

SUITABILITY OF SALT DOMES IN  
THE EAST TEXAS BASIN FOR NUCLEAR-WASTE ISOLATION:  
FINAL SUMMARY OF GEOLOGIC AND HYDROGEOLOGIC RESEARCH  
(1978 - 1983)

M.P.A. Jackson and Steven J. Seni

Milestone Contract Report for the U. S. Department of  
Energy under Contract No. DE-AC97-80ET46617, formerly DE-AC97-79ET44605  
(formerly EW-78-S-05-5681)

Bureau of Economic Geology  
W. L. Fisher, Director  
The University of Texas at Austin  
University Station, P. O. Box X  
Austin, Texas 78712

1983

SUITABILITY OF SALT DOMES IN  
 THE EAST TEXAS BASIN FOR NUCLEAR-WASTE ISOLATION:  
 FINAL SUMMARY OF GEOLOGIC AND HYDROGEOLOGIC RESEARCH  
 (1978-1983)

|   |    |
|---|----|
| Summary . . . . .   | 1  |
| 0.0 Evaluation . . . . .  | 4  |
| 1.0 Introduction to the East Texas Basin . . . . .                    | 9  |
| 1.1 The East Texas Waste Isolation Program . . . . .                  | 9  |
| 1.2 Tectonic Evolution . . . . .                                      | 16 |
| 1.3 Structural Framework . . . . .                                    | 18 |
| 1.4 Stratigraphic Framework . . . . .                                 | 20 |
| 1.5 Regional Hydrogeology . . . . .                                   | 23 |
| 1.6 Inventory of East Texas Salt Domes . . . . .                      | 26 |
| 2.0 Regional Geologic Studies . . . . .                               | 29 |
| 2.1 Present Distribution and Geometry of Salt Structures . . . . .    | 29 |
| 2.2 Mechanisms Initiating Salt Flow . . . . .                         | 32 |
| 2.3 Initiation of Salt Flow . . . . .                                 | 34 |
| 2.4 Diapirism . . . . .   | 37 |
| 2.5 Effects of Dome Growth on Facies in Enclosing Strata . . . . .    | 39 |
| 2.6 Effects of Dome Growth on Structure of Enclosing Strata . . . . . | 43 |
| 2.7 Effects of Dome Growth on Surface Processes . . . . .             | 45 |
| 2.8 Rates of Dome Growth . . . . .                                    | 48 |
| 2.9 Fault Tectonics . . . . .   | 50 |
| 2.10 Seismicity . . . . .   | 52 |
| 2.11 Petroleum Potential of Domes . . . . .                           | 55 |
| 3.0 Regional Hydrogeologic Studies . . . . .                          | 57 |
| 3.1 Ground-Water Hydraulics . . . . .                                 | 57 |
| 3.2 Ground-Water Chemistry . . . . .                                  | 61 |

|     |  |     |
|-----|--|-----|
| 3.3 | Subsurface Salinity Near Salt Domes . . . . .  | 63  |
| 3.4 | Ground-Water Age . . . . .   | 67  |
| 3.5 | Surface Salines . . . . .  | 70  |
| 3.6 | Saline Aquifers . . . . .  | 73  |
| 4.0 | Core Studies of Oakwood Dome, East Texas . . . . .   | 77  |
| 4.1 | Salt-Core Lithology . . . . .  | 77  |
| 4.2 | Salt-Core Structure . . . . .  | 80  |
| 4.3 | Salt-Core Strain . . . . .   | 83  |
| 4.4 | Cap-Rock - Rock-Salt Interface . . . . .   | 86  |
| 4.5 | Cap Rock . . . . .   | 91  |
| 5.0 | Hydrogeologic Studies of Oakwood Dome and Vicinity . . . . .   | 96  |
| 5.1 | Hydrogeologic Monitoring and Testing . . . . .   | 96  |
| 5.2 | Ground-Water Modeling: Wilcox Multiple-Aquifer System . . . . .  | 100 |
| 5.3 | Ground-Water Modeling: Flow Rates and Travel Times. . . . .  | 102 |
|     | Acknowledgments . . . . .  | 104 |
|     | Selected References. . . . .   | 105 |
|     | References. . . . .  | 107 |
|     | Appendix 1 - Lithologic descriptions, correlation notes, and<br>selected references, East Texas Basin . . . . .  | 116 |
|     | Appendix 2 - Dome catalog. . . . .   | 120 |
|     | Appendix 3 - Schematic stages of dome growth showing typical<br>lithologic and thickness variations in strata around domes . . . . .                   | 226 |
|     | Appendix 4 - Methods for calculating net and gross rates of<br>diapir growth with applications, assumptions,<br>restrictions, and advantages . . . . . | 227 |
|     | Appendix 5 - Log of Oakwood Dome salt core . . . . .   | 230 |
|     | Appendix 6 - Log of Oakwood Dome cap rock . . . . .  | 247 |

## Figures

|  |    |
|--|----|
| 1.2-1 Schematic cross sections showing evolutionary stages in formation of East Texas Basin and adjoining Gulf of Mexico . . . . .                   | 17 |
| 1.3-1 Regional structural framework of the East Texas Basin . . . . .  | 19 |
| 1.3-2 Structural cross section across East Texas Basin . . . . .   | 19 |
| 1.4-1 Stratigraphic column, East Texas Basin.<br>See also Appendix 1 . . . . .   | 21 |
| 1.4-2 Typical geophysical and lithic log, Rains County, Texas . . . . .  | 22 |
| 1.5-1 Ground-water flow lines for Wilcox-Carrizo system, East Texas Basin. . . . .   | 25 |
| 1.6-1 Major-axis orientation and proportional axial ratios of salt diapirs . . . . .   | 27 |
| 1.6-2 Rose diagrams of major axis orientation of (A) turtle structures,<br>(B) salt pillows, and (C) salt diapirs . . . . .                          | 27 |
| 1.6-3 Graph of axial ratio versus percentage overhang for 15 East Texas diapirs. . . . .   | 28 |
| 2.1-1 Isometric block diagram of salt structures in the East Texas Basin . . . . .   | 30 |
| 2.1-2 Map of salt provinces and salt-structure contours, East Texas Basin. . . . .   | 31 |
| 2.2-1 Salt-flow directions with dipping source layer and uniform,<br>onlapping overburden . . . . .  | 33 |
| 2.2-2 Fluid gradient in salt pillow below denser cover . . . . .   | 33 |
| 2.2-3 Fluid gradient in tabular salt below P <sub>3</sub> and P <sub>4</sub> , induced by<br>differential loading by dense sand-rich delta . . . . . | 33 |
| 2.3-1 Model of Late Jurassic-Early Cretaceous salt mobilization . . . . .  | 36 |
| 2.4-1 Map of diapir groups . . . . .   | 38 |
| 2.4-2 Block diagram of depositional facies during Washita-Glen Rose time . . . . .   | 39 |
| 2.5-1 Block diagram of depositional facies during Wilcox time . . . . .  | 41 |
| 2.5-2 Net sandstone, Paluxy Formation showing decrease in sandstone<br>over crests of pillows . . . . .  | 42 |
| 2.5-3 Cross section through Wilcox Group around Bethel Dome . . . . .  | 42 |
| 2.6-1 Isometric block diagram of salt diapirs and structure<br>contours on top of Woodbine Group . . . . .   | 44 |

|        |   |    |
|--------|---|----|
| 2.7-1  | Significant correlation between depth to dome and index of preferred orientation . . . . .                                    | 47 |
| 2.7-2  | Cross section of Quaternary floodplain deposits above Oakwood Dome . . . . .  | 47 |
| 2.8-1  | Comparison of long-term rates of dome growth . . . . .  | 49 |
| 2.9-1  | Fault traces on base of Austin Chalk and their relation to salt diapirs, salt pillows, and turtle structures . . . . .        | 51 |
| 2.9-2  | Time-to-depth-converted seismic section showing symmetric buried graben over crest of Van-Ash salt pillow. . . . .            | 51 |
| 2.10-1 | Jacksonville main shock and aftershock from Mt. Enterprise fault zone . . . . .   | 54 |
| 2.10-2 | Time-to-depth-converted seismic section across Mt. Enterprise listric-normal growth fault. . . . .                            | 54 |
| 2.11-1 | Map of salt-related structures and petroleum fields in central part of East Texas Basin . . . . .                             | 56 |
| 2.11-2 | Production statistics for central part of East Texas Basin . . . . .  | 56 |
| 3.1-1  | Map of regional potentiometric surface of Wilcox-Carrizo aquifer in East Texas . . . . .                                      | 59 |
| 3.1-2  | Elevations of Wilcox-Carrizo water levels and major stream beds . . . . .   | 59 |
| 3.1-3  | Fluid-pressure versus depth in fresh-water Wilcox-Carrizo aquifers . . . . .  | 60 |
| 3.2-1  | Piper diagrams of Wilcox-Carrizo water chemistry. . . . .   | 62 |
| 3.3-1  | Map showing relationship of percentage thickness of fresh water in Wilcox aquifer to trends of high sand percentage . . . . . | 65 |
| 3.3-2  | Location of possible saline plume associated with Oakwood Dome . . . . .  | 66 |
| 3.4-1  | <sup>14</sup> C ages of ground water in Wilcox-Carrizo aquifer near Oakwood Dome . . . . .                                    | 68 |
| 3.5-1  | Depths to top of East Texas domes . . . . .   | 71 |
| 3.5-2  | Duggey's Lake overlies possible dissolution-induced collapse over Palestine Dome . . . . .                                    | 72 |
| 3.6-1  | Fluid pressure versus depth for saline aquifers in East Texas Basin . . . . .   | 75 |
| 3.6-2  | Calcium concentration versus total dissolved solids in saline aquifers in East Texas Basin. . . . .                           | 75 |
| 3.6-3  | $\delta^{2}\text{H}$ and $\delta^{18}\text{O}$ in East Texas ground water and meteoric water line . . . . .                   | 76 |
| 4.1-1  | Oakwood Dome cross section showing location of TOG-1 well . . . . .   | 78 |

|       |   |     |
|-------|---|-----|
| 4.1-2 | Profile of TOG-1 rock-salt core showing R-1, R-2, and R-3 zones, dip of foliation in R-1 zone, and disseminated-anhydrite layers. See also Appendix 5 . . . . . | 78  |
| 4.1-3 | Photomicrograph of brine inclusions within halite in R-3 zone at depth of 354.7 m (1163.7 ft) . . . . .   | 79  |
| 4.2-1 | Schistosity and anhydrite-rich layers in TOG-1 rock-salt core . . . . .   | 81  |
| 4.2-2 | Structure section along TOG-1 rock-salt core . . . . .  | 82  |
| 4.2-3 | Inferred flow patterns within a laterally spreading, rising diapir fed by multiple emplacement of salt tongues as overthrust folds . . . . .                    | 82  |
| 4.3-1 | Flinn diagram showing mean strains in Oakwood Dome rock salt . . . . .  | 84  |
| 4.3-2 | Statistically significant upward decrease in percentage shortening with decreasing depth . . . . .  | 85  |
| 4.4-1 | Photograph of tight contact between salt and overlying caprock . . . . .  | 89  |
| 4.4-2 | Schematic diagram showing processes at cap-rock - rock-salt interface . . . . .   | 90  |
| 4.5-1 | Photograph of 1 mm-wide stylolitic laminae in anhydrite cap-rock from TOG-1. . . . .  | 95  |
| 5.1-1 | Potentiometric surface of Carrizo aquifer over Oakwood Dome . . . . .   | 98  |
| 5.1-2 | Electric-log resistivity values in the Wilcox Group compared with lab-derived K values . . . . .  | 98  |
| 5.2-1 | View of upper surface (top of Wilcox-Carrizo aquifer) of finite-difference model of ground-water flow, Oakwood Dome area . . . . .                              | 101 |
| 5.2-2 | Regional ground-water flow lines in Wilcox-Carrizo aquifer near Oakwood Dome . . . . .  | 101 |
| 5.3-1 | Ground-water velocity vectors computed in model simulation A . . . . .  | 103 |

Tables

|       |  |    |
|-------|--|----|
| 0.0-1 | Evaluation of Oakwood Salt Dome as potential repository . . . . .                          | 6  |
| 1.1-1 | Data base for the East Texas Waste Isolation program . . . . .                             | 11 |
| 1.1-2 | Studies in the East Texas Waste Isolation program . . . . .                                | 12 |
| 3.4-1 | <sup>14</sup> C ages of ground water in Wilcox-Carrizo aquifer near Oakwood Dome . . . . . | 69 |

|       |   |    |
|-------|---|----|
| 4.4-1 | Inferred processes at Oakwood Dome that are favorable<br>for storage of nuclear waste in salt diapirs . . . . . | 87 |
| 4.4-2 | Inferred processes at Oakwood Dome that are unfavorable<br>to storage of nuclear waste in salt diapirs. . . . . | 88 |
| 4.5-1 | Comparison of porosities and permeabilities of cap rock from<br>Oakwood and Gyp Hill Salt Domes . . . . .       | 93 |
| 5.1-1 | Test data from monitoring wells around Oakwood Dome . . . . .   | 99 |

## SUMMARY

Consideration of guidelines from the Nuclear Waste Policy Act of 1982 indicates that Oakwood Salt Dome has 23 favorable factors, 15 potentially adverse factors, and three disqualifying factors. Based on our survey of domes in East Texas, we find no factor generic to salt domes that precludes their use as a repository of nuclear waste.

This report summarizes results of the East Texas Waste Isolation program from January 1, 1978, to March 30, 1983. Using an extensive data base, the study comprised 33 different lines of research by 67 scientists and research assistants. The program covered both basin-wide and site-specific (mainly around Oakwood Dome) studies using surface and subsurface data. A wide range of pertinent geologic and economic data for all 15 shallow salt domes is summarized in Appendix 2.

Mesozoic opening of the Gulf of Mexico accompanied thermal processes that controlled sedimentation during filling of the East Texas Basin. The basin contains up to 7,000 m of shallow-marine and continental sediments overlying the Louann Salt. Deformation in the basin resulted from subsidence of its floor and gravitational flow of salt.

The East Texas Basin is divided into four provinces based on the shape of salt structures. Five forces make salt flow; they operate from near surface to the deepest parts of the basin. Salt flow began in pre-Gilmer (Late Jurassic) time with the growth of salt pillows. Three groups of diapirs can be differentiated on the basis of age and distribution. The growing salt structures affected topography, thereby influencing depositional facies. Low-permeability facies generally surround the salt stocks. Two types of structural inversion affected the structure of strata during diapirism. Geomorphic evidence does not preclude Quaternary uplift over Oakwood Dome, but its southern flank may have subsided. The rates of dome growth declined exponentially with time to rates less than 0.6 m per  $10^4$  yr. All regional fault systems in the basin appear to be related to slow gravitational creep of salt. Nevertheless at least eight probable earthquakes were recorded near the southern margin of the basin in 1981 and 1982, and their probable focus - the Mount Enterprise fault - is poorly understood.

The following conclusions were drawn from geologic study of a core into Oakwood Dome. Salt core from the dome is greater than 98 percent pure halite, (anhydrite is the only other mineral) and displays evidence for two distinct periods of recrystallization. Geometric analysis and strain analysis suggest that the crest of the dome was truncated, probably by ground-water dissolution, during the formation of anhydrite cap rock. Diapiric rise of salt formed a tight contact between salt and cap rock. The cap rock formed in a deep saline environment and appears to be a low-permeability barrier to dome dissolution.

Two major aquifer systems lie above and below the hypothetical repository level in a dome: the Wilcox-Carrizo fresh-brackish aquifer system and the Woodbine saline aquifer. Only the five shallowest domes have surface salines and are poor sites for potential repositories. False cap rock over two of these domes suggest that their salines may originate from upward discharge of deep-basin brines.

Of the domes that penetrate the Wilcox-Carrizo aquifer system, only Oakwood Dome has a slightly brackish plume, possibly caused by salt dissolution. None of the salt domes show evidence of large exposure to circulating ground water. The salt domes are generally isolated by low-permeability cap rock and mud-rich facies.

Regional circulation in the Wilcox-Carrizo aquifer system correlates closely with topography and geologic structure. A potential for downward flow prevails except beneath the Trinity and Sabine River drainage systems, especially beneath the Trinity River flood plain. Potential for downward flow between the Wilcox-Carrizo and the Woodbine is due to large basinwide pressure declines in the Woodbine caused by oil and gas production.

Wilcox-Carrizo ground-water chemistry evolves from an acidic, oxidizing, Ca-Mg-HCO<sub>3</sub>-SO<sub>4</sub> water to a basic, reduced, Na-HCO<sub>3</sub> water. <sup>14</sup>C dating of the ground water indicates ages of 10<sup>3</sup> yr in recharge areas to 1.5 x 10<sup>4</sup> yr in the artesian section.

Three-dimensional modeling of ground-water flow in the Wilcox-Carrizo aquifer near Oakwood Dome shows that the stratified sand-mud fabric causes poor vertical connection of sand bodies and very low ( $\approx 10^{-3}$  to  $10^{-4}$ ) ratios of vertical to horizontal hydraulic conductivity.

Rates of vertical ground-water flow are only 11 m/10<sup>4</sup> yr. Ground-water travel times from Oakwood Dome to potential discharge areas are approximately 10<sup>4</sup> yr in well-connected, channel-fill sand bodies and 10<sup>5</sup> to 10<sup>6</sup> yr in poorly connected interchannel facies. These interchannel facies constitute large potential aquitards. Realistic modeling of flow rates in the Wilcox or in similar aquifers is invalid without incorporating sand-body geometry and interconnection.

The shallower of the two deep saline aquifer systems surrounds salt domes immediately below hypothetical repository level. Mixing of deep saline waters with the overlying fresh-water system is limited.

## 0.0 EVALUATION

Oakwood Dome is evaluated as a potential repository for high-level nuclear waste.

*Consideration of guidelines from the Nuclear Waste Policy Act of 1982 indicates that Oakwood Salt Dome has 23 favorable factors, 15 potentially adverse factors, and three disqualifying factors. We find no factor generic to salt domes that precludes their use as a repository of nuclear waste.*

The East Texas Waste Isolation project is one of three subprograms studying interior salt basins in the Gulf Coast area. These subprograms constitute part of the National Waste Terminal Storage program, which is designed to assess the suitability of dome salt, bedded salt, basalt, tuff, and crystalline rock as host media for deep underground containment of high-level nuclear waste. In common with other projects, the goal of the East Texas project was a progressive screening in which the best site (in this case, a salt stock in the core of a salt dome) could be selected by eliminating less favorable sites.

All 15 shallow salt domes in the East Texas Basin were examined. These were then narrowed down to three domes: Keechi, Oakwood, and Palestine. By 1980 Palestine Dome had been eliminated because of ongoing collapse of strata above the dome induced by earlier brining operations. By 1981 further screening had eliminated Keechi Dome because it was too small and too shallow (ONWI-109 Technical Report). From this point, therefore, research in the ETWI program was directed to (1) a better understanding of Oakwood Dome and vicinity, and (2) supplying information generic to salt domes in general, which could be applied to the other three candidate domes in the North Louisiana and Mississippi interior salt basins.

In accordance with the requirements of the Nuclear Waste Policy Act of 1982, the Department of Energy has proposed "General Guidelines for Recommendation of Sites for Nuclear Waste Repositories," which appear in the Federal Register, Part II, of February 7, 1983. Based on these guidelines, the Oakwood Dome area is evaluated in table 0.0-1. With regard to its suitability as a repository for high-level nuclear waste, Oakwood Dome has 23 favorable factors, 15 potentially adverse factors, and three disqualifying factors. These three

disqualifying factors are related to petroleum exploration and are specific to Oakwood Dome. Based on our survey of the East Texas Basin, we find no factor generic to salt domes that precludes their use as a repository for nuclear waste.

Table 0.0-1. Evaluation of Oakwood Dome as potential repository in terms of guidelines set by Nuclear Waste Policy Act of 1982

|  | Favorable | Potentially Adverse |
|--|-----------|---------------------|
| <b>Geologic and Hydrologic Factors</b>                                       |           |                     |
| <u>SITE GEOMETRY (OAKWOOD)</u>   |           |                     |
| Potential repository depth >300 m  | *         |                     |
| Erosional denudation in $10^4$ yr = 1-2 m                                    | *         |                     |
| Thickness and lateral extent   | *         |                     |
| <u>HYDROGEOLOGY (OAKWOOD AND REGIONAL)</u>                                   |           |                     |
| Predominantly downward vertical hydraulic gradient basinwide                 | *         |                     |
| Local recharge over Oakwood Dome to shallow (Carrizo) aquifer                | *         |                     |
| No evidence for interaction between saline and fresh aquifers around Oakwood | *         |                     |
| Upward discharge of deep-basin fluids at Butler Dome                         |           | *                   |
| Saline plume at Oakwood Dome   |           | *                   |
| Travel time of ground water to discharge areas:                              |           |                     |
| Modeling: connected Wilcox sands = $10^3$ - $10^4$ yr                        |           | *                   |
| : disconnected Wilcox sands = $10^5$ - $10^6$ yr                             | *         |                     |
| $^{14}\text{C}$ dating: Wilcox = $1.6 \times 10^4$ yr                        | *         |                     |
| Oakwood area modeled with reasonable accuracy                                | *         |                     |
| Low-permeability Wilcox facies around dome                                   | *         |                     |
| Low-permeability cap rock above, and partly flanking dome                    | *         |                     |

Table 0.0-1 (cont.)

|   | Favorable | Potentially Adverse | Disqualifying |
|---|-----------|---------------------|---------------|
| Tight seal in core between rock salt and cap rock   | *         |                     |               |
| Vertical extension fractures in anhydrite cap rock  |           | *                   |               |
| Possible subsidence over southern part of Oakwood salt stock  |           | *                   |               |
| Inferred escape of brines from former dissolution cavity below caprock (inferred to be >3 Ma ago)   |           | *                   |               |
| Structural evidence for truncation of dome crest (mainly in Cretaceous)   |           | *                   |               |
| 62 boreholes through salt overhang probably connect shallow, fresh-water aquifer and deep, saline aquifer, possibly allowing rapid salt dissolution by fresh water                |           |                     | *             |
| <u>ROCK CHARACTERISTICS (OAKWOOD)</u>   |           |                     |               |
| Evidence for self sealing in anhydrite cap rock during strain   | *         |                     |               |
| Rock-salt mineral assemblage unchanged during thermal loading   | *         |                     |               |
| Recrystallization of uppermost 2 m of rock salt probably caused by entry of water from cap-rock base (inferred to be >3 Ma ago)   |           | *                   |               |
| In-place concentration of intracrystalline fluid in foliated (R-1) rock salt at level of hypothetical repository is unknown because of artificial introduction of water into core |           | *                   |               |
| Preferred migration paths of intercrystalline fluids are partly predictable from strain analysis and geometric analysis of rock salt  | *         |                     |               |
| Structure of rock salt reasonably understood where intersected by borehole  | *         |                     |               |

Table 0.0-1 (cont.)

|  | Favorable | Potentially Adverse | Disqualifying |
|--|-----------|---------------------|---------------|
| <u>TECTONIC ENVIRONMENT (MAINLY REGIONAL)</u>  |           |                     |               |
| Uplift rates over fastest domes, estimated by extrapolation of growth rates from 112 Ma to 48 Ma, is $<0.6 \text{ m}/10^4 \text{ yr}$ .                    | *         |                     |               |
| Geomorphic evidence does not preclude current differential uplift over most of Oakwood Dome  |           | *                   |               |
| Geomorphic evidence suggests subsidence of the southern part of Oakwood Dome   |           | *                   |               |
| No evidence for rapid regional uplift or subsidence  | *         |                     |               |
| Most regional fault systems are reasonably understood and apparently aseismic  | *         |                     |               |
| No regional faults within 10 km of dome  | *         |                     |               |
| Small Quaternary faults at surface 18 km from Oakwood Dome   |           | *                   |               |
| Vertical extent of small, post-Queen City surface faults over Oakwood Dome is unknown  |           | *                   |               |
| Historical earthquakes, if repeated, would not significantly affect Oakwood site   | *         |                     |               |
| Seismicity probably due to movement on Mt. Enterprise fault, but because cause of faulting is not yet understood, seismic risk cannot be reliably assessed |           | *                   |               |
| No Quaternary igneous activity   | *         |                     |               |
| <u>HUMAN INTRUSION (OAKWOOD)</u>   |           |                     |               |
| Petroleum reserves below overhang and 4 km to SE   |           |                     | *             |
| Intensive exploratory and production drilling through salt overhang, partly to level of hypothetical repository; sites of 3 holes have not been located    |           |                     | *             |
| <u>SURFACE CHARACTERISTICS (OAKWOOD)</u>   |           |                     |               |
| Gently rolling terrain   | *         |                     |               |
| Dikes possibly required for flood protection   |           | *                   |               |

## 1.0 INTRODUCTION TO THE EAST TEXAS BASIN

### 1.1 THE EAST TEXAS WASTE ISOLATION PROGRAM

This report summarizes results of the East Texas Waste Isolation program from January 1, 1978 to March 30, 1983.

*The East Texas Waste Isolation program began on January 1, 1978 and ceased on March 30, 1983. The program goals were to assist in the selection of a suitable salt dome in the East Texas Basin through geologic and hydrogeologic characterization of the domes and surrounding strata and to provide generic information applicable to other salt dome basins.*

This report, in STOP format (Carte and Landers, 1975), summarizes results of the East Texas Waste Isolation program from January 1, 1978 to March 30, 1983. As part of the Area Characterization Phase of evaluating U.S. Gulf Coast salt-dome basins, the East Texas program was designed to characterize the geology and geohydrology of salt domes and surrounding strata in the East Texas Basin and to provide generic information applicable to other salt-dome basins. The data base for this program is extensive because the basin is a mature petroleum province and contains major fresh-water aquifers (table 1.1-1). Table 1.1-2 lists the 32 principal lines of geologic research, the scale of examination, and the pertinent sections of the report covering these aspects. Most of these lines of research have generic application to other salt-dome basins as well, and some are exclusively generic. The most important generic studies are listed in column 1 of table 1.1-2. Selected References show the principal references for individual sections of this report. A more complete list is given under References.

In addition to M.P.A. Jackson and S. J. Seni, the following geologists coauthored reports summarized in this paper (see bibliography for details): C. W. Kreitler (project director), O. K. Agagu, J. M. Basciano, B. Bracken, E. W. Collins, R. D. Conti, E. D. Davidson, Jr., O. R. Dix, G. A. Donaldson, S. P. Dutton, G. E. Fogg, A. B. Giles, E. H. Guevara, D. W. Harris, D. K. Hobday, C. M. Lopez, M. K. McGowen, W. R. Muehlberger, D. Pass, W. D. Pennington,

B. Wilson, D. H. Wood, and H. V. Wuerch. Research assistants who compiled and processed data include F. Boyd, E. Bramson, R. Burks, S. Carlson, C. Chomicky, R. Cobb, S. Cumella, D. Dann, R. Debus, E. Duncan, S. Ghazi, S. Hovorka, J. Hultman, J. Karabaic, D. Legett, E. Lindgren, S. Lovell, J. Lundelius, D. Magouirk, S. Mann, J. McIntyre, G. Meyer, D. Miser, J. O'Neal, L. Orr, E. Pisasale, K. Pollman, D. Prouty, K. Rader, B. Richter, V. Riggert, J. Rogers, L. Ruiz, R. Senger, R. Sherrill, T. Simmons, J. Smith, J. Sugmann, P. Talamas, D. Wiggins, D. Worrell, and D. Young.

Table 1.1-1. Data base for the East Texas Waste Isolation program

Surface

Geologic Atlas of Texas map sheets 1:250,000  
Geologic maps from unpublished theses  
Topographic maps 1:62,500 and 1:24,000  
Texas General Highway Maps 1:63,360 and 1:253,440  
Aerial photographs 1:12,000 to 1:25,500  
Landsat imagery 1:250,000, band-5  
Re-leveling profile of 28 stations across Mount Enterprise fault zone.  
Microseismic monitoring data from 1-3 seismograph stations near Mount Enterprise.

Subsurface

Geophysical logs from ~4,600 wells  
Water-level data from >2,000 water wells  
Water-chemistry data from ~1,500 water wells  
29 shallow borings to depths of 7-120 m (20-400 ft) over Oakwood Dome, 9 of which were monitored for water levels.  
Hydrologic test data from 5 production wells, one of which was cored.  
TOG-1 412 m (1,352 ft) core through Oakwood Dome salt, cap rock, and overburden; TOH-2AO 563 m (1,847 ft) core through Wilcox Group near Oakwood Dome.  
13 cores borrowed from Well Sample Library and oil companies.  
475 km of 6-fold C.D.P. reflection seismic line.  
Residual gravity map 1:96,000

Table 1.1-2 Studies in the East Texas Waste Isolation program

|  | 1. GENERIC | 2. BASIN-WIDE | 3. ALL 15 DOMES | 4. OAKWOOD, KEECHI<br>PALESTINE, BUTLER<br>DOMES | 5. LOCAL NON-DOME |
|--|------------|---------------|-----------------|--|-------------------|
| <b>SITE GEOMETRY</b>   |            |               |                 |  |                   |
| Measurement of size and shape of salt domes: to determine if criteria of minimum thickness and lateral extent are met. Based on analysis of structure-contour maps from gravity, seismic, and well data. |            |               | 1.6             |  |                   |
| Measurement of depth to salt and cap rock: to determine if minimum-depth criterion is met. Based on interpretation of well logs and seismic profiles.  |            |               | 1.6             |  |                   |
| <b>SURFACE GEOLOGY</b>   |            |               |                 |  |                   |
| Calculation of denudation rates by surveys of suspended-sediment loads and reservoir sedimentation: to assess risk of erosional breaching of dome.   |            | 2.7           |                 |  |                   |
| Measurement of stream and terrace profiles: to determine the effects of possible dome uplift or collapse.  |            | 2.7           |                 | 2.7  |                   |
| Shallow drilling of Quaternary valley fill over Oakwood Dome: to determine the effects of possible dome uplift or collapse.  |            |               |                 | 2.7  |                   |
| Analysis of slopes above domes: to recognize possible dome uplift or collapse.   |            |               |                 | 2.7  |                   |
| Analysis of link-lengths of drainage networks: to determine the existence of possible dome uplift or collapse.   |            |               | 1.6             | 2.7  | 2.7               |
| Stratigraphic and structural mapping, including fault zones, over domes: to determine the effects of possible dome uplift or collapse.   |            |               |                 | 2.7<br>2.9                                       |                   |
| Lineament analysis of aerial photographs and Landsat imagery: to study regional and over-dome fracture patterns.   |            | 2.7           |                 |  | 2.7               |
| Releveling over Mount Enterprise fault zone: to measure elevation changes from faulting in the past 30 years.  |            |               |                 |  | 2.10              |

Studies in the East Texas Waste Isolation program (continued)

|   | 1. GENERIC | 2. BASIN-WIDE     | 3. ALL 15 DOMES | 4. OAKWOOD, KEECHI<br>PALESTINE, BUTLER<br>DOMES | 5. LOCAL NON-DOME |
|---|------------|-------------------|-----------------|--|-------------------|
| Microseismic monitoring of the Mount Enterprise fault zone: to determine magnitudes and locations of earthquakes.   |            |                   |                 |  | 2.10              |
| <b>SUBSURFACE GEOLOGY</b>   |            |                   |                 |  |                   |
| Interpretation of geophysical logs to elucidate lithology, depositional systems, structure, tectonic evolution, and geometry of sedimentary units in the basin.                         | 2.5        | 1.2               | 1.3             |  |                   |
|   | 2.6        | 1.3<br>1.4<br>2.1 | 1.4<br>1.6      |  |                   |
| Construction of 49 stratigraphic and structural regional cross sections: to carry out basin analysis.   |            | 1.3               | 1.3             |  |                   |
|   |            | 1.4               | 1.4             |  |                   |
| Construction of structural cross sections around 15 domes: to determine geometry of near-dome stratigraphic units.  | 2.4        |                   | 1.6             |  |                   |
| <del>Interpretation of reflection seismic data and time-to-depth conversion of events: to examine seismic stratigraphy, especially of units below depth of abundant well control.</del> |            | 1.3               |                 | 1.3  |                   |
|   |            | 1.4               |                 | 1.4  |                   |
|   |            | 2.1               |                 |  |                   |
|   |            | 2.3               |                 |  |                   |
|   |            | 2.9               |                 |  |                   |
| Interpretation of residual gravity: to define salt-related structures.  |            | 1.3               | 1.6             |  |                   |
|   |            | 2.1               |                 |  |                   |
| Analysis of regional fault systems: to examine distribution, geometry, displacement history, and origin, especially with regard to seismic potential.                                   |            | 2.9               |                 |  |                   |
| Examination of subsurface data around 15 salt domes: to infer times and patterns of salt movement over 64 Ma.   | 2.4        |                   | 1.6             |  |                   |
|   | 2.5        |                   | 2.3             |  |                   |
|   |            |                   | 2.4             |  |                   |
|   |            |                   | 2.5             |  |                   |
|   |            |                   | 2.6             |  |                   |

13

Studies in the East Texas Waste Isolation program (continued)

|  | 1. GENERIC               | 2. BASIN-WIDE | 3. ALL 15 DOMES   | 4. OAKWOOD, KEECHI<br>PALESTINE, BUTLER<br>DOMES | 5. LOCAL NON-DOME |
|--|--------------------------|---------------|-------------------|--|-------------------|
| Measurement of thickness changes around 15 salt domes: to quantify rates of dome growth over 64 Ma to predict future dome growth.                        | 2.8                      |               | 1.6<br>2.4<br>2.8 |  |                   |
| Oakwood salt-core studies of lithology, geochemistry, fluid inclusions, structure, and strain: to evaluate host-rock characteristics.                    | 4.1<br>4.2<br>4.3<br>4.4 |               |                   | 4.1<br>4.2<br>4.3<br>4.4                         |                   |
| Oakwood cap-rock studies of lithology, geochemistry, isotopic chemistry, structure, and origin: to evaluate the effects of geologic sealing by cap rock. | 4.4<br>4.5               |               |                   | 4.4<br>4.5                                       |                   |
| Literature review of internal structure of salt glaciers and diapirs generally: to evaluate host-rock characteristics.                                   | *                        |               |                   |  |                   |
| Review of mechanisms for initiating salt flow generally: to understand structural evolution of host rock.  | 2.2                      | 2.2           |                   |  |                   |
| Synthesis of petroleum potential of salt domes: to evaluate probability of future exploration for resources.   |                          | 1.6           | 1.6               |  |                   |
| Documentation of petroleum storage in salt domes: to eliminate domes with prior economic use.  |                          |               | 1.6               |  |                   |
| Documentation of hydrocarbon accumulation patterns   | 2.11                     | 2.11          | 2.11              | 2.11   | 2.11              |
| GEOHYDROLOGY   |                          |               |                   |  |                   |
| Documentation of surface salines: to determine their relation to shallow salt domes.   | 3.5                      |               | 1.6<br>3.5        |  |                   |
| Monitoring ground-water levels: to deduce ground-water flow paths.   |                          | 1.5<br>3.1    |                   | 3.1  |                   |

Studies in the East Texas Waste Isolation program (continued)

|   | 1. GENERIC        | 2. BASIN-WIDE     | 3. ALL 15 DOMES | 4. OAKWOOD, KEECHI PALESTINE, BUTLER DOMES | 5. LOCAL NON-DOME |
|---|-------------------|-------------------|-----------------|--|-------------------|
| Pumping tests of producing wells around Oakwood Dome: to determine hydrologic properties of fresh-water aquifers.   |                   |                   |                 | 3.1<br>5.1                                 |                   |
| Analysis of water and existing water-chemistry data: to determine geochemical evolution of fresh and saline aquifers.   | 3.2<br>3.6        | 1.5<br>3.2<br>3.6 |                 | 3.2<br>3.6                                 | 3.2               |
| Isotopic analysis of ground water: to determine age, residence time and source.   |                   | 3.4               |                 | 3.4  | 3.2               |
| 5 Construction of hydrodynamic models around Oakwood Dome: to evaluate the effects of changing several hydrologic variables on flow patterns around the dome. | 3.3<br>5.2<br>5.3 |                   |                 | 3.3<br>5.2<br>5.3                          |                   |
| Examination of petrography, isotopes, and stratigraphic relations of Butler Dome false cap rock: to determine origin and age of alteration.                   |                   |                   |                 | 3.6  |                   |

\*See separate contract report.

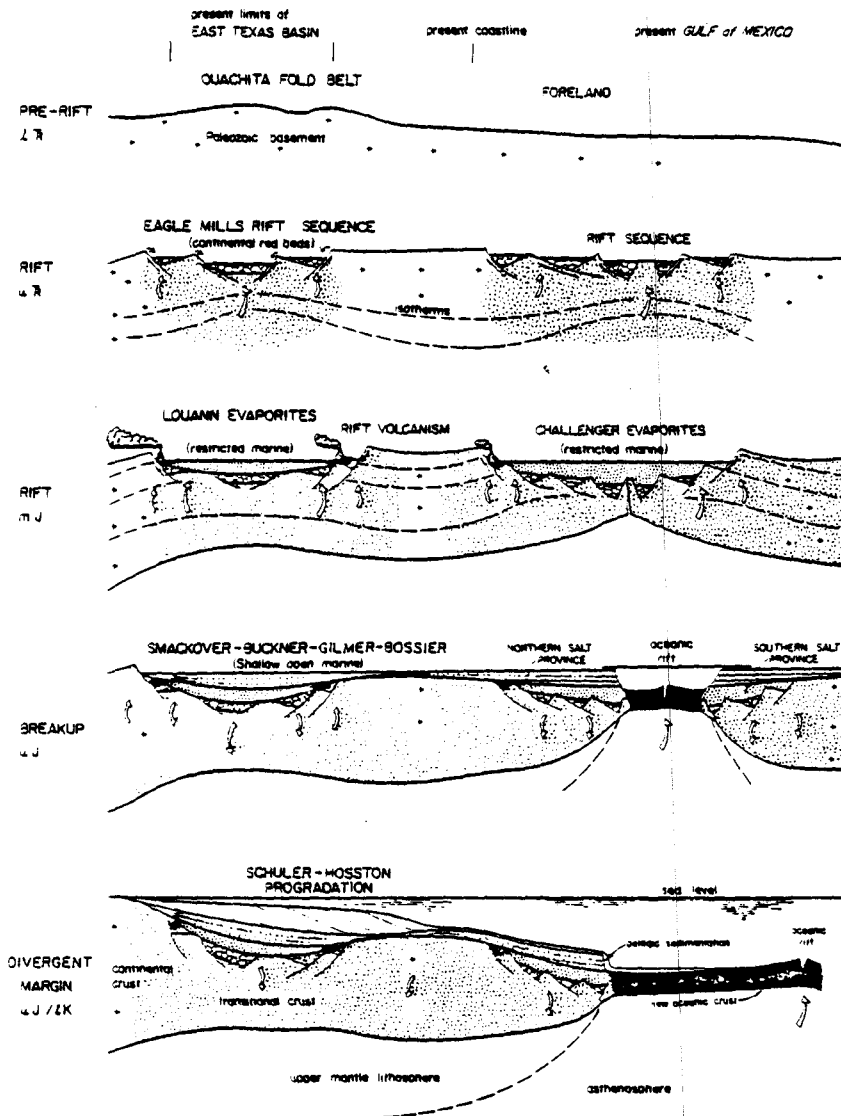
Mesozoic opening of the Gulf of Mexico accompanied thermal processes that controlled sedimentation during filling of the East Texas Basin.

*The character of Mesozoic sedimentary fill in the East Texas Basin closely reflects underlying thermally induced tectonic processes characteristic of initial uplift, rifting, and thinning of Paleozoic continental crust. The subsequent tectonic subsidence allowed restricted-marine incursions accompanied by rift volcanism. Further subsidence resulted in the accumulation of open shallow-marine deposits followed by progradation of the continental margin by delta-dominated systems toward an oceanic spreading center in the Gulf of Mexico.*

The East Texas Basin originated as a Jurassic failed rift north of the principal rift zone that ultimately formed the Gulf of Mexico (fig. 1.2-1). During the pre-rift stage, lithospheric expansion and uplift exposed the Paleozoic Ouachita Fold Belt to erosion. With the onset of rifting, diverging zones of maximum uplift (upward arrows in fig. 1.2-1) migrated outward from the rift axes as the lithosphere rose and stretched, probably as a result of an underlying thermal anomaly. These zones of uplift were followed by diverging zones of collapse (downward arrows). Upper Triassic red beds were deposited unconformably as continental rift fill on eroded basement. Widespread erosion formed the sub-salt angular unconformity across Triassic rift fill and Paleozoic basement.

By mid-Jurassic the basin had subsided sufficiently to allow marine incursions along the linear trough and its flanks, forming the Louann Salt. Rift volcanism is recorded by lava flows and ash falls immediately above and below the salt.

In the late Jurassic, open shallow-marine deposits accumulated on the subsiding continental shelf in the basin during continental breakup. The paucity of terrigenous sediment on this shelf suggests that the rift margin was still sufficiently elevated to divert rivers elsewhere. Continued, cooling-induced subsidence of the divergent continental margin eventually allowed massive progradation of terrigenous clastics in the Late Jurassic and Early Cretaceous at which time the Gulf of Mexico had completely formed. Throughout the Cretaceous, rates of basin subsidence and sediment accumulation declined and virtually ceased by the Early Tertiary.



1.2-1 Schematic cross sections showing evolutionary stages in formation of East Texas Basin and adjoining Gulf of Mexico (from Jackson and Seni, 1983).

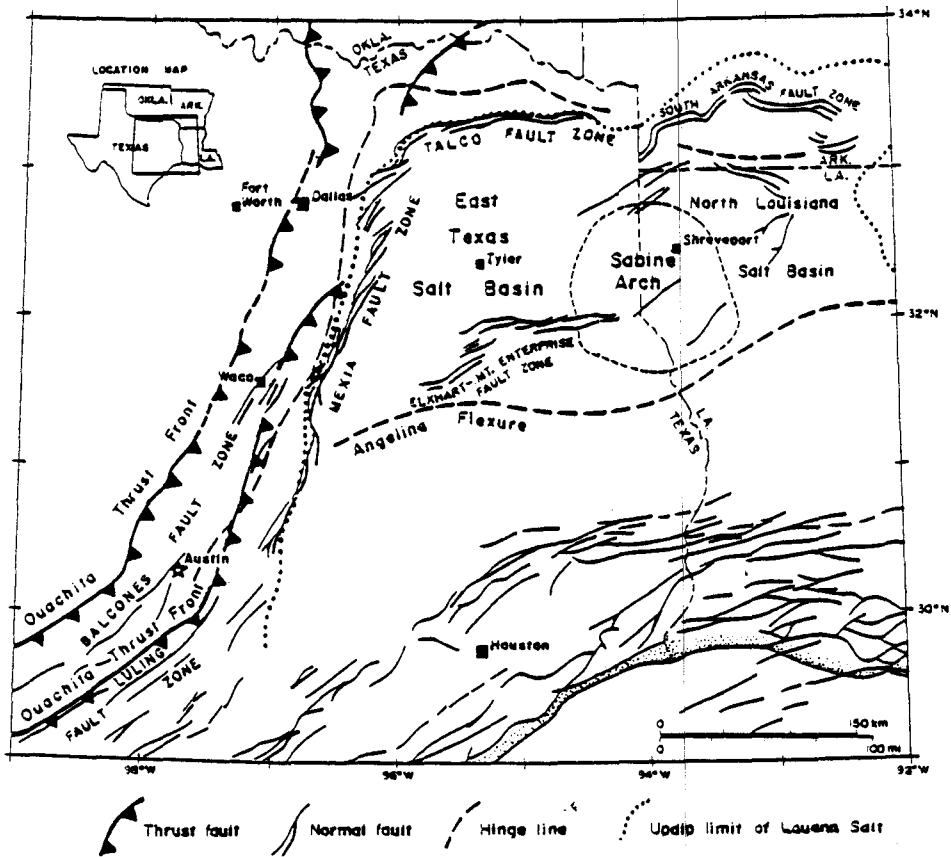
Deformation in the basin resulted from basin subsidence and gravitational flow of salt.

*The East Texas Basin has been distorted by second-order anticlines, including salt pillows, salt diapirs, and turtle structures, formed directly by gravity creep of salt. The basin is bounded by the Mexia-Talco fault zone in the north and west, by the Sabine Arch in the east, and the Angelina Flexure in the south.*

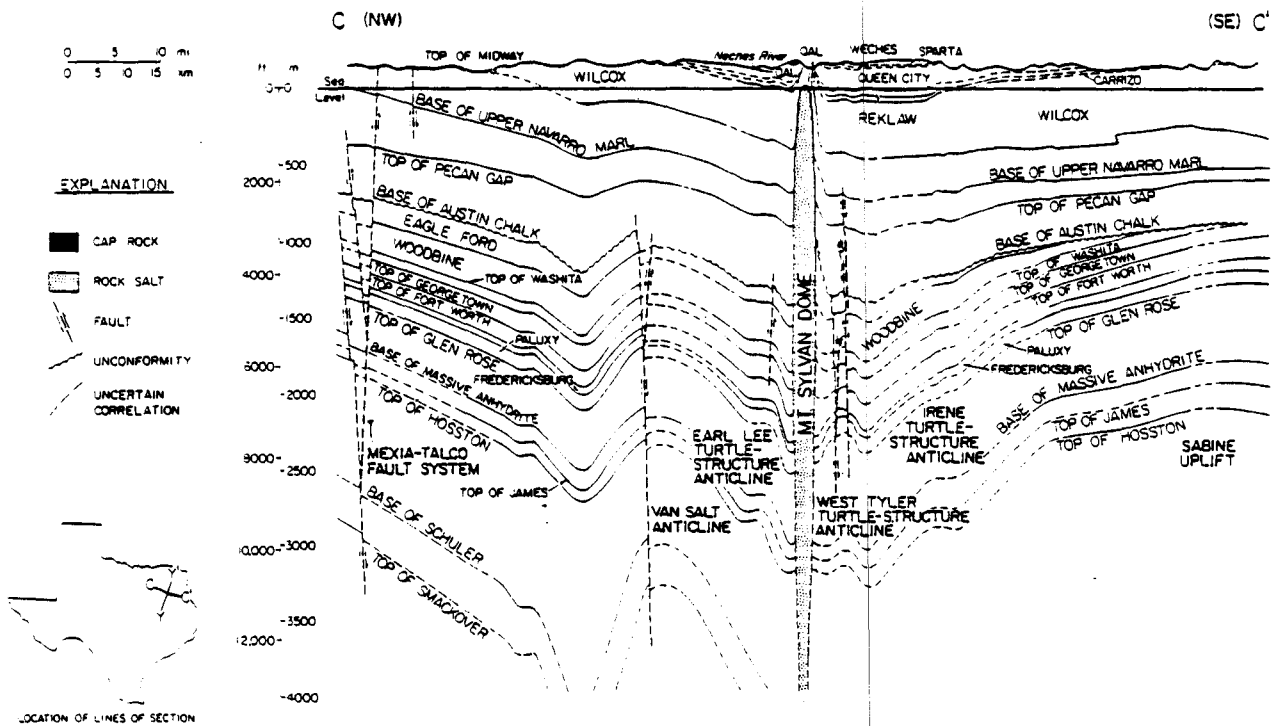
The western and northern margins of the East Texas Basin coincide with other geologic structures varying from Pennsylvanian to Tertiary age (fig. 1.3-1): (1) the Pennsylvanian Ouachita fold and thrust belt beneath Mesozoic cover; and (2) Triassic rift grabens and half grabens parallel to the Ouachita trends. This part of the basin margin is defined by the Mexia-Talco Fault Zone, a Jurassic to Eocene peripheral graben system that coincides with the updip limit of the Louann Salt.

The Sabine Arch forms the eastern margin of the basin (fig. 1.3-2). The southern margin of the basin is defined by the Angelina Flexure, a hinge line that is generally monoclinal at its ends and anticlinal in the middle. The Elkhart-Mount Enterprise fault zone extends from just north of the western end of the Angelina Flexure to the center of the Sabine Arch (fig. 1.3-1).

The gross structure of the East Texas Basin consists of regular basinward dips in the east, west, and north and a low rim in the south along the Angelina Flexure. Deformation within the basin appears to be related solely to large-scale, gravitationally induced creep of salt (halokinesis). The synclinal East Texas Basin has been distorted by three types of second-order, salt-related anticlines: (1) salt pillows--large, low-amplitude upwarps cored by salt; (2) salt diapirs--subvertical, cylindrical salt stocks that have pierced the adjacent strata; and (3) turtle structures--salt-free growth anticlines formed by subsidence of their flanks due to collapse of underlying salt pillows during salt diapirism.



1.3-1 Regional structural framework of the East Texas Basin (from Jackson, 1982).



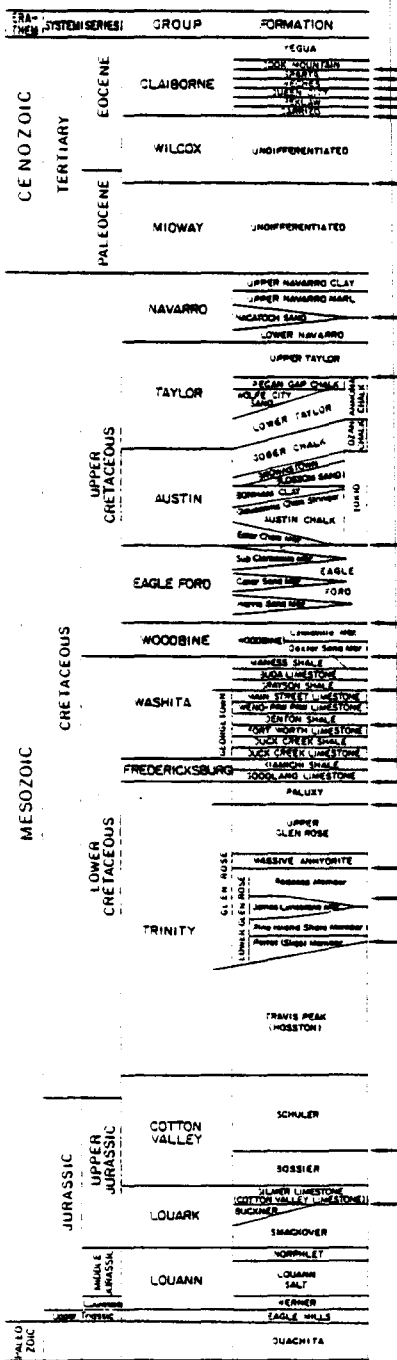
1.3-2 Structural cross section across East Texas Basin (from Wood and Guevara, 1981).

The basin contains up to 7,000 m of shallow marine and continental sediments overlying the Louann Salt.

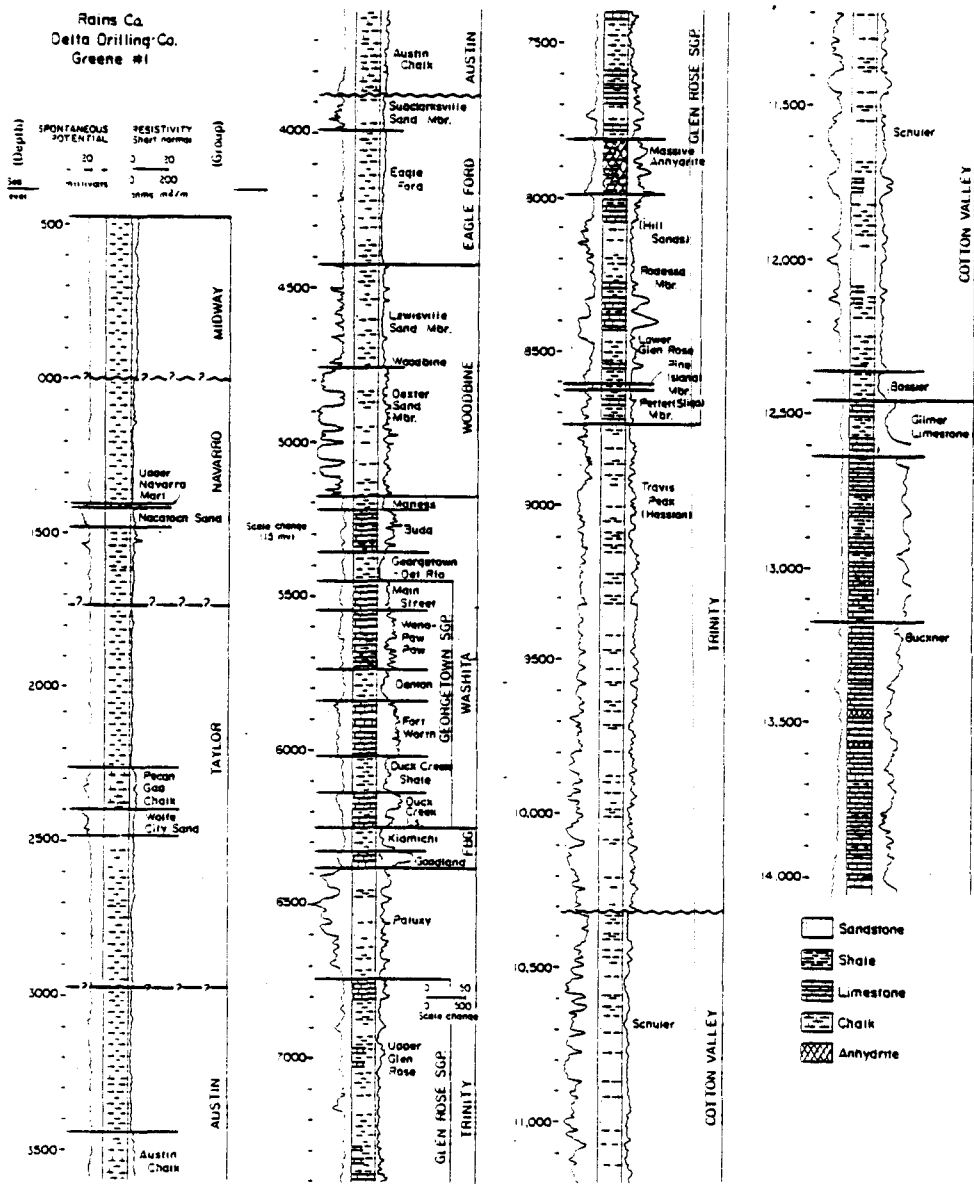
*The East Texas Basin contains 5,500-7,000 m (18,000-23,000 ft) of Mesozoic and Cenozoic evaporites, fluviodeltaic sandstones, shales, and shelf carbonates. Apart from certain Upper Jurassic shales, deep-water (>300 m; >1,000 ft) facies are absent.*

The basin fill in East Texas followed a typical path from purely continental (Late Triassic) through restricted marine (Early Jurassic) to open shallow marine (Late Jurassic). This was succeeded by episodes of terrigenous clastic and carbonate accumulation (Cretaceous), terminating with largely fluvial deposition (Tertiary) (figs. 1.4-1, 1.4-2, Appendix 1). During the Late Triassic rift stage, Eagle Mills red beds were deposited unconformably on eroded basement. Mid-Jurassic marine incursions along the rifts deposited the Werner Formation, consisting of red beds and evaporites, and the evaporitic Louann Salt.

Open shallow-marine deposits in the Upper Jurassic Smackover, Buckner, Gilmer, and Bossier Formations represent breakup accumulations on the subsiding continental shelf. Sand-rich Schuler-Hosston deltas prograded across the divergent continental shelf during the Late Jurassic and Early Cretaceous. A rapid marine transgression allowed the accumulation of Glen Rose carbonates, minor evaporites and shale. In the Mid- and Late Cretaceous, deltaic and fluvial sequences like the Woodbine and Eagle Ford repeatedly prograded and built out the continental shelf. By the Early Tertiary the basin was essentially full and fluvial systems prograded over the southern rim of the basin into the Gulf of Mexico. Net erosion characterized the last 40 Ma (million years) of geologic time.



1.4-1 Stratigraphic column, East Texas Basin. Arrows show contacts on figure 1.3-2 (after Wood and Guevara, 1981). See also Appendix 1.



1.4-2 Typical geophysical and lithic log, Rains County, Texas (after Wood and Guevara, 1981).

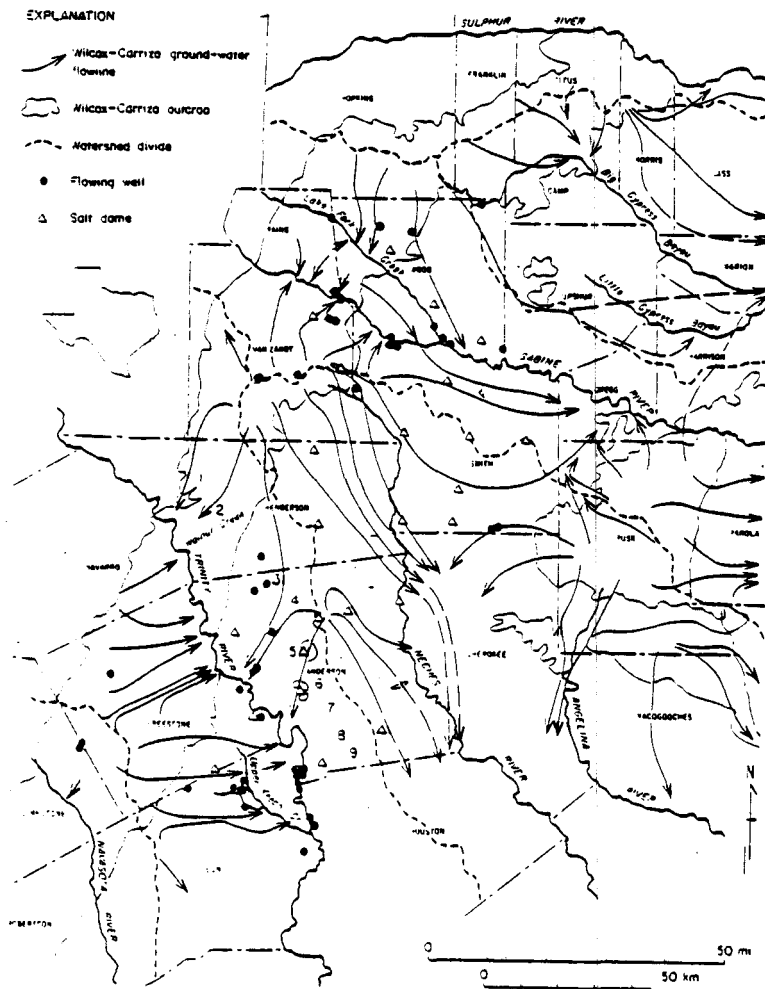
The Wilcox-Carrizo is the most important fresh-water aquifer system in the East Texas Basin.

*The Wilcox-Carrizo fresh-water aquifer system is separated from deeper saline aquifers by 600-1,200 m (2,000-4,000 ft) of aquitards and aquicludes. A salt-dome repository would lie at the depth of aquitards and aquicludes between the fresh Wilcox-Carrizo and saline Woodbine systems.*

Major fresh-water aquifers are (youngest to oldest) the Queen City Formation, Carrizo Formation, and Wilcox Group. The Queen City is a water-table (unconfined) system in which topographic effects create a series of local ground-water basins. Immediately below is the leaky Reklaw aquitard which causes artesian conditions in parts of the underlying Wilcox-Carrizo aquifer system. The Wilcox-Carrizo aquifer system includes (1) an artesian (confined) section overlain by the Reklaw aquitard, and (2) a water-table (unconfined) system where the Wilcox-Carrizo crops out along the west, north, and east margins of the basin. The fresh-brackish water interface (1,000 mg/L) generally lies from 90 to 150 m (300 to 500 ft) above the base of the Wilcox. The major saline aquifer is the Woodbine Group, separated from the fresh-water systems by (600-1,200 m) (2,000-4,000 ft) of aquitards and aquicludes. Deeper saline aquifers include the Paluxy Formation and Glen Rose Subgroup and Hosston Formation (section 4.6). A repository at a depth of 600-900 m (2,000-3,000 ft) would be situated at the depth of the 600-1,200 m (2,000-4,000 ft) interval between the Wilcox and Woodbine aquifers.

Regional ground-water flow patterns in the Wilcox-Carrizo system are shown in figure 1.5-1. Owing to a shallow water table (depth  $\approx$  12 m, 40 ft), flow in the large outcrop areas along the west and east margins of the basin correlates closely with topography. Ground-water flow lines in outcrops emanate from large recharge areas at watershed divides and either converge on streams or veer downdip. Topographic control on flow is also evident in the confined (artesian) section of the basin where flow lines tend to veer away from watershed

divides and generally converge toward the Trinity, Neches, and Sabine Rivers. This indicates that the Reklaw aquitard leaks in some areas, and that the Wilcox-Carrizo aquifer may discharge upward through it to streams. Both Oakwood and Keechi domes are located within the artesian section. Pressure-depth relations (section 3.1) indicate that upward leakage is confined to the area around the lower Trinity River.



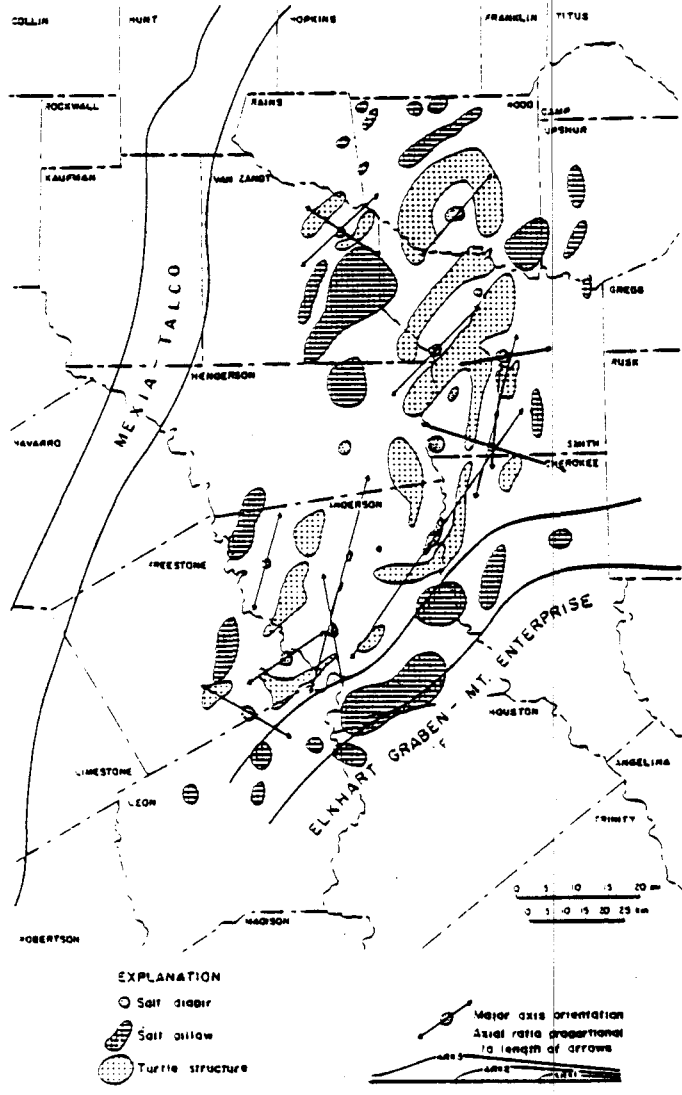
1.5-1 Ground-water flow lines for Wilcox-Carrizo system, East Texas Basin (from Fogg and Kreitler, 1981).

Pertinent data for all 15 shallow salt domes are provided in Appendix 2.

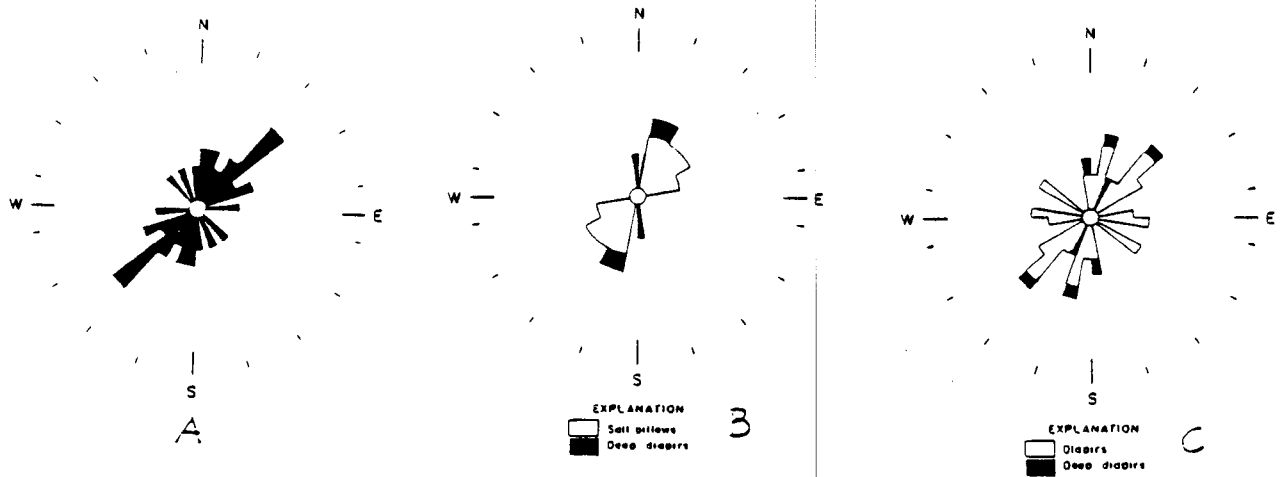
*A wide range of pertinent geologic and economic data for all 15 shallow salt domes is summarized. Salt stock morphology provides a guide to structural maturity.*

The primary purpose of this program was to examine the feasibility of isolating nuclear waste in East Texas salt domes. Appendix 2 presents pertinent geologic and economic data for all 15 shallow domes: location, residual-gravity expression, depths to cap rock and salt, orientation and lateral dimensions, shape, cap-rock thickness and composition, geometry of adjacent strata, faulting around dome, growth history, evidence for collapse, topographic expression, surface salines, resources, and uses of the domes. Graphics for each dome include structure contours of the salt stock on a topographic base, isometric block diagram of the salt stock, cross sections showing salt-stock shape along major and minor axes, and a cross section through the dome showing adjacent strata.

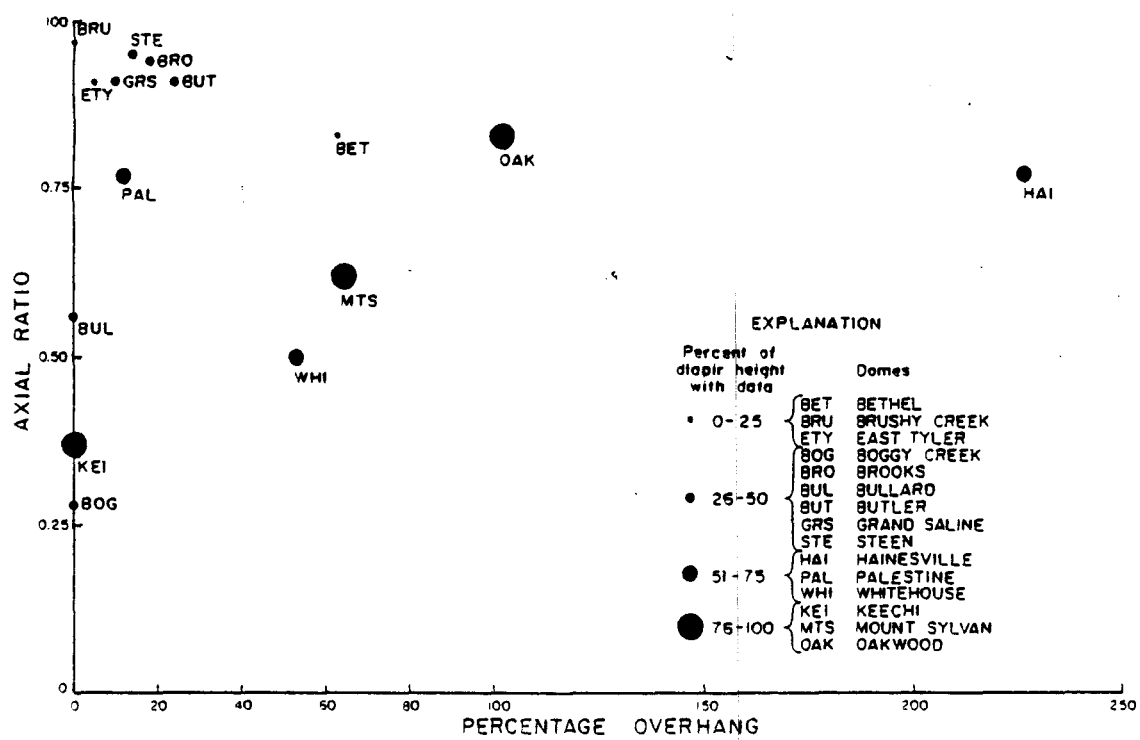
The orientation of precursor Jurassic-Lower Cretaceous salt ridges controlled the following aspects of the diapirs that evolved from them: major-axis orientation, diapir-family orientation, and overhang directions (figs. 1.6-1, 1.6-2). The following variables generally correlate with increasing structural maturity in salt stocks: decreasing axial ratio, increasing percentage overhang, increasing planar crest area. The best variables for indicating structural maturity in salt stocks are axial ratio and percentage overhang (fig. 1.6-3). But no one variable is totally reliable and this approach should be treated with caution.



1.6-1 Major-axis orientation and proportional axial ratios of salt diapirs.



1.6-2 Rose diagrams of major axis orientation of (A) turtle structures, (B) salt pillows, and (C) salt diapirs.



1.6-3 Graph of axial ratio versus percentage overhang for 15 East Texas diapirs.

## 2.0 REGIONAL GEOLOGIC STUDIES

### 2.1 PRESENT DISTRIBUTION AND GEOMETRY OF SALT STRUCTURES

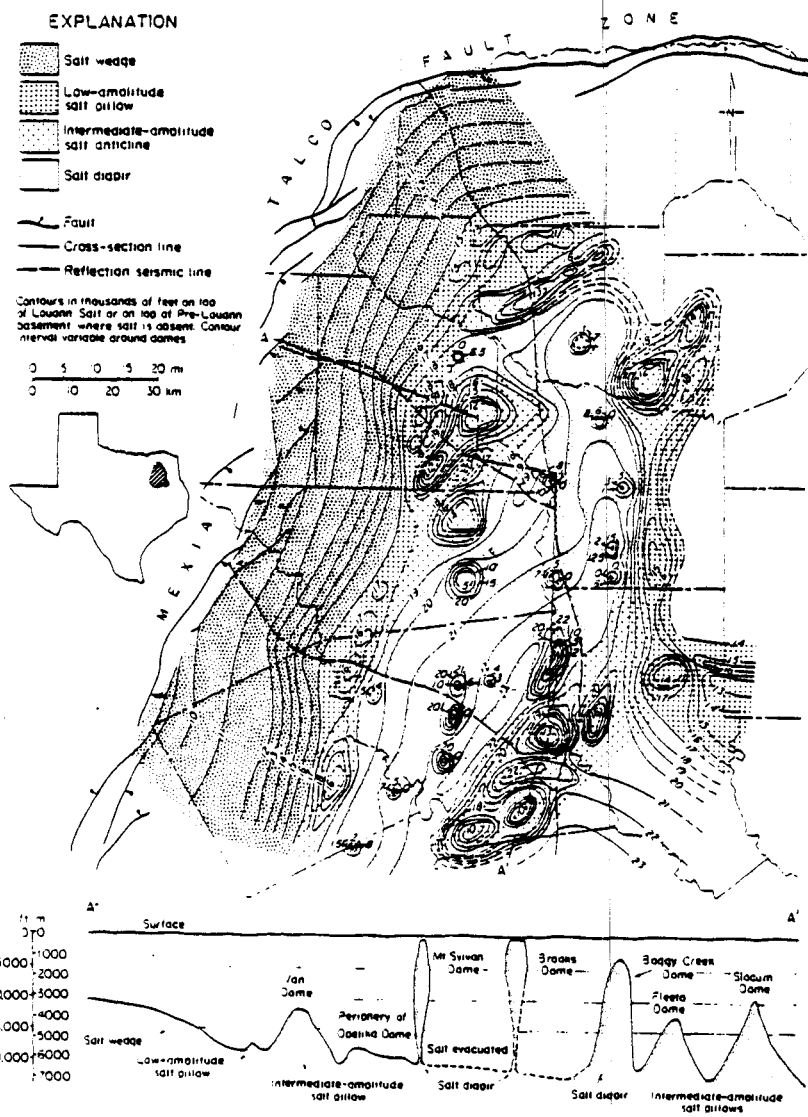
The East Texas Basin is divided into four provinces based on the shape of salt structures.

*A central province of salt diapirs is surrounded by three other provinces: intermediate-amplitude salt pillows (inner), low-amplitude salt pillows, and a salt wedge (outer). These provinces reflect increasing thicknesses of the original salt-source layer toward the basin center.*

The present distribution and morphology of salt structures in the East Texas Basin are portrayed in figure 2.1-1. Undeformed salt, 2.7-4.6 km (8,800-15,000 ft) deep and 225 km (135 mi) long, encircles an array of salt structures. In much of the basin center the Louann Salt is apparently absent. Salt structures (fig. 2.1-2) are classified into provinces.

- (1) An outermost salt wedge consists of apparently undeformed salt from 0 to 340-640 m (0 to 1,115-2,100 ft) thick. Its updip pinchout coincides with the Mexia-Talco Fault Zone.
- (2) Periclinal salt structures with low amplitude/wavelength ratios are called low-amplitude salt pillows. These pillows are flanked by synclines of Louann Salt. The Louann Salt was originally at least 550-625 m (1,800-2,050 ft) thick before deformation. Overburden thickness was about 500 m (1,640 ft) throughout provinces 1 through 3 at the start of salt movement.
- (3) Intermediate-amplitude salt pillows are commonly separated by synclines evacuated of salt and are larger than pillows of province 2. Original thickness of the salt source layer here is estimated as 550 - >760 m (1,800 - >2,500 ft).
- (4) The salt diapirs of the diapir province in the basin center are the most mature salt structures. They have all partially "pierced" their overburden and have risen to within 23 m (75 ft) (Steen Dome) to about 2,000 m (6,560 ft) (Girlie Caldwell Dome) of the present surface.





2.1-2 Map of salt provinces and salt-structure contours, East Texas Basin (from Seni and Jackson, 1983).

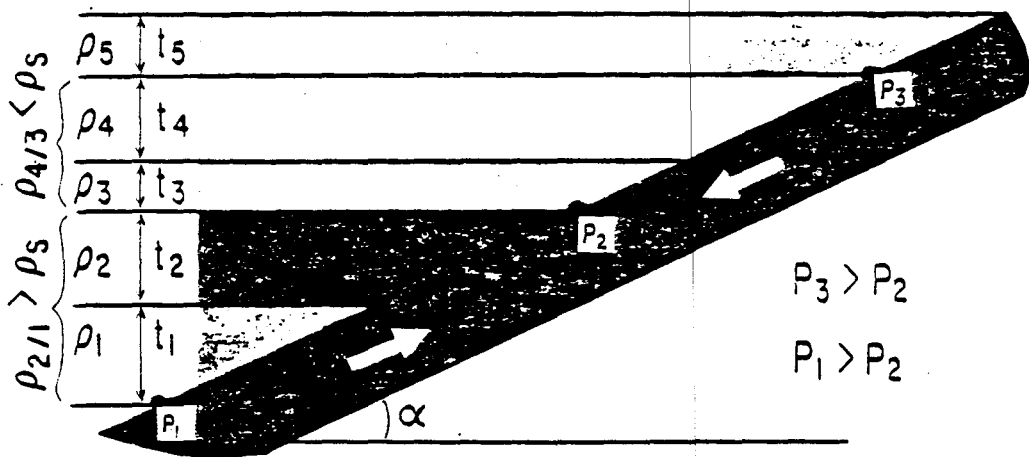
Five forces make salt flow; they operate from near surface to the deepest parts of the basin.

*Salt pillows formed by: (1) differential loading by delta fronts where salt was shallow; (2) passive rise of salt into gravity-glide anticlines; (3) buoyancy at depths <700 m (<2,300 ft), where salt was loaded by dense carbonates; (4) buoyancy at depths >700 m (>2,300 ft), where salt was loaded by compacted terrigenous clastics and most other sediments; and (5) thermal convection may operate in thick salt masses >1,000 m (>3,280 ft) deep.*

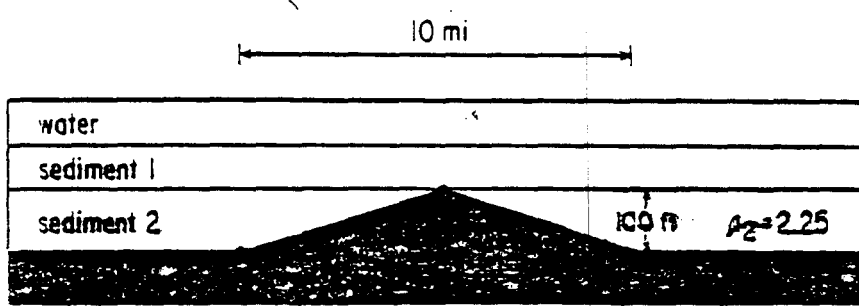
For salt to undergo steady-state creep (rheid flow) several conditions must be present although many combinations of factors permit this ductile behavior. Increasing water content, high temperatures, and low strain rates encourage ductile behavior. Differential stress (equivalent to hydraulic gradient in fluids) must exceed the elastic limit of the salt for plastic flow. Numerous geologic variations in thickness, density, viscosity, or temperature (such as folds, faults, facies changes) provide differential stresses and trigger salt flow.

In the case of a dipping salt layer of uniform thickness overlain by parallel layers of uniform thickness, salt will flow downhill, regardless of the overburden density. This causes updip thinning and downdip thickening of the salt; cover extends updip and shortens downdip by gravity-glide buckling. Where a dipping layer of uniformly thick salt is overlain by progressively thicker, denser cover downdip, updip salt flows downhill and downdip salt flows uphill converging to a point where the gravity head is balanced by the pressure head ( $P_2$  in fig. 2.2-1), possibly nucleating salt pillows.

East Texas salt pillows initially grew by buoyancy because a density inversion was induced by dense Upper Jurassic carbonates overlying less dense salt (fig. 2.2-2). Salt rise was probably augmented by folding of the carbonates as they glided into the basin over the salt detachment zone. Younger, larger pillows grew from salt ridges formed by intense differential loading at the leading edge of prograding sandy deltas (fig. 2.2-3). In at least one dome (Hainesville) diapirism was triggered by erosional breaching of a pillow. After deep burial had compacted terrigenous sediments, diapir buoyancy was driven by density inversion. Salt may be thermally convecting in the deepest parts of salt stocks.

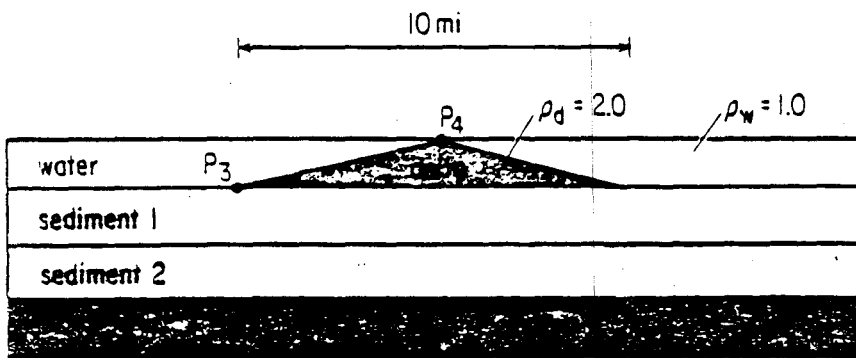


2.2-1 Salt-flow directions with dipping source layer and uniform, overlapping overburden (after Kehle, in press)



Fluid gradient =  $2 \times 10^{-4} g$  ( $\rho_2 = 2.25$ )  
 or  $2 \times 10^{-3} g$  ( $\rho_2 = 2.75$ )

2.2-2 Fluid gradient in salt pillow (black) below denser cover (after Kehle, in press).



Fluid gradient =  $4 \times 10^{-3} g$

2.2-3 Fluid gradient in tabular salt below P3 and P4, induced by differential loading by dense sand-rich delta (after Kehle, in press).

Salt flow first formed pillows in pre-Gilmer (Late Jurassic) time.

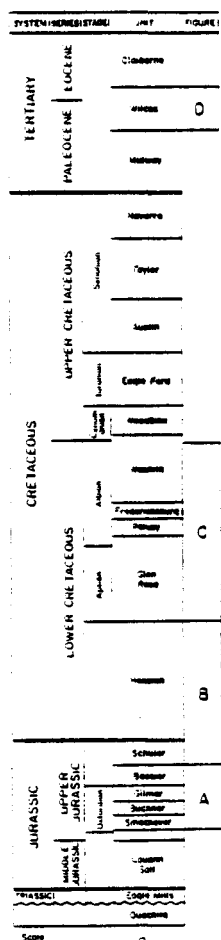
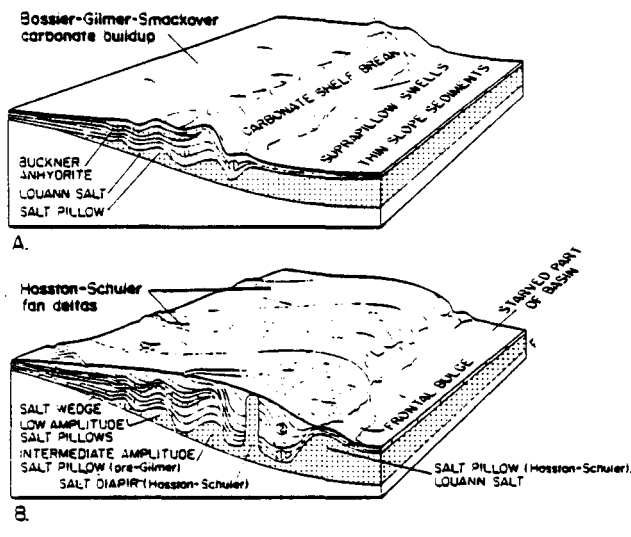
*Seismic data indicate that the oldest salt structures were low-amplitude pillows. The pillows grew beneath the Smackover-Gilmer carbonate platform. Subsequently Schuler-Hosston deltas prograded across the platform and formed more-distal salt anticlines.*

The earliest record of movement in the Louann Salt is in the overlying shallow-marine interval below the top of the Upper Jurassic Gilmer Limestone. This seismic unit thins over salt anticlines of province 2, and overlying units onlap these anticlines. Low-amplitude salt pillows therefore grew in pre-Gilmer time. Pillows grew along the western margin of the basin in the pillow provinces 2 and 3 (section 2.1). Oakwood Dome, and possibly Grand Saline Dome, on the western fringe of the diapiric province 4 also began to grow as pillows in pre-Gilmer time.

The overlying Upper Jurassic marine strata formed an aggrading, slowly prograding, carbonate wedge that loaded the salt fairly uniformly. The evaporitic Buckner Anhydrite pinches out seaward in the pillow provinces 2 and 3 (fig. 2.3-1A), possibly because topographic swells over pillows restricted circulation of seawater. The carbonate shelf break is inferred from abrupt thickening of overlying terrigenous clastics along this line. In Gilmer time the basin was still starved and the slope sediments were thin (fig. 2.3-1A). This accounts for the lack of contemporaneous halokinesis in the central basin, despite the great thickness of salt there.

In the Late Jurassic and Early Cretaceous the Schuler-Hosston clastics prograded rapidly across the carbonate platform as coalescing sand-rich deltas. Progradation slowed on crossing the shelf break, but the thick deltas continued to advance as a linear front into the previously starved basin (fig. 2.3-1B). Subsurface mapping delineates strike-parallel thicks in provinces 3 and 4, indicating the existence of parallel ridges and troughs. Loading of the pre-Schuler

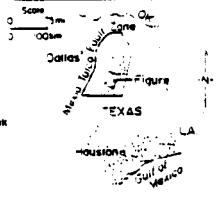
substrate by the advancing linear depocenters would have squeezed salt ahead as a frontal bulge to form salt anticlines (fig. 2.3-1B). Increase in sediment supply or progradational rate would have buried the frontal anticline, thereby initiating a parallel, but more distal, salt anticline. These anticlines were ridges of salt from which the salt diapirs grew by budding upward.



**EXPLANATION**

- Primary peripheral sink
- ⊙ Secondary peripheral sink
- ▭ Salt dome
- ▭ Fault Zone

Index map



2.3-1 Model of Late Jurassic-Early Cretaceous salt mobilization. (A) Block diagram of depositional facies during Bossier-Gilmer-Smackover time (after Jackson and Seni, 1983). (B) Block diagram of depositional facies during Hosston-Schuler time (after Jackson and Seni, 1983).

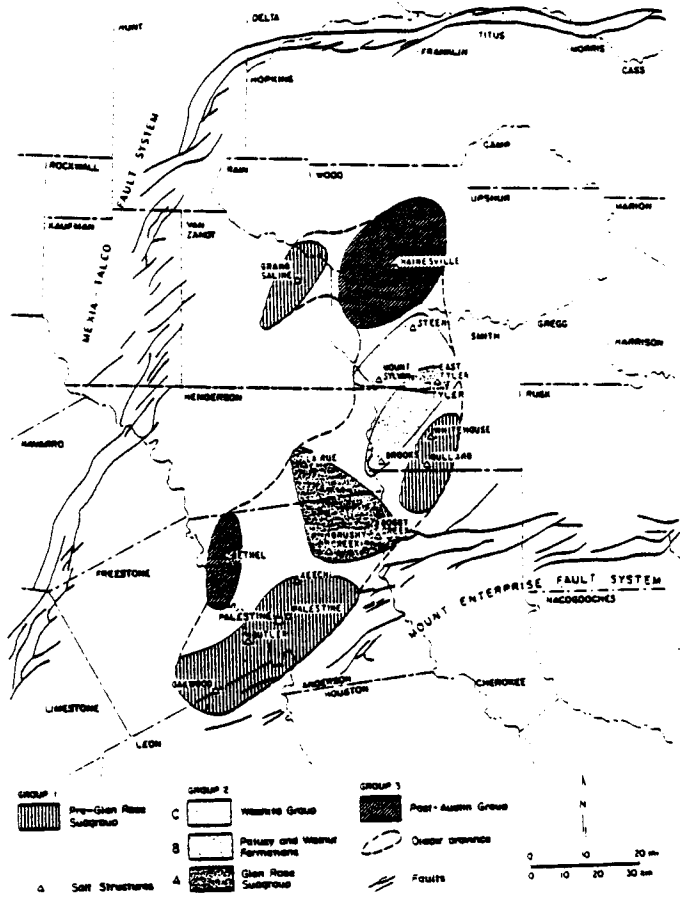
Three groups of diapirs can be differentiated on the basis of age and distribution.

*Group 1 diapirs grew along the margins of the diapir province in Late Jurassic-Early Cretaceous time. Group 2 diapirs grew along the basin axis in mid Cretaceous. Group 3 diapirs grew along the northwestern margins of the diapir province in Late Cretaceous.*

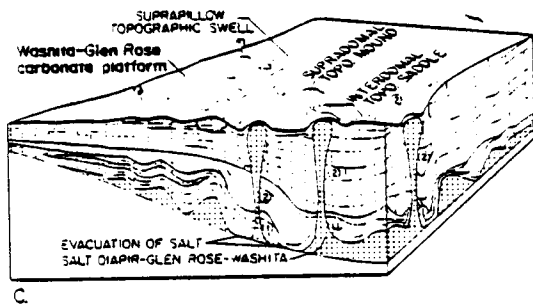
By Glen Rose time (mid-Early Cretaceous) salt diapirs were growing in three areas around the periphery of the diapir province, (fig. 2.4-1), starting at about 130 Ma. At least two areas coincide with known Schuler-Hosston clastic depocenters described above. These group 1 diapirs thus appear to have been localized by loading on the salt-cored anticlines in front of the prograding Schuler-Hosston deltas.

By mid-Cretaceous when maximum sedimentation was taking place in the basin center, a second generation of diapirs evolved, via a pillow stage, from the thick salt (fig. 2.4-2). Sites of group 2 diapir initiation migrated from the basin center northward along the basin axis.

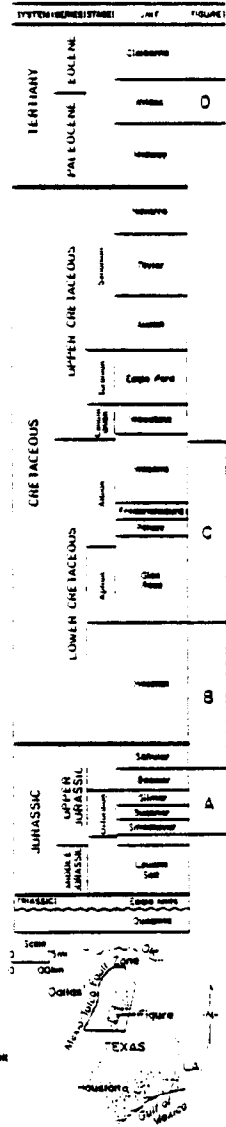
The group 3 diapirs on the northern and western margin of the diapir province had different origin. In the Late Cretaceous subsidence of the East Texas Basin had declined exponentially to relatively low rates. Tilting of the basin margins by loading of the basin center would have encouraged basin-edge erosion. Local unconformities exist over Hainesville Dome and 150-200 km<sup>3</sup> (37-49 mi<sup>3</sup>) of salt are calculated to be missing. The precursor salt pillow was breached by erosion; salt withdrawal through extrusion formed the largest secondary peripheral sink in the East Texas Basin. Erosional breaching of the faulted crests of salt pillows might also have initiated diapirism of the first and second generations of diapirs.



2.4-1 Map of diapir groups (from Seni and Jackson, 1983).



2.4-2 Block diagram of depositional facies during Washita-Glen Rose time (after Jackson and Seni, 1983).



## 2.5 EFFECTS OF DOME GROWTH ON FACIES IN ENCLOSING STRATA

Growing salt structures affected topography, thereby influencing depositional facies.

*Studies of paleoenvironments of the East Texas Basin and of modern environments elsewhere show that growing salt structures formed topographic mounds and depressions. The topographic influence on sedimentation patterns is characteristic for different dome-growth stages and sedimentary environments.*

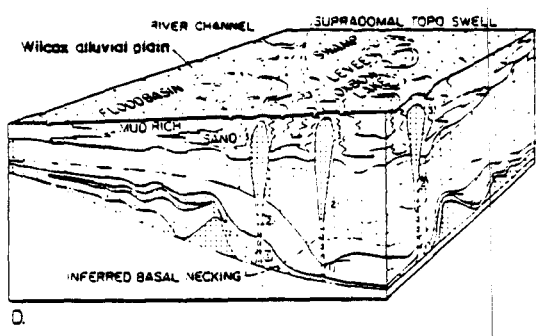
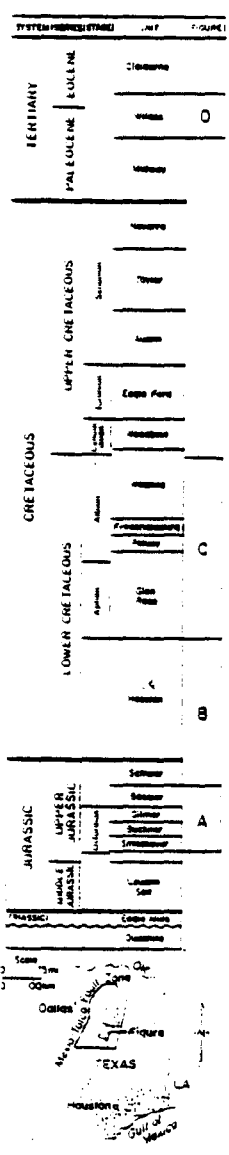
Syn depositional lithostratigraphic variations in response to salt flow highlight the interdependence between sediment accumulation and dome evolution (Appendix 3). These lithostratigraphic variations were primarily controlled by paleotopography. Salt uplift formed broad swells and small mounds over salt pillows and diapirs, respectively. Concurrently, topographic and structural basins formed over zones of salt withdrawal, leaving saddles with residual elevation between the basins (fig. 2.5-1). This salt-related topography influenced sedimentation patterns, which, in turn, enhanced continued salt flow because of increased loading by vertically stacked facies in the peripheral sink.

In the East Texas Basin, growth of salt pillows was responsible for uplift and thinning over broad areas, whereas diapir growth caused uplift and thinning over smaller areas (Appendix 3). During diapirism the effect of the topographic depression in the large peripheral sink is much greater than the effect of the diapir mound. Continued domal "piercement" commonly destroyed the uplifted strata by erosion or by shoving the uplifted units aside. In contrast, much of the broad, thinned zone over pillow crests was preserved after pillow collapse when diapirism buried the thinned region deep below secondary and tertiary peripheral sinks. The locations of sinks are related to evolutionary stage and regional dip. Axial traces of primary peripheral sinks tend to be updip of the salt pillow. In contrast, secondary and tertiary peripheral sinks commonly encircle the diapir. This change in position results from the transition from predominantly downdip lateral flow in the pillow stage to a combination of centripetal and upward flow in the diapir stage.

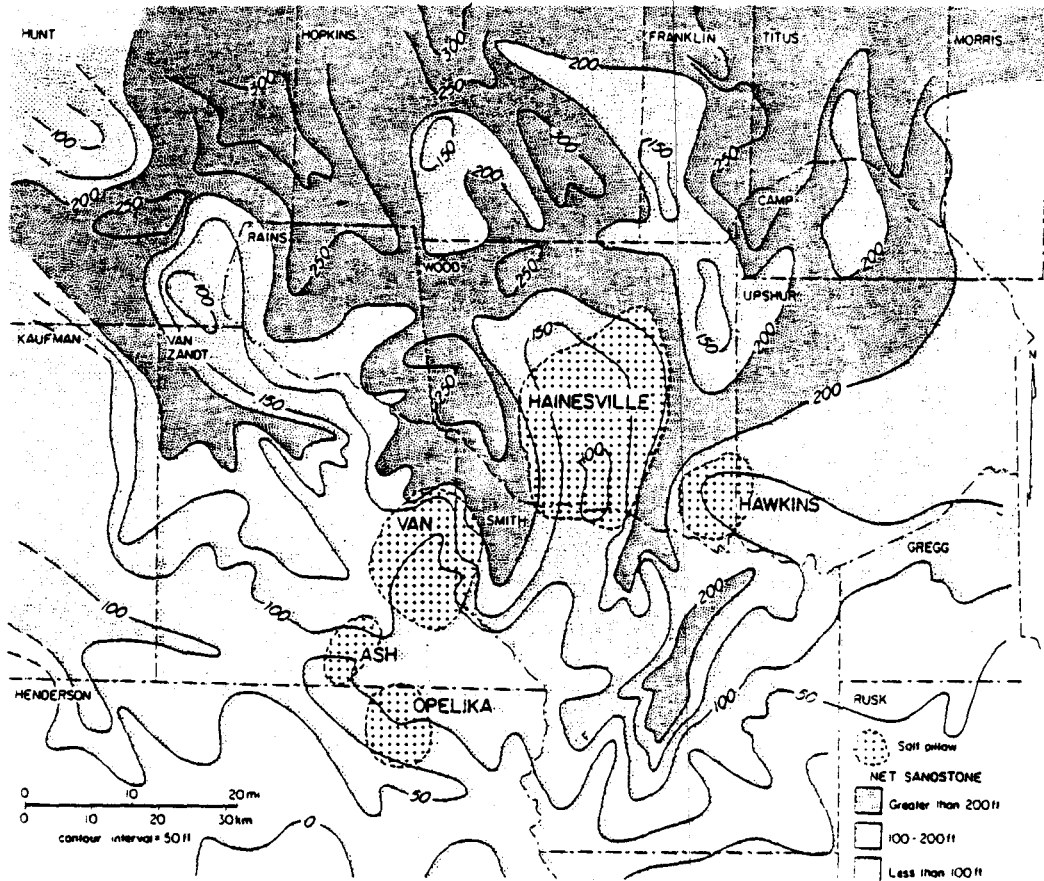
In fluvial and deltaic environments the sedimentary response to salt-influenced topography was quite different. Fluvial systems bypassed topographic mounds above domes and

pillows (fig. 2.5-2). Uplifted areas, therefore, tend to be thin and sand poor (fig. 2.5-3). Subsidence of the peripheral sinks promoted aggradation of sand-rich fluvial-channel facies.

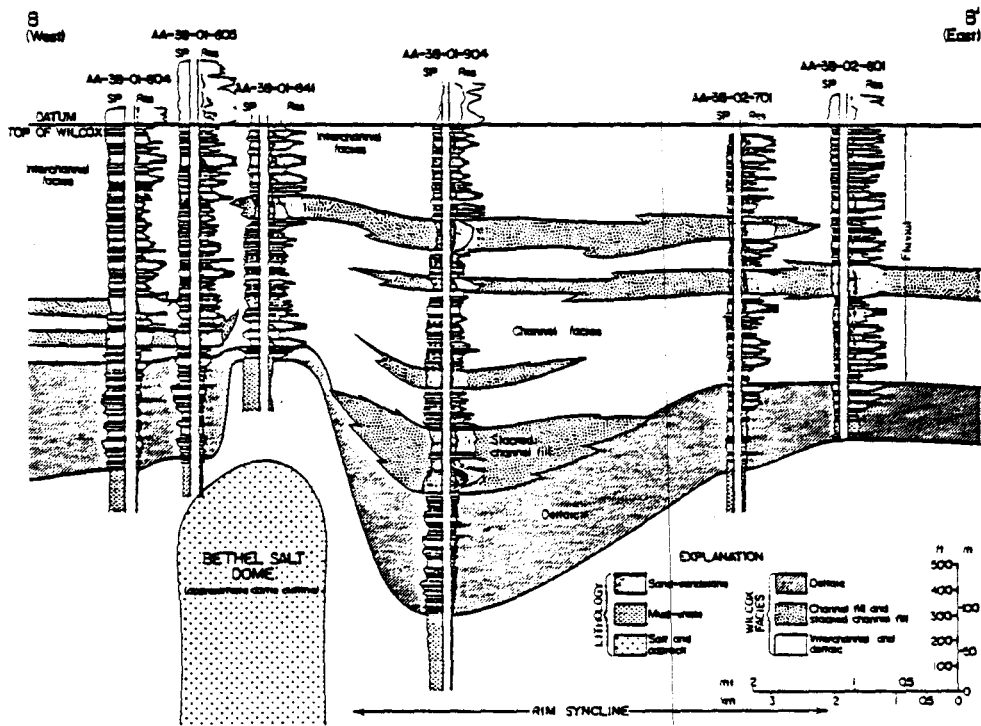
In terrigenous shelf and shallow-marine carbonate environments sand can accumulate by winnowing on bathymetric shoals, so that salt domes with sufficient surface expression, such as those in the modern Persian Gulf, are overlain by sand-rich sediments. Lower Cretaceous reefs have been found in East Texas on saddles with residual elevation between salt-withdrawal basins (fig. 2.5-1). Dome-crest reefs have been recognized in Oligocene sediments of the Texas Gulf Coast, in Holocene strata in the northwestern Gulf of Mexico, and in the modern Persian Gulf. This type of reef has not been recognized in East Texas.



2.5-1 Block diagram of depositional facies during Wilcox time (after Jackson and Seni, 1983).



2.5-2 Net sandstone, Paluxy Formation showing decrease in sandstone over crests of pillows (from Seni and Jackson, 1983).



2.5-3 Cross section through Wilcox Group around Bethel Dome (from Seni and Jackson, 1983).

## 2.6 THE EFFECTS OF DOME GROWTH ON STRUCTURE OF ENCLOSING STRATA

Two types of structural inversion affect the structure of strata during diapirism.

*Strata immediately adjacent to diapirs invert from anticlinal to synclinal, whereas interdomal strata invert from synclinal to anticlinal creating a turtle-structure anticline.*

During pillow stage of growth strata over the pillow crest and flanks are anticlinal while strata in the primary peripheral sink over the area of salt withdrawal are synclinal (fig. 2.6-1). Sediments over the pillow crests undergo extension, commonly with antithetic faults and central grabens, drape compaction, and differential compaction. But most thinning of strata above pillows is syndepositional and caused by salt flow.

During the subsequent diapir stage the flanks of the pillow deflate because of salt withdrawal into the central growing diapir. Pillow deflation results in collapse of the originally anticlinal strata forming a synclinal secondary peripheral sink (e.g. Bethel and Hainesville Domes, fig. 2.6-1). The core of the primary peripheral sink remains unaffected by collapse. But the flanks of the sink, which overlie the pillow flanks, collapse during diapirism, thereby forming a turtle-structure anticline. Thickening in secondary peripheral sinks is mainly due to syndepositional salt flow rather than post-depositional distortion by folding. Diapiric piercement is commonly assisted by erosional breaching of a salt pillow, as evidenced by angular unconformities centered around diapirs like Hainesville Dome.

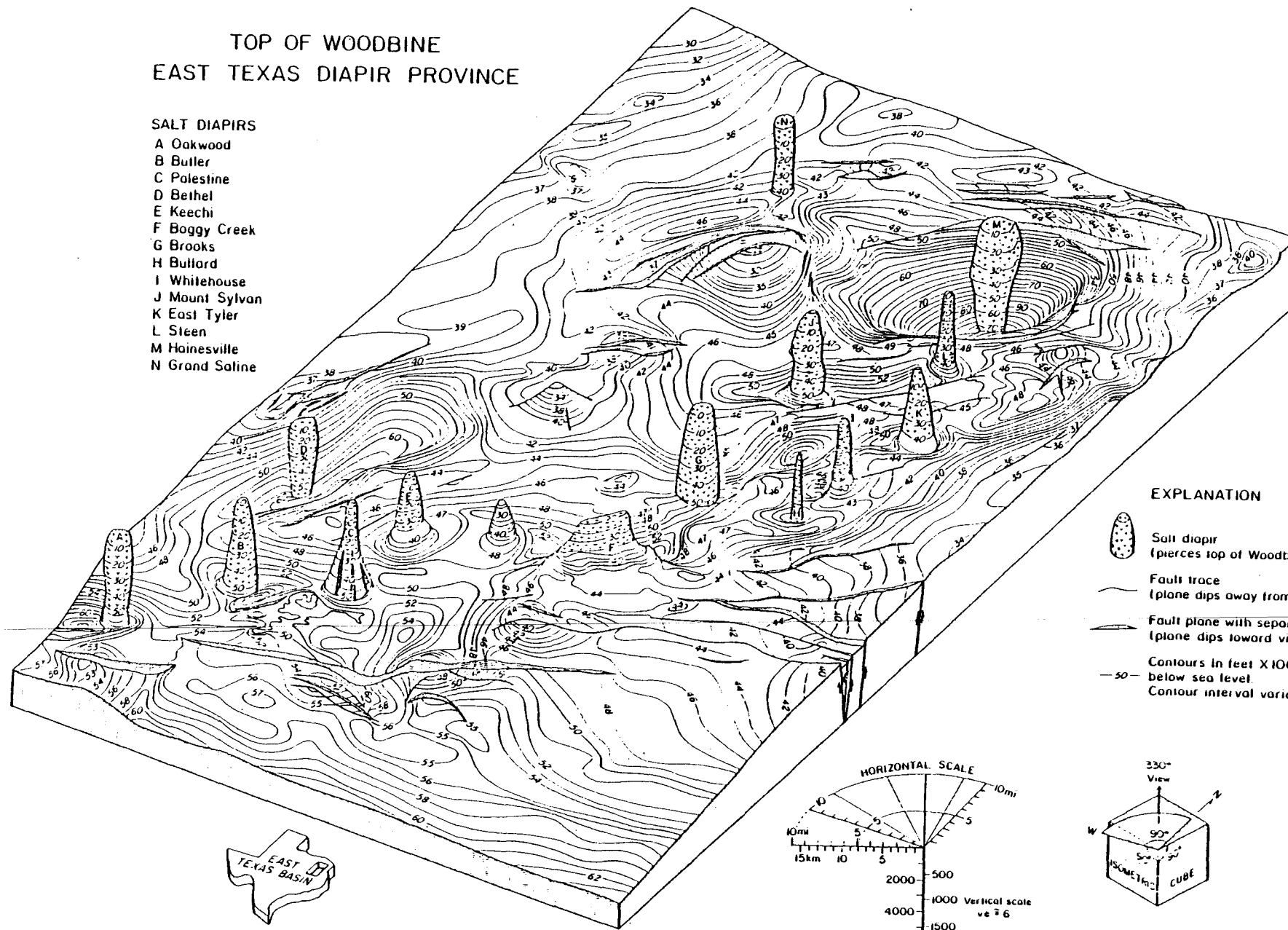
Salt stocks with upward converging sides (e.g., Palestine and Boggy Creek Domes) drag up adjacent strata. In contrast, stocks with upward diverging or vertical sides (e.g., Bethel and Grand Saline Domes) have negligible effect on adjacent strata; this suggests that friction along the salt contact has only a local effect. All salt stocks examined are bounded by ring faults along their sides. Antithetic faults are more abundant than homothetic faults over diapirs. Thus the effects of lateral extension and collapse predominate over uplift.

TOP OF WOODBINE  
EAST TEXAS DIAPIR PROVINCE

SALT DIAPIRS

- A Oakwood
- B Butler
- C Palestine
- D Bethel
- E Keechi
- F Boggy Creek
- G Brooks
- H Bullard
- I Whitehouse
- J Mount Sylvan
- K East Tyler
- L Steen
- M Hainesville
- N Grand Saline

47



2.6-1 Isometric block diagram of salt diapirs and structure contours on top of Woodbine Group.

Geomorphic evidence does not preclude Quaternary uplift over Oakwood Dome, but its southern flank may have subsided.

*Anomalous geomorphic features over Oakwood Dome include a drainage system that is less mature and erosional slopes that are steeper than over Keechi and Palestine Domes. These features are equivocal and do not preclude Quaternary uplift. Scattered depositional terraces show no evidence of dome-related uplift. On the contrary, the southern part of Oakwood Dome may have subsided in Quaternary time.*

Fracturing induced by dome growth is apparently recorded in the pattern of lineaments above salt domes. Shallower domes have lineament distributions with lower degrees of preferred orientation than do deeper domes (fig. 2.7-1). Southern domes (Bethel, Boggy Creek, Butler, Keechi, Oakwood, and Palestine) tend to have lower degrees of lineament preferred orientation than do northern domes of the same depth. The lower preferred orientations are ascribed to a higher proportion of radial and concentric fractures induced by dome growth. Southern domes have a significantly higher lineament density than do the northern domes.

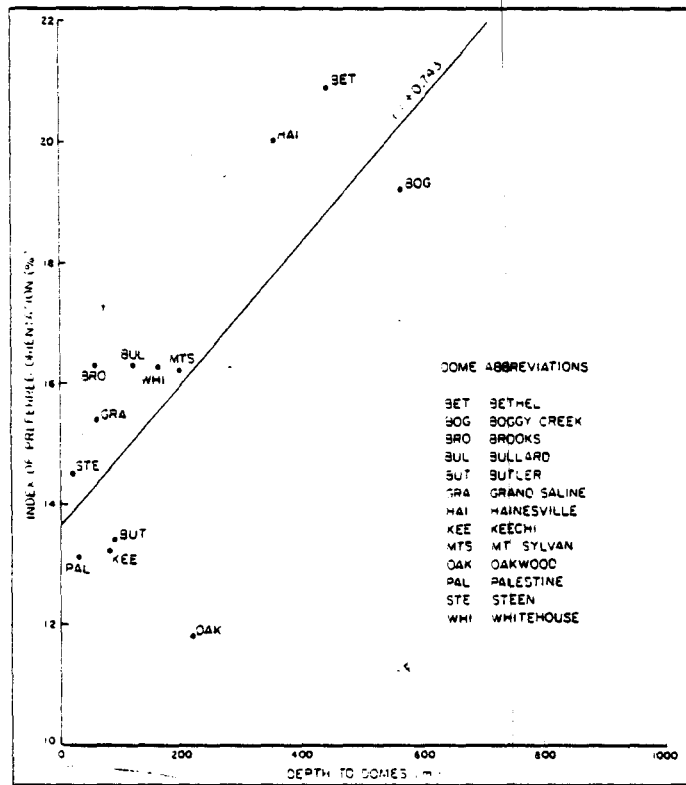
Channels over the central part of Oakwood Dome are incised up to 4 m, unlike the dome flanks. Some creek channels have migrated away from the dome, leaving cutoff channels possibly caused by dome uplift. Link-length-distribution analysis of East Texas drainage networks over various salt domes indicates that Oakwood Dome has a less mature drainage system than do other domes.

Morphologic maps of Palestine, Keechi, and Oakwood Domes distinguish between slopes formed by erosional processes and slopes formed by depositional processes. Hillside erosional slopes at Oakwood are considerably steeper than at the other two domes. Erosional slopes above Oakwood and Palestine Domes are steeper than slopes near each dome. All three domes display depositional slopes, commonly in a central depression. Above Palestine Dome a man-

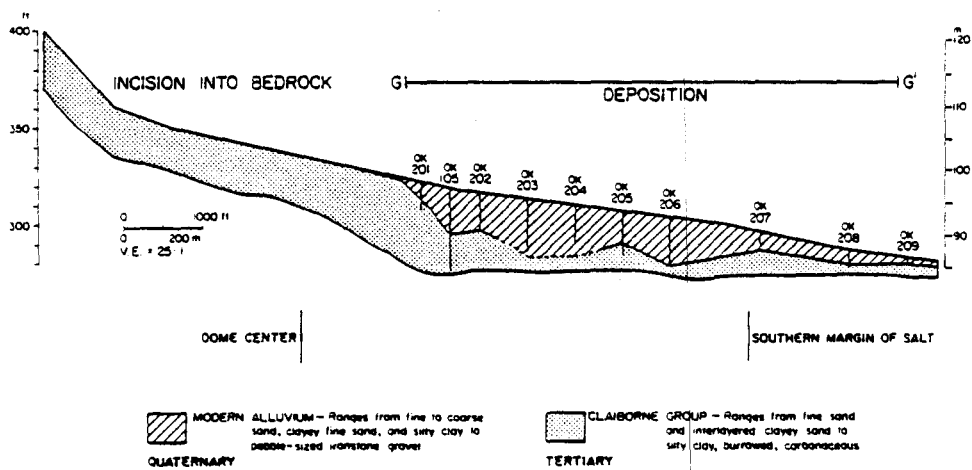
made lake is surrounded by a ring of hills. In the south-central part of Oakwood Dome, a relatively large floodplain has filled with alluvium twice as thick as in adjacent downstream areas (fig. 2.7-2). Topographic lows suggest subsidence over domes, possibly due to dissolution of cap rock or salt by ground water.

Palestine, Keechi, and Oakwood Domes are located in the Trinity River drainage basin where four Quaternary terrace levels have been identified. The regional gradient of these terraces shows no significant domal uplift. On a local scale outcrop and borehole data from Quaternary terrace deposits at Oakwood and Palestine Domes show no indication of warping due to dome uplift. However these deposits are too patchy to be sure.

Average denudation rates computed from suspended-sediment-load data (Trinity, Neches, and Sabine River Basins) and sedimentation resurvey data from four reservoirs are  $0.9 \text{ m}/10^4 \text{ yr}$  ( $3 \text{ ft}/10^4 \text{ yr}$ ) and  $1.7 \text{ m}/10^4 \text{ yr}$  ( $5.6 \text{ ft}/10^4 \text{ yr}$ ), respectively. These rates are slightly higher than the estimated maximum rates of dome uplift (see section 2.8).



2.7-1 Significant correlation between depth to dome and index of preferred orientation (from Dix and Jackson, 1981).



2.7-2 Cross section of Quaternary floodplain deposits above Oakwood Dome (from Collins and others, 1981).

Rates of dome growth declined exponentially with time.

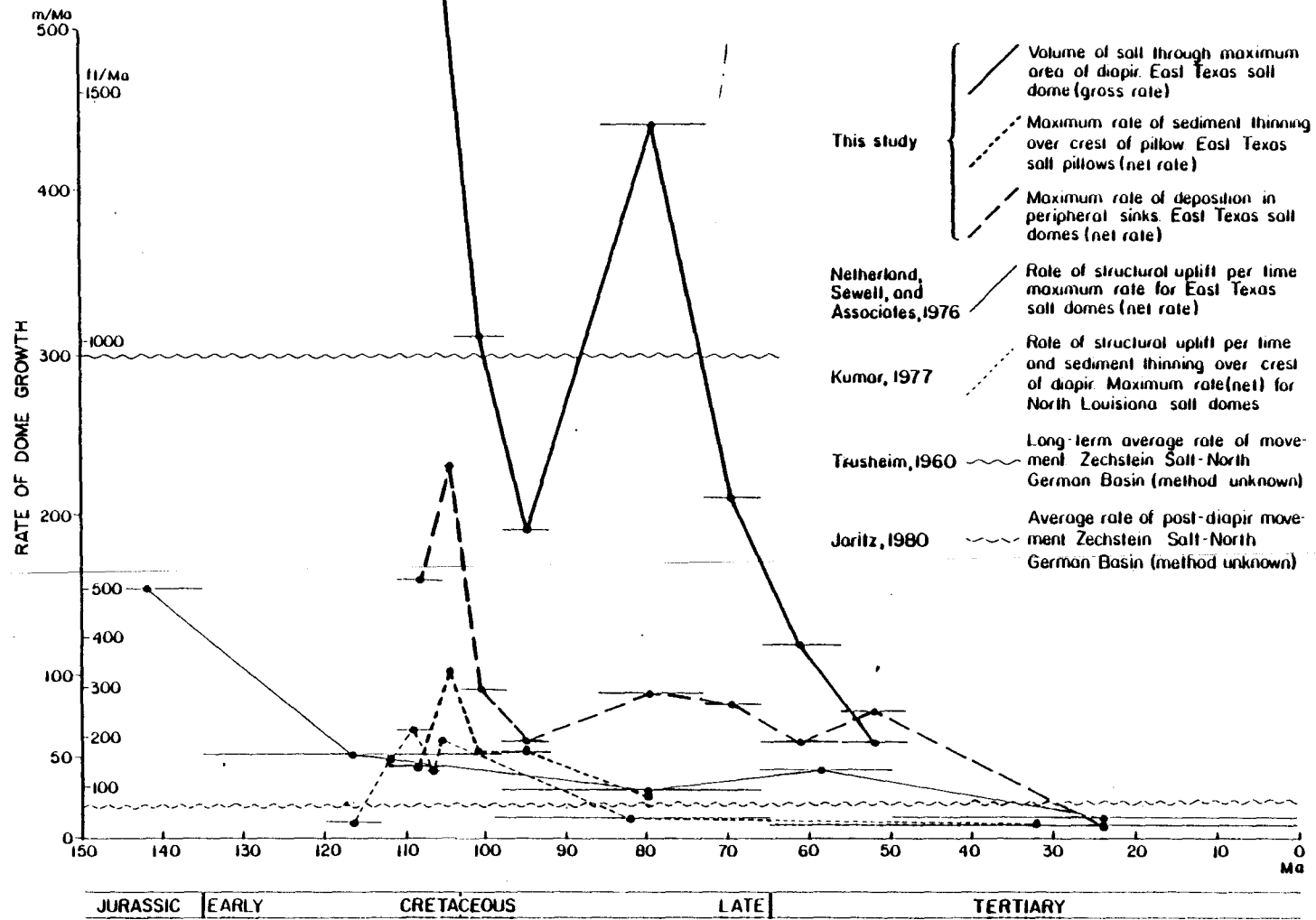
*Three different techniques of calculating dome-growth rates show that growth declined exponentially from 112 Ma to 48 Ma. Extrapolation indicates that none of the East Texas salt domes are likely to rise more than 0.6 m (2 ft) in the next  $10^4$  yr.*

Syn depositional thickness variations in surrounding strata allow measurement of the volumes and rates of salt flow.

The concept of gross rate of growth versus net rate of growth is of fundamental importance (Appendix 4). Gross rates are a function of the volume of salt evacuated from the withdrawal basin and mobilized up the diapir. Net rates are a function of this process, and all other processes that affect diapir height and growth rate, such as salt dissolution, extrusion, and lateral intrusion. Thus gross rates of growth approximate the true rate of salt flow regardless of the independent motion of the diapir crest. On the other hand, net rates of growth approximate the actual movement of the diapir crest.

Average growth rates were calculated for 16 salt domes for successive periods of 1-17 Ma and combined to yield curves of long-term growth over 64 Ma (fig. 2.8-1). Maximum gross rates of dome growth (400-530 m/Ma; 1,310-1,740 ft/Ma) coincided with maximum regional rates of deposition in the Early Cretaceous from 112 to 104 Ma. Rapid gross rates of dome growth (180-460 m/Ma gross; 590-1,510 ft/Ma) recurred along the northern and western margins of the diapir province in the Late Cretaceous from 86 to 56 Ma with growth of Hainesville and Bethel Domes.

All three growth-rate curves show the same trend of exponential decline with time, regardless of whether they are based on compacted or "decompacted" sediment thicknesses. Extrapolation of the most recent well-documented episode of dome growth 65 Ma ago indicates that none of the East Texas domes are likely to rise by more than 0.6 m (2 ft) in the next  $10^4$  yr.



2.8-1 Comparison of long-term rates of dome growth (from Seni and Jackson, 1983).

All regional fault systems appear to be related to slow gravitational creep of salt.

*All the regional faults studied (1) are normal, (2) moved steadily during the Mesozoic and Early Tertiary, and (3) appear to be related to salt mobilization.*

All the regional fault systems were examined in terms of their distribution, geometry, displacement history, and possible origins. Their relation to salt structures is shown in figure 2.9-1.

The Mexia-Talco fault zone is a graben between salt-free strata and strata underlain by mobile salt that allowed overburden creep into the East Texas Basin. The Elkhart Graben and the central-basin faults formed by crestal stretching and collapse of strata above salt pillows and turtle structures (fig. 2.9-2). At least one western fault in the Mount Enterprise fault zone is a long-active listric-normal growth fault, downthrown to the north and based in the Louann Salt. Once initiated, its growth would have been perpetuated by loading induced by sediments trapped on the downthrown side and by the tensile stress regime near the basin margins.

Faulting ceased before the Quaternary except for a westward extension of the north flank of the Elkhart Graben and small faults south of the Mount Enterprise fault zone.



At least 8 probable earthquakes were recorded near the Mount Enterprise fault zone in 1981 and 1982.

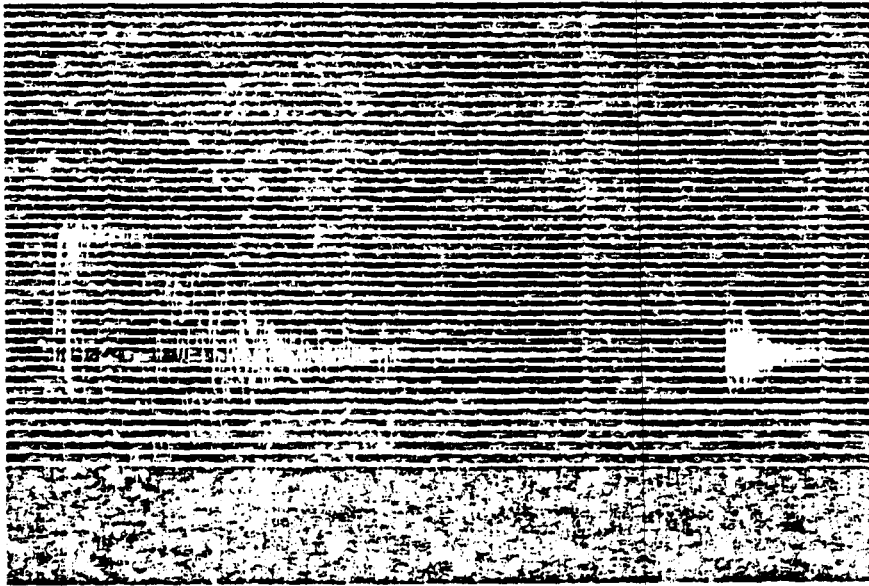
*At least 8 probable earthquakes were recorded by microseismic stations in the Mount Enterprise fault zone, East Texas, during June 1981 to August 1982. The Jacksonville main shock on 11/6/81 registered 3.0-3.2  $m_bLg$ , Richter magnitude 3.5-4.0, Mercalli intensity III-V, and was felt over 500 km<sup>2</sup>. It is ascribed to normal faulting in the Mount Enterprise fault zone.*

The East Texas Basin is generally considered an area of low seismic risk. However, historic evidence of apparent earthquakes in 1891 (near Rusk), in 1932 (near Wortham), in 1957 (near Mount Enterprise), and in 1964 (near Hemphill) suggested that seismic monitoring should be carried out if the area was a potential site for nuclear-waste storage. The first stage of monitoring consisted of a single-channel, smoked-paper seismograph from 2/80 to 5/81. The second stage comprised a three-station, telemetered network from 6/81 to 8/82.

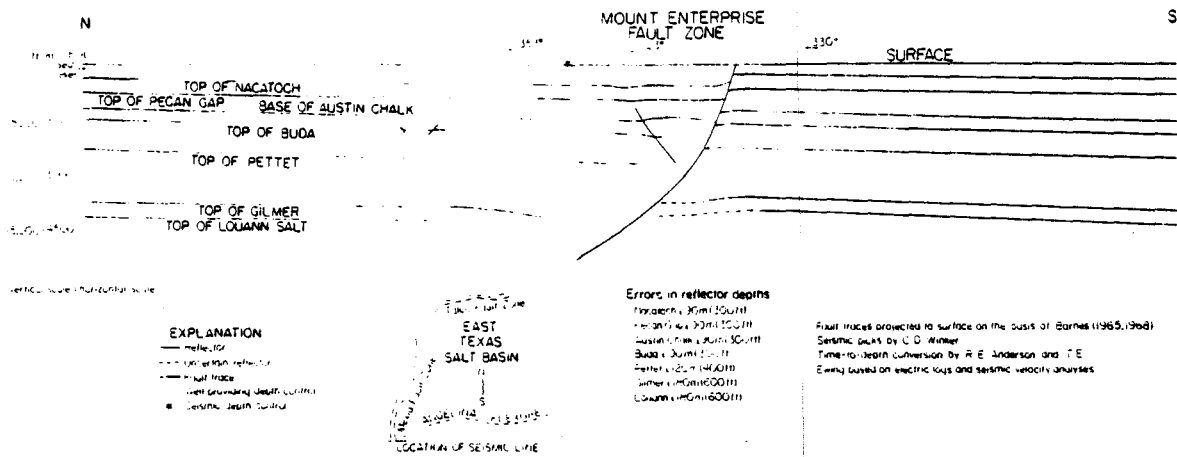
The following four earthquakes were recorded and located: (1) 3.0  $m_bLg$  (approximates Richter magnitude [ $m_b$ ] by using high-mode Love waves [ $Lg$ ]), Center, Texas, 6/9/81 U.T.C. (Universal Corrected Time); (2) 3.2  $m_bLg$ , Jacksonville, Texas, 11/6/81 U.T.C.; (3) 1.7  $M_{coda}$  ( $\approx m_bLg$ ) aftershock, Jacksonville, Texas, 11/9/81 U.T.C.; and (4) 1.8  $M_{coda}$ , Mount Enterprise, Texas, 12/11/81 U.T.C. The following four earthquakes were recorded but not precisely located: (1) 2.1  $M_{coda}$ , probable aftershock of Jacksonville, Texas, 11/6/81 U.T.C.; (2) 1.6  $M_{coda}$ , possible aftershock of Jacksonville, Texas, 1/5/82 U.T.C.; (3) 2.3  $M_{coda}$  and 1.9  $M_{coda}$ , 5/13/82 U.T.C.

The Jacksonville main shock was felt over 500 km<sup>2</sup> (200 mi<sup>2</sup>) and the aftershock over 75 km<sup>2</sup> (30 mi) (fig. 2.10-1). This event is ascribed to normal faulting along the Mount Enterprise fault zone, which surrounds the epicenter. The Mount Enterprise Fault Zone is the

least understood zone in East Texas because of poor subsurface information. Nevertheless, at least one seismic profile (fig. 2.10-2) indicates that, like the Mexia-Talco Fault Zone, it is based in the Louann Salt, which suggests that the Mount Enterprise fault zone is also related to salt creep, indicating a low seismic potential. A releveling profile across the Mount Enterprise fault zone indicates approximately 14 cm displacement in the past 30 yr.



2.10-1 Jacksonville main shock (left), magnitude 3.2, and aftershock (right) from Mt. Enterprise fault zone (from Jackson and others, 1982).



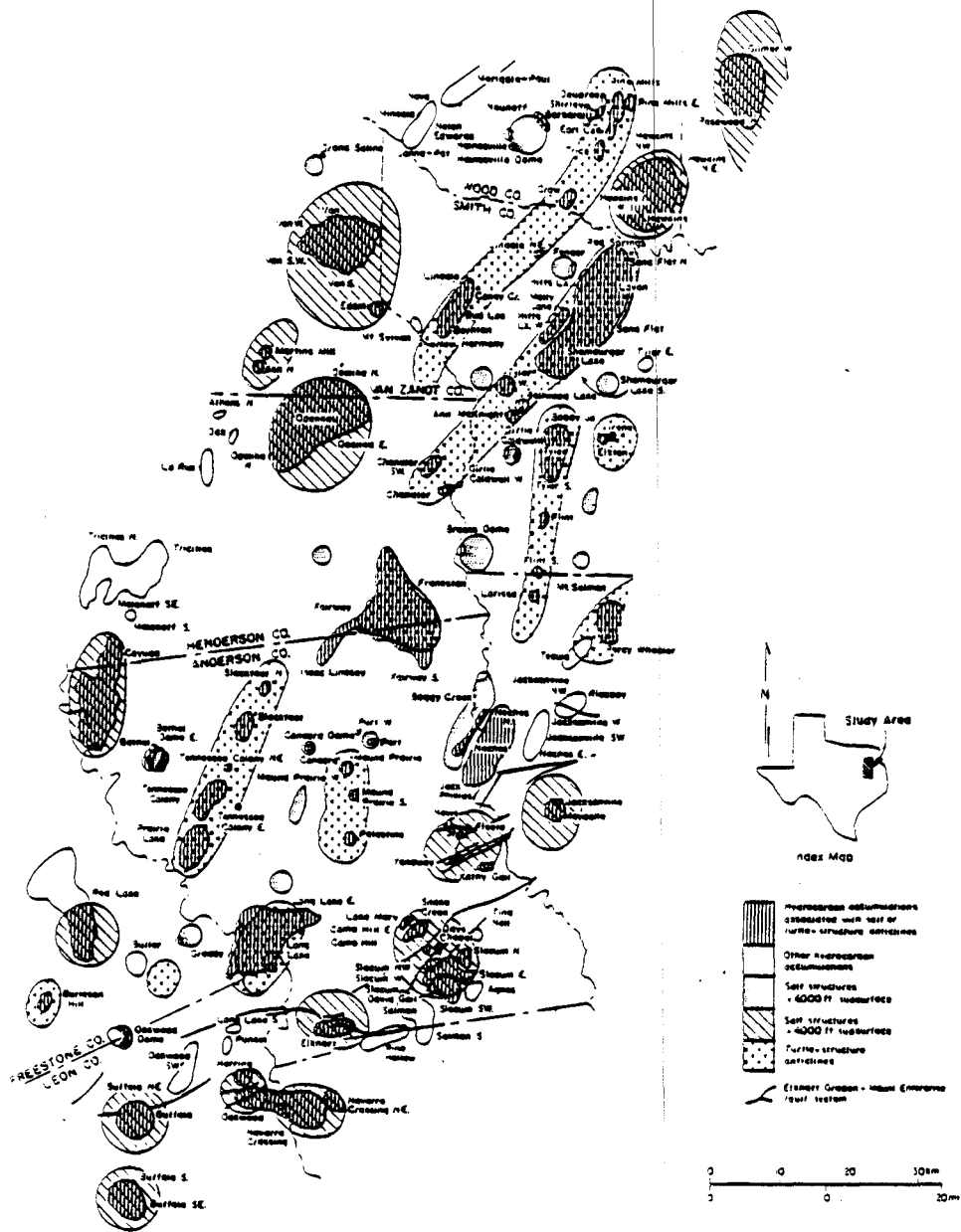
2.10-2 Time-to-depth-converted seismic section across Mt. Enterprise listric-normal growth fault (from Jackson, 1982).

Relatively small petroleum reserves have been discovered around East Texas diapirs.

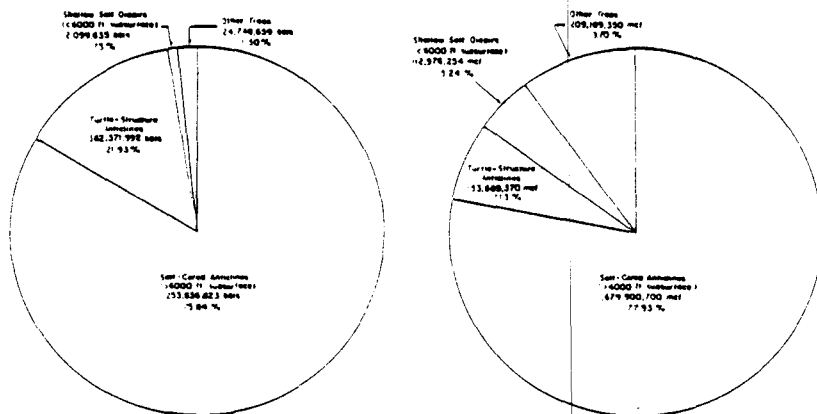
*In the central part of the East Texas Basin most oil and gas has been produced from anticlines over salt pillows because of their large structural closure. In contrast, little oil and gas has been produced near salt diapirs because of their much smaller traps.*

Petroleum in the East Texas Basin is produced from three types of salt-related anticlines, listed in order of production: salt pillows, turtle-structure anticlines, and salt diapirs (figs. 2.11-1). Production statistics from the central part of the basin are shown in figure 2.11-2. Salt pillows have trapped more hydrocarbons than have turtle-structure anticlines because pillows formed earlier and uplifted thicker sections, thereby creating multiple-zoned fields.

Only relatively small ( $<10^7$  bbls) hydrocarbon reservoirs have been discovered at the shallow salt diapirs, despite intense exploration drilling for traps similar to those around productive shallow salt domes in the Gulf Coast Basin. The paucity of hydrocarbons is probably due to the relatively small structural closure characteristic of mature East Texas diapirs. Boggy Creek Dome, a large, immature, ridgelike diapir, uplifts a large stratigraphic section and contains the largest known accumulation of oil associated with an East Texas Dome. Additional hydrocarbon reserves might be discovered by deep drilling of dome flanks below the Woodbine Group. Thus the present apparent scarcity of petroleum around salt domes does not necessarily preclude future drilling close to domes or through dome overhangs.



2.11-1 Map of salt-related structures and petroleum fields in central part of East Texas Basin (from Wood and Giles, 1982).



2.11-2 Production statistics for central part of East Texas Basin (from Wood and Giles, 1982).

### 3.0 REGIONAL HYDROGEOLOGIC STUDIES

#### 3.1 GROUND-WATER HYDRAULICS

Three-dimensional analysis of hydraulic-head data reveals a correlation of ground-water circulation with topography and geologic structure.

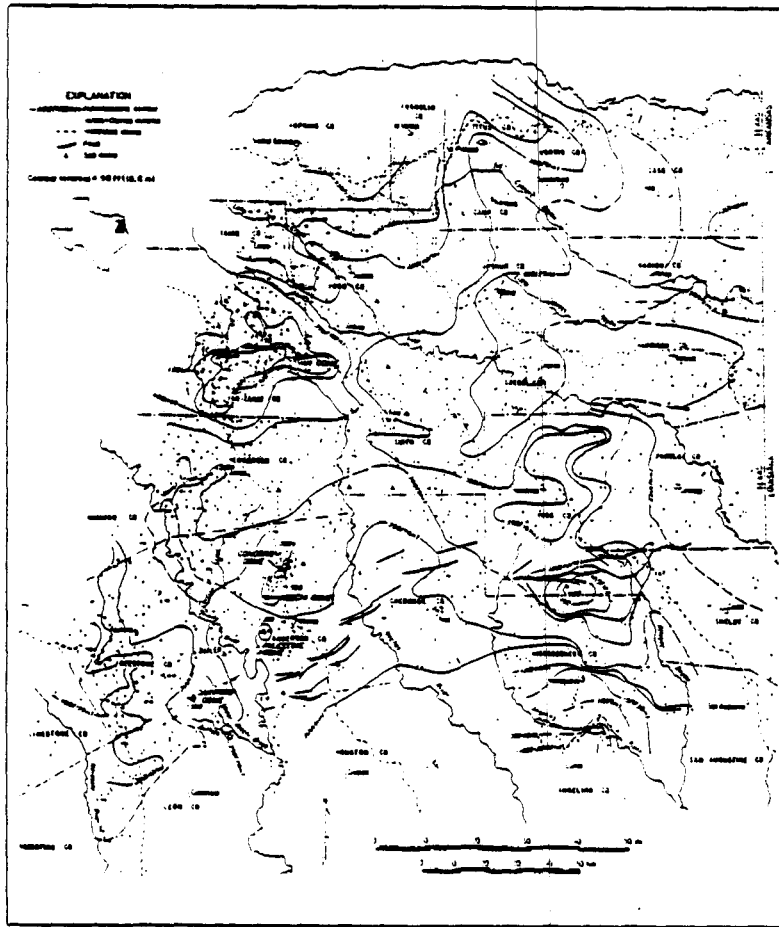
*Regional ground-water circulation in the Wilcox-Carrizo aquifer system correlates closely with topography and geologic structure. A potential for downward vertical flow prevails except beneath the major streams and their tributaries. Potential for upward flow is greatest beneath the Trinity River floodplain.*

Regional potentiometric surfaces in Eocene aquifers are controlled primarily by topography and structure. Outcrop flow patterns closely follow topography as water moves away from high recharge areas to low discharge areas (fig. 3.1-1). Thus the Queen City does not form a regionally coherent flow system but, instead, a series of smaller flow cells of closely spaced recharge and discharge areas. In the confined Wilcox-Carrizo system, flow approximately follows the structural dip as ground water moves eastward in the northern half of the basin and southward in the southern half. The ground-water divide lies in southern Smith County.

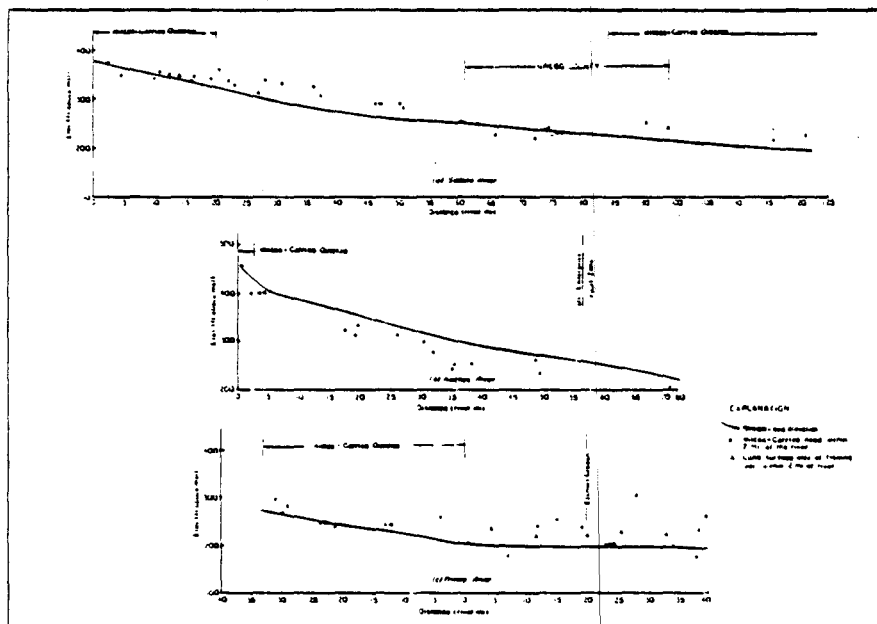
Topography affects flow in the confined Wilcox-Carrizo indirectly through leakage between the Queen City and Wilcox-Carrizo. The leakage is indicated by a subtle correlation between the Wilcox-Carrizo potentiometric surface and topography (fig. 3.1-2). Analyses of vertical head differentials and the distribution of flowing wells confirm the occurrence of leakage and show its direction. The leakage is predominantly downward, except beneath the Trinity and Sabine Rivers, which appear to be discharge areas for the confined section (fig. 3.1-2). In comparison, the Neches River is not a discharge area because it does not incise deeply enough to intersect the Wilcox-Carrizo potentiometric surface.

Fluid-pressure versus depth (P-D) relations in the Wilcox-Carrizo aquifers (fig. 3.1-3), measured by well-screen depths and depths to water levels, help locate areas where there is a hydraulic potential for vertical flow. Almost all the 598 points plot below the hydrostatic

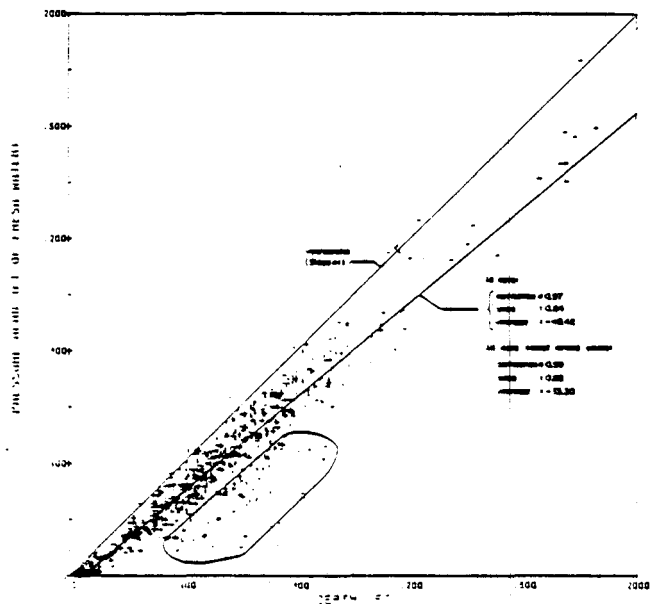
pressure line (slope  $<1.0$ ) indicating that, on the whole, vertical flow is downward (fig. 3.1-3). A high correlation coefficient shows that the P-D relationship is predictable. This hydraulic potential for downward flow increases toward higher elevations and from the artesian section to the outcrops.



3.1-1 Map of regional potentiometric surface of Wilcox-Carrizo aquifer in East Texas (from Fogg and Kreitler, 1982).



3.1-2 Elevations of Wilcox-Carrizo water levels and major stream beds (from Fogg and Kreitler, 1982).



3.1-3 Fluid-pressure versus depth in fresh-water Wilcox-Carrizo aquifers (from Fogg and Kreitler, 1982).

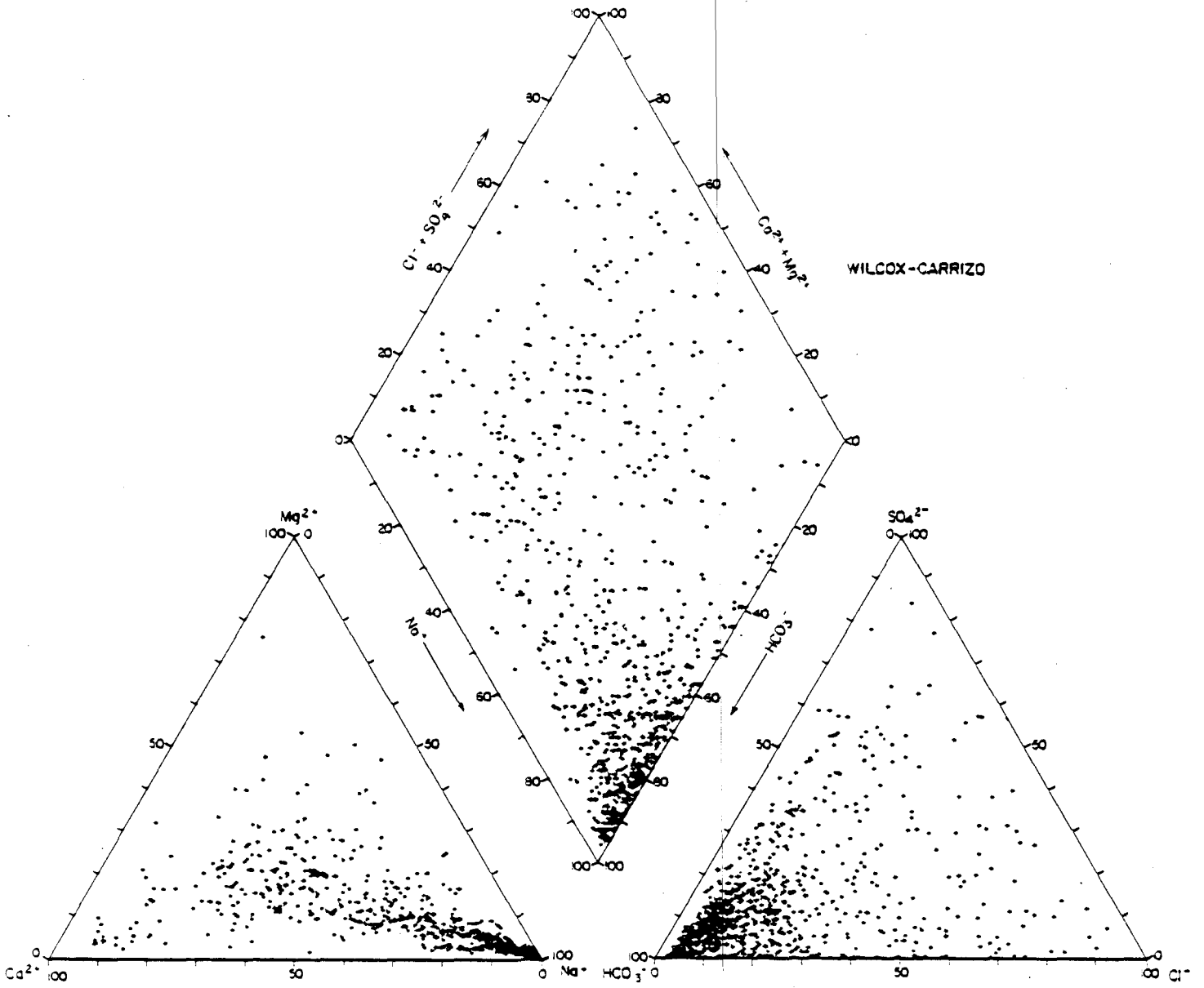
Ground-water chemistry indicates recharge over Oakwood Dome.

*Ground water in the Wilcox-Carrizo aquifer around most domes in the basin is fresh. Carrizo water indicates recharge over Oakwood and Keechi Domes.*

As ground water flows from recharge areas to discharge areas in the Wilcox-Carrizo aquifer it generally alters from an acidic, oxidized calcium-magnesium-bicarbonate-sulfate type to a basic, reduced, sodium-bicarbonate water (fig. 3.2-1). This change in the water chemistry is controlled predominantly by calcite dissolution and cation exchange with montmorillonitic clays. Water that departs from regional chemical patterns indicates anomalous hydrologic conditions such as possible dissolution of salt domes or relatively high rates of recharge to the artesian portion of the Wilcox-Carrizo.

Water from the Carrizo aquifer at Oakwood Dome characteristically displays low pH and low anion and cation concentrations indicative of a recharge zone. This is supported by light  $\delta^{13}\text{C}$  values (derived from soil carbon dioxide) from the same waters. Carrizo water at Keechi Dome has similar anomalous chemistry, indicating shallow recharge. Water from deeper Wilcox wells near the dome does not indicate recharge or vertical mixing with overlying Carrizo waters. The continuous rise of pH with depth indicates the existence of a closed carbonate system. Deep Wilcox artesian waters are strongly reducing, probably from coalification of organic material. The high exchange capacity of the montmorillonite and overall reducing nature of the Wilcox probably would inhibit migration of radionuclides if they were accidentally released into the aquifer.

The Wilcox Group is pierced by Oakwood Dome, but its ground water around the dome is primarily fresh (<1,000 mg/L total dissolved solids, TDS). The same is also true of most other domes in the basin, suggesting that the domes are generally isolated from ground-water circulation in the Wilcox by cap rocks or muddy facies around the domes.



3.2-1 Piper diagrams of Wilcox-Carrizo water chemistry (from Fogg and Kreitler, 1982).

Three sources of salinity in the Wilcox Group include a possible saline plume by Oakwood Dome.

*Estimates of the salinities of formation water in the Woodbine, Nacatoch, and Wilcox stratigraphic units have been accomplished using electric-log interpretation (SP and resistivity). Three sources of salinity affect the Wilcox Group: (1) upward leakage of deep saline waters along faults, (2) incomplete flushing of saline water in muddy areas of the Wilcox Group, and (3) salt-dome dissolution. A high TDS plume in the Wilcox northeast of Oakwood Dome may represent sodium-chloride waters formed by dome dissolution.*

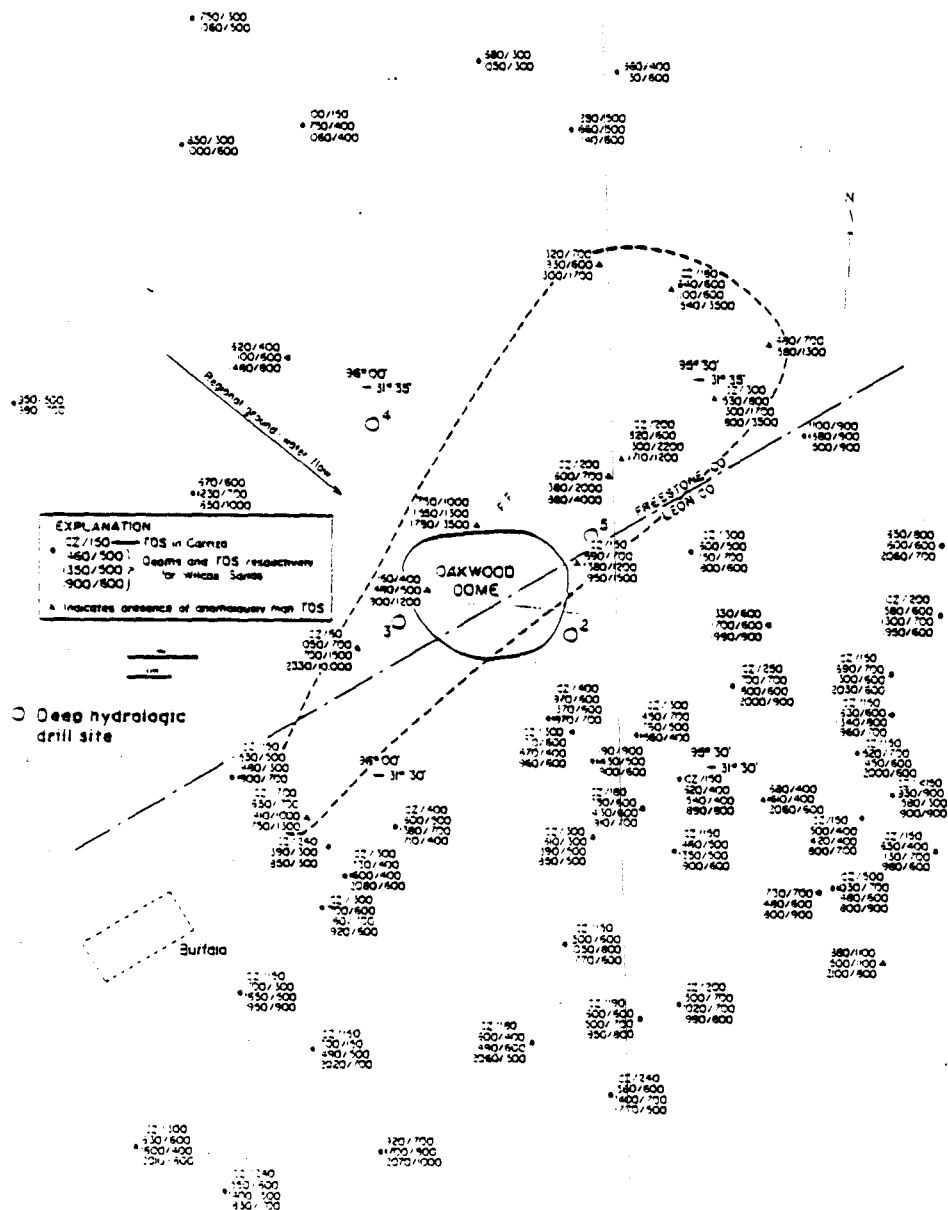
Maximum salinity in sands of the Woodbine Formation was mapped from SP logs using methods outlined by Keys and MacCary (1971). Maximum salinity values range from 30,000 to 300,000 ppm. Salinities in the Woodbine do not characteristically increase toward salt domes. Sodium chloride in the Woodbine waters probably originates from dissolution of salt stocks. But there is no evidence for ongoing solution. The Nacatoch Formation is either missing, very thin, or tightly cemented everywhere except in the northern part of the basin. The thin Nacatoch aquifer poses a negligible threat to the stability of Oakwood and Keechi Domes.

Salinity of the Wilcox Group was estimated by an empirical relationship between electric-log resistivity and total dissolved solids (TDS). A map of percentage thickness of fresh water (TDS less than 1,000 mg/L) in the Wilcox aquifer (fig. 3.3-1) indicates three sources of salinity: (1) upward leakage of deep, saline water along faults, (2) incomplete flushing of saline water in muddy areas of the Wilcox Group, and (3) salt-dome dissolution. Faults may allow upward leakage in the Mount Enterprise-Elkhart Graben in southern Anderson and Cherokee and northern Houston Counties, where salinities increase abruptly. High salinities from salt-dome dissolution could be confused with high salinities resulting from upward flow along numerous faults associated with the domes. The lack of high salinities around domes depicted in figure 3.3-1, however, suggests that the domes are neither dissolving significantly nor inducing upward leakage.

Incomplete flushing of saline water in muddy areas of the Wilcox Group is suggested by a good correlation between saline zones and muddy zones on the sand-percentage map in Upshur County, southeast of Mount Sylvan Dome and east of Whitehouse and Bullard Domes. The saline intervals near the three domes are not caused solely by dome dissolution, because salinities decrease and fresh-water thicknesses increase toward the domes. The saline water in the muddy sediments may be derived from salt-dome dissolution during the geologic past or from seas that submerged the Wilcox at least twice since deposition 40 million years ago. The persistence of saline water in muddy facies is possibly enhanced by ground-water velocities that are probably as low as 0.0015 to 0.9150 m/10<sup>4</sup> yr (0.0049 to 3.0020 ft/10<sup>4</sup> yr). Maximum TDS in the Wilcox was invariably found in muddy sands near the base of the aquifer. In nearly every case these concentrations are around 5,000 ppm ( $\pm$  1,000 ppm), and in a few isolated areas appear to reach 10,000 ppm.

Of all the domes, only Oakwood is associated with a ground-water plume of anomalously high TDS (fig. 3.3-2). The plume has not been verified by water sampling, but it is assumed to be saline and caused by dome dissolution, because it flanks the dome and is consistent with ground-water modeling (section 5.3). Modeling indicates that the northeast orientation of the plume is caused by sand-body distribution and interconnection. If salt was dissolved from the entire surface of Oakwood Dome, the dissolution rate would be  $\sim$ 10 m/10<sup>4</sup> yr; with localized dissolution over 10<sup>4</sup>m<sup>2</sup> the salt would dissolve at 2,000 m/10<sup>4</sup> yr. The relatively muddy Wilcox strata surrounding Oakwood Dome provides a barrier, in addition to salt-dome cap rock, that may isolate the dome from the high-permeability, channel-fill sand bodies, except perhaps near the brackish water plume.





3.3-2 Location of possible saline plume associated with Oakwood Dome (from Fogg and Kreitler, 1982).

Youngest  $^{14}\text{C}$  ages are found closest to the recharge area over Oakwood Dome, and ages decrease with depth and distance from the dome.

*$^{14}\text{C}$  ages of ground waters (1,000-15,000 yr) near Oakwood Dome increase down the hydraulic gradient from the outcrop recharge area toward the Trinity River.  $^{14}\text{C}$  ages also increase as the water chemistry evolves. Waters in the shallow Carrizo are younger than waters in the deeper Wilcox Aquifer.*

$^{14}\text{C}$  ages of bicarbonate in ground water at the Oakwood Dome help confirm directions and rates of ground-water flow, previously determined by hydraulic head data, and rates for the chemical evolution of the ground water. Ages were corrected for dissolution of carbonates.  $\delta^{13}\text{C}$  values, and  $^{14}\text{C}$  ages of ground water in the Wilcox, Carrizo, and Queen City aquifers near Oakwood Dome indicate that ground water flows from outcrop toward the Trinity River, possibly discharging into Upper Keechi Creek, a tributary of the Trinity River (fig. 3.4-1). Ground-water ages increase from approximately 1,000 to 4,000 years in the Carrizo aquifer over Oakwood Dome to 7,000 to 8,000 years in the deeper Carrizo Wilcox aquifers to approximately 15,000 years near Upper Keechi Creek. Thus, the youngest ages are closest to the recharge area over the dome, and ages generally increase with depth and distance away from the dome (compare section 5.2).

Evolution of the ground-water chemistry (section 3.2) from a Ca-Mg-Cl-SO<sub>4</sub> water (recharge water) to a Na-HCO<sub>3</sub> water coincides with increased  $^{14}\text{C}$  age of the samples (table 3.4-1).



3.4-1  $^{14}\text{C}$  ages of ground water in Wilcox-Carrizo aquifer near Oakwood Dome (from Kreitler and Wuerch, 1981).

3.4-1 <sup>14</sup>C ages of ground water in Wilcox-Carrizo aquifer near Oakwood Dome (from Kreitler and Wuerch, 1981).

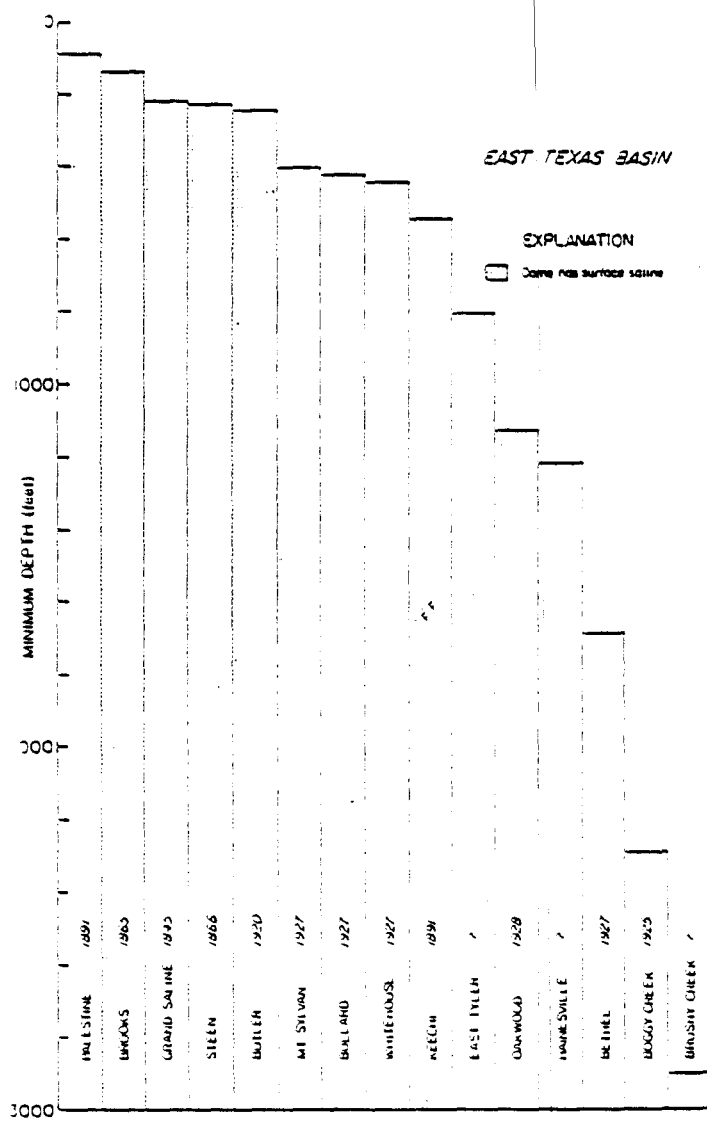
|                               | 1                  | 2           | 3            | 4            | 5          |
|-------------------------------|--------------------|-------------|--------------|--------------|------------|
| Sample no.                    | 3601               | 3666        | 3665         | 3693         | 3598       |
| Screened Interval (ft)        | 350-371<br>501-578 | 400-482     |              |              | 340-380    |
| Depth (ft)                    | 591                | 482         | 640          | 190          | 380        |
| δC <sup>13</sup>              | 7.2                | 15.5        | 6.3          | -15.1        | -18.6      |
| C <sup>14</sup> age           | 22,960 ± 460       | 8,920 ± 220 | 21,550 ± 400 | 18,840 ± 340 | 3,160 ± 90 |
| Corrected C <sup>14</sup> age | 14,670             | 6,890       | 12,200       | 14,820       | 2,182      |
| pH                            | 8.8                | 7.4         | 8.1          | 8.6          | 5.5        |
| Temp. (°C)                    | 26.2               | 26.7        | 24.0         | 29.6         | 23.0       |
| Ca <sup>2+</sup>              | 6.1                | 27.2        | 5.5          | 30.8         | 5.2        |
| Na                            | 297.8              | 46.7        | 120.6        | 22.2         | —          |
| Mg <sup>2+</sup>              | 0.53               | 9.88        | 1.05         | 7.83         | 2.2        |
| K <sup>+</sup>                | 3.1                | 7.0         | 4.0          | 7.1          | 4.2        |
| Cl                            | 38.5               | 34.6        | 27.0         | 45.0         | 12.6       |
| SO <sub>4</sub> <sup>2-</sup> | 3.0                | 36.0        | 5.0          | 16.5         | 13.0       |
| HCO <sub>3</sub> <sup>-</sup> | 640.0              | 181.0       | 540.0        | 236.0        | 34.0       |
| Br                            | 0.76               | 1.42        | 1.27         | 1.41         | 0.1        |
| F                             | 0.68               | 0.01        | 0.21         | 0.19         | 0.1        |
| SiO <sub>2</sub>              | 13.6               | 19.5        | 13.6         | 13.0         | 36.7       |
| Fe                            | 0.01               | 0.39        | 0.17         | 0.03         | 0.6        |
| Sr                            | —                  | —           | —            | —            | —          |
| H.S                           | 0.02               | 0.02        | 0.02         | 0.02         | —          |
| I                             | —                  | —           | —            | —            | —          |
| Mn                            | 0.01               | 0.03        | 0.01         | 0.01         | 0.02       |

All chemical analyses measured in mg/L

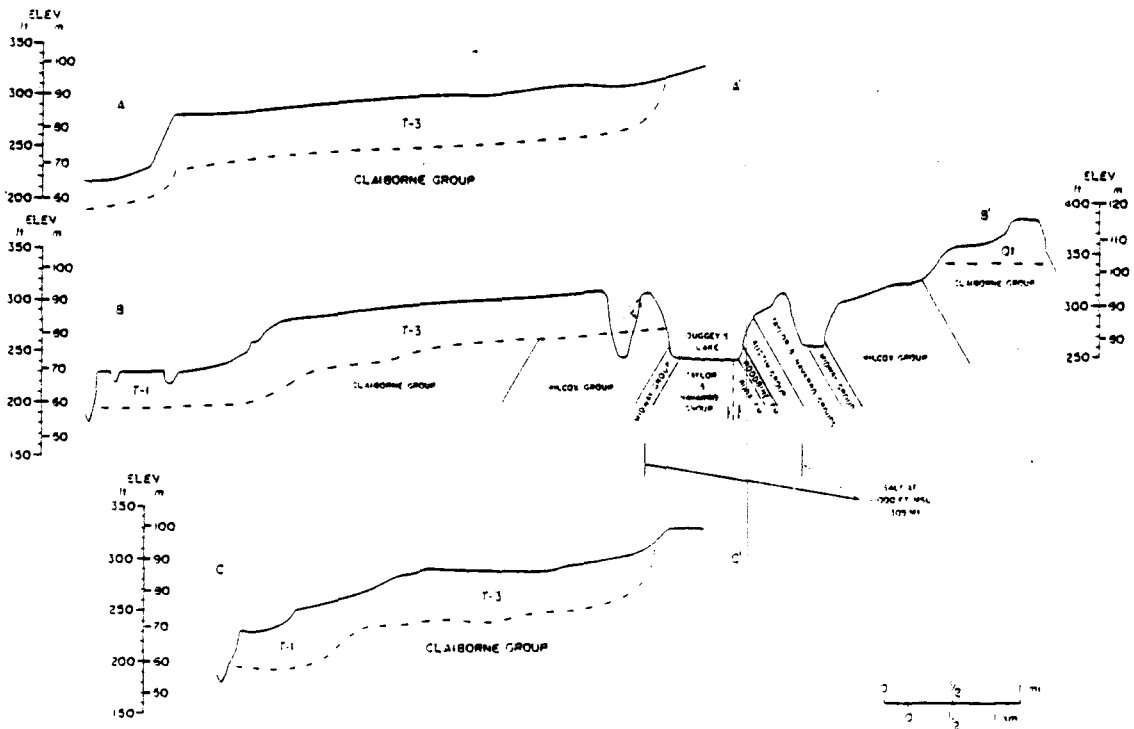
The shallowest salt domes are poor, leaky sites for potential repositories.

*The shallowest salt domes in the basin all have surface saline features above them, most of which are located in depressions. Not only are such areas hydrologically unstable, but they also make obvious targets for salt mining in the future.*

The five shallowest salt domes in the East Texas Basin have overlying surface saline features (fig. 3.5-1). With the possible exception of Butler, these features occur within or below well-defined depressions, suggestive of dissolution-induced collapse (fig. 3.5-2). The shallower domes (1) tended to be discovered earlier, (2) are the most hydrologically unstable, and (3) are most likely to be breached by future exploration for salt resources. Accordingly shallow domes (<125 m, <400 ft, depth to salt) are much less favorable as waste repositories than deeper domes. In the deeper flow systems, the presence of cap rock and muddy facies around a dome and generally lower flow velocities may be sufficient to reduce dissolution rates to negligible values.



3.5-1 Depths to top of East Texas domes. Five shallowest domes have surface salines and were discovered early (from Fogg and others, 1982).



3.5-2 Duggey's Lake overlies possible dissolution-induced collapse over Palestine Dome.

The shallower of two deep saline aquifer systems surrounds salt stocks immediately below hypothetical repository level.

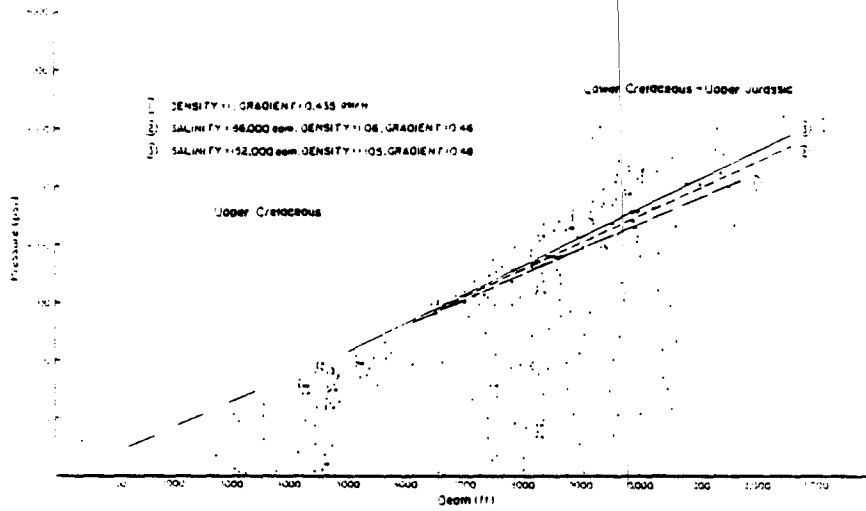
*Hydrodynamic and geochemical data reveal two deep, saline aquifer systems: (1) generally normally pressured, slowly circulating, meteoric sodium-chloride waters in Upper Cretaceous sands less than 6,000 ft deep; and (2) slightly overpressured, slowly circulating, underlying meteoric sodium-calcium-chloride waters. The only known example of mixing between these saline systems and the fresh-water system is at Butler Dome, where pre-Pleistocene false cap rock formed by near-surface discharge of deep-basin brines.*

Given a repository depth of 3,000 ft, which is below the base of fresh ground water, we need to know whether potential release of radionuclides could enter deep saline aquifers below the Wilcox Group.

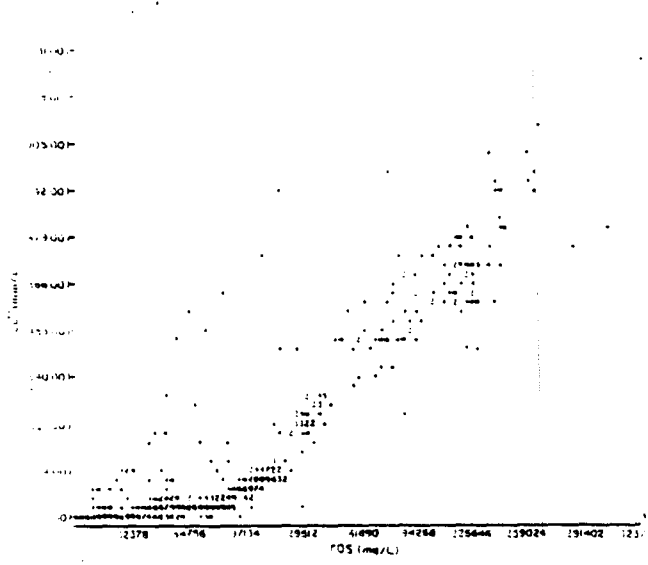
Pressure data from the deep saline aquifers suggest that there are two hydrologic systems: (1) the generally normally pressured, circulating, Upper Cretaceous aquifers <1,800 m (<6,000 ft) deep and (2) the partly overpressured, slow circulating, Lower Cretaceous and Upper Jurassic aquifers >1,800 m (>6,000 ft) deep (fig. 3.6-1). Basin-wide pressures in the extensive, hydrologically continuous Woodbine sands have dropped significantly because of oil production in East Texas since the 1930's. Hydraulic potential is presently inadequate to drive fluids from the Woodbine into overlying meteoric aquifers. Pressure may never recover.

Saline waters in the Upper Cretaceous aquifers are predominantly sodium-chloride type (fig. 3.6-2). The deeper waters are mainly sodium-calcium-chloride type with much higher total dissolved solids due to clay reactions, albitization, and other chemical reactions in an older, more closed system than the shallower sodium-chloride waters surrounding a repository. Based on  $\delta^2\text{H}$  and  $\delta^{18}\text{O}$  isotopic composition of the water (fig. 3.6-3), both saline systems have been flushed of their original connate waters and recharged by continental meteoric waters. The presence of meteoric water, rather than connate seawater, implies that both systems are hydrodynamically active rather than stagnant. The sodium and chlorine in both systems is the result of dissolution of salt in pillows and diapirs.

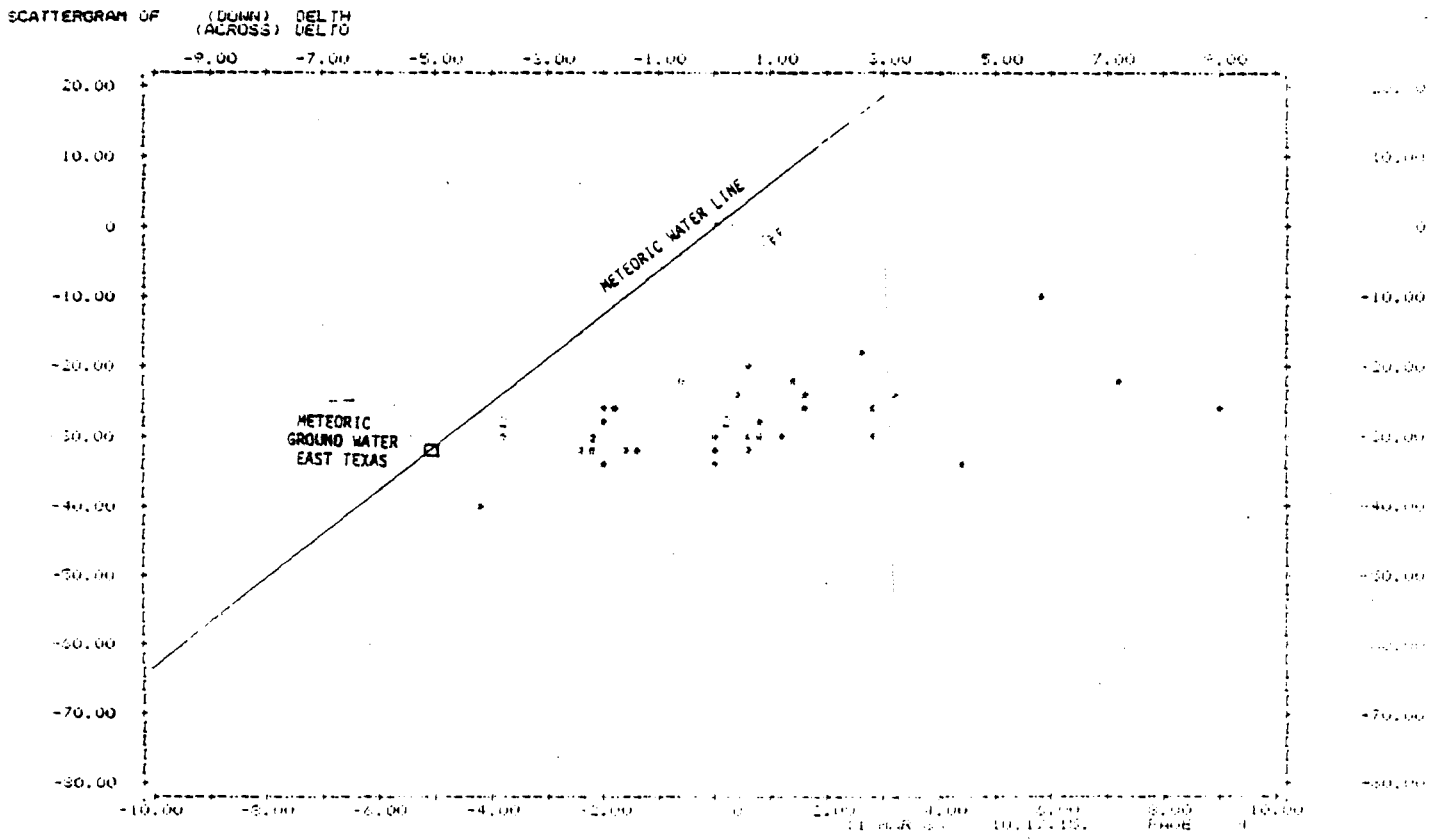
Deep basinal waters have discharged up the flanks of Butler Dome, or a radial fault associated with it, and possibly Palestine Dome. A false cap rock of calcite-cemented Carrizo sandstone has resulted. The  $\delta^{13}\text{C}$  and  $\delta^{18}\text{O}$  values of the calcite suggest the waters originated from the deep basin. Butler Dome is located where the potentiometric surface is depressed and the Wilcox aquifer is discharging. Lowering of the hydraulic head in the shallow aquifers may have permitted discharge of deep basin saline waters. In general salt domes in discharge zones of meteoric aquifers have the greatest potential for migration of deep-basin fluids up the flanks of diapirs and diapir-associated faults.



3.6-1 Fluid pressure versus depth for saline aquifers in East Texas Basin (from Kreitler and others, 1982).



3.6-2 Calcium concentration versus total dissolved solids (TDS) in saline aquifers in East Texas Basin (from Kreitler and others, 1982).



3.6-3  $\delta^{2}\text{H}$  and  $\delta^{18}\text{O}$  in East Texas ground water and meteoric water line (from Kreitler, personal communication).

## 4.0 CORE STUDIES OF OAKWOOD DOME, EAST TEXAS

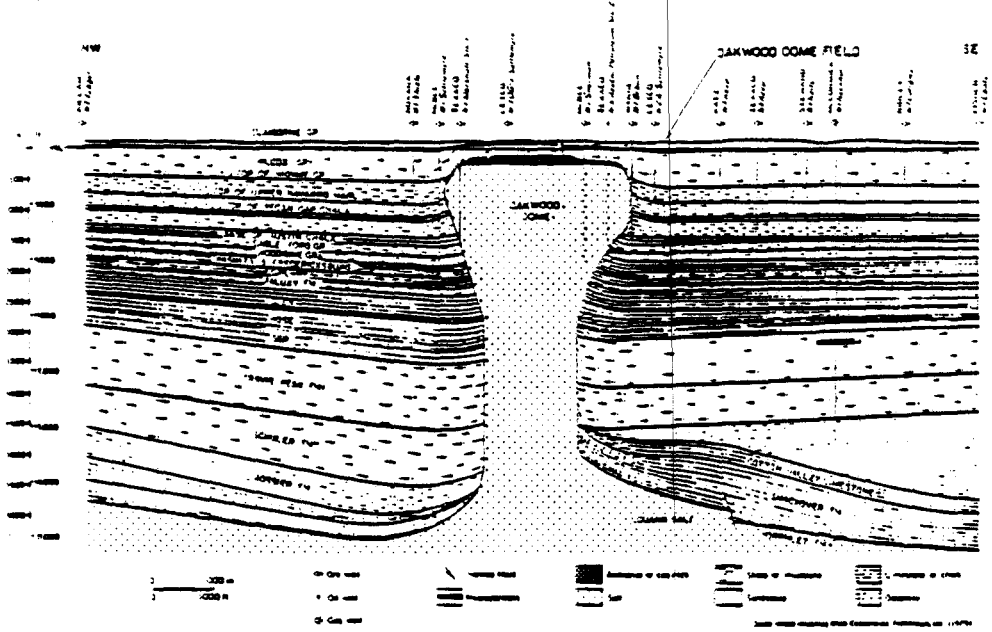
### 4.1 SALT-CORE LITHOLOGY

Salt core from Oakwood Dome is greater than 98 percent pure, and displays evidence of two distinct periods of recrystallization.

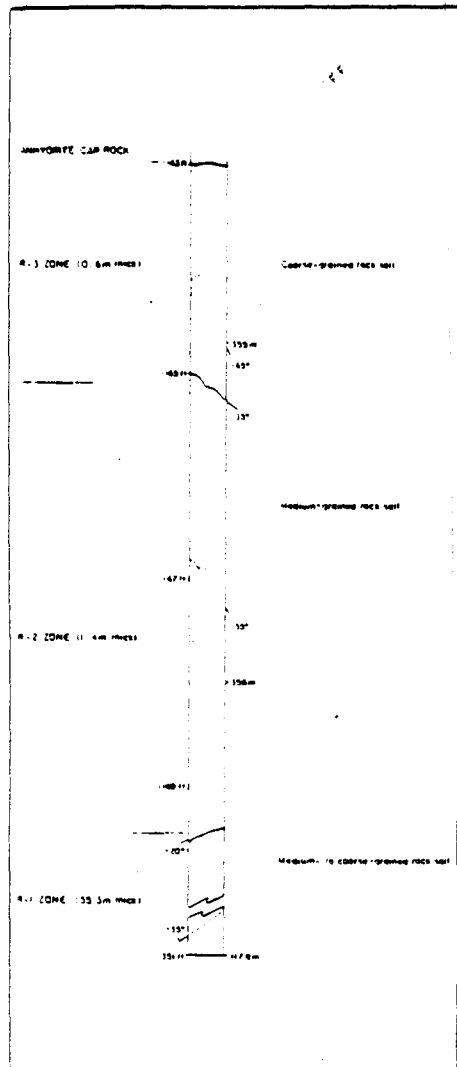
*Salt core from Oakwood Dome is greater than 98 percent pure halite, and displays evidence of two distinct periods of recrystallization. Deformation and recrystallization during diapir growth produced a penetrative schistosity. Later recrystallization of the upper 2 m of salt in the presence of ground water under conditions of low differential stress produced a granoblastic fabric.*

A vertical drill core, LETCO TOG-1, was obtained just north of the axis of the Oakwood Dome salt stock, Freestone County, East Texas (fig. 4.1-1). It intersects rock salt at 354.5 m (1,163 ft) and ends at a depth of 411.8 m (1,351 ft), yielding 57.3 m (188 ft) of rock-salt core (fig. 4.1-2, Appendix 5). The rock-salt core contains an average of  $1.3 \pm 0.7$  percent anhydrite. If all the cap rock was derived by residual accumulation of such low concentrations of anhydrite, dissolution of a column of rock salt more than 6 km high would be required.

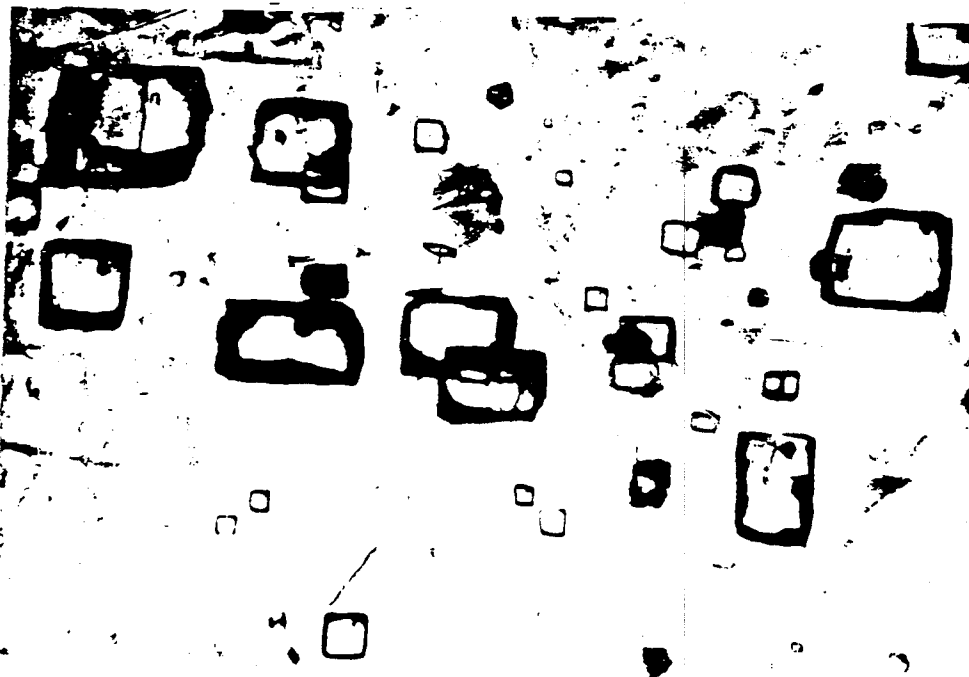
The lower 55.4 m (181.5 ft) of rock salt, the R-1 zone, displays a strong schistosity induced by diapiric flow of salt (fig. 4.1-2). Recrystallization of previously foliated rock salt produced a granoblastic polygonal texture of the upper 2 m (6.5 ft) of salt core. Consideration of homologous temperatures, geothermal gradients and present erosion rates suggest that this recrystallization occurred at least 3 Ma ago at a minimum depth of 760 m (2,493 ft). Microstructure, fluid inclusions, and bromine concentrations in halite suggest that recrystallization of the R-1 and R-2 zones was promoted by downward movement of intercrystalline brine from the lower contact of the anhydrite cap rock. Bromine concentrations in halite suggest that rock salt of the recrystallized R-3 zone has been chemically recycled by limited resolution to a greater degree than has the remainder of the rock salt. Intracrystalline fluid inclusions are confined to the R-3 zone (fig. 4.1-3). Their volume increases upward from 0.0005 percent 60 cm (2 ft) below the cap rock to 0.05 percent at the cap-rock contact.



4.1-1 Oakwood Dome cross section showing location of TOG-1 well (after Giles and Wood, 1983).



4.1-2 Profile of TOG-1 rock-salt core showing R-1, R-2, and R-3 zones, dip of foliation in R-1 zone (dashed line), and disseminated-anhydrite layers (stippled) (from Dix and Jackson, 1982). See also Appendix 5.



4.1-3 Photomicrograph of brine inclusions within halite in R-3 zone at depth of 354.7 m (1163.7 ft) (from Dix and Jackson, 1982).

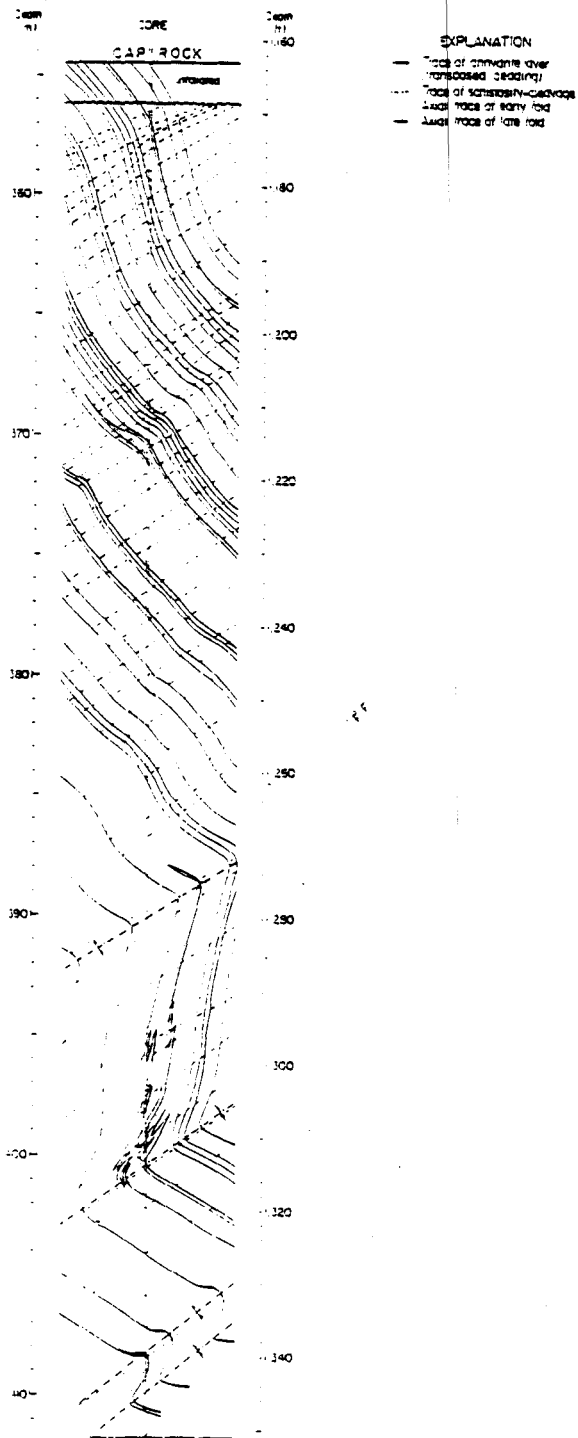
Geometric analysis suggests that the crest of Oakwood salt stock has been truncated.

*Geometric analysis of the megascopic structure in the Oakwood salt core suggests that the core has penetrated the hinge zone and lower part of a large inclined overthrust antiform representing one of the highest and youngest of a series of salt tongues that fed the spreading diapir cap. The fold geometry also suggests that tens or hundreds of meters of overlying salt have been truncated from the top of the diapir, most probably by ground-water dissolution.*

Geometric synthesis of mesoscopic structures in the Oakwood salt core has determined the form and orientation of the macroscopic structures intersected by the vertical drill core, TOG-1. Nongraded layering, defined by disseminated anhydrite grains in halite, and a tectonite fabric constitute the basic structural elements (fig. 4.2-1). The fabric has a strong schistosity, defined by the preferred orientation of disc-like halite grains, and a weak mineral lineation.

The structures have been extrapolated to zones adjacent to the core by assuming similar-type shear folding. The schistosity is axial planar to a series of younger major folds that jointly define the lower part of a large inclined anticlinorium. The younger major folds refold older minor isoclinal, which are transected by the fabric (fig. 4.2-2).

The core has penetrated the hinge zone and lower limb of an inclined, overturned antiform. This is inferred to represent one of several salt tongues that have fed the diapir, rising upward and outward, and changing in orientation from steeply plunging folds to recumbent, overthrust folds (fig. 4.2-3). Fold structures originally situated deep in the diapir have been bared by ground-water dissolution and are now juxtaposed against the base of the cap rock.



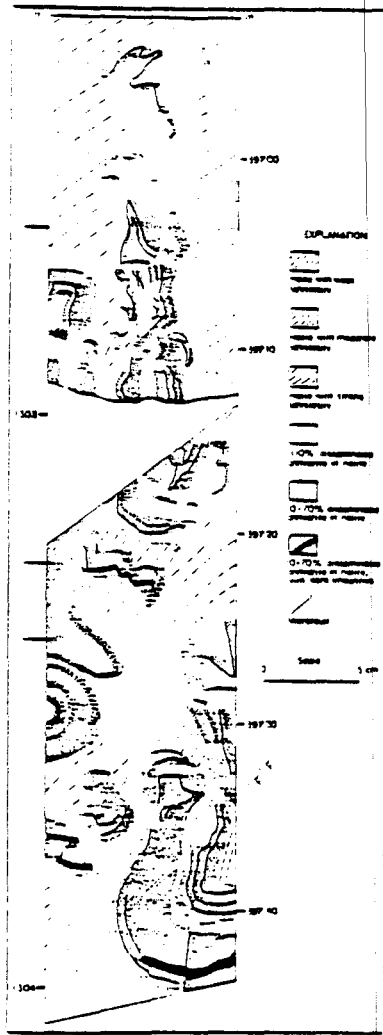
4.2-1 Schistosity and anhydrite-rich layers in TOG-1 rock-salt core (from Dix and Jackson, 1982).

Strain analysis of halite provides further evidence for past truncation of the Oakwood salt stock.

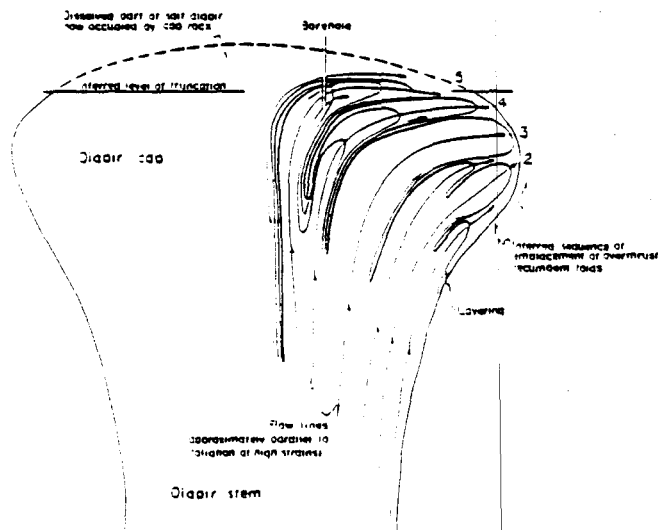
*Strain analysis of 2,400 halite grains in the TOG-1 core indicates that flattening strains predominate, the ratio of flattening to constriction increases upward, whereas strain intensity decreases upward. These results provide further evidence for truncation of the crest of the salt stock in the past.*

Measurement of the orientations and axial ratios of 2,400 halite grains at eight sample sites along the TOG-1 core has allowed the minimum finite strains to be determined by three different methods: the Harmonic Mean Method, the Theta Curve Method, and the Shape Factor Grid Method. All the strains recorded (fig. 4.3-1) are of the flattening type ( $0.544 > k > 0.000$ ) and the ratio of flattening to constriction increases upward. The strain intensity decreases upward through the foliated salt from 52 to 37 percent shortening (fig. 4.3-2); the unfoliated R-2 salt underwent about 15 percent shortening. This upward decrease in strain intensity may mark the trend toward a "neutral" zone of low strain (present in some model diapirs), since removed by dissolution during diapir truncation.

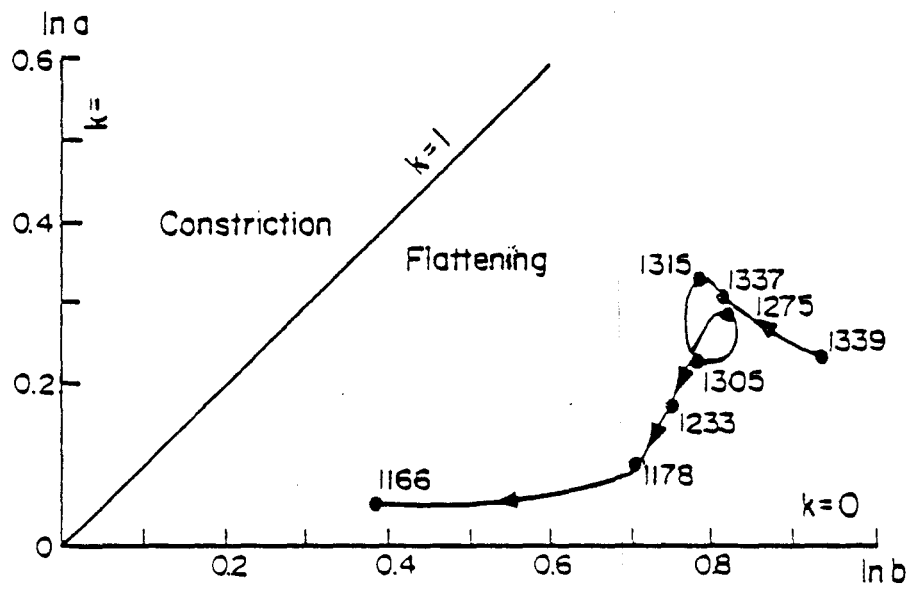
The orientations of maximum extension directions vary widely even though the foliation plane, which contains these directions, dips uniformly. Thus the preferred directions of salt creep or intergranular fluid flow are also likely to vary within the foliation plane.



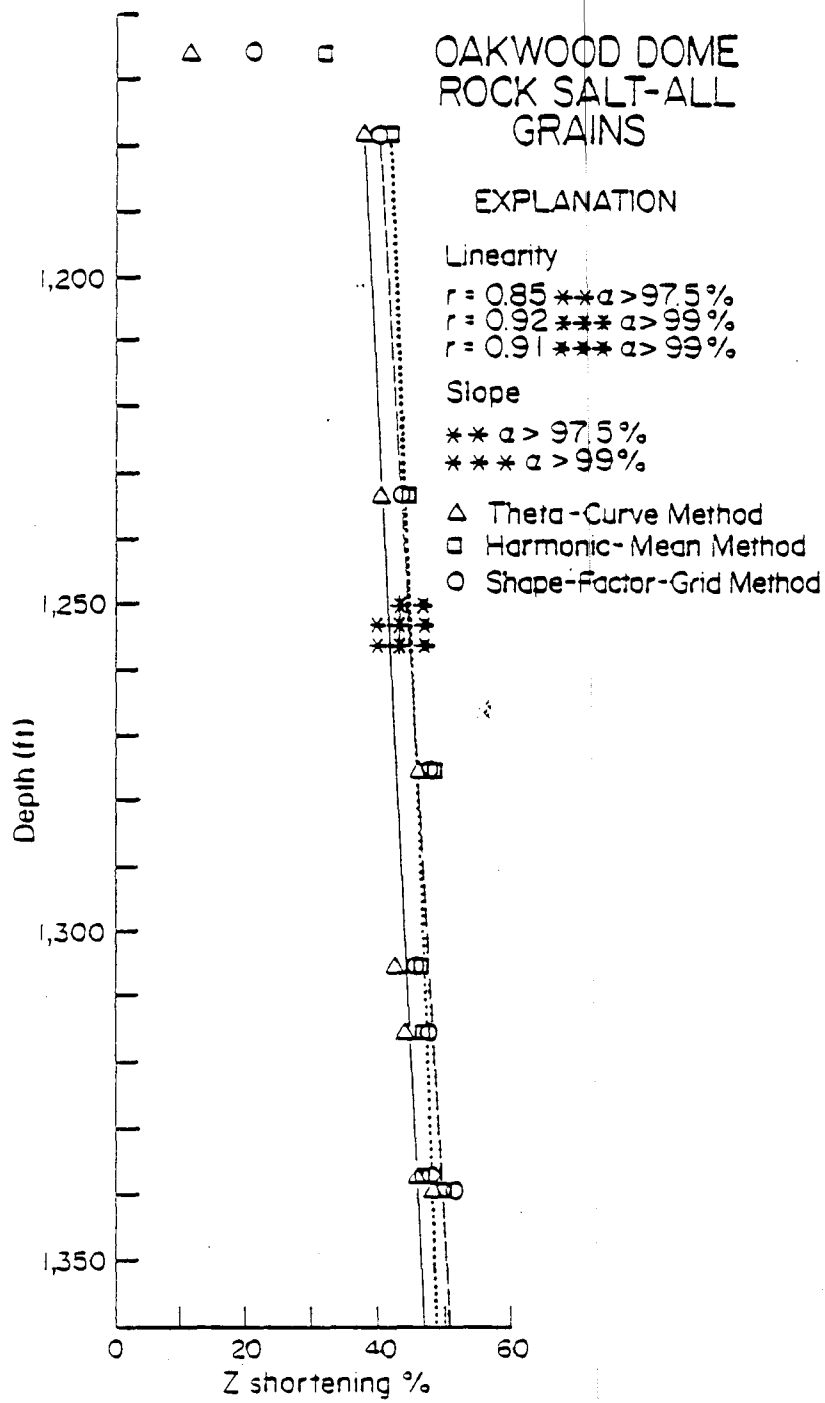
4.2-2 Structure section along TOG-1 rock-salt core (from Jackson, 1983).



4.2-3 Inferred flow patterns within a laterally spreading, rising diapir fed by multiple emplacement of salt tongues as overthrust folds (from Jackson, 1983).



4.3-1 Flinn diagram showing mean strains in Oakwood Dome rock salt. Numbers refer to depth in ft (from Jackson, 1983).



(A)

4.3-2 Statistically significant upward decrease in percentage shortening with decreasing depth (from Jackson, 1983).

Diapiric rise of salt formed a tight contact with the Oakwood cap rock.

*Dissolution of halite at the crest of the salt stock released disseminated anhydrite that accumulated as loose sand on the floor of the dissolution cavity. Renewed rise of the salt tightly closed the cavity and accreted the anhydrite sand against the base of the cap rock.*

Intracrystalline fluid inclusions in the R-3 rock salt are most concentrated directly below the cap-rock contact (section 4.1). This implies that fluids moved down from the base of the cap rock. The absence of a cavity between rock salt and cap rock (fig. 4.4-1) indicates that the salt stock is not being dissolved where intersected by the borehole.

The presence of an anhydrite-rich lamina across halite-filled extension fractures at the base of the cap rock indicates that anhydrite lamina have accreted against the base of the cap rock as residual sand released by halite dissolution (fig. 4.4-2). Horizontal lamination throughout the anhydrite cap rock is thought to reflect this process.

Upward force from the rising salt stock probably induced the observed vertical shortening in the cap rock just above the contact. This strain resulted in horizontal, spaced, stylolitic cleavage formed by pressure solution and mass transfer of anhydrite. The stylolitic cleavage, which is marked by a dark, insoluble pyritic residue, transects the older lamination. Further lateral extension and vertical shortening in the base of the cap rock resulted in halite-filled vertical extension fractures and inclined shear fractures (fig. 4.4-2).

Ingress of water resulted in dissolution of the salt stock, formation of cap rock and addition of sodium chloride to the ground water. These processes are both detrimental and favorable to waste isolation (tables 4.4-1 and 4.4-2). Despite the strong evidence for repeated attrition and uplift of the salt stock, the geologic system of rock salt and cap rock has the ability to offset, at least partially, these negative processes by self-sealing and recovery.

Table 4.4-1. Inferred processes at the cap-rock - rock-salt contact of Oakwood Dome that are favorable for storage of nuclear wastes.

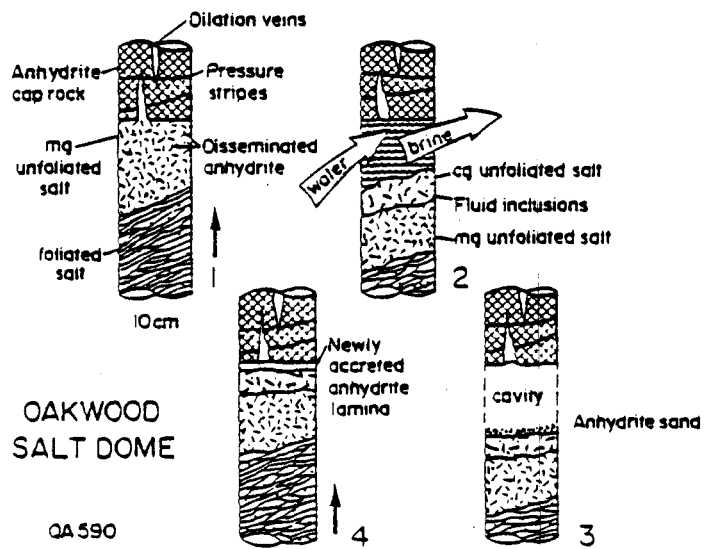
| OBSERVATION  | FAVORABLE SIGNIFICANCE  |
|--|---|
| 1. Tight seal between rock salt and anhydrite cap rock. Extension fractures and spaced cleavage in anhydrite cap rock. | Ability of salt flow driven by diapirism to close cavities and apply upward pressure on cap rock to keep cavity closed.   |
| 2. Halite-filled extension fractures in anhydrite cap rock.  | Ability of halite to grow in opening fractures, thereby sealing them.   |
| 3. Horizontal, stylolitic spaced cleavage in anhydrite cap rock.   | Ability of anhydrite aggregates to respond to stresses by migrating in solution to nearby pressure shadows and pore spaces, thereby reducing porosity and enhancing sealing properties of the cap rock. |

Table 4.4-2. Inferred processes at the cap-rock - rock-salt contact of Oakwood Dome that are unfavorable to storage of nuclear wastes.

| PROCESS OR OBSERVATION  | DETRIMENTAL SIGNIFICANCE   |
|---|--|
| 1. Structural truncation of diapiric crest.                                   | Considerable diapiric uplift.  |
| 2. Water-induced recrystallization of uppermost 2 m of rock salt.             | Introduction of water to diapiric crest and destruction of up to 6 km of rock salt by repeated episodes of dissolution.                                    |
| Greater abundance of fluid inclusions in rock salt close to cap-rock contact. |  |
| Accretion of anhydrite lamina against base of cap rock.                       |  |
| Similar appearance of lamination throughout anhydrite cap rock.               |  |
| 3. Tight seal between rock salt and anhydrite cap rock.                       | Renewed uplift of salt diapir after most recent episode of dissolution.  |
| 4. Vertical extension fractures in anhydrite cap rock.                        | Fracturing and dilation of cap rock because of rise of salt stock, creating further avenues for ground water to enter and wastes to escape.                |
| 5. Low bromine content of halite in lens of rock salt in anhydrite cap rock.  | Passage of brines through fractures in cap rock, precipitation of halite in cavities, and possible escape of brines from cap rock into surrounding strata. |



4.4-1 Photograph of tight contact between salt and overlying caprock (from Dix and Jackson, 1982).



4.4-2 Schematic diagram showing processes at cap-rock - rock-salt interface (from Jackson, 1983).

Oakwood Dome cap rock formed in a deep saline environment and appears to be a low-permeability barrier to dome dissolution.

*Cap rock at Oakwood Dome consists of low-permeability anhydrite resting in sharp contact on the underlying rock salt. A more porous calcite section overlies the anhydrite. The cap rock appears to be an effective barrier that inhibits dome dissolution.*

Salt-dome cap rock in general may or may not be an effective low-permeability barrier to future dissolution of salt stocks. Some cap rock, such as that on Gyp Hill Dome, is presently forming by salt dissolution. Other cap rock such as that on Oakwood Dome, formed in the geologic past and appears to be an effective low-impermeability seal. Cap rock on top of Oakwood Salt Dome is 137 m (450 ft) thick in the TOG-1 well (Appendix 6). Above a tight contact with salt (section 4.4) the following zones are present:

(1) Anhydrite zone, 354 - 277 m (1,163-908 ft), containing low-permeability, low-porosity granoblastic anhydrite devoid of gypsum (table 4.5-1). The rock is horizontally laminated on millimeter scale by primary variations in organic content and by stylolitic pressure stripes induced by diapiric rise of the underlying salt (fig. 4.5-1).

(2) Transitional zone, 277 - 275 m (908-902 ft), containing anhydrite partly altered to calcite and gypsum.

(3) Calcite zone, 275 - 217 m (902-713 ft), consisting of high-porosity (table 4.5-1), alternating layers of dark-grey, fine-grained calcite and younger, white, coarse-grained calcite replacing fractures and occluding porosity.

The anhydrite zone is postulated to have formed by dissolution of 6 km of rock salt over 100 Ma ago in a relatively deep, hot, saline environment. The calcite zone, characterized by extremely depleted  $\delta^{13}\text{C}$  calcite and traces of biodegraded hydrocarbons, formed in a similar environment by reduction of anhydrite and oxidation of organics introduced by groundwater. Vacherie Dome cap rock, Louisiana, has a similar diagenetic history.

In contrast the anhydrite cap rock of Gyp Hill, South Texas, is statistically more porous (table 4.5-1). Textural evidence, chiefly gypsum-cemented anhydrite, indicates that it formed--and probably still is forming--in a shallower, cooler, and less saline environment, as is the case for Rayburn's Dome, Louisiana.

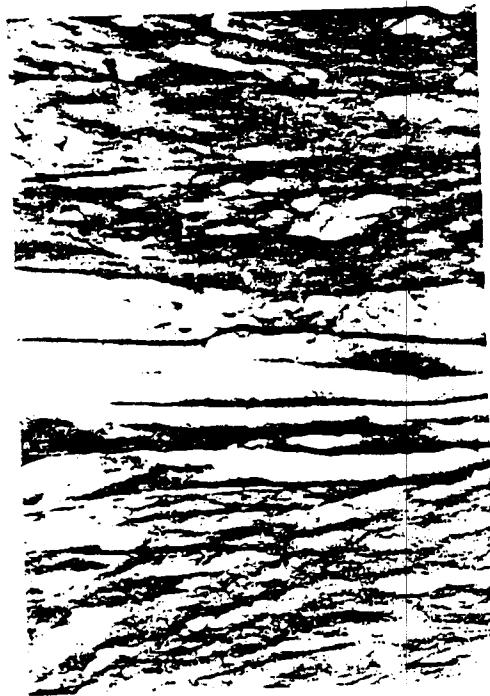
Table 4.5-1. Comparison of porosities and permeabilities of cap rock from Oakwood and Gyp Hill Salt Domes (from Kreitler and Dutton, 1982).

OAKWOOD CAP ROCK

| <u>Caprock Zones</u> | <u>Depth (ft)</u> | <u>Permeability (millidarcys)</u> | <u>Porosity (percent)</u> |
|----------------------|-------------------|-----------------------------------|---------------------------|
| CALCITE              | 720               | <0.01                             | 1.3                       |
|                      | 740               | <0.01                             | 2.2                       |
|                      | 760               | 0.04                              | 3.1                       |
|                      | 780               | 0.02                              | 3.8                       |
|                      | 800               | 43.0                              | 9.1                       |
|                      | 820               | 16.0                              | 6.2                       |
|                      | 820               | 0.01                              | 4.0                       |
|                      | 840               | <0.01                             | 13.0                      |
|                      | 880               | <0.01                             | 5.1                       |
| TRANSITION           | 904               | 0.05                              | 5.7                       |
|                      | 907               | <0.01                             | 2.3                       |
|                      | 907               | 0.29                              | 8.3                       |
| ANHYDRITE            | 920               | <0.01                             | 0.7                       |
|                      | 940               | <0.01                             | 0.7                       |
|                      | 960               | <0.01                             | 0.8                       |
|                      | 1,040             | <0.01                             | 0.9                       |
|                      | 1,060             | <0.01                             | 0.8                       |
|                      | 1,080             | <0.01                             | 0.8                       |
|                      | 1,100             | <0.01                             | 0.9                       |
|                      | 1,100             | <0.01                             | 1.0                       |
|                      | 1,120             | <0.01                             | 1.3                       |
|                      | 1,138             | 0.02                              | 3.3                       |
|                      | 1,162             | <0.01                             | 1.1                       |

GYP HILL CAP ROCK

| <u>Caprock<br/>Zones</u> | <u>Depth<br/>(ft)</u> | <u>Permeability<br/>(millidarcys)</u> | <u>Porosity<br/>(percent)</u> |
|--------------------------|-----------------------|---------------------------------------|-------------------------------|
| Gypsum                   | 50                    | <0.01                                 | 1.6                           |
|                          | 123                   | <0.01                                 | 3.0                           |
|                          | 152                   | <0.01                                 | 1.4                           |
|                          | 171                   | <0.01                                 | 2.0                           |
|                          | 230                   | <0.01                                 | 2.5                           |
|                          | 272                   | <0.01                                 | 1.2                           |
|                          | 284                   | <0.01                                 | 3.4                           |
| Anhydrite                | 310                   | <0.01                                 | 1.3                           |
|                          | 340                   | <0.01                                 | 1.5                           |
|                          | 370                   | <0.01                                 | 1.3                           |
|                          | 400                   | <0.01                                 | 2.6                           |
|                          | 428                   | <0.01                                 | 1.6                           |
|                          | 500                   | <0.01                                 | 5.1                           |
|                          | 600                   | <0.01                                 | 2.6                           |
|                          | 690                   | <0.01                                 | 3.1                           |
|                          | 740                   | <0.01                                 | 3.3                           |
|                          | 794                   | <0.01                                 | 1.6                           |
|                          | 815                   | <0.01                                 | 2.2                           |
|                          | 835                   | <0.01                                 | 1.6                           |
|                          | 855                   | <0.01                                 | 3.6                           |
| 875                      | <0.01                 | 4.4                                   |                               |
| 890                      | 45                    | 20.0                                  |                               |



0 40 mm

4.5-1 Photograph of 1 mm-wide stylolitic laminae in anhydrite cap-rock from TOG-1 (from Dix and Jackson, 1982).

## 5.0 HYDROGEOLOGIC STUDIES OF OAKWOOD DOME AND VICINITY

### 5.1 HYDROGEOLOGIC MONITORING AND TESTING

The area over Oakwood Dome is a recharge zone and boreholes through the overhang could permit flow of fresh water into the salt stock.

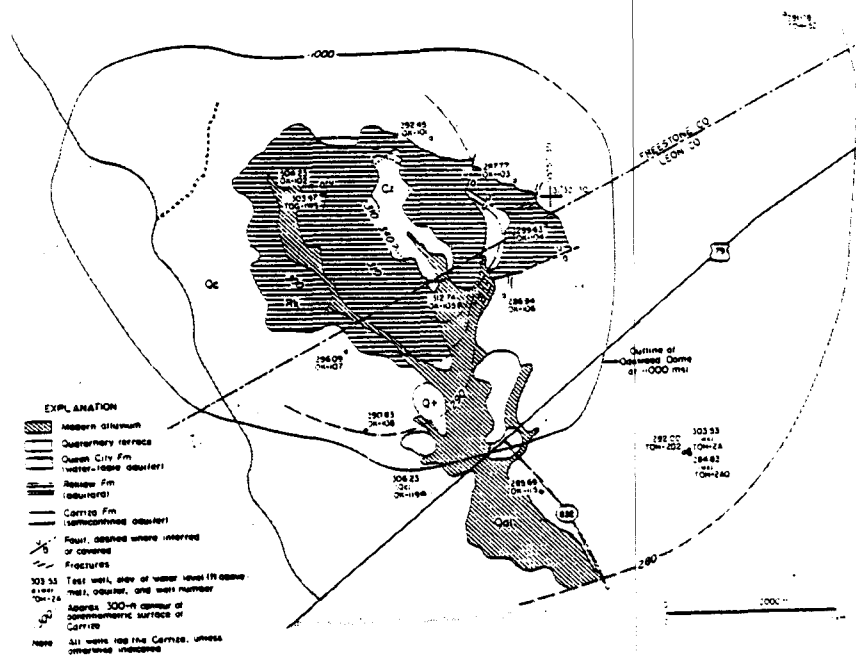
*Results of pumping tests conducted around Oakwood Dome have been used to calculate transmissivity, hydraulic conductivity, and storativity. Distribution of water levels in wells directly over the dome delineates a recharge area in the vicinity of the Carrizo outcrop and correlates with water-chemistry data from the same wells. Unplugged drillholes through the Oakwood salt overhang could initiate rapid salt dissolution by descending fresh water.*

Data collected from monitoring help to detect magnitudes and effects of recharging over Oakwood Dome. Water levels in all wells were monitored weekly and biweekly from July 1979 to October 1981.

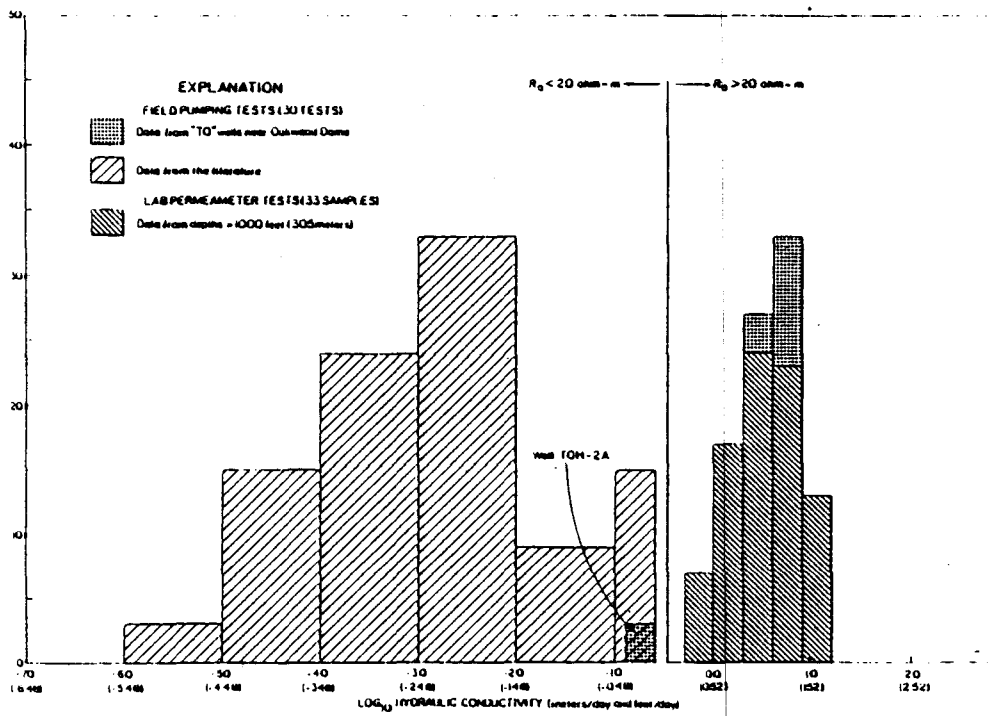
The water levels of the Carrizo aquifer were measured on May 15, 1980 (fig. 5.1-1). Contours clearly indicate a recharge area near the Carrizo and Reklaw outcrops, which is consistent with the water-chemistry data for Oakwood Dome (see section 3.2). Faults in the east apparently impede flow, causing the steeper hydraulic gradients. Short-term water-level fluctuations in all the wells reflect barometric pressure changes and artesian conditions.

In 1979 and 1980, pumping tests were conducted in 14 wells around Oakwood Salt Dome. Most wells were screened in the Carrizo Formation and the Wilcox Group. Each pumping test lasted 8 to 24 hours. Values of transmissivity (T), hydraulic conductivity (K), and storativity obtained from analysis of test data from production wells are shown in table 5.1-1. Lab-derived K values from depths greater than 1,000 ft (305 m) and the field-derived K values are related to electric-log resistivity values in the Wilcox Group (fig. 5.1-2). The distributions barely overlap and their median values differ by a factor of about  $10^3$ . All the field-derived K values (except from well TOH-2A) are apparently from thick, channel-fill sand bodies that consistently register high electric-log resistivities ( $R_o$ ). The lab-derived values, however, are from thinner interchannel sand bodies that consistently register low resistivities.

Several boreholes through the salt overhang of Oakwood Dome represent a potential hazard. The boreholes may connect the shallow, fresh-water aquifer with the deep, saline aquifer. The holes could allow rapid salt dissolution by descending fresh water with greater hydraulic head than the saline water. The problem is increased because some of these boreholes remain unlocated.



5.1-1 Potentiometric surface of Carrizo aquifer over Oakwood Dome (from Fogg and Kreitler, 1982).



5.1-2 Electric-log resistivity values in the Wilcox Group compared with lab-derived K values.

5.1-1 Test data from monitoring wells around Oakwood Dome (from Fogg, 1981).

| Well      | Unit,<br>screened interval<br>(m) | Aquifer interval,<br>thickness<br>(m) | Transmissivity<br>(m <sup>2</sup> /d)              |   | Hydraulic<br>conductivity<br>(m/d)                 |   | Storativity  |   | Remarks   |
|-----------|-----------------------------------|---------------------------------------|--|---|--|---|--|---|---|
|           |                                   |                                       | Cooper/Jacob <sup>c</sup><br>drawdown/<br>recovery | Theis <sup>d</sup><br>drawdown/<br>recovery | Cooper/Jacob <sup>c</sup><br>drawdown/<br>recovery | Theis <sup>d</sup><br>drawdown/<br>recovery | Cooper/Jacob <sup>c</sup><br>drawdown/<br>recovery | Theis <sup>d</sup><br>drawdown/<br>recovery |   |
| TOG-1WS   | Carrizo                           | 23.8-51.5                             | 76.0   | 75.   | 2.7  | 2.7   | --   | --  | 1. Barrier boundary detected.<br>2. Head in 1WS dropped below<br>bottom of upper aquitard<br>during test.   |
|           | 30.8-49.4                         | 27.7                                  | 80.0   | 75.   | 2.9  | 2.7   | --   | --  |   |
| Obs. well | Carrizo                           | 27.4-48.8                             | --a  | 32.?  | --a  | 1.5?  | --a  | 8.2 x 10 <sup>-5</sup> ?                    |   |
| OK-102    | 42.1-45.1                         | 21.4                                  | --   | --  | --   | --  | --   | --  |   |
| TOH-5D    | Carrizo                           | 142.3-154.5,<br>157.0-183.5           | 270.0  | 220.  | 7.0  | 5.7   | --   | --  | 1. The observation well re-<br>sults are questionable<br>owing to their great dis-<br>tances from TOH-5D, small<br>drawdown responses, and<br>sparsity of measurements.<br>2. Observation well data was<br>corrected for barometric<br>effects. |
|           | 144.5-150.6,<br>158.2-182.6       | 38.7                                  | 270.0  | 240.0                                       | 7.0  | 6.2   | --   | --  |   |
| Obs. well | Carrizo                           | 60.4-79.9                             | --a  | 440.?                                       | --a  | 23.?  | --a  | 1.4 x 10 <sup>-4</sup> ?                    |   |
| OK-103    | 70.1-73.2                         | 19.5                                  | --   | 440.?                                       | --   | 23.?  | --   | 1.2 x 10 <sup>-4</sup> ?                    |   |
| Obs. well | Carrizo                           | 39.6-57.9                             | --a  | 680.?                                       | --a  | 37.?  | --a  | 3.3 x 10 <sup>-4</sup> ?                    |   |
| OK-104    | 51.8-54.9                         | 18.3                                  | --   | --b   | --   | --b   | --   | --b   |   |
| TOH-2D2   | Carrizo                           | 155.8-176.2                           | 170.0  | 200.0                                       | 8.3  | 9.8   | --   | --  | 1. Values of T and K from<br>2D0 are lower because of<br>poor connection to aquifer.<br>2. During pumping, water lev-<br>els rose 6.7 cm in<br>TOH-2AO and 45.7 cm in<br>TOH-2A.  |
|           | 157.3-175.9                       | 20.4                                  | 160.0  | 150.0                                       | 7.8  | 7.4   | --   | --  |   |
| Obs. well | Carrizo                           | 155.8-176.2                           | 140.0  | 140.0                                       | 6.5  | 6.9   | 1.1 x 10 <sup>-4</sup>                             | 1.3 x 10 <sup>-4</sup>                      |   |
| TOH-2D0   | 158.2-176.8                       | 20.4                                  | 140.0  | 140.0                                       | 6.9  | 6.9   | 2.2 x 10 <sup>-4</sup>                             | 1.7 x 10 <sup>-3</sup>                      |   |
| TOH-2A    | Wilcox                            | 579.0-586.0                           | 1.4  | 1.4   | 0.21   | 0.21  | --   | --  | 1. Incomplete recovery.   |
|           | 579.0-585.0                       | 6.7                                   | 1.8  | 1.6   | 0.27   | 0.24  | --   | --  |   |
| TOH-2AO   | Wilcox                            | 253.9-285                             | 190.0  | 170.0                                       | 6.1  | 5.5   | --   | --  | 1. Early data used.<br>2. Barrier boundary detected.<br>3. During pumping, water<br>level rose 345.0 cm in<br>TOH-2A.   |
|           |                                   | 31.1                                  | 195.0  | 200.0                                       | 6.3  | 6.4   | --   | --  |   |

<sup>a</sup>Jacob method of analysis inappropriate because u too large.

<sup>b</sup>Recovery measurements were too sparse to use.

<sup>c</sup>From Cooper and Jacob (1946)

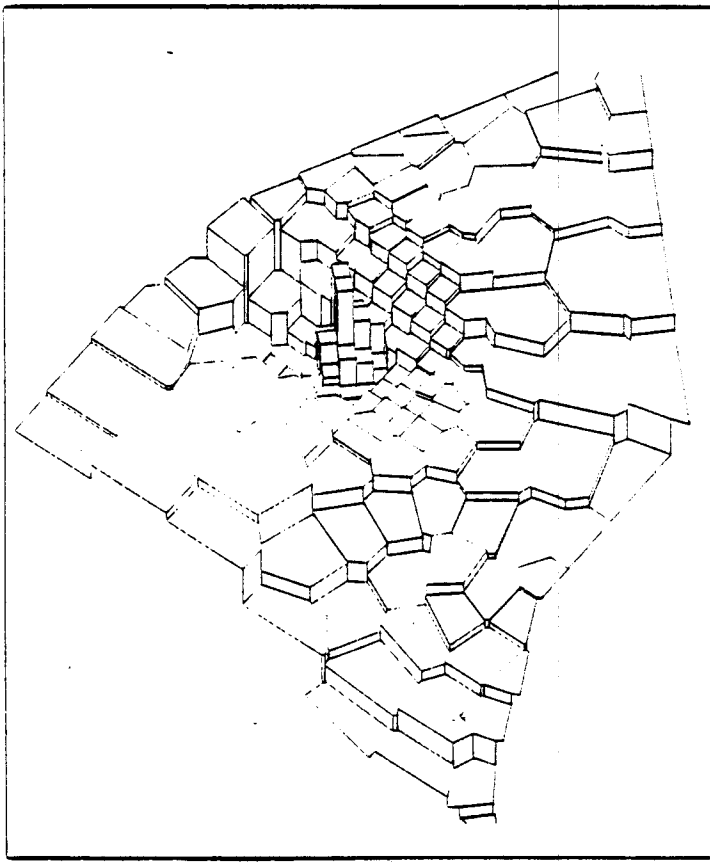
<sup>d</sup>From Theis (1935)

A three dimensional steady-state ground-water flow model has been constructed for the Wilcox around Oakwood Dome.

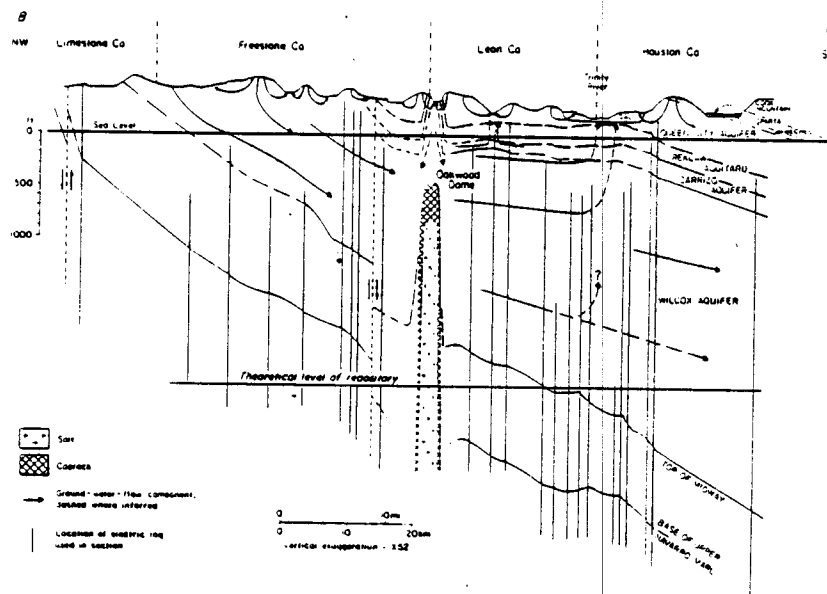
*A three-dimensional steady-state ground-water flow model has been constructed with an integrated finite-difference mesh for the Oakwood Dome vicinity (fig. 5.2-1). The model includes: (1) regional ground-water circulation patterns (fig. 5.2-2), (2) vertical leakage across the Reklaw aquitard, (3) recharge over Oakwood Dome, and (4) large-scale heterogeneity and anisotropy of the Wilcox-Carrizo aquifer system. Heterogeneity is a volume-averaged distribution of horizontal hydraulic conductivity ( $K_h'$ ). Anisotropy was introduced by lowering the ratio of vertical to horizontal ( $K_v'/K_h'$ ) until the model simulated observed pressure-depth trends. Sensitivity of the model to vertical and horizontal and sand-body interconnection was tested by simulating different distributions of  $K_h'$  and  $K_v'/K_h'$ .*

The Wilcox multiple aquifer system contains channel-fill sand bodies complexly distributed in a less permeable matrix of interchannel sands, silts, and clays. Key uncertainties in the model are the degree of connection between channel-fill sands and the hydraulic conductivity ( $K$ ) of interchannel sands. It appears, however, that channel-fill sands are laterally disconnected in low-sand-percentage areas and laterally interconnected in high-sand-percentage areas, resulting in considerable variations in values of  $K_h'$  and ground-water flux. Sand-body vertical interconnection is generally poor, resulting in an anisotropy ratio ( $K_v'/K_h'$ ) of at most  $10^{-4}$  to  $10^{-3}$ . Vertical flow may be locally large where relatively permeable avenues are vertical. Oakwood Dome apparently lies in a transition zone where the hydraulic potential for vertical flow in the Wilcox-Carrizo is relatively small.

The northeast orientation of the brackish plume associated with Oakwood Dome can be modeled by flow resulting from variable sand-body distribution and interconnection. The relatively muddy Wilcox strata surrounding Oakwood Dome provide a barrier, in addition to salt-dome caprock, that may isolate the dome from the high-permeability, channel-fill sand bodies, except perhaps near the brackish water plume.



5.2-1 View of upper surface (top of Wilcox-Carrizo aquifer) of finite-difference model of ground-water flow, Oakwood Dome area (after Fogg, 1981).



5.2-2 Regional ground-water flow lines in Wilcox-Carrizo aquifer near Oakwood Dome (from Fogg, 1981).

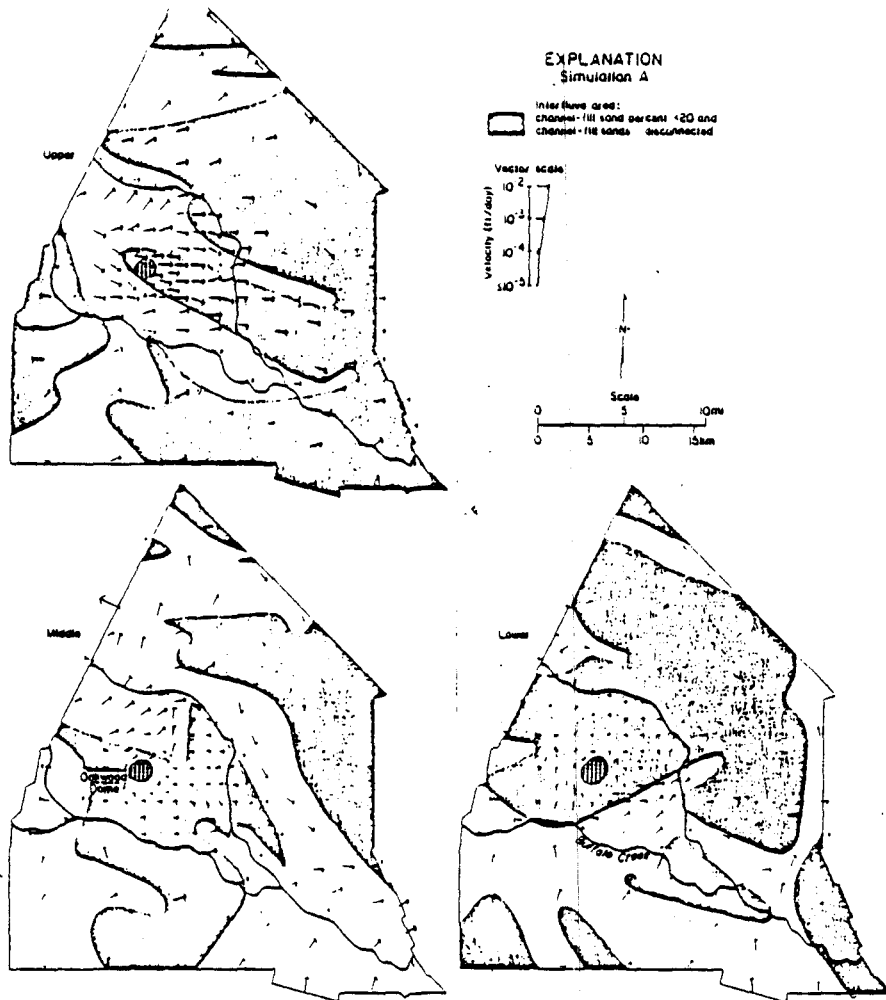
Model hydraulic-head contours and velocity vectors demonstrate that local fluxes can differ significantly from regional hydraulic gradients.

*Computed flow rates are 11 m/10<sup>4</sup> yr (36 ft/10<sup>4</sup> yr) in the fine-grained Wilcox facies enclosing the dome and 1,113 m/10<sup>4</sup> yr (3,652 ft/10<sup>4</sup> yr) in sandy facies near the dome.*

Model hydraulic-head contours and velocity vectors demonstrate that local fluxes can differ significantly from regional hydraulic gradients. Ground-water flow rates computed from the model are 11 m/10<sup>4</sup> yr (36 ft/10<sup>4</sup> yr) in the fine-grained facies in the Wilcox around the dome and 1,113 m/10<sup>4</sup> yr (3,652 ft/10<sup>4</sup> yr) in the high-percentage sand facies near Oakwood Dome (fig. 5.3-1). These flow rates may decrease by as much as 10<sup>2</sup> from top to bottom of the Wilcox-Carrizo aquifer system. Thus the model predicts a residence time of 10<sup>5</sup>-10<sup>6</sup> yr in the fine-grained facies and 10<sup>3</sup>-10<sup>4</sup> yr in high-percentage sand facies.

Because Oakwood Dome is practically surrounded by interchannel facies as a result of syndepositional dome growth, the dome may be virtually isolated from circulating Wilcox ground water. A possible exception is where channel-fill sandy facies abut against the northeast flank, coinciding with a brackish plume that apparently results from dissolution of salt or cap rock (section 3.3).

Recharge over Oakwood Dome probably is very small and affects only shallow ground-water conditions directly over the dome. Almost all the recharge water is discharged in the outcrop area. Ground-water flow rates in the artesian section are consequently sluggish compared with the outcrop section.



5.3-1 Ground-water velocity vectors computed in model simulation A (from Fogg and others, 1982).

### Acknowledgments

We thank all those whose writings we have borrowed freely to produce this summary. We are particularly grateful to G. E. Fogg and C. W. Kreidler for their constructive suggestions on hydrogeologic aspects of this report. A. B. Giles constructed the cross sections showing dome stratigraphy in Section 1.6. The manuscript was typed by Virginia Zeikus and Jean Wilke. Twyla Coker word processed the typescript under Lucille Harrell's supervision. Figures were drafted by cartographic staff under the supervision of Dan Scranton and James Macon. Susan H. Shaw coordinated the production of this report.

This work was supported by the U.S. Department of Energy, Office of Nuclear Waste Isolation, and funded under contract number DE-AC97-80ET46617, formerly DE-AC97-79ET44605, formerly EW-78-S-05-5681.

## SELECTED REFERENCES

- 1.1 Kreitler (1979); Kreitler and others (1980); Kreitler and others (1981a); Kreitler and others (1982a)
- 1.2 Jackson and Seni (1983); Jackson (1981a); Seni and Kreitler (1981); Jackson and others (1982)
- 1.3 Jackson (1982); Agagu and others (1980b)
- 1.4 Wood and Guevara (1981); Agagu and others (1980a)
- 1.5 Fogg and Kreitler (1982); Fogg and Kreitler (1981); Fogg (1980a); Fogg and others (1982a)
- 1.6 Jackson and Seni (in preparation); Giles and Wood (1983); Wood and Giles (1982); Giles (1980)
- 2.1 Jackson and Seni (1983); Seni and Jackson (1983); Giles and Wood (1983); Giles (1980); Giles (1981); Wood and Giles (1982)
- 2.2 Woodbury and others (1980); Kehle (in preparation); Jackson and Seni (1983); Jackson and Harris (1981)
- 2.3 Jackson and Seni (1983); McGowen and Harris (1983); Jackson and Harris (1981); Kehle (in preparation)
- 2.4 Seni and Jackson (1983); Jackson and Seni (1983); Giles (1981); Loocke (1978)
- 2.5 Seni and Jackson (1983); Jackson and Seni (1983); Seni and Fogg (1982); McGowen and Harris (1981); Seni (1981)
- 2.6 Seni and Jackson (1983); Jackson (1982); Wood and Guevara (1981); Jackson and Harris (1981); McGowen and Harris (1981); Wood (1981); Wood and Giles (1982)
- 2.7 Collins and others (1981); Collins (1982); Dix and Jackson (1981a); Collins and Hobday (1980); Dix (1980); Collins (1981a); Dix and Jackson (1981b); Collins (1981b); Collins (1981c)
- 2.8 Seni and Jackson (1983); Giles and Wood (1983); Giles (1981); Netherland, Sewell, and Associates (1976); Kumar (1977); Trusheim (1960); Jaritz (1980)
- 2.9 Jackson (1982); Jackson and others (1982); Collins and others (1980)
- 2.10 Pennington and Carlson (in preparation); Jackson and others (1982)
- 2.11 Wood and Giles (1982); Giles and Wood (1983)
- 3.1 Fogg and Kreitler (1982); Fogg and Kreitler (1981); Fogg (1981a)
- 3.2 Fogg and Kreitler (1982); Fogg and Kreitler (1981); Fogg and others (1982a); Kreitler and Wuerch (1981); Kreitler and Fogg (1980); Fogg (1980b)
- 3.3 Fogg and Kreitler (1982); Fogg and Kreitler (1981); Fogg (1981b); Fogg (1981c)

- 3.4 Fogg and Kreitler (1982); Fogg and Kreitler (1981); Fogg and others (1982a); Kreitler and Wuerch (1981)
- 3.5 Fogg and others (1982); Fogg and Kreitler (1980)
- 3.6 Fogg and Kreitler (1982); Fogg and Kreitler (1982); Kreitler and others (1982b)
- 4.1 Dix and Jackson (1982); Dix and Jackson (1981c)
- 4.2 Jackson (1983); Dix and Jackson (1982); Jackson and Dix (1981)
- 4.3 Jackson (1983); Jackson (1981b)
- 4.4 Dix and Jackson (1982)
- 4.5 Kreitler and Dutton (1982); Dutton and others (1982); Dix and Jackson (1982); Kreitler and others (1981b); Dutton and Kreitler (1981)
- 5.1 Fogg and Kreitler (1982); Fogg and Kreitler (1981); Fogg (1981b); Fogg and others (1981)
- 5.2 Fogg and others (1982b); Fogg and Kreitler (1982); Fogg and Kreitler (1981); Fogg (1981c)
- 5.3 Fogg and others (1982b); Fogg and Kreitler (1982); Fogg and Kreitler (1981); Fogg (1981c)

## REFERENCES

- Agagu, O. K., Guevara, E. H., and Wood, D. H., 1980a, Stratigraphic framework and depositional sequences of the East Texas Basin, in Kreitler and others, *Geology and geohydrology of the East Texas Basin, A report on the progress of nuclear waste isolation feasibility studies (1979)*; The University of Texas at Austin, Bureau of Economic Geology Geological Circular, 80-12, p. 4-10.
- Agagu, O. K., McGowen, M. K., Wood, D. H., Basciano, J. M., and Harris, D. W., 1980b, Regional tectonic framework of the East Texas Basin, in C. W. Kreitler and others, *Geology and geohydrology of the East Texas Basin, A report on the progress of nuclear waste isolation feasibility studies (1979)*; The University of Texas at Austin, Bureau of Economic Geology Geological Circular 80-12, p. 11-19.
- Carte, J. A., and Landers, R. A., 1975, STOP: A path to more useful Earth science reports: *Geology*, v. 3, no. 7, p. 405-407.
- Cloos, H., 1928, Über antithetische Bewegungen: *Geologische Rundschau*, v. 19, p. 246-251.
- Collins, E. W., 1980, The Reklaw Formation of East Texas, in Middle Eocene coastal plain and nearshore deposits of East Texas: a field guide to the Queen City Formation and related papers: Society of Economic Paleontologists and Mineralogists, Gulf Coast Section, Guidebook, p. 67-70.
- Collins, E. W., 1981a, Morphologic Mapping of Oakwood, Palestine, and Keechi Salt Domes, East Texas, in C. W. Kreitler and others, *Geology and geohydrology of the East Texas Basin, A report on the progress of nuclear waste isolation feasibility studies (1980)*; The University of Texas at Austin, Bureau of Economic Geology Geological Circular 81-7, p. 102-112.
- Collins, E. W., 1981b, Trinity River terraces near Palestine Salt Dome, East Texas, in C. W. Kreitler and others, *Geology and geohydrology of the East Texas Basin, A report on the progress of nuclear waste isolation feasibility studies (1980)*; The University of Texas at Austin, Bureau of Economic Geology Geological Circular 81-7, p. 78-82.
- Collins, E. W., 1981c, Denudation rates in East Texas, in C. W. Kreitler and others, *Geology and geohydrology of the East Texas Basin, A report on the progress of nuclear waste isolation feasibility studies (1980)*; The University of Texas at Austin, Bureau of Economic Geology Geological Circular 81-7, p. 88-92.
- Collins, E. W., 1982; Surface evidence of tectonic activity and erosion rates, Palestine, Keechi, and Oakwood Salt Domes, East Texas: The University of Texas, Bureau of Economic Geology Geological Circular 82-3, 39 p.
- Collins, E. W., Dix, O. R., and Hobday, D. K., 1981, Oakwood Salt Dome, East Texas: Surface geology and drainage analysis: The University of Texas, Bureau of Economic Geology Geological Circular 81-6, 23 p.
- Collins, E. W., and Hobday, D. K., 1980, Surface geology and shallow borehole investigations of Oakwood Dome--preliminary studies, in C. W. Kreitler and others, *Geology and geohydrology of the East Texas Basin, A report on the progress of nuclear waste isolation feasibility studies (1979)*; The University of Texas at Austin, Bureau of Economic Geology Geological Circular 80-12, p. 88-92.

- Collins, E. W., Hobday, D. K., and Kreitler, C. W., 1980, Quaternary faulting in East Texas: The University of Texas, Bureau of Economic Geology Geological Circular 80-1, 20 p.
- Dennis, J. G., and Kelley, V. C., 1980, Antithetic and homothetic faults: *Geologische Rundschau*, v. 69, no. 1, p. 186-193.
- Dix, O., 1980, Analysis of selected stream drainage systems in the East Texas Basin, in C. W. Kreitler and others, *Geology and geohydrology of the East Texas Basin, A report on the progress of nuclear waste isolation feasibility studies (1979)*: The University of Texas at Austin, Bureau of Economic Geology Geological Circular 80-12, p. 93-100.
- Dix, O. R., and Jackson, M.P.A., 1981a, Statistical analysis of lineaments and their relation to fracturing, faulting, and halokinesis in the East Texas Basin: The University of Texas at Austin, Bureau of Economic Geology Report of Investigations No. 110, 30 p.
- Dix, O. R., and Jackson, M.P.A., 1981b, Statistical analysis of lineaments on aerial photographs and Landsat imagery of the East Texas Basin and their relation to regional structure, in Kreitler and others, *Geology and geohydrology of the East Texas Basin, A report on the progress of nuclear waste isolation feasibility studies (1981)*: The University of Texas, Bureau of Economic Geology, Report prepared for the U.S. Department of Energy under Contract No. DE-AC-97-80ET 46617, p. 83-87.
- Dix, O. R., and Jackson, M.P.A., 1981c, Lithology of the Oakwood Salt Core, in C. W. Kreitler and others, *Geology and geohydrology of the East Texas Basin, A report on the progress of nuclear waste isolation feasibility studies (1980)*: The University of Texas at Austin, Bureau of Economic Geology Geological Circular 81-7, p. 172-178.
- Dix, O. R., and Jackson, M.P.A., 1982, Lithology, microstructures, fluid inclusions, and geochemistry of rock salt and of the cap rock contact in Oakwood Dome, East Texas: significance for nuclear waste storage: The University of Texas at Austin, Bureau of Economic Geology Report of Investigations No. 120, 59 p.
- Dutton, S. P., and Kreitler, C. W., 1980, Cap rock formation and diagenesis, Gyp Hill salt dome, South Texas: *Gulf Coast Association of Geological Societies Transactions*, v. 30, p. 333-339.
- Dutton, S. P., and Kreitler, C. W., 1981, Cap-rock studies of Oakwood Dome, in C. W. Kreitler and others, *Geology and geohydrology of the East Texas Basin, A report on the progress of nuclear waste isolation feasibility studies (1980)*: The University of Texas at Austin, Bureau of Economic Geology Geological Circular 81-7, p. 162-166.
- Dutton, S. P., Kreitler, C. W., and Bracken, B., 1982, Formation and diagenesis of salt-dome cap rock, Texas Gulf Coast: *Society of Economic Paleontologists and Mineralogists Core Workshop No. 3*, p. 100-129.
- Dutton, S. P., Kreitler, C. W., and Bracken, B., 1982a, Cap rock, in C. W. Kreitler and others, *Geology and geohydrology of the East Texas Basin, A report on the progress of nuclear waste isolation feasibility studies (1980)*: The University of Texas at Austin, Bureau of Economic Geology, Report prepared for U.S. Department of Energy under Contract No. DE-AC97-80ET 46617.

- Finley, R. J., Wermund, E. G., and Ledbetter, J. O., 1981, The feasibility of locating a Texas salt test facility: The University of Texas at Austin, Bureau of Economic Geology, U.S. Department of Energy Milestone Report, 171 p.
- Fogg, G. E., 1980a, Regional aquifer hydraulics, East Texas Basin, in C. W. Kreitler and others, Geology and geohydrology of the East Texas Basin, A report on the progress of nuclear waste isolation feasibility studies (1979): The University of Texas at Austin, Bureau of Economic Geology Geological Circular 80-12, p. 55-67.
- Fogg, G. E., 1980b, Salinity of formation waters, in C. W. Kreitler and others, Geology and geohydrology of the East Texas Basin, A report on the progress of nuclear waste isolation feasibility studies (1979): The University of Texas at Austin, Bureau of Economic Geology Geological Circular 80-12, p. 68-72.
- Fogg, G. E., 1981a, Fluid-pressure versus depth relationships in the Wilcox-Carrizo aquifer system, East Texas, in C. W. Kreitler and others, Geology and geohydrology of the East Texas Basin, A report on the progress of nuclear waste isolation feasibility studies (1980): The University of Texas at Austin, Bureau of Economic Geology Geological Circular 81-7, p. 115-122.
- Fogg, G. E., 1981b, Aquifer testing and monitoring around Oakwood Salt Dome, East Texas, in C. W. Kreitler and others, Geology and geohydrology of the East Texas Basin, A report on the progress of nuclear waste isolation feasibility studies (1980): The University of Texas at Austin, Bureau of Economic Geology Geological Circular 81-7, p. 126-135.
- Fogg, G. E., 1981c, Aquifer modeling of the Oakwood Salt Dome area, in C. W. Kreitler and others, Geology and geohydrology of the East Texas Basin, A report on the progress of nuclear waste isolation feasibility studies (1980): The University of Texas at Austin, Bureau of Economic Geology Geological Circular 81-7, p. 139-149.
- Fogg, G. E., and Kreitler, C. W., 1980, Impacts of salt-brining on Palestine Salt Dome, in C. W. Kreitler and others, Geology and geohydrology of the East Texas Basin, A report on the progress of nuclear waste isolation feasibility studies (1979): The University of Texas at Austin, Bureau of Economic Geology, Geological Circular 80-12, p. 46-54.
- Fogg, G. E., and Kreitler, C. W., 1981, Ground-water hydrology around salt domes in the East Texas Basin: A practical approach to the contaminant transport problem: Bulletin of Association of Engineering Geologists, v. 18, no. 4, p. 387-411.
- Fogg, G. E., and Kreitler, C. W., 1982, Ground-water hydraulics and hydrochemical facies of Eocene aquifers in the East Texas Basin: The University of Texas, Bureau of Economic Geology Report of Investigations 127, 75 p.
- Fogg, G. E., Kreitler, C. W., and Wuerch, H. V., 1982a, Meteoric Hydrology, in C. W. Kreitler and others, Geology and geohydrology of the East Texas Basin, A report on the progress of nuclear waste isolation feasibility studies (1981): The University of Texas at Austin, Bureau of Economic Geology, Report prepared for the U.S. Department of Energy under Contract No. DE-AC97-80ET46617, p. 12-27.
- Fogg, G. E., Seni, S. J., and Dutton, S. P., 1981, Core analysis of hydrologic parameters, Eocene Wilcox aquifer, East Texas, in C. W. Kreitler and others, Geology and geohydrology of the East Texas Basin, A report on the progress of nuclear waste isolation feasibility studies

- (1980): The University of Texas at Austin, Bureau of Economic Geology Geological Circular 81-7, p. 136-138.
- Fogg, G. E., Seni, S. J., and Kreitler, C. W., 1982b, Three-dimensional modeling of ground-water flow through depositional systems in the Oakwood Salt Dome vicinity, East Texas: The University of Texas, Bureau of Economic Geology, Report prepared for the U.S. Department of Energy under Contract No. DE-AC97-80ET46617, 56 p.
- Giles, A. B., 1980, Evaluation of East Texas salt domes, *in* C. W. Kreitler and others, Geology and geohydrology of the East Texas Basin, A report on the progress of nuclear waste isolation feasibility studies (1979): The University of Texas at Austin, Bureau of Economic Geology Geological Circular 80-12, p. 20-29.
- Giles, A. B., 1981, Growth history of Oakwood Salt Dome, East Texas, *in* C. W. Kreitler and others, Geology and geohydrology of the East Texas Basin, A report on the progress of nuclear waste isolation feasibility studies (1980): The University of Texas at Austin, Bureau of Economic Geology Geological Circular 81-7, p. 39-42.
- Giles, A. B., and Wood, D. H., 1983, Oakwood Salt Dome, East Texas: geologic framework, growth history, and hydrocarbon production: The University of Texas, Bureau of Economic Geology Geological Circular 83-1, 55 p.
- Guevara, E. H., and Giles, A. B., 1979, Upper Cretaceous-Lower Eocene strata, Hainesville, Keechi, and Oakwood salt domes, East Texas: Gulf Coast Association of Geological Societies Transactions, v. 29, p. 112-120.
- Hobday, D. K., 1980, Geology of the Queen City Formation and associated units, *in* Middle Eocene coastal plain and nearshore deposits of East Texas, a field guide to the Queen City Formation and related papers: Society of Economic Paleontologists and Mineralogists, Gulf Coast Section, Guidebook, p. 1-45.
- Hobday, D. K., Morton, R. A., and Collins, E. W., 1979, The Queen City Formation in the East Texas Embayment: a depositional record of riverine, tide and wave interaction: Gulf Coast Association of Geological Societies Transactions, v. 29, p. 136-146.
- Hobday, D. K., Morton, R. A., and Collins, E. W., 1980, The Queen City Formation in the East Texas Embayment: a depositional record of riverine, tide and wave interaction: The University of Texas at Austin, Bureau of Economic Geology Geological Circular 80-4, 11 p.
- Hobday, D. K., and Perkins, B. F., 1980, Sedimentary facies and trace fossils of a large aggrading delta margin embayment: upper Woodbine Formation of northeast Texas: Gulf Coast Association of Geological Societies Transactions, v. 30, p. 131-142.
- Jackson, M.P.A., 1981a, Tectonic environment during early infilling of the East Texas Basin, *in* C. W. Kreitler and others, Geology and Geohydrology of the East Texas Basin, A report on the progress of nuclear waste isolation feasibility studies (1980): The University of Texas at Austin, Bureau of Economic Geology Geological Circular 81-7, p. 7-11.
- Jackson, M.P.A., 1981b, Strain analysis of halite in the Oakwood core, *in* C. W. Kreitler and others, Geology and geohydrology of the East Texas Basin, A report on the progress of nuclear waste isolation feasibility studies (1980): The University of Texas at Austin, Bureau of Economic Geology Geological Circular 81-7, p. 183-187.

- Jackson, M.P.A., 1982, Fault tectonics of the East Texas Basin: The University of Texas at Austin, Bureau of Economic Geology Geological Circular 82-4, 31 p.
- Jackson, M.P.A., 1983, Natural strain in glacial and diapiric rock salt, with emphasis on Oakwood Dome, East Texas: The University of Texas at Austin, Bureau of Economic Geology, Report prepared for the U.S. Department of Energy under Contract No. DE-AC97-80ET46617, 75 p.
- Jackson, M.P.A., and Dix, O. R., 1981, Geometric analysis of macroscopic structures in Oakwood salt core, *in* Kreitler, C. W., and others, Geology and geohydrology of the East Texas Basin, A report on the progress of nuclear waste isolation feasibility studies (1980): The University of Texas at Austin, Bureau of Economic Geology Geological Circular 81-7, p. 177-182.
- Jackson, M.P.A., and Harris, D. W., 1981, Seismic stratigraphy and salt mobilization along the northwestern margin of the East Texas Basin, *in* Kreitler, C. W., and others, Geology and geohydrology of the East Texas Basin, A report on the progress of nuclear waste isolation feasibility studies (1980): The University of Texas at Austin, Bureau of Economic Geology Geological Circular 81-7, p. 28-32.
- Jackson, M.P.A., and Seni, S. J., 1983, Geometry and evolution of salt structures in a marginal rift basin of the Gulf of Mexico, East Texas: *Geology*, v. 11, no. 3, p. 131-135.
- Jackson, M.P.A., and Seni, S. J., in preparation, Salt domes of the East Texas Basin: The University of Texas at Austin, Bureau of Economic Geology Report of Investigations.
- Jackson, M.P.A., Wilson, B., and Pennington, W. D., 1982, Basin tectonics, *in* Kreitler, C. W., and others, Geology and geohydrology of the East Texas Basin--a report on the progress of nuclear waste isolation feasibility studies (1981): The University of Texas at Austin, Bureau of Economic Geology, Report prepared for the U.S. Department of Energy under Contract No. DE-AC97-80ET46617, p. 54-59.
- Jaritz, W., 1980, Einige Aspekte der Entwicklungsgeschichte der nordwestdeutschen Salzstocke: *Z. dt. geol. Ges.*, v. 131, p. 387-408.
- Keys, W. C., and MacCary, L. M., 1971, Application of borehole geophysics to water resources investigations, Techniques of water resource investigations of the U.S. Geological Survey: Washington, D. C., U.S. Government Printing Office.
- Kreitler, C. W., 1979, Evaluating the potential of East Texas salt domes for isolation of nuclear waste: The University of Texas at Austin, Bureau of Economic Geology, Report prepared for the U.S. Department of Energy under Contract No. EW-78-S-05-5681, 29 p.
- Kreitler, C. W., 1980, Studies of the suitability of salt domes in East Texas Basin for geologic isolation of nuclear wastes: The University of Texas at Austin, Bureau of Economic Geology Geological Circular 80-5, 7 p.
- Kreitler, C. W., Agagu, O. K., Basciano, J. M., Collins, E. W., Dix, O., Dutton, S. P., Fogg, G. E., Giles, A. B., Guevara, E. H., Harris, D. W., Hobday, D. K., McGowen, M. K., Pass, D., and Wood, D. H., 1980, Geology and geohydrology of the East Texas Basin, a report on

the progress of nuclear waste isolation feasibility studies (1979): The University of Texas at Austin, Bureau of Economic Geology Geological Circular 80-12, 112 p.

Kreitler, C. W., Collins, E. W., Davidson, E. D., Jr., Dix, O. R., Donaldson, G. W., Dutton, S. P., Fogg, G. E., Giles, A. B., Harris, D. W., Jackson, M.P.A., Lopez, C. M., McGowen, M. K., Muehlberger, W. R., Pennington, W. D., Seni, S. J., Wood, D. H., and Wuerch, H. V., 1981a, Geology and geohydrology of the East Texas Basin, A report on the progress of nuclear waste isolation feasibility studies (1980): The University of Texas at Austin, Bureau of Economic Geology Geological Circular 81-7, 207 p.

Kreitler, C. W., Bracken, B., Collins, E. W., Conti, R., Dutton, S. P., Fogg, G. E., Jackson, M.P.A., McGowen, M. K., Pennington, W. C., Seni, S. J., Wilson, B., Wood, D. H., and Wuerch, H. V., 1982a, Geology and geohydrology of the East Texas Basin--A report on the progress of nuclear waste isolation feasibility studies (1981): The University of Texas at Austin, Bureau of Economic Geology, Report prepared for the U.S. Department of Energy under Contract No. DE-AC97-80ET46617, 62 p.

Kreitler, C. W., and Dutton, S. P., 1982, Origin and diagenesis of cap rock: The University of Texas at Austin, Bureau of Economic Geology, Report submitted to U.S. Department of Energy under Contract No. DE-AC97-80ET46617, 45 p.

Kreitler, C. W., Dutton, S. P., and Fogg, G. E., 1981b, Geochemistry of ground water and cap rock from Gyp Hill Salt Dome, South Texas, in Kreitler, C. W., and others, Geology and geohydrology of the East Texas Basin, A report on the progress of nuclear waste isolation feasibility studies (1980): The University of Texas at Austin, Bureau of Economic Geology Geological Circular 81-7, p. 167-171.

Kreitler, C. W., and Fogg, G. E., 1980, Geochemistry of ground water in the Wilcox aquifer, in Kreitler, C. W., and others, Geology and geohydrology of the East Texas Basin, A report on the progress of nuclear waste isolation feasibility studies (1979): The University of Texas at Austin, Bureau of Economic Geology Geological Circular 80-12, p. 73-78.

Kreitler, C. W., Fogg, G. E., and Collins, E. W., 1982b, Deep-basin hydrology, in Kreitler, C. W., and others, Geology and geohydrology of the East Texas Basin, A report on the progress of nuclear waste isolation feasibility studies (1980): The University of Texas at Austin, Report prepared for U.S. Department of Energy under Contract No. DE-AC97-80ET46617, p. 28-34.

Kreitler, C. W., and Wuerch, H. V., 1981, Carbon-14 dating of ground water near Oakwood Dome, East Texas, in Kreitler, C. W., and others, Geology and geohydrology of the East Texas Basin, A report on the progress of nuclear waste isolation feasibility studies (1980): The University of Texas at Austin, Bureau of Economic Geology Geological Circular 81-7, p. 156-161.

Kehle, R. O., in preparation, The origin of salt structures.

Kumar, M. B., 1977, Growth rates of salt domes of the North Louisiana Salt Basin, in Martinez, J. D., and others, An investigation of the utility of Gulf Coast Salt Domes for the storage or disposal of radioactive wastes: Institute for Environmental Studies, Louisiana State University, Baton Rouge, Louisiana, p. 225-229.

- Loocke, J. E., 1978, Growth history of the Hainesville Salt dome, Wood County, Texas: The University of Texas at Austin, Master's thesis, 95 p.
- Lotze, F., 1931, Uber Zerrungsformen: Geologische Rundschau, v. 22, p. 353-371.
- McGowen, M. K., and Lopez, C. M., in press, Depositional systems in the Nacatoch Formation (Upper Cretaceous), East Texas and southwest Arkansas: The University of Texas at Austin, Bureau of Economic Geology Report of Investigations.
- McGowen, M. K., and Harris, D. W., 1981, Preliminary study of the upper Jurassic (Cotton Valley) and lower Cretaceous (Hosston/Travis Peak) Formations of the East Texas Basin, in Kreitler, C. W., and others, Geology and geohydrology of the East Texas Basin, A report on the progress of nuclear waste isolation feasibility studies (1980): The University of Texas at Austin, Bureau of Economic Geology Geological Circular 81-7, p. 43-47.
- McGowen, M. K., and Harris, D. W., in press, Cotton Valley (Upper Jurassic) and Hosston (Lower Cretaceous) depositional systems and their influence on salt tectonics in the East Texas Basin: The University of Texas at Austin, Bureau of Economic Geology.
- Netherland, Sewell and Associates, 1976, Geological study of the interior salt domes of northeast Texas Salt Dome Basin to investigate their suitability for possible storage of radioactive waste material as of May, 1976: Report prepared for the Office of Waste Isolation, Energy Research and Development Administration, Union Carbide Corporation, Nuclear Division, 57 p.
- Pennington, W. D., and Carlson, S., in preparation, Summary of observations-East Texas seismic network: The University of Texas, Bureau of Economic Geology.
- Seni, S. J., 1981, The effect of salt tectonics on deposition of the lower Cretaceous Paluxy Formation, East Texas, in Kreitler, C. W., and others, Geology and geohydrology of the East Texas Basin, A report on the progress of nuclear waste isolation feasibility studies (1980): The University of Texas at Austin, Bureau of Economic Geology Geological Circular 81-7, p. 53-59.
- Seni, S. J., and Fogg, G. E., 1982, Wilcox Group facies and syndepositional dome growth, southern East Texas Basin: The University of Texas at Austin, Bureau of Economic Geology, Report prepared for the U.S. Department of Energy under Contract No. DE-AC97-80ET46617, 33 p.
- Seni, S. J., and Jackson, M.P.A., 1983, Sedimentary record of Cretaceous and Tertiary salt movement, East Texas Basin: Times, rates, and volumes of salt flow, implications to nuclear-waste isolation and petroleum exploration: The University of Texas at Austin, Bureau of Economic Geology Report of Investigations (in press).
- Seni, S. J., and Jackson, M.P.A., in press, Evolution of salt structures, East Texas diapir province, Part I: Sedimentary record of halokinesis: American Association of Petroleum Geologists Bulletin.
- Seni, S. J., and Jackson, M.P.A., in press, Evolution of salt structures, East Texas diapir province, Part II: Patterns and rate of halokinesis: American Association of Petroleum Geologists Bulletin.

- Seni, S. J., and Kreitler, C. W., 1981, Evolution of the East Texas Basin, in Kreitler, C. W., and others, Geology and geohydrology of the East Texas Basin, A report on the progress of nuclear waste isolation feasibility studies (1980): The University of Texas at Austin, Bureau of Economic Geology Geological Circular 81-7, p. 12-20.
- Trusheim, F., 1960, Mechanism of salt migration in northern Germany: American Association of Petroleum Geologists Bulletin, v. 44, no. 9, p. 1519-1540.
- Wood, D. H., 1981, Structural effects of salt movement in the East Texas Basin, in Kreitler, C. W., and others, Geology and geohydrology of the East Texas Basin, A report on the progress of nuclear waste isolation feasibility studies (1980): The University of Texas at Austin, Bureau of Economic Geology Geological Circular 81-7, p. 21-27.
- Wood, D. H., and Giles, A. B., 1982, Hydrocarbon accumulation patterns in the East Texas salt dome province: The University of Texas at Austin, Bureau of Economic Geology Geological Circular 82-6, 36 p.
- Wood, D. H., and Guevara, E. H., 1981, Regional structural cross sections and general stratigraphy, East Texas Basin: The University of Texas at Austin, Bureau of Economic Geology, 21 p.
- Woodbury, H. O., Murray, I. B., Jr., and Osborné, R. E., 1980, Diapirs and their relation to hydrocarbon accumulation, in Miall, A. D., ed., Facts and principles of world petroleum occurrence: Calgary, Canadian Society of Petroleum Geologists, p. 119-142.

Appendix 1. Lithologic descriptions, correlation notes, and selected references, East Texas Basin (from Wood and Guevara, 1981).

| STRATIGRAPHIC UNITS |            |   | LITHOLOGY, FACIES RELATIONSHIPS,* AND STRATIGRAPHIC NOTES   | SELECTED REFERENCES†   |   |  |
|---------------------|------------|---|---|--|---|--|
| SYSTEM              | SERIES     | GROUP   | FORMATION   | *Lithic composition is from Sellards and others (1932), Bailey and others (1945), Barrow (1953) Waters and others (1955), Nichols and others (1968), and Forgotson and Forgotson (1976).<br><br>†The following references describe the entire stratigraphic column in the East Texas Basin: Sellards and others (1932), Waters and others (1955), Eaton (1956), Nichols and others (1968), Agagu and others (1980a). Other references listed below discuss the specific units and refer specifically to basin strata. See text for further references on adjacent areas. |   |  |
|                     |            |   |   |  |   |  |
| TERTIARY            | EOCENE     | CLAIBORNE<br>Shallow marine to nonmarine clastic strata. Weches, Queen City, and Reklaw sometimes have been combined to form Mount Selman Formation. Contacts between formations are typically difficult to delineate by electric logs. | Yegua Fm.   | Sand, sandy clay, and compact clay; contains minor bentonite and lignite.  | Barnes (1965, 1966, 1967b, 1970), Guevara and Garcia (1972), Hobday and others (1980).  |  |
|                     |            |   | Cook Mountain Fm.   | Clay and shale that are brown, glauconitic, fossiliferous; contains some sandy shale, some limestone. Formerly known as "Crockett Member" of Cook Mountain Formation.  |   |  |
|                     |            |   | Sparta Fm.  | Gray to buff sand with erratic sandy shale or clays; contains some glauconitic sand, limonite, and lignite. Formerly member of Cook Mountain Formation.  |   |  |
|                     |            |   | Weches Fm.  | Glauconite that is sand sized, dark green to black, fossiliferous, bedded; contains significant glauconitic clay and glauconitic sand.   |   |  |
|                     |            |   | Queen City Fm.  | Sand and sandy clay that are thin bedded, white and red.   |   |  |
|                     |            |   | Reklaw Fm.  | Green to black, glauconitic clay; locally sandy or gypsiferous.  |   |  |
|                     |            |   | Carrizo Fm.   | Medium-grained sand to sandy clay; locally ferruginous. Formerly considered part of underlying Wilcox Group.   |   |  |
|                     |            | WILCOX  | Undifferentiated  | Nonmarine clastic strata. Poorly consolidated silt to coarse-grained sandstone; interbedded with medium-brown-gray, very carbonaceous, micaceous, pyritic, soft and flaky shale; contains lignite, siderite, clay ironstone, and bentonite stringers. Wilcox locally is very calcareous. In outcrop Wilcox divides into Calvert Bluff, Simsboro, and Hooper Formations. Wilcox in outcrop was formerly called "Rockdale Formation." Some workers place Wilcox entirely within the Eocene; others (including this paper) contend that it includes upper Paleocene strata. | Barnes (1965, 1966, 1967b, 1970, 1972), Fisher and McGowen (1967), Kaiser (1978).   |  |
|                     |            | PALEOCENE   | MIDWAY  | Undifferentiated   | Marine shale that is medium gray to brown gray, micaceous, calcareous to noncalcareous; contains thin beds of fine-grained sandstone and siderite near top, thin beds of glauconitic quartz sandstone toward base, black phosphatic nodules at base. Upper contact with Wilcox Group is gradational; this report places top of Midway at base of last sand greater than 10 ft thick. In outcrop Midway subdivides into Willis Point and Kincaid Formations. | Barnes (1965, 1966, 1967b, 1970, 1972).  |
|                     | CRETACEOUS | GULFIAN   | NAVARRO<br>Upper contact is an unconformity that is difficult to delineate in subsurface without paleontological data. Locally, black phosphatic nodules at base of Midway Group have been used as contact. | Upper Navarro Clay   | Microfossiliferous and micaceous clay and shale. Unit has been included with Upper Navarro Marl and called "Kemp Clay."   | Barrow (1953), Granata (1963), Barnes (1966, 1967b, 1972), Stehli and others (1972), McGowen and Lopez (in press). |
| Upper Navarro Marl  |            |   |   | Marl; occurs throughout basin.   |   |  |
| Nacatoch Sand       |            |   |   | Sandstone that is fine grained, well sorted, somewhat calcareous. Thins and pinches out to the south.  |   |  |
| Lower Navarro Fm.   |            |   |   | Shale that is microfossiliferous, micaceous, and flaky. Has been called "Neylandville Marl."   |   |  |
|                     |            | TAYLOR<br>Upper contact with Navarro Group is difficult to determine without paleontological data.  | Upper Taylor Fm.  | Marl and shale. Marl is gray, microfossiliferous. Shale is brown gray, flaky, slightly calcareous. A limy shale, the Saratoga, occurs at base of unit at eastern edge of basin.  | Ellisor and Teagle (1934), Stephenson (1937), Barrow (1953), Granata (1963), Stehli and others (1972), Thompson and others (1978).  |  |
| Pecan Gap Chalk     |            |   | Light-gray, microfossiliferous chalk throughout most of basin. Thickens and is transitional to east with Annona Chalk.  |  |   |  |
| Wolfe City Sand     |            |   | Sandstone that is very fine grained, thinly bedded, argillaceous, and glauconitic. In the western part of the basin, locally porous and thick.  |  |   |  |
| Lower Taylor Fm.    |            |   | Shale that is medium gray, fissile, micaceous, glauconitic, and calcareous to noncalcareous. Transitional to east with Annona Chalk and Ozan Chalk.   |  |   |  |

Appendix I (cont.)

| STRATIGRAPHIC UNITS    |   |  | LITHOLOGY, FACIES RELATIONSHIPS, AND STRATIGRAPHIC NOTES | SELECTED REFERENCES  |   |  |
|------------------------|---|--|--|--|---|--|
| SYSTEM                 | SERIES  | GROUP  | FORMATION  |  |   |  |
| CRETACEOUS             | GULFIAN   | AUSTIN<br>No definitive stratigraphic study of group has been accomplished for basin. Thus, major differences are cited in the literature for stratigraphic and facies relationships, as well as nomenclature. | Gober Chalk  | Chalk that occurs throughout most of basin, but may be discontinuous. "Gober" has been applied to any chalk in this stratigraphic position. Top of Gober conventionally has been called "top of Austin Group," but lithologic unit appears to grade into Ozan Chalk (Taylor Group) to east.  | Barrow (1953), Forgotson (1958), Granata (1963), Nichols (1964), Stehli and others (1972), Thompson and others (1978).  |  |
|                        |   |  | Brownstown Fm.   | Clay or shale. Where underlying Blossom Sand is absent, Brownstown is indistinguishable on electric logs from Bonham Clay.   |   |  |
|                        |   |  | Blossom Sand   | Sand, discontinuous. Most sands in this stratigraphic position have been called "Blossom."   |   |  |
|                        |   |  | Bonham Clay  | Clay or shale.   |   |  |
|                        |   |  | Austin Chalk   | Limestone that is light gray, argillaceous, fossiliferous, and chalky; interbedded with thin shale beds. Top is marked by "glauconitic chalk stringer" across much of basin. Discontinuous sand below glauconitic chalk stringer is sometimes known as "Second Blossom." At base of Austin Chalk there is a distinctive member, Ector Chalk, which is white to dark gray and brown, and massive. Austin Group becomes sandier to east and grades into Tokio Formation. Due to uplift and erosion of Sabine Uplift, base of Austin Chalk is marked by unconformity that truncates Eagle Ford, Woodbine, and part of Washita along eastern margin of study area. |   |  |
|                        | COMANCHEAN  | WASHITA  | EAGLE FORD   | Undifferentiated   | Shale with sand members. Shale is very fine grained, medium gray, platy, and micaceous; becomes sandy, particularly to north. Sand members, Subclarksville, Coker, and Harris Sands, are fine grained, glauconitic, micaceous, and locally porous. "Subclarksville Sand" has come to mean youngest sand beneath unconformity at base of Austin Chalk and commonly has been applied to sands that correlate with other sand members. Notations such as "first," "second," and "third" Subclarksville Sand are also common. Harris Sand may consist of reworked Woodbine sands. Eagle Ford is missing in eastern part of basin because of overlying unconformity. | Barrow (1953), Forgotson (1958), Granata (1963), Nichols (1964), Stehli and others (1972).   |
|                        |   |  | WOODBINE   | Undifferentiated   | Sand that is very fine to medium grained, well sorted, friable, calcareous to noncalcareous; interbedded with multicolored and waxy shales; conglomeratic; containing abundant bentonitic volcanic ash. There are two members: Lewisville is shelf-strandplain facies and underlying Dexter is fluvial facies. Woodbine is overlain by Austin Chalk along eastern part of basin where Eagle Ford has been removed. Farther east, Woodbine is also truncated by unconformity. Some workers indicate a significant pre-Woodbine unconformity in basin; this report shows an unconformity below Woodbine only where Maness Shale is missing.                       | Bailey and others (1945), Barrow (1953), Forgotson (1958), Granata (1963), Nichols (1964), Oliver (1971), Stehli and others (1972).            |
|                        |   |  | GEORGETOWN SUBGROUP                                      | Maness Shale   | Shale that is dark gray, faintly laminated; distinguished by copper or bronze color, and conchoidal fractures. Transitional between Washita Group and Woodbine Group and sometimes has been included in Woodbine Group.   | Bailey and others (1945), Eaton and Reynolds (1951), Barrow (1953), Granata (1963), Nichols (1964), Mosteller (1970), Scott and others (1978). |
|                        | Buda Limestone  | Limestone that is white, dense; marly near top, slightly porous to southwest.  |  |  |   |  |
|                        | Grayson-Del Rio Fm  | Gray, calcareous shale; contains interbedded limestone that is brown gray, microcrystalline, dense, slightly argillaceous.   |  |  |   |  |
| Mainstreet Limestone   | Limestone that is gray or white, fossiliferous; marly to south.   |  |  |  |   |  |
| Weno-Paw Paw Limestone | Gray limestone; interbedded with shales. Paw Paw is sandy and shaly facies in outcrop and in extreme northwest part of basin.                             |  |  |  |   |  |
| Denton Shale           | Gray shale and marl in northwest part of basin. Thins and includes limestone beds in southeast.   |  |  |  |   |  |
| Fort Worth Limestone   | Limestone that is white to light gray, hard, dense; containing some marly streaks; becomes shaly to north. Nonporous in north and west; porous elsewhere. |  |  |  |   |  |
| Duck Creek Shale       | Dark-gray marl; interbedded with gray, fossiliferous, nodular limestone.  |  |  |  |   |  |
| Duck Creek Limestone   | Gray limestone; contains some marl. Commonly combined with overlying shale and named Duck Creek Formation.  |  |  |  |   |  |

Appendix I (cont.)

| STRATIGRAPHIC UNITS |            |                     | LITHOLOGY, FACIES RELATIONSHIPS, AND STRATIGRAPHIC NOTES | SELECTED REFERENCES  |   |   |
|---------------------|------------|---------------------|--|--|---|---|
| SYSTEM              | SERIES     | GROUP               | FORMATION  |  |   |   |
| CRETACEOUS          | COMANCHEAN | Fredericksburg      | Kiamichi Shale   | Black, laminated shale; contains thin beds of fossiliferous limestone; becomes porous to southeast. Interfingers with limestones of overlying Washita Group; in this report upper boundary is base of last Washita limestone.  | Bailey and others (1945), Eaton and Reynolds (1951), Barrow (1953), Granata (1963), Nichols (1964), Mosteller (1970), Scott and others (1978).  |   |
|                     |            |                     | Goodland Limestone                                       | Limestone that is white to light grayish-brown, dense; contains calcite veins. Grades into porous Edwards Limestone at southeastern extremity of basin.  |   |   |
|                     |            | TRINITY             | Paluxy Fm.   | Very fine to medium-grained sandstone; interbedded with varicolored, waxy shale, and with mudstone; contains thin carbonaceous laminae, and thin lenses of conglomerate. Grades southward into shale that is dark gray, pyritic, sideritic, fissile, and interbedded limestone. Shale and limestone facies in southern third of the basin is Walnut Formation and is difficult to distinguish from overlying Goodland Limestone. Paluxy grades into Antlers Sandstone in northern extremities of basin. Walnut is considered to be of Fredericksburg age, but Paluxy is normally grouped with Trinity Group because it is difficult to distinguish from clastic facies of underlying Upper Glen Rose in northern part of basin. In Louisiana, "Paluxy" has come to include clastic facies of underlying Upper Glen Rose. In this report, Walnut is undistinguished from Paluxy.  | Bailey and others (1945), Barrow (1953), Granata (1963), Nichols (1964), Mosteller (1970), Caughey (1977).  |   |
|                     |            |                     | GLEN ROSE SUBGROUP                                       | Upper Glen Rose Fm.  | Limestone that is light to medium brown-gray, dense, locally porous; interbedded with medium- to dark-gray, fissile shale. Anhydrite zones in lower part of formation are called "stray," "first," "second," and "third" anhydrite stringers and can be correlated over large areas. Toward northeast uppermost Glen Rose becomes Paluxy-like clastic facies, and limestone occurs only at base of formation. Upper Glen Rose in Texas is equivalent to Rusk Formation in Louisiana, where term "Glen Rose" excludes Paluxy-like clastic facies mentioned above.                | Barrow (1953), Forgotson (1956, 1957), Nichols (1964)   |
|                     |            |                     |  | Massive Anhydrite  | White, saccharoidal anhydrite; interbedded with red to gray shale, light- to medium-gray, dense, pelletal limestone, and some dolomite. Anhydrite has mottled, chicken-wire texture. Ferry Lake Anhydrite of Louisiana is equivalent to Massive Anhydrite of Texas. "Mooringsport Formation" has been used for interval from top of anhydrite stringer in the Upper Glen Rose to base of Massive Anhydrite. Bacon Lime is local limestone, porous, pelletal, oolitic, at base of Massive Anhydrite. Top of Massive Anhydrite is difficult to correlate but base is good marker. | Jones (1945), Barrow (1953), Forgotson (1956, 1957), Granata (1963), Nichols (1964), Bushaw (1968). |
|                     |            | Lower Glen Rose Fm. |  | Composed of the Rodessa Member (interbedded shale, anhydrite, limestone, and sandstone), James Limestone Member (limestone is gray, dense, nonporous, locally oolitic and coquinoideal; contains shale), Pine Island Shale Member (dark shale with some interbedded limestone and sandstone), and Pettet (Sligo) Member (medium- to dark-brown-gray, dense limestone, interbedded with dark-gray shale). Pettet is fossiliferous, pelletal, and colitic to north and west; it is transitional with underlying Travis Peak (Hosston) and is commonly considered a member of Travis Peak. This report includes Pettet with Lower Glen Rose primarily because of lithology; sands of Travis Peak are easily identified, but top of Pettet is difficult to identify in northern part of basin. All members of Lower Glen Rose become more terrigenous in northern part of basin; James Limestone becomes indistinguishable, and a sandy unit called "Pittsburg" appears near base. Rodessa includes local porous, productive zones such as Hill, Neugent, and Henderson sandy zones, and Gloyd, Dees, and Young limestones. Shale between Rodessa and James is normally called "Bexar Shale"; in this report it is included with Rodessa. "Pettet" is commonly used in East Texas; however, in Louisiana and South Texas, same unit is called "Sligo." In Louisiana, "Pettet" refers only to porous limestone facies of Sligo. | Barrow (1953), Forgotson (1956, 1957), Granata (1963), Nichols (1964), Bushaw (1968).   |   |

Appendix 1 (cont.)

| STRATIGRAPHIC UNITS |  |                   | LITHOLOGY, FACIES RELATIONSHIPS,<br>AND STRATIGRAPHIC NOTES  | SELECTED REFERENCES  |   |
|---------------------|--|-------------------|--|--|---|
| SYSTEM              | SERIES   | GROUP             | FORMATION  |  |   |
| CRETACEOUS          | COMANCHEAN   | TRINITY<br>(con.) | Travis Peak Fm.  | Predominantly fine- to medium-grained sandstone and interbedded dull-red and gray-green, arenaceous shale. Pale-green, carbonaceous siltstone found in upper part of unit; lenticular chert and quartz pebble conglomerate beds found throughout. "Hosston," commonly used in Louisiana and Arkansas, is generally favored over "Travis Peak"; however, "Travis Peak" has been retained within East Texas Basin by common usage. Confusion persists because subsurface unit is not equivalent to Travis Peak in outcrop in Central Texas; Travis Peak at outcrop is equivalent to part of Lower Glen Rose. Base of unit is unconformable except in southern part of basin, but it is rarely distinguishable on electric logs due to similar composition of Travis Peak and underlying Schuler. | Barrow (1953), Forgotson (1957), Granata (1963), Bushaw (1968).   |
|                     |  | JURASSIC          | COTTON VALLEY  | Schuler Fm.  | Fine- to medium-grained sandstone interbedded with varicolored, waxy shale. Locally conglomeratic. Fossiliferous limestones occur in the lower portion. |
| Bossier Fm.         | Shale that is gray, micaceous, and noncalcareous; interbedded with microcrystalline limestone. |                   |  |  |   |
| LOUARK              | Gilmer Limestone   |                   | Limestone that is gray to brown, dense, micritic; sometimes oolitic and pseudo-oolitic, or sometimes argillaceous; interbedded with thin beds of dark-gray shale. Unit occurs over most of study area and becomes increasingly shaly to southeast. Gilmer previously has been informally known as "Cotton Valley Limestone," "Lower Cotton Valley Lime," or "Haynesville." However, unit is not part of Cotton Valley Group, and it is lithically different from, but does grade laterally into, terrigenous Haynesville Formation of Louisiana. | Forgotson (1954a, b), Forgotson and Forgotson (1976), Todd and Mitchum (1977), Collins (1980).   |   |
|                     | Buckner Fm.  |                   | Pink to white anhydrite and halite, red shale, and pink dolomite. Evaporites occur primarily in northeast. Buckner grades into Smackover Formation to southeast.   |  | Imlay (1943), Swain (1949), Barrow (1953), Forgotson (1954a, b), Todd and Mitchum (1977).   |
|                     | Smackover Fm.  |                   | Limestone that is brownish gray, dense, microcrystalline. At north and west parts of basin are some moderately fossiliferous oolitic limestones and some tan, porous to nonporous dolomite.  |  | Eaton (1961), Collins (1980).   |
| MIDDLE              | LOUANN   | Norphlet Fm.      | Red beds consisting of very fine grained, well-sorted, slightly calcareous sandstone; interbedded with siltstone and small amounts of red to maroon, plastic shale; some halite at base; some thin dolomites, anhydrites, and conglomerates throughout. Unit becomes more fine grained to south.   | Barrow (1953), Eaton (1961), Nichols (1964), Todd and Mitchum (1977).  |   |
|                     |  | Louann Salt       | Halite that is white to pale gray or pale blue. Gradational with overlying Norphlet and underlying Werner Formations.  |  |   |
|                     |  | Werner Fm.        | Anhydrite containing local sandstone and conglomerate at base.   |  |   |
|                     |  | Eagle Mills Fm.   | Red shale, some fine-grained red to pink sandstone, and red to brown, dense limestone. May not extend into center of basin.  |  |   |
| LOWER               |  |                   |  |  |   |
| TRIASSIC            | UPPER  |                   |  |  |   |
| PALEOZOIC           |  | PRE-EAGLE MILLS   |  | Pennsylvanian and older, partially metamorphosed shales.   | Swain (1949), Nichols (1964).   |

Appendix 2. Dome catalog.

1.0 DOME NAME:

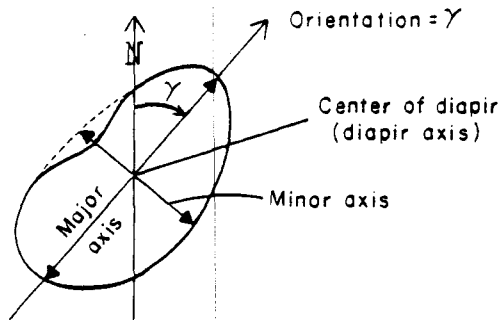
- 1.1 LOCATION: N - north  
 E - east  
 S - south  
 W - west

- 1.2 RESIDUAL GRAVITY EXPRESSION: Based on data from Exploration Techniques (1979) and a basinwide residual gravity map from Exploration Techniques (1979).  
 GU: gravity units (0.1 milligal)

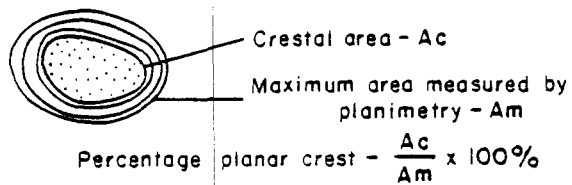
- 1.3 DEPTH: Depths in ft (m) below topographic surface.  
 Contour elevations in ft (m) below sea level.

- 1.4 ORIENTATION AND MAXIMUM LATERAL DIMENSIONS OF SALT STOCK: Modified from structure-contour maps of top of salt from Netherland, Sewell, and Associates (1976).

Orientation: Map view

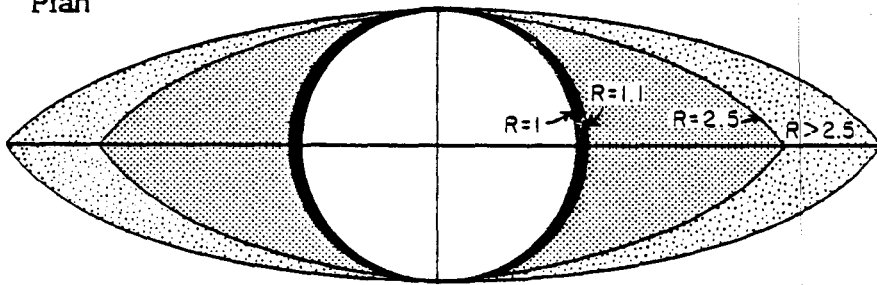


Structure-contour map



1.5 SHAPE OF SALT STOCK: Modified from structure-contour maps of top of salt from Netherland, Sewell, and Associates (1976).

Plan

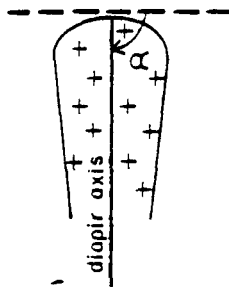


$$\text{Axial ratio } R = \frac{\text{major axis}}{\text{minor axis}}$$

$$\frac{1}{R} = \frac{\text{minor axis}}{\text{major axis}}$$

- Circular  $R=1.0-1.1$
- Elliptical  $R=1.1-2.5$
- Highly elliptical  $R>2.5$

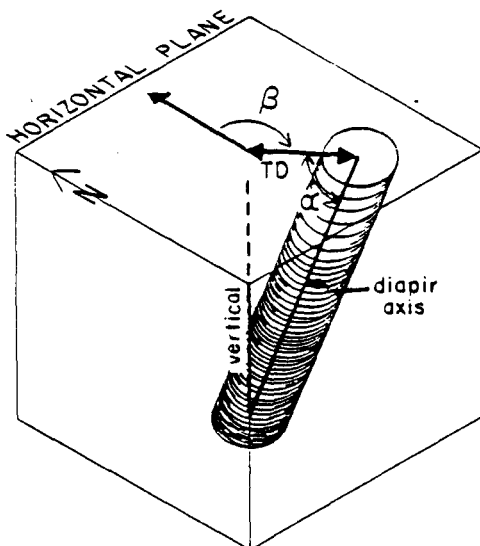
Cross section



Vertical axis  $\alpha = 90^\circ$

$\alpha$  = axial plunge

$\beta$  = axial tilt

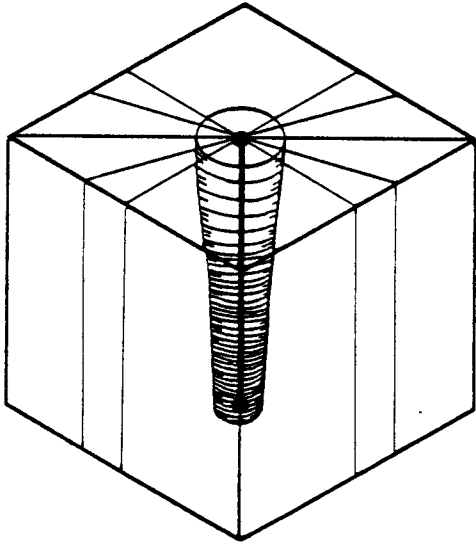


$\beta$  = tilt orientation

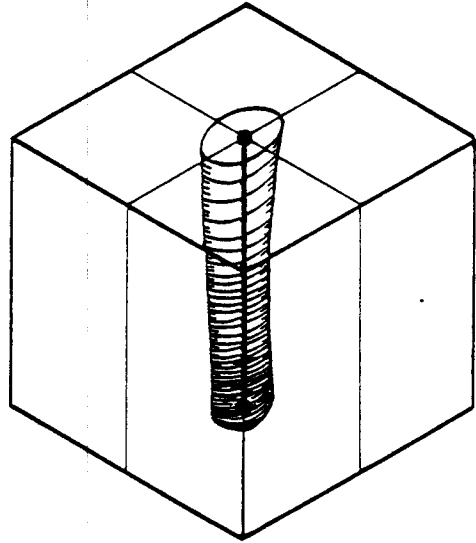
TD = tilt distance

$\alpha$  = axial plunge

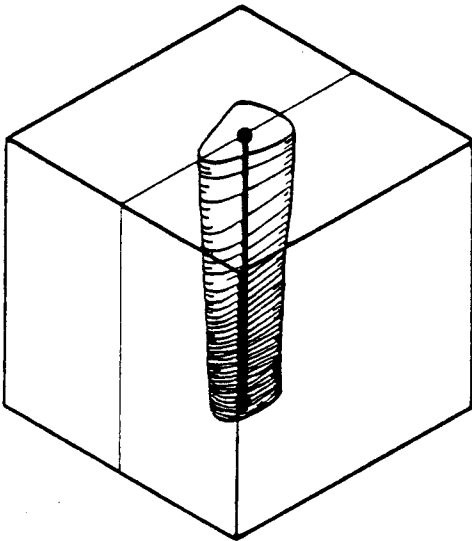
Symmetry



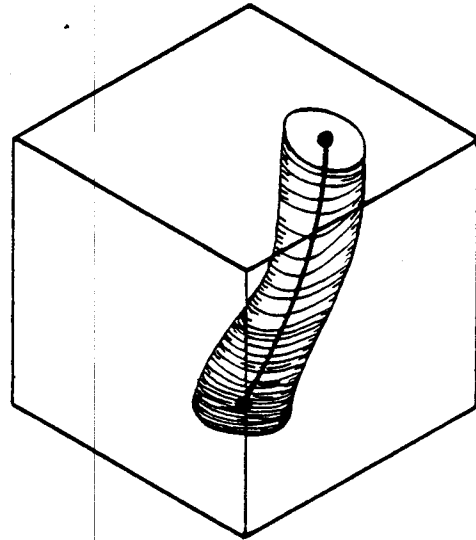
Axial - infinite number of planes of symmetry, one axis of symmetry



Orthorhombic - two planes of symmetry, one axis of symmetry

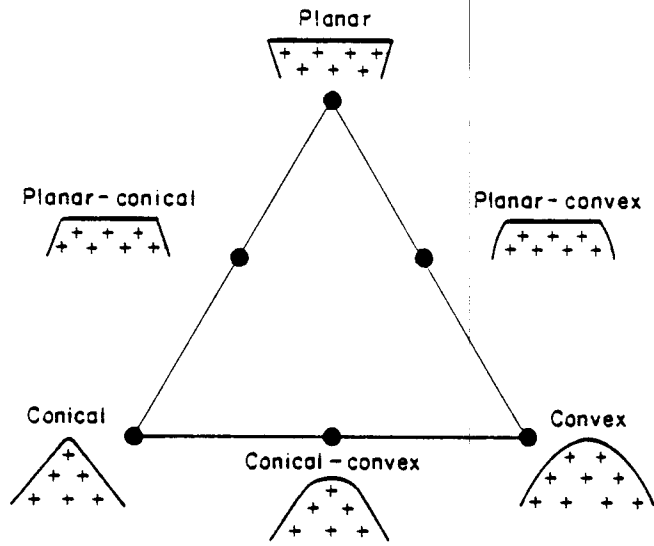


Monoclinic - one plane of symmetry, one axis of symmetry



Triclinic - no planes or axes of symmetry

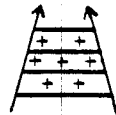
Crest shape



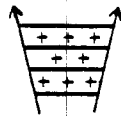
Sides

Cross section

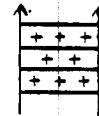
Upward converging



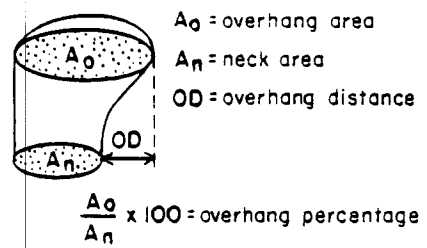
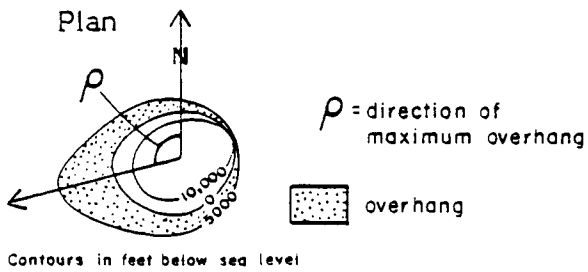
Upward diverging



Parallel

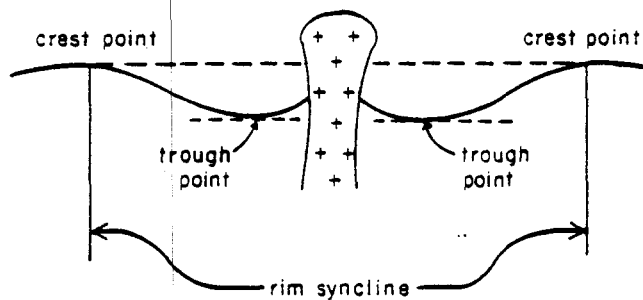


Overhang



### 1.7 GEOMETRY OF ADJOINING STRATA:

Lateral extent of rim anticline measured from trough point to trough point and rim syncline measured from crest point to crest point on dome cross sections.



Vertical variation in limb dip measured from dome cross sections.

$\delta$  = Dihedral angle between strata and dome flank.

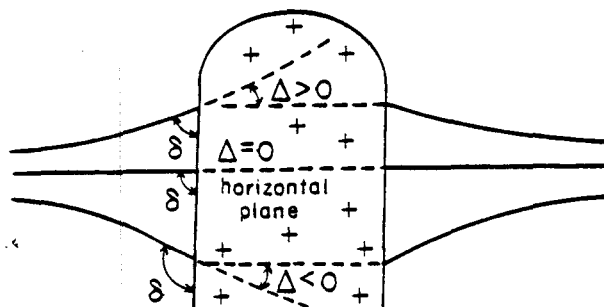
$\Delta$  = Dip of strata at flank of salt stock.

Note sign convention.

$\Delta > 0$  Strata dip away from dome.

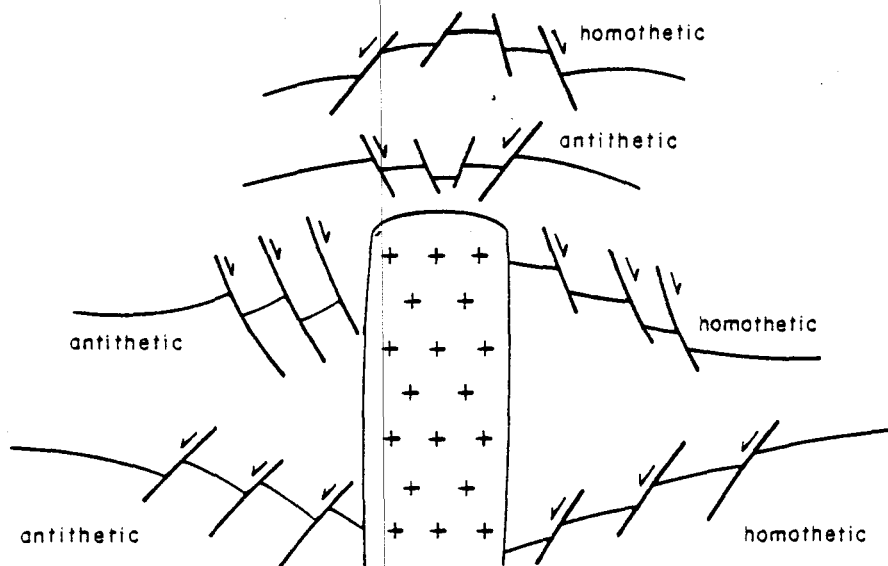
$\Delta = 0$  Strata are horizontal.

$\Delta < 0$  Strata dip toward dome.



### 1.8 FAULTING OF ADJACENT STRATA:

Usage after Cloos (1928) and Dennis and Kelley (1980).



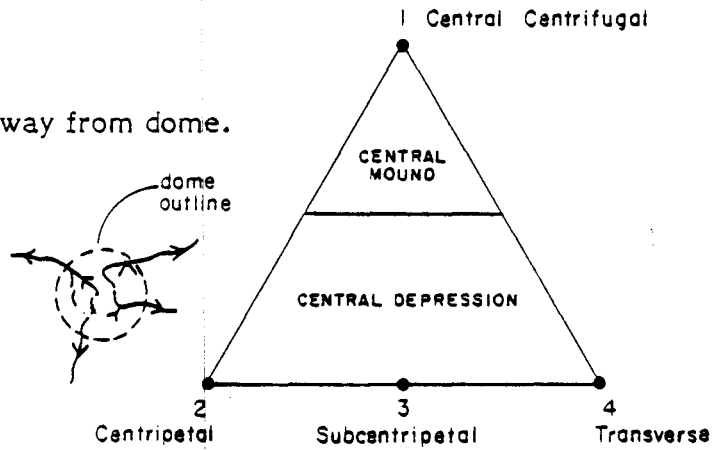
2.0 GROWTH HISTORY:

After Jackson and Seni (1983) and Seni and Jackson (in press).  
One million years equals 1 Ma.

2.7 EVIDENCE FOR COLLAPSE:

Drainage system

Type 1 - Centrifugal -- radial drainage away from dome.



Type 2 - Centripetal -- radial drainage toward center of dome.



Type 3 - Subcentripetal -- partial drainage toward center of dome.



Type 4 - Transverse -- drainage across dome.



1.0 DOME NAME: BETHEL

1.1 LOCATION: NW Anderson Co.  
31° 53' 23" N; 96° 54' 54" W

1.2 RESIDUAL GRAVITY EXPRESSION: -88 GU

1.3 DEPTH: Depth to Cap Rock: 1,440 ft (439 m)

Depth to Salt Stock: 1,600 ft (488 m)

Depth to Top of Louann Salt (approximate): 20,000 ft (6,100 m)

1.4 ORIENTATION AND MAXIMUM LATERAL DIMENSIONS OF SALT STOCK:

Major Axis: Length: 2.3 mi (3.7 km)  
Orientation: 015°

Minor Axis: Length: 1.9 mi (3.0 km)

Area: 3.4 mi<sup>2</sup> (8.7 km<sup>2</sup>)

Area of Planar Crest: 2.8 mi<sup>2</sup> (7.2 km<sup>2</sup>)

Percentage Planar Crest: 82%

1.5 SHAPE OF SALT STOCK:

General: Piercement stock

Plan: Elliptical (axial ratio: 1.2)

Cross Section:

Axis: Vertical, axial plunge 90°

Approximate Overall Symmetry: Orthorhombic

Crest: Planar-conical

Sides: Upward diverging from -2,500 ft to -5,000 ft (-762 m to -1,524 m);  
upward converging above -2,500 ft (-762 m); deepest data -5,000 ft (-1,524 m)

## BETHEL

**Overhang:** Well developed, circum-domal, symmetrical, elevation -2,500 ft (-762 m); maximum lateral overhang 2,100 ft (640 m) on S flank; percentage overhang 63%

### 1.6 CAP ROCK:

**Maximum Stratigraphic Thickness:** 493 ft (150 m) in center, thins toward flanks of dome

**Minimum Stratigraphic Thickness:** 62 ft (19 m)

**Composition:** Calcite, anhydrite

### 1.7 GEOMETRY OF ADJACENT STRATA:

**Lateral Extent of Rim Syncline:** 48,000 ft (14,600 m)

**Lateral Extent of Rim Anticline:** 12,000 ft (3,650 m)

**Vertical Variation in Maximum Limb Dip:**  $\Delta = -2$  to  $-6^\circ$  from elevation -1,650 ft to -10,000 ft (-500 to -3,000 m)  
 $\Delta = 0^\circ$  at -1,000 ft (-300 m)  
 $\Delta = +8^\circ$  above -1,000 ft (-300 m)

**$\delta$  Angle Between Salt and Surrounding Strata:**

$\delta \approx 90^\circ$  at -9,300 ft (-2,800 m) to -1,650 ft (-500 m),  
 $\delta = 20^\circ$  at -1,300 ft (-400 m), declines to  
 $\delta = 0^\circ$  at -650 ft (-200 m); ring fault below -200 m

**Oldest Planar Overburden:** Claiborne Group

### 1.8 FAULTING OF ADJACENT STRATA:

**Faults at Flanks:** On both sides, single offset, normal, antithetic, down-to-dome faults NW side, Woodbine and Eagle Ford age (growth). SE side, Paluxy age.

**Crestal Faults:** Single offset, normal, antithetic, down-to-dome fault on NW side.

**Youngest Faulted Strata:** Claiborne Group

**Oldest Strata Brought to Surface:** Claiborne Group

BETHEL

2.0 GROWTH HISTORY:

2.1 PRIMARY PERIPHERAL SINK:

Age of Initiation: Pre-112 Ma

Age of Cessation: 86 Ma

Duration of Growth: At least 26 Ma

Distance of Axial Trace from Center of Dome: 6 mi (10 km)

2.2 SECONDARY PERIPHERAL SINK:

Age of Initiation: 86 Ma

Age of Cessation: 50 Ma

2.3 TERTIARY PERIPHERAL SINK:

Age of Initiation: 50 Ma

Age of Cessation: Post-48 Ma

2.4 AGE OF MIGRATION OF SINK TO SALT-STOCK CONTACT: 73 Ma

2.5 DOME-RELATED UNCONFORMITIES: None recognized, but timing of diapirism is similar to that of Hainesville Dome

Evidence for Extrusion and Erosion of Salt: None recognized, but timing of diapirism is similar to that of Hainesville Dome.

2.6 YOUNGEST DEFORMATION: Fault in Wilcox Group

2.7 EVIDENCE FOR COLLAPSE:

Configuration of Overburden Strata: Flat-lying Claiborne Group

Drainage System: Type 4, supradomal depression, transverse drainage

Sinkholes: None

Surface Salines: None

3.0 RESOURCES AND USES:



1.0 **DOME NAME:** BOGGY CREEK

1.1 **LOCATION:** NE Anderson Co., NW Cherokee Co.  
31° 58' 07" N; 95° 26' 26" W

1.2 **RESIDUAL GRAVITY EXPRESSION:** -108 GU

1.3 **DEPTH:** Depth to Cap Rock: 1,692 ft (516 m)

Depth to Salt Stock: 1,829 ft (557 m)

Depth to Top of Louann Salt (approximate): 22,000 ft (6,700 m)

1.4 **ORIENTATION AND MAXIMUM LATERAL DIMENSIONS OF SALT STOCK:**

Major Axis: Length: > 9 mi (> 14 km)  
Orientation: 035°

Minor Axis: Length: > 2.5 mi (4.0 km)

Area: > 19.5 mi<sup>2</sup> (50 km<sup>2</sup>)

Area of Planar Crest: 2.3 mi<sup>2</sup> (5.9 km<sup>2</sup>)

Percentage Planar Crest: 12%

1.5 **SHAPE OF SALT STOCK:**

General: Elongated piercement stock

Plan: Highly elliptical (axial ratio 3.5), slightly sinuous

Cross Section:

Axis: Axial plunge 83°; tilt direction 013°; tilt distance 1,056 ft (322 m)

Approximate Overall Symmetry: Triclinic

Crest: Convex-planar, crestline depression near S end

Sides: Upward converging above -10,000 ft (-3,048 m); deepest data -10,000 ft (-3,048 m)

Overhang: None recognized above -10,000 ft (-3,048 m)

## BOGGY CREEK

### 1.6 CAP ROCK:

**Maximum Stratigraphic Thickness:** 123 ft (37 m) on upper flanks of dome, absent on dome crest

**Minimum Stratigraphic Thickness:** 14 ft (4 m)

**Composition:** Anhydrite, calcite

### 1.7 GEOMETRY OF ADJACENT STRATA:

**Lateral Extent of Rim Anticline:** 15,000 ft (4,570 m)

**Vertical Variation in Maximum Limb Dip:**  $\Delta = 0^\circ$  at -10,000 ft (-3,100 m) (Glen Rose)  
 $\Delta = +48^\circ$  at -5,000 ft (-1,500 m) (Woodbine)  
 $\Delta = +15^\circ$  at -1,500 ft (-500 m) (Wilcox)

**Angle Between Salt and Surrounding Strata:**  $\delta = 60^\circ$  extends upward to Washita at -2,000 m (-6,500 m)

**Oldest Planar Overburden:** Quaternary

### 1.8 FAULTING OF ADJACENT STRATA:

**Faults at Flanks:** Graben to SE, faulted in Taylor time

**Crestal Faults:** Antithetic, normal, down-to-dome, simple offset in Navarro time

**Youngest Faulted Strata:** Navarro Group

**Oldest Strata Brought to Surface:** Wilcox Group

### 2.0 GROWTH HISTORY:

#### 2.1 PRIMARY PERIPHERAL SINK:

**Age of Initiation:** Pre-112 Ma

**Age of Cessation:** Pre-112 Ma

**Duration of Growth:** Unknown

**Distance of Axial Trace from Center of Dome:** 4-6 mi (7-10 km)

#### 2.2 SECONDARY PERIPHERAL SINK:

**Age of Initiation:** Pre-112 Ma

**Age of Cessation:** 105 Ma

BOGGY CREEK

2.3 TERTIARY PERIPHERAL SINK:

Age of Initiation: 105 Ma

Age of Cessation: 48 Ma

2.4 AGE OF MIGRATION OF SINK TO SALT-STOCK CONTACT: Sink has not migrated to salt stock

2.5 DOME-RELATED UNCONFORMITIES:

Evidence for Extrusion and Erosion of Salt: None recognized

2.6 YOUNGEST DEFORMATION: Fault in upper Navarro Marl

2.7 EVIDENCE FOR COLLAPSE:

Configuration of Overburden Strata: Claiborne strata not present over dome crest, Quaternary alluvium present over dome crest

Drainage System: Type 4, central supradomal depression, transverse drainage

Sinkholes: None

Surface Salines: None

3.0 RESOURCES AND USES:

3.1 HYDROCARBONS:

Number of Producing Wells: Current: ?

Total: ?

Production: Current: 12,877 bbls - Woodbine; 222 bbls - Wilcox

Total: 6,751,841 bbls - Woodbine; 8,888 bbls - Wilcox ; 292,718 mcf (cumulative to 1980) - Woodbine

Stratigraphic Reservoir: Woodbine Group; Wilcox Group

Traps: Truncation by side of salt stock; supradomal fault or anticline (Wilcox)

3.2 BRINE: None

3.3 SULFUR: None

3.4 GAS STORAGE: None

1.0 DOME NAME: BROOKS

1.1 LOCATION: SW Smith Co.  
32° 09' 42" N; 95° 26' 38" W

1.2 RESIDUAL GRAVITY EXPRESSION: -134 G.U.

1.3 DEPTH: Depth to Cap Rock: 195 ft (59 m)

Depth to Salt Stock: 220 ft (67 m)

Depth to Top of Louann Salt (approximate): 21,000 ft (6,400 m)

1.4 ORIENTATION AND MAXIMUM LATERAL DIMENSIONS OF SALT STOCK:

Major Axis: Length: 3.5 mi (5.6 km)  
Orientation: 042°

Minor Axis: Length: 3.3 mi (5.3 km)

Area: 8.8 mi<sup>2</sup> (23 km<sup>2</sup>)

Area of Planar Crest: 2.7 mi<sup>2</sup> (6.9 km<sup>2</sup>)

Percentage Planar Crest: 31%

1.5 SHAPE OF SALT STOCK:

General: Piercement stock

Plan: Circular (axial ratio = 1.06)

Cross Section:

Axis: Vertical, axial plunge 90°

Approximate Overall Symmetry: Axial

Crest: Planar, conical

Sides: Upward diverging from -5,500 ft to -7,000 ft (-1,676 m to -2,134 m);  
upward converging above -5,500 ft (-1,676 m); deepest data -7,000 ft (-2,134 m)

## BROOKS

**Overhang:** Well-developed, circum-domal, symmetrical, elevation -5,500 ft (-1,676 m); maximum lateral overhang 600 ft (183 m) on N and S flanks; percentage overhang 18%.

### 1.6 CAP ROCK:

**Maximum Stratigraphic Thickness:** 268 ft (82 m)

**Minimum Stratigraphic Thickness:** 20 ft (6 m)

**Composition:** Calcite, anhydrite, gypsum

### 1.7 GEOMETRY OF ADJOINING STRATA:

**Lateral Extent of Rim Syncline:** 42,000 ft (12,800 m)

**Lateral Extent of Rim Anticline:** 18,000 ft (5,500 m)

**Vertical Variation in Maximum Limb Dip:**

|                      |                         |            |
|----------------------|-------------------------|------------|
| $\Delta = -10^\circ$ | at -10,000 ft (3,000 m) | Glen Rose  |
| $\Delta = 0^\circ$   | at -6,000 ft (-1,800 m) | U. Washita |
| $\Delta = +50^\circ$ | at -3,000 ft (-1,000 m) | Austin     |
| $\Delta = +10^\circ$ | at 0 ft (0 m)           | Claiborne  |

**Angle Between Salt and Surrounding Strata:**  $\delta = 130^\circ$ , extends upward to -1,300 m (-4,300 ft)(Woodbine)

**Oldest Planar Overburden:** None

### 1.8 FAULTING OF ADJACENT STRATA:

**Faults at Flanks:** No faults in section

**Crestal Faults:** None

**Youngest Faulted Strata:** None

**Oldest Strata Brought to Surface:** Austin Group

### 2.0 GROWTH HISTORY:

#### 2.1 PRIMARY PERIPHERAL SINK:

**Age of Initiation:** Pre-112 Ma

**Age of Cessation:** Pre-112 Ma

**Duration of Growth:** Unknown

**Distance of Axial Trace from Center of Dome:** 7 mi (12 km)

**BROOKS:**

**2.2 SECONDARY PERIPHERAL SINK:**

Age of Initiation: Pre-112 Ma

Age of Cessation: 92 Ma

**2.3 TERTIARY PERIPHERAL SINK:**

Age of Initiation: 92 Ma

Age of Cessation: Post-50 Ma

**2.4 AGE OF MIGRATION OF SINK TO SALT-STOCK CONTACT: 106 Ma**

**2.5 DOME-RELATED UNCONFORMITIES: None recognized**

Evidence for Extrusion and Erosion of Salt: None recognized

**2.6 YOUNGEST DEFORMATION: Unknown**

**2.7 EVIDENCE FOR COLLAPSE:**

Configuration of Overburden Strata: Claiborne and Wilcox strata absent over dome

Drainage System: Type 3, supradomal depression, subcentripetal drainage

Sinkholes: Man-made lake over dome crest

Surface Salines: Present

**3.0 RESOURCES AND USES:**

**3.1 HYDROCARBONS:**

Number of Producing Wells: Current: 0

Total: 1

Production: Current: 0

Total: 1,199 bbls

Stratigraphic Reservoir: Paluxy Formation

Traps: Beneath overhang

BROOKS

3.2 BRINE: Yes

3.3 SULFUR: None

3.4 GAS STORAGE: None

1.0 DOME NAME: BRUSHY CREEK

1.1 LOCATION: NE Anderson Co.  
31° 55' 27" N; 95° 35' 50" W

1.2 RESIDUAL GRAVITY EXPRESSION: -36 G.U.

1.3 DEPTH: Depth to Cap Rock: 3,522 ft (1,074 m)

Depth to Salt Stock: 3,570 ft (1,038 m)

Depth to Top of Louann Salt (approximate): 22,000 ft (6,700 m)

1.4 ORIENTATION AND MAXIMUM LATERAL DIMENSIONS OF SALT STOCK:

Major Axis: Length: >1.6 mi (>2.6 km)  
Orientation: None, circular

Minor Axis: Length: >1.56 mi (>2.5 km)

Area: >1.9 mi<sup>2</sup> (>4.9 km<sup>2</sup>)

Area of Planar Crest: 0.5 mi<sup>2</sup> (1.3 km<sup>2</sup>)

Percentage Planar Crest: 26%

1.5 SHAPE OF SALT STOCK:

General: Probably piercement stock (configuration below -4,000 ft [-1,219 m ]  
unknown)

Plan: Circular (axial ratio = 1.03)

Cross Section:

Axis: Insufficient deep data

Approximate Overall Symmetry: Unknown

Crest: Convex-conical

Sides: Upward converging above -4,000 ft (-1,219 m); deepest data -4,000 ft  
(-1,219 m)

## BRUSHY CREEK

**Overhang:** None recognized above -4,000 ft (-1,219 m)

### 1.6 CAP ROCK:

**Maximum Stratigraphic Thickness:** 187 ft (57 m) on upper flanks of dome, absent on dome crest

**Minimum Stratigraphic Thickness:** 81 ft (25 m)

**Composition:** Calcite, anhydrite, minor celestite

### 1.7 GEOMETRY OF ADJOINING STRATA:

**Lateral Extent of Rim Syncline:** 25,500 ft (7,800 m)

**Lateral Extent of Rim Anticline:** 15,000 ft (4,570 m)

**Vertical Variation in Maximum Limb Dip:**  $\Delta = -3^\circ$  at -11,000 ft (3,350 m) Hosston  
 $\Delta = 0^\circ$  from -7,000 ft (-2,100 m) Paluxy  
to -4,500 ft (1,370 m) Austin  
 $\Delta$  decreases from  $+15^\circ$  at 3,000 ft (-900 m)  
to  $+5^\circ$  at 0 ft (0 m)

**Angle Between Salt and Surrounding Strata:**  $\delta \sim 90^\circ$  at -11,500 ft (-3,500 m)  
declining to  
 $\delta = 40^\circ$  at -4,000 ft (-1,200 m) and  
 $\delta = 0^\circ$  at -3,300 ft (-1,000 m)

**Oldest Planar Overburden:** None

### 1.8 FAULTING OF ADJACENT STRATA:

**Faults at Flanks:** SW side: multiple offset, normal, down-to-dome, antithetic (m. Glen Rose); multiple offset, normal, up-to-dome, antithetic (Paluxy); normal, down-to-dome (Austin)

**Crestal Faults:** Central graben, antithetic pair, in domal crest

**Youngest Faulted Strata:** Claiborne Group

**Oldest Strata Brought to Surface:** Claiborne Group

### 2.0 GROWTH HISTORY:

#### 2.1 PRIMARY PERIPHERAL SINK:

**Age of Initiation:** Pre-112 Ma

BRUSHY CREEK

Age of Cessation: Pre-112 Ma

Duration of Growth: Unknown

Distance of Axial Trace from Center of Dome: 5-8 mi (8-13 km)

2.2 SECONDARY PERIPHERAL SINK:

Age of Initiation: Pre-112 Ma

Age of Cessation: 105 Ma

2.3 TERTIARY PERIPHERAL SINK:

Age of Initiation: 105 Ma

Age of Cessation: Post-48 Ma

2.4 AGE OF MIGRATION OF SINK TO SALT-STOCK CONTACT: Sink has not migrated to salt stock

2.5 DOME-RELATED UNCONFORMITIES: None recognized

Evidence for Extrusion and Erosion of Salt: None recognized

2.6 YOUNGEST DEFORMATION: Fault in Claiborne Group

2.7 EVIDENCE FOR COLLAPSE: Central graben over dome crest

Configuration of Overburden Strata: Central graben over dome crest

Drainage System: Type 4, transverse drainage

Sinkholes: None

Surface Salines: None

3.0 RESOURCES AND USES:

3.1 HYDROCARBONS: 2 Fields; Purt (Woodbine) & West Purt (Rodessa)

Number of Producing Wells: Current: 2 (West Purt; Purt)

Total: 6 (1 Rodessa; 5 Woodbine)

Production: Current: 3,866 bbls (Purt)  
2,087 bbls (West Purt)

Total: 137,976 bbls (Purt)  
35,992 bbls (West Purt)

BRUSHY CREEK

**Stratigraphic Reservoir:** Woodbine Group (Purt); Rodessa Member (West Purt)

**Traps:** Supradomal faults and anticline (Purt); flank fault (West Purt)

3.2 **BRINE:** None

3.3 **SULFUR:** None

3.4 **GAS STORAGE:** None

1.0 DOME NAME: BULLARD

1.1 LOCATION: S central Smith Co.  
32° 09' 20" N; 95° 17' 38" W

1.2 RESIDUAL GRAVITY EXPRESSION: -48 G.U.

1.3 DEPTH: Depth to Cap Rock: 375 ft (114 m)

Depth to Salt Stock: 527 ft (161 m)

Depth to Top of Louann Salt (approximate): 22,000 ft (6,700 m)

1.4 ORIENTATION AND MAXIMUM LATERAL DIMENSIONS OF SALT STOCK:

Major Axis: Length: 1 mi (1.6 km)  
at -4,000 ft  
Orientation: 095°

Major axis: Length: 2.6 mi (4.2 km)  
at -10,000 ft  
Orientation: 058°

Minor Axis: Length: 0.5 mi<sup>2</sup> (1.3 km<sup>2</sup>)

Minor axis: Length: 2.5 mi (4.0 km)

Area: 0.5 mi<sup>2</sup> (1.3 km<sup>2</sup>)

Area: 5.0 mi<sup>2</sup> (12.8 km<sup>2</sup>)

Area of Planar Crest: 0.1 mi<sup>2</sup> (0.26 km<sup>2</sup>)

Percentage Planar Crest: 20%

1.5 SHAPE OF SALT STOCK:

General: Piercement stock

Plan: Irregular; circular (axial ratio = 1.07) at -6,000 ft to -10,000 ft (-1,828 m to -3,048 m); elliptical (axial ratio = 1.8) above -6,000 ft (-1,828 m)

Cross Section:

Axis: Axial plunge 75°; tilt direction 213°; tilt distance 2,112 ft (644 m)

Approximate Overall Symmetry: Triclinic

Crest: Convex upward

Sides: Irregularly upward converging above -10,000 ft (-3,048 m); deepest data -10,000 ft (-3,048 m)

Overhang: Minor overhang on W flank, elevation -4,000 ft (-1,219 m); maximum lateral overhang 500 ft (152 m)

BULLARD

1.6 CAP ROCK:

Maximum Stratigraphic Thickness: 152 ft (46 m)

Minimum Stratigraphic Thickness: 145 ft (44 m)

Composition: Anhydrite, calcite

1.7 GEOMETRY OF ADJOINING STRATA:

Lateral Extent of Rim Syncline: 24,000 ft (7,300 m)

Lateral Extent of Rim Anticline: 9,000 ft (2,740 m)

Vertical Variation in Maximum Limb Dip:  $\Delta = 2^\circ$  at 4,900 ft (-1,500 m) Woodbine  
 $\Delta = 0^\circ$  at -4,500 ft (1,370 m) Austin Chalk  
 $\Delta = +35^\circ$  at 3,000 ft (914 m) Pecan Gap  
decreases to  $+5^\circ$  at 0 ft Claiborne

Angle Between Salt and Surrounding Strata:  $\delta > 30^\circ$ , extends upward to 0 ft (Claiborne)

Oldest Planar Overburden: None

1.8 FAULTING OF ADJACENT STRATA:

Faults at Flanks: No faults in section

Crestal Faults: No faults in section

Youngest Faulted Strata: None faulted

Oldest Strata Brought to Surface: Queen City Formation

2.0 GROWTH HISTORY:

2.1 PRIMARY PERIPHERAL SINK:

Age of Initiation: Pre-112 Ma

Age of Cessation: Pre-112 Ma

Duration of Growth: Unknown

Distance of Axial Trace from Center of Dome: 5-6 mi (8-10 km)

BULLARD

2.2 SECONDARY PERIPHERAL SINK:

Age of Initiation: Pre-112 Ma

Age of Cessation: Pre-112 Ma

2.3 TERTIARY PERIPHERAL SINK:

Age of Initiation: Pre-112 Ma

Age of Cessation: Post-48 Ma

2.4 AGE OF MIGRATION OF SINK TO SALT-STOCK CONTACT: Unknown

2.5 DOME-RELATED UNCONFORMITIES: None recognized

Evidence for Extrusion and Erosion of Salt: None recognized

2.6 YOUNGEST DEFORMATION: Wilcox strata arch over dome crest

2.7 EVIDENCE FOR COLLAPSE:

Configuration of Overburden Strata: Claiborne strata flat lying over crest of dome

Drainage System: Type 3, subcentripetal drainage

Sinkholes: None

Surface Salines: None

3.0 RESOURCES AND USES:

3.1 HYDROCARBONS:

Number of Producing Wells: Current: 0

Total: 0

Production: Current: 0

Total: 0

Stratigraphic Reservoir: None

Traps: None

3.2 BRINE: None

3.3 SULFUR: None

3.4 GAS STORAGE: None

1.0 DOME NAME: BUTLER

1.1 LOCATION: SE Freestone Co.  
31° 40' 07" N; 95° 51' 52" W

1.2 RESIDUAL GRAVITY EXPRESSION: -80 G.U.

1.3 DEPTH: Depth to Cap Rock: No caprock

Depth to Salt Stock: 312 ft (95 m)

Depth to Top of Louann Salt (approximate): 21,000 ft (6,400 m)

1.4 ORIENTATION AND MAXIMUM LATERAL DIMENSIONS OF SALT STOCK:

Major Axis: Length: 2.5 mi (4.0 km)  
Orientation: 055°

Minor Axis: Length: 2.2 mi (3.6 km)

Area: 4.4 mi<sup>2</sup> (11.3 km<sup>2</sup>)

Area of Planar Crest: 0.5 mi<sup>2</sup> (1.3 km<sup>2</sup>)

Percentage Planar Crest: 11%

1.5 SHAPE OF SALT STOCK:

General: Piercement stock

Plan: Slightly elliptical (axial ratio = 1.1)

Cross Section:

Axis: Vertical, axial plunge 90°

Approximate Overall Symmetry: Orthorhombic

Crest: Conical-planar

Sides: Upward diverging from -5,000 ft to -8,000 ft (-1,524 m to -2,438 m);  
upward converging above -5,000 ft (-1,524 m); deepest data  
-8,000 ft (-2,438 m)

Overhang: Moderate, circum-domal, symmetrical, elevation -5,000 ft (-1,524 m),  
maximum lateral overhang 1,200 ft (366 m) on N flank; percentage  
overhang 24%

BUTLER

1.6 CAP ROCK:

Maximum Stratigraphic Thickness: Cap rock absent

Minimum Stratigraphic Thickness: Cap rock absent

Unusual calcite-cemented Carrizo Formation (false cap rock) overlies NW flank of dome

1.7 GEOMETRY OF ADJOINING STRATA:

Lateral Extent of Rim Syncline: 32,800 ft (7,500 m)

Lateral Extent of Rim Anticline: 16,400 ft (3,750 m)

Vertical Variation in Maximum Limb Dip:  $\Delta = -13^\circ$  at -9,000 ft (2,750 m)  
 $\Delta = 0^\circ$  at -5,600 ft (-1,700 m)  
 $\Delta = +30^\circ$  at -1,600 ft (-500 m)

Angle Between Salt and Surrounding Strata:  $\delta = 115^\circ$ , extends upwards to U. Taylor Group

Oldest Planar Overburden: None

1.8 FAULTING OF ADJACENT STRATA:

Faults at Flanks: None

Crestal Faults: One in SW, normal, homothetic, up-to-dome, simple offset, central half-horst of trapdoor type (L. Austin Group to surface)

Youngest Faulted Strata: Claiborne Group

Oldest Strata Brought to Surface: Navarro Group

2.0 GROWTH HISTORY:

2.1 PRIMARY PERIPHERAL SINK:

Age of Initiation: 150 Ma

Age of Cessation: 135 Ma

Duration of Growth: 15 Ma

Distance of Axial Trace from Center of Dome: 5-7 mi (8-11 km)

BUTLER

2.2 SECONDARY PERIPHERAL SINK:

Age of Initiation: 135 Ma

Age of Cessation: 125 Ma

2.3 TERTIARY PERIPHERAL SINK:

Age of Initiation: 125 Ma

Age of Cessation: Post-48 Ma

2.4 AGE OF MIGRATION OF SINK TO SALT-STOCK CONTACT: 112 Ma

2.5 DOME-RELATED UNCONFORMITIES: Common in Claiborne strata above salt stock.

Evidence for Extrusion and Erosion of Salt: None recognized

2.6 YOUNGEST DEFORMATION: Fault in Claiborne Group

2.7 EVIDENCE FOR COLLAPSE:

Configuration of Overburden Strata: Anticlinal

Drainage System: Type 2, supradomal depression, central centripetal drainage  
Man-made lake over NE flank.

Sinkholes: Common

Surface Salines: Present

3.0 RESOURCES AND USES:

3.1 HYDROCARBONS:

Number of Producing Wells: Current: 0

Total: 1

Production: Current: 0

Total: 763 bbls

Stratigraphic Reservoir: Woodbine Group

Traps: Truncation by side of salt stock

3.2 BRINE: None

3.3 SULFUR: None

3.4 GAS STORAGE: 3 wells for ethane storage

1.0 DOME NAME: EAST TYLER

1.1 LOCATION: Central Smith Co.  
32° 22' 30" N; 95° 15' 45" W

1.2 RESIDUAL GRAVITY EXPRESSION: -84 G.U.

1.3 DEPTH: Depth to Cap Rock: 800 ft (244 m)

Depth to Salt Stock: 890 ft (271 m)

Depth to Top of Louann Salt (approximate): 21,000 ft (6,400 m)

1.4 ORIENTATION AND MAXIMUM LATERAL DIMENSIONS OF SALT STOCK:

Major Axis: Length: 3.3 mi (5.2 km)  
Orientation: 080°

Minor Axis: Length: 2.9 mi (4.6 km)

Area: 7.4 mi<sup>2</sup> (19 km<sup>2</sup>)

Area of Planar Crest: 0.7 mi<sup>2</sup> (1.8 km<sup>2</sup>)

Percentage Planar Crest: 9%

1.5 SHAPE OF SALT STOCK:

General: Piercement stock

Plan: Slightly elliptical (axial ratio = 1.1)

Cross Section:

Axis: Axial plunge 83°; tilt direction 305°; tilt distance 520 ft (158 m)

Approximate Overall Symmetry: Monoclinic

Crest: Convex-planar, small trough in SE flank

Sides: Upward diverging from -5,000 ft to -6,000 ft (-1,524 m to -1,829 m)  
along NE flank; upward converging above -5,000 ft (-1,524 m);  
deepest data -6,000 ft (-1,829 m) on NE flank, -5,000 ft (-1,524 m) elsewhere

## EAST TYLER

**Overhang:** Moderate overhang on NE flank only, insufficient data elsewhere; maximum lateral overhang (on NE flank) 600 ft (183 m); percentage overhang 5% (assuming symmetrical shape)

### 1.6 CAP ROCK:

**Maximum Stratigraphic Thickness:** 277 ft (84 m)

**Minimum Stratigraphic Thickness:** 90 ft (27 m)

**Composition:** Anhydrite, calcite

### 1.7 GEOMETRY OF ADJOINING STRATA:

**Lateral Extent of Rim Syncline:** 28,500 ft (8,687 m)

**Lateral Extent of Rim Anticline:** 13,500 ft (4,115 m)

**Vertical Variation in Maximum Limb Dip:**  $\Delta = 5^\circ$  at -4,600 ft (-1,500 m) Woodbine  
 $\Delta = 0^\circ$  at -2,500 ft (760 m) U. Navarro Marl  
 $\Delta = +15^\circ$  at -1,640 ft (500 m) Wilcox

**Angle Between Salt and Surrounding Strata:**  $\delta = 50^\circ$  at -6,000 ft (-1,829 m)  
 $\delta = 0^\circ$  at -4,600 ft (-1,500 m)  
 $\delta = +20^\circ$  at -1,640 ft (-500 m)

**Oldest Planar Overburden:** Claiborne Group

### 1.8 FAULTING OF ADJACENT STRATA:

**Faults at Flanks:** None

**Crestal Faults:** Homothetic, normal, up-to-dome on S flank

**Youngest Faulted Strata:** Wilcox Group

**Oldest Strata Brought to Surface:** Sparta Formation

### 2.0 GROWTH HISTORY:

#### 2.1 PRIMARY PERIPHERAL SINK:

**Age of Initiation:** Pre-112 Ma

**Age of Cessation:** Pre-112 Ma

**Duration of Growth:** Unknown

EAST TYLER

Distance of Axial Trace from Center of Dome: 3-5 mi (5-8 km)

2.2 SECONDARY PERIPHERAL SINK:

Age of Initiation: Pre-112 Ma

Age of Cessation: 92 Ma

2.3 TERTIARY PERIPHERAL SINK:

Age of Initiation: 92 Ma

Age of Cessation: Post-48

2.4 AGE OF MIGRATION OF SINK TO SALT-STOCK CONTACT: 112 Ma

2.5 DOME-RELATED UNCONFORMITIES: None recognized

Evidence for Extrusion and Erosion of Salt: None recognized

2.6 YOUNGEST DEFORMATION: Fault in Wilcox Group

2.7 EVIDENCE FOR COLLAPSE:

Configuration of Overburden Strata: Claiborne strata arch over dome crest

Drainage System: Type 2, central supradomal depression, central centripetal drainage

Sinkholes: None

Surface Salines: None

3.0 RESOURCES AND USES:

3.1 HYDROCARBONS:

Number of Producing Wells: Current: 0

Total: 0

Production: Current: 0

Total: 0

Stratigraphic Reservoir: None

Traps: None

EAST TYLER

3.2 BRINE: None

3.3 SULFUR: None

3.4 GAS STORAGE: 9 wells

1.0 DOME NAME: GRAND SALINE

1.1 LOCATION: NE Van Zandt Co.  
32° 39' 58" N; 95° 42' 34" W

1.2 RESIDUAL GRAVITY EXPRESSION: -56 G.U.

1.3 DEPTH: Depth to Cap Rock: 171 ft (52 m)

Depth to Salt Stock: 213 ft (65 m)

Depth to Top of Louann Salt (approximate): 20,000 ft (6,100 m)

1.4 ORIENTATION AND MAXIMUM LATERAL DIMENSIONS OF SALT STOCK:

Major Axis: Length: 1.6 mi (2.6 km)  
Orientation: 050°

Minor Axis: Length: 1.5 mi (2.4 km)

Area: 2.1 mi<sup>2</sup> (5.4 km<sup>2</sup>)

Area of Planar Crest: 1.8 mi<sup>2</sup> (4.6 km<sup>2</sup>)

Percentage Planar Crest: 86%

1.5 SHAPE OF SALT STOCK:

General: Piercement stock

Plan: Circular (axial ratio 1.07) at -100 ft (-30 m); elliptical (axial ratio 1.3)  
at -3,000 ft (-914 m)

Cross Section:

Axis: Axial plunge 74°; tilt direction 339°; tilt distance 2,112 ft (644 m)

Approximate Overall Symmetry: Monoclinic

Crest: Planar

Sides: Parallel above -7,500 ft (-2,286 m);  
deepest data -7,500 ft (-2,286 m)

Overhang: Minor overhang on SE flank, elevation -6,500 ft (-1,981 m);  
Maximum lateral overhang 500 ft (152 m); percentage overhang 10%;  
axial tilt produces apparent overhang on NW flank of 2,640 ft (805 m).

## GRAND SALINE

### 1.6 CAP ROCK:

Maximum Stratigraphic Thickness: 61 ft (19 m)

Minimum Stratigraphic Thickness: 5 ft (2 m)

Composition: Anhydrite, gypsum, calcite

### 1.7 GEOMETRY OF ADJOINING STRATA:

Lateral Extent of Rim Syncline: None above -7,500 ft (-2,286 m)

Lateral Extent of Rim Anticline: 21,000 ft (6,400 m)

Vertical Variation in Maximum Limb Dip:  $\Delta = +5^\circ$  at -6,000 ft (-1,800 m) Washita  
 $\Delta = +5^\circ$  at 0 ft Wilcox

Angle Between Salt and Surrounding Strata:  $\delta = 85^\circ$ , extends from 2,600 m (8,600 ft)  
(mid. Glen Rose) to  $\delta = 30^\circ$  at 0 m (Wilcox)  
at crest

Oldest Planar Overburden: Wilcox Group

### 1.8 FAULTING OF ADJACENT STRATA:

Faults at Flanks: Small graben on NE flank

Crestal Faults: None

Youngest Faulted Strata: Woodbine Group

Oldest Strata Brought to Surface: Wilcox Group

### 2.0 GROWTH HISTORY:

#### 2.1 PRIMARY PERIPHERAL SINK:

Age of Initiation: Pre-112 Ma

Age of Cessation: Pre-112 Ma

Duration of Growth: Unknown

Distance of Axial Trace from Center of Dome: 3-5 mi (5-8 km)

GRAND SALINE

2.2 SECONDARY PERIPHERAL SINK:

Age of Initiation: Pre-112 Ma

Age of Cessation: Unknown

2.3 TERTIARY PERIPHERAL SINK:

Age of Initiation: Pre-112 Ma

Age of Cessation: Post-48 Ma

2.4 AGE OF MIGRATION OF SINK TO SALT-STOCK CONTACT: 98 Ma

2.5 DOME-RELATED UNCONFORMITIES: None recognized

Evidence for Extrusion and Erosion of Salt: None recognized

2.6 YOUNGEST DEFORMATION: Unknown

2.7 EVIDENCE FOR COLLAPSE:

Configuration of Overburden Strata: Wilcox strata flat lying over dome

Drainage System: Type 2 central supradomal depression, central centripetal drainage

Sinkholes: Common, central marshy area

Surface Salines: Present

3.0 RESOURCES AND USES:

3.1 HYDROCARBONS:

Number of Producing Wells: Current: 1

Total: 1

Production: Current: 3,854 bbls

Total: 84,463 bbls

Stratigraphic Reservoir: Paluxy Formation

Traps: Flank fault

GRAND SALINE

3.2 BRINE: Yes

3.3 SULFUR: None

3.4 GAS STORAGE: None

- 1.0 DOME NAME: HAINESVILLE
- 1.1 LOCATION: S central Wood Co.;  
32° 41' 40" N; 95° 22' 20" W
- 1.2 RESIDUAL GRAVITY EXPRESSION: -110 GU
- 1.3 DEPTH: Depth to Cap Rock: 1,100 ft (335 m)  
Depth to Salt Stock: 1,200 ft (366 m)  
Depth to Top of Louann Salt (approximate): 20,000 ft (6,100 m)
- 1.4 ORIENTATION AND MAXIMUM LATERAL DIMENSIONS OF SALT STOCK:
- Major Axis: Length: 4.3 mi (6.9 km)  
Orientation: 040°
- Minor Axis: Length: 3.2 mi (5.1 km)
- Area: 8.9 mi<sup>2</sup> (22.9 km<sup>2</sup>)
- Area of Planar Crest: 4.8 mi<sup>2</sup> (12.2 km<sup>2</sup>)
- Percentage Planar Crest: 54%
- 1.5 SHAPE OF SALT STOCK:
- General: Piercement stock
- Plan: Elliptical (axial ratio = 1.3), small lobes on NE and SW flanks
- Cross Section:
- Axis: Vertical, axial plunge 90°
- Approximate Overall Symmetry: Monoclinic
- Crest: Planar-convex
- Sides: Upward converging from -10,000 ft to -15,000 ft (-3,048 m to -4,572 m);  
upward diverging from -4,000 ft to -10,000 ft (-1,219 m to -3,048 m);  
upward converging above -4,000 ft (-1,219 m)

## HAINESVILLE

**Overhang:** Broad, circum-domal, symmetrical, elevation -3,000 ft (-914 m); maximum lateral overhang 8,400 ft (2,560 m) on NE flank; percentage overhang 226%.

### 1.6 CAP ROCK:

**Maximum Stratigraphic Thickness:** 105 ft (32 m)

**Minimum Stratigraphic Thickness:** 43 ft (13 m)

**Composition:** Anhydrite

### 1.7 GEOMETRY OF ADJOINING STRATA:

**Lateral Extent of Rim Syncline:** 54,000 ft (16,450 m)

**Lateral Extent of Rim Anticline:** 21,000 ft (6,400 m)

**Vertical Variation in Maximum Limb Dip:**  $\Delta = -7^\circ$  at -8,000 ft (-2,450 m) Woodbine  
 $\Delta = 0^\circ$  at -1,500 ft (450 m) Wilcox  
 $\Delta = +30^\circ$  at -1,200 ft (365 m) Wilcox

**Angle Between Salt and Surrounding Strata:**  $\delta = 90^\circ$  at -7,500 ft (2,300 m) Austin  
 $\delta = 150^\circ$  at -4,000 ft (-1,200 m) Pecan Gap  
 $\delta = 0^\circ$  at -1,000 ft (-300 m) Wilcox

**Oldest Planar Overburden:** Claiborne Group

### 1.8 FAULTING OF ADJACENT STRATA:

**Faults at Flanks:** None

**Crestal Faults:** None

**Evidence for Growth Faulting:** None

**Youngest Faulted Strata:** Wilcox Group

**Oldest Strata Brought to Surface:** Wilcox Group

### 2.0 GROWTH HISTORY:

#### 2.1 PRIMARY PERIPHERAL SINK:

**Age of Initiation:** Pre-112 Ma

**Age of Cessation:** 86 Ma

## HAINESVILLE

**Duration of Growth:** At least 26 Ma

**Distance of Axial Trace from Center of Dome:** 5-7 mi (8-12 km)

### 2.2 SECONDARY PERIPHERAL SINK:

**Age of Initiation:** 86 Ma

**Age of Cessation:** 60 Ma

### 2.3 TERTIARY PERIPHERAL SINK:

**Age of Initiation:** 60 Ma

**Age of Cessation:** Post-48 Ma

### 2.4 AGE OF MIGRATION OF SINK TO SALT-STOCK CONTACT: 73 Ma

### 2.5 DOME-RELATED UNCONFORMITIES: Common in Lower and Upper Cretaceous

**Evidence for Extrusion and Erosion of Salt:** Unconformities, large volume of salt withdrawn, small volume of salt dissolved to form cap rock.

### 2.6 YOUNGEST DEFORMATION: Faults in Wilcox strata

### 2.7 EVIDENCE FOR COLLAPSE:

**Configuration of Overburden Strata:** Wilcox strata downfaulted over crest of dome

**Drainage System:** Type 4, central supradomal depression, transverse drainage

**Sinkholes:** Common

**Surface Salines:** None

### 3.0 RESOURCES AND USES:

#### 3.1 HYDROCARBONS: 3 Fields: Hainesville, Hainesville Dome, Neuhoff

**Number of Producing Wells:** **Current:** 0 (Hainesville Field);  
1 (Hainesville Dome Field); ? (Neuhoff Field)

**Total:** 1 (Hainesville Field);  
2 (Hainesville Dome Field); ?(Neuhoff Field)

HAINESVILLE

Production:      Current }  
                  Total    } see chart below

Stratigraphic Reservoir:      Woodbine Group, Paluxy Formation (Neuhoff); Hosston Formation (Hainesville Dome); Sub-Clarksville Member (Hainesville)

Traps:      Hosston Formation, all production beneath overhang, associated with possible angular unconformity

3.2 BRINE: None

3.3 SULFUR: None

3.4 GAS STORAGE: Yes

HAINESVILLE

|                         | <u>Current<br/>Oil Production<br/>(bbls)</u> | <u>Total<br/>Oil Production<br/>(bbls)</u> | <u>Current<br/>Gas Production<br/>(mcf)</u> | <u>Total<br/>Gas Production<br/>(mcf)</u> |
|-------------------------|--|--|---|---|
| Hainesville Field:      |  |  |   |   |
| Sub-Clarksville         | 0  | 0  | 0   | 3,882,866                                 |
| Hainesville Dome Field: |  |  |   |   |
| Hosston                 | 1,038  | 37,443                                     | 0   | 0   |
| Neuhoff Field:          |  |  |   |   |
| Woodbine                | 311,104                                      | 364,440                                    | 0   | 0   |
| Paluxy                  | 4,575  | 4,575                                      | 0   | 0   |

1.0 DOME NAME: KEECHI

1.1 LOCATION: Central Anderson  
31° 50' 19" N; 95° 42' 20" W

1.2 RESIDUAL GRAVITY EXPRESSION: -128 GU

1.3 DEPTH: Depth to Cap Rock: 250 ft (76 m)

Depth to Salt Stock: 300 ft (91 m)

Depth to Top of Louann Salt (approximate): 21,000 ft (6,400 m)

1.4 ORIENTATION AND MAXIMUM LATERAL DIMENSIONS OF SALT STOCK:

Major Axis: Length: >4.6 mi (>7.4 km)  
Orientation: 015°

Minor Axis: Length: >1.7 mi (>2.7 km)

Area: >5.9 mi (>15 km<sup>2</sup>)

Area of Planar Crest: 0.2 mi<sup>2</sup> (0.5 km<sup>2</sup>)

Percentage Planar Crest: 3%

1.5 SHAPE OF SALT STOCK:

General: Elongate piercement stock

Plan: Highly elliptical (axial ratio = 2.7)

Cross Section:

Axis: Axial plunge 8°; tilt direction 059°; tilt distance 686 ft (209 m)

Approximate Overall Symmetry: Monoclinic

Crest: Convex-planar

Sides: Upward converging above -20,000 ft (-6,096 m)

## KEECHI

**Overhang:** Minor overhang on SSE flank, elevation -2,000 ft (610 m);  
maximum lateral overhang 500 ft (152 m); percentage overhang  $\approx$  1%.

### 1.6 CAP ROCK:

**Maximum Stratigraphic Thickness:** 300 ft (91 m)

**Minimum Stratigraphic Thickness:** Zero

**Composition:** Anhydrite

### 1.7 GEOMETRY OF ADJOINING STRATA:

**Lateral Extent of Rim Syncline:** None present above 20,000 ft (6,096 m)

**Lateral Extent of Rim Anticline:** 30,000 ft (9,144 m)

**Vertical Variation in Maximum Limb Dip:**  $\Delta = +20^\circ$  at -4,900 ft (-7,500 m) Woodbine  
 $\Delta = +10^\circ$  at -1,000 ft (300 m) Wilcox

**Angle Between Salt and Surrounding Strata:**  $\delta = 68^\circ$  at 2,250 ft (-685 m)  
 $\delta = 20^\circ$  at -500 ft (-150 m)

**Oldest Planar Overburden:** Claiborne Group

### 1.8 FAULTING OF ADJACENT STRATA:

**Faults at Flanks:** None

**Crestal Faults:** Simple graben on N flank, antithetic pair

**Youngest Faulted Strata:** Claiborne Group

**Oldest Strata Brought to Surface Group:** Taylor Group

### 2.0 GROWTH HISTORY:

#### 2.1 PRIMARY PERIPHERAL SINK:

**Age of Initiation:** 150 Ma

**Age of Cessation:** 135 Ma

**Duration of Growth:** 15 Ma

**Distance of Axial Trace from Center of Dome:** 7-8 mi (11-13 km)

KEECHI

2.2 SECONDARY PERIPHERAL SINK:

Age of Initiation: 135 Ma

Age of Cessation: 125 Ma

2.3 TERTIARY PERIPHERAL SINK:

Age of Initiation: 125 Ma

Age of Cessation: Post-48 Ma

2.4 AGE OF MIGRATION OF SINK TO SALT-STOCK CONTACT: 105 Ma

2.5 DOME-RELATED UNCONFORMITIES: None recognized

Evidence for Extrusion and Erosion of Salt: None recognized

2.6 YOUNGEST DEFORMATION: Faults through Wilcox Group to surface

2.7 EVIDENCE FOR COLLAPSE:

Configuration of Overburden Strata: Crestal grabens over dome

Drainage System: Type 4, supradomal depression, transverse drainage

Sinkholes: None reported

Surface Salines: Present

3.0 RESOURCES AND USES:

3.1 HYDROCARBONS:

Number of Producing Wells: Current: 0

Total: 0

Production: Current: 0

Total: 0

Stratigraphic Reservoir: None

Traps: None

KEECHI

3.2 BRINE: None

3.3 SULFUR: None

3.4 GAS STORAGE: None

1.0 DOME NAME: MOUNT SYLVAN

1.1 LOCATION: W. Central Smith Co.  
32° 23' 09" N; 95° 26' 55" W

1.2 RESIDUAL GRAVITY EXPRESSION: -104 GU

1.3 DEPTH: Depth to Cap Rock: 550 ft (168 m)

Depth to Salt Stock: 613 ft (187 m)

Depth to Top of Louann Salt (approximate): 20,000 ft (6,100 m)

1.4 ORIENTATION AND MAXIMUM LATERAL DIMENSIONS OF SALT STOCK:

|   |  |
|---|--|
| Major Axis: Length: 2.3 mi (3.7 km)<br>at 2,000 ft<br>Orientation: 045° | Major Axis: Length: 2.7 mi (4.4 km)<br>at -18,000 ft (5,486 m)<br>Orientation: None (circular) |
|---|--|

|                                     |                                     |
|-------------------------------------|-------------------------------------|
| Minor Axis: Length: 1.5 mi (2.4 km) | Minor Axis: Length: 2.7 mi (4.4 km) |
|-------------------------------------|-------------------------------------|

Area: 2.5 mi<sup>2</sup> (6.5 km<sup>2</sup>)

Area: 5.9 mi<sup>2</sup> (15.1 km<sup>2</sup>)

Area of Planar Crest: 0.3 mi<sup>2</sup> (0.8 km<sup>2</sup>)

Percentage Planar Crest: 12%

1.5 SHAPE OF SALT STOCK:

General: Piercement stock

Plan: Irregular; circular (axial ratio 1.0) at -18,000 ft (-5,486 m); irregular elliptical (axial ratio 1.53) at -2,000 ft (-610 m)

Cross Section:

Axis: Axial plunge 61°; tilt direction 211°; tilt distance 10,000 ft (3,048 m)

Approximate Overall Symmetry: Triclinic

Crest: Convex

Sides: Upward converging from -10,000 ft to 18,000 ft (-3,048 m to -5,486 m);  
upward diverging from -6,000 ft to -10,000 ft (-1,829 m to -3,048 m);  
upward converging above -6,000 ft (-1,829 m)

## MOUNT SYLVAN

**Overhang:** Multiple overhangs; major, circum-domal, near symmetrical, elevation -6,000 ft (-1,829 m), maximum lateral overhang 3,300 ft (1,006 m) on NE flank, percentage overhang 64%; minor, asymmetrical, SW flank only, elevation -2,000 ft (-610 m), maximum lateral overhang 2,000 ft (610 m), percentage overhang 12%; axial tilt produces apparent overhang on SW flank of 10,000 ft (3,048 m)

### 1.6 CAP ROCK:

**Maximum Stratigraphic Thickness:** 112 ft (34 m)

**Minimum Stratigraphic Thickness:** 60 ft (18 m)

**Composition:** Calcite, anhydrite

### 1.7 GEOMETRY OF ADJOINING STRATA:

**Lateral Extent of Rim Syncline:** 25,500 ft (7,770 m)

**Lateral Extent of Rim Anticline:** 13,500 ft (4,100 m)

**Vertical Variation in Maximum Limb Dip:**  $\Delta = -7^\circ$  at -7,500 ft (-2,300 m) Paluxy  
 $\Delta = 0^\circ$  at -1,500 ft (-450 m) Wilcox  
 $\Delta = +20^\circ$  at -1,000 ft (-300 m) Wilcox

**Angle Between Salt and Surrounding Strata:**  $\delta = 135^\circ$  at -7,500 ft (-2,300 m) Paluxy  
 $\delta = 45^\circ$  at -4,000 ft (-1,200 m) Austin  
Chalk  
 $\delta = 2^\circ$  at 0 ft (0 m) Wilcox

**Oldest Planar Overburden:** Quaternary strata

### 1.8 FAULTING OF ADJACENT STRATA:

**Faults at Flanks:** SE flank, normal, antithetic faults, multiple offset, down-to-dome

**Crestal Faults:** None

**Evidence for Growth Faulting:** None

**Youngest Faulted Strata:** Wilcox Group

**Oldest Strata Brought to Surface:** Queen City Formation

### 2.0 GROWTH HISTORY:

### 2.1 PRIMARY PERIPHERAL SINK:

MOUNT SYLVAN

Age of Initiation: 150 Ma

Age of Cessation: 135 Ma

Duration of Growth: 15 Ma

Distance of Axial Trace from Center of Dome: 4-5 mi (7-8 km)

2.2 SECONDARY PERIPHERAL SINK:

Age of Initiation: 135 Ma

Age of Cessation: 73 Ma

2.3 TERTIARY PERIPHERAL SINK:

Age of Initiation: 73 Ma

Age of Cessation: Post-48 Ma

2.4 AGE OF MIGRATION OF SINK TO SALT-STOCK CONTACT: 112 Ma

2.5 DOME-RELATED UNCONFORMITIES: None recognized

Evidence for Extrusion and Erosion of Salt: None recognized

2.6 YOUNGEST DEFORMATION: Faults in Wilcox Group

2.7 EVIDENCE FOR COLLAPSE: Half grabens over SE flank

Configuration of Overburden Strata: Wilcox strata arch over dome

Drainage System: Type 4, transverse drainage

Sinkholes: None

Surface Salines: None

3.0 RESOURCES AND USES:

3.1 HYDROCARBONS:

Number of Producing Wells: Current: 0

Total: 0

MOUNT SYLVAN

Production: Current: 0

Total: 0

Stratigraphic Reservoir: None

Traps: None

3.2 BRINE: None

3.3 SULFUR: None

3.4 GAS STORAGE: None

1.0 DOME NAME: OAKWOOD

1.1 LOCATION: SE Freestone Co., N-Central Leon Co.;  
31° 32' 10" N; 95° 58' 13" W

1.2 RESIDUAL GRAVITY EXPRESSION: -48 GU

1.3 DEPTH: Depth to Cap Rock: 703 ft (214 m)

Depth to Salt Stock: 800 ft (244 m)

Depth to Top of Louann Salt (approximate): 20,000 ft (6,100 m)

1.4 ORIENTATION AND MAXIMUM LATERAL DIMENSIONS OF SALT STOCK:

Major Axis: Length: 2.5 mi (3.9 km)  
Orientation: 120°

Minor Axis: Length: 2.0 mi (3.2 km)

Area: 3.8 mi<sup>2</sup> (9.7 km<sup>2</sup>)

Area of Planar Crest: 2.8 mi<sup>2</sup> (7.2 km<sup>2</sup>)

Percentage Planar Crest: 74%

1.5 SHAPE OF SALT STOCK:

General: Piercement stock

Plan: Irregular elliptical (axial ratio = 1.24)

Cross Section:

Axis: Vertical, axial plunge 90°

Approximate Overall Symmetry: Monoclinic

Crest: Planar-conical

Sides: Parallel from -10,000 ft to -18,000 ft (-3,048 m to -5,486 m);  
upward diverging from -2,000 ft to -10,000 ft (-610 m to -3,048 m);  
upward converging above -2,000 ft (-610 m)

## OAKWOOD

**Overhang:** Well-developed, circum-domal, symmetrical, elevation -2,000 ft (-610 m); maximum lateral overhang 3,600 ft (1,097 m) on NW flank; percentage overhang 102%.

### 1.6 CAP ROCK:

**Maximum Stratigraphic Thickness:** 533 ft (162 m), thickest at center of dome crest

**Minimum Stratigraphic Thickness:** 50 ft (15 m)

**Composition:** Anhydrite, calcite

### 1.7 GEOMETRY OF ADJOINING STRATA:

**Lateral Extent of Rim Syncline:** 22,500 ft (6,850 m)

**Lateral Extent of Rim Anticline:** 13,500 (4,100 m)

**Vertical Variation in Maximum Limb Dip:**

- $\Delta = 3^\circ$  at -5,600 ft (-1,700 m) Woodbine
- $\Delta = 0^\circ$  at -1,500 ft (-450 m) Wilcox
- $\Delta = +25^\circ$  at -1,300 ft (-400 m) Wilcox
- $\Delta = +6^\circ$  at -250 ft (-75 m) Claiborne

**Angle Between Salt and Surrounding Strata:**  $\delta = 90^\circ$  at -5,000 m (-16,500 ft) to crest

**Oldest Planar Overburden:** Quaternary strata

### 1.8 FAULTING OF ADJACENT STRATA:

**Faults at Flanks:** Normal, single offset

**Crestal Faults:** Small, central graben, antithetic

**Youngest Faulted Strata:** Queen City Formation

**Oldest Strata Brought to Surface:** Carrizo Formation

### 2.0 GROWTH HISTORY:

#### 2.1 PRIMARY PERIPHERAL SINK:

**Age of Initiation:** 150 Ma

OAKWOOD

Age of Cessation: 135 Ma

Duration of Growth: 15 Ma

Distance of Axial Trace from Center of Dome: 7 mi (11 km)

2.2 SECONDARY PERIPHERAL SINK:

Age of Initiation: 135 Ma

Age of Cessation: 125 Ma

2.3 TERTIARY PERIPHERAL SINK:

Age of Initiation: 125 Ma

Age of Cessation: Post-48 Ma

2.4 AGE OF MIGRATION OF SINK TO SALT-STOCK CONTACT: 104 Ma

2.5 DOME-RELATED UNCONFORMITIES: None recognized

Evidence for Extrusion and Erosion of Salt: None recognized

2.6 YOUNGEST DEFORMATION: Fault in Claiborne Group

2.7 EVIDENCE FOR COLLAPSE:

Configuration of Overburden Strata: Claiborne strata arched over dome

Drainage System: Type 3, supradomal depression, subcentripetal drainage

Sinkholes: None

Surface Salines: None

3.0 RESOURCES AND USES:

3.1 HYDROCARBONS:

Number of Producing Wells: Current: 2

Total: 24

Production: Current: 5,004 bbls

Total: 2,120,719 bbls

Stratigraphic Reservoir: Woodbine Group

OAKWOOD

Trap: Beneath overhang

3.2 BRINE: None

3.3 SULFUR: None

3.4 GAS STORAGE: None

1.0 DOME NAME: PALESTINE

1.1 LOCATION: SW Anderson Co.,  
35° 44' 33" N; 95° 43' 41" W

1.2 RESIDUAL GRAVITY EXPRESSION: 110 GU

1.3 DEPTH: Depth to Cap Rock: 120 ft (36 m)

Depth to Salt Stock: 122 ft (37 m)

Depth to Top of Louann Salt (approximate): 22,000 ft (6,700 m)

1.4 ORIENTATION AND MAXIMUM LATERAL DIMENSIONS OF SALT STOCK:

Major Axis: Length: 3.4 mi (5.4 km) at 20,000 ft  
Orientation: 170°

Minor Axis: Length: 2.7 mi (4.3 km)

Area: 7.0 mi<sup>2</sup> (17.9 km<sup>2</sup>)

Area of Planar Crest: 0.7 mi<sup>2</sup> (1.8 km<sup>2</sup>)

Percentage Planar Crest: 11%

1.5 SHAPE OF SALT STOCK:

General: Piercement stock

Plan: Elliptical (axial ratio 1.3)

Cross Section:

Axis: Axial plunge 82°; tilt direction 094°; tilt distance 1,584 ft (483 m)

Approximate Overall Symmetry: Monoclinic

Crest: Conical-planar

Sides: Nearly parallel from -7,000 ft to -15,000 ft (-2,134 m to -4,572 m);  
upward converging above -7,000 ft (-2,134 m)

Overhang: Well-developed, E flank only, elevation -6,000 ft (-1,829 m),  
maximum lateral overhang 2,640 ft (805 m), percentage overhang 11%

PALESTINE

1.6 CAP ROCK:

Maximum Stratigraphic Thickness: 32 ft (10 m)

Minimum Stratigraphic Thickness: 9 ft (3 m)

Composition: Calcite, calcite-cemented Carrizo Formation as false cap rock.

1.7 GEOMETRY OF ADJOINING STRATA:

Lateral Extent of Rim Syncline: 32,000 ft (9,140 m)

Lateral Extent of Rim Anticline: 16,200 (4,900 m)

Vertical Variation in Maximum Limb Dip:  $\Delta = 72^\circ$  at -10,800 ft (-3,300 m) Hosston  
 $\Delta = 0^\circ$  at -6,000 ft (-1,800 m) Washita  
 $\Delta = 40^\circ$  at -4,500 ft (1,370 m) Austin  
 $\Delta = 20^\circ$  at -1,800 ft (550 m) Wilcox

Angle Between Salt and Surrounding Strata:  $\delta = 90^\circ$  from -11,000 ft to -7,500 ft  
(-3,350 to -2,300 m) Hosston to Washita  
 $\delta = 20$  to  $30^\circ$  at -2,500 ft  
(760 m) Navarro Marl

Oldest Planar Overburden: Quaternary strata

1.8 FAULTING OF ADJACENT STRATA:

Faults at Flanks: None

Crestal Faults: Horst and graben, normal, homothetic, up-to-dome

Youngest Faulted Strata: Claiborne Group

Oldest Strata Brought to Surface: Buda Limestone

2.0 GROWTH HISTORY:

2.1 PRIMARY PERIPHERAL SINK:

Age of Initiation: 150 Ma

Age of Cessation: 135 Ma

Duration of Growth: 15 Ma

Distance of Axial Trace from Center of Dome: 5-7 mi (8-12 km)

PALESTINE

2.2 SECONDARY PERIPHERAL SINK:

Age of Initiation: 135 Ma

Age of Cessation: 125 Ma

2.3 TERTIARY PERIPHERAL SINK:

Age of Initiation: 125 Ma

Age of Cessation: Post-48 Ma

2.4 AGE OF MIGRATION OF SINK TO SALT-STOCK CONTACT: 104 to 112 Ma

2.5 DOME-RELATED UNCONFORMITIES: None recognized

Evidence for Extrusion and Erosion of Salt: None recognized

2.6 YOUNGEST DEFORMATION: Faults in Wilcox Group to surface

2.7 EVIDENCE FOR COLLAPSE: Grabens over dome crest

Configuration of Overburden Strata: Wilcox, Claiborne strata arch over dome

Drainage System: Type 2, central, supradomal depression, central centripetal drainage, man-made lake over center of dome

Sinkholes: Common

Surface Saline: Present

3.0 RESOURCES AND USES:

3.1 HYDROCARBONS:

Number of Producing Wells: Current: 0

Total: 0

Production: Current: 0

Total: 0

Stratigraphic Reservoir: None

Traps: None

PALESTINE

3.2 BRINE: Yes

3.3 SULFUR: None

3.4 GAS STORAGE: None

1.0 DOME NAME: STEEN

1.1 LOCATION: N Central Smith Co.;  
32° 31' 0" N; 95° 19' 30" W

1.2 RESIDUAL GRAVITY EXPRESSION: -54 GU

1.3 DEPTH: Depth to Cap Rock: 75 ft (23 m)

Depth to Salt Stock: 300 ft (91 m)

Depth to Top of Louann Salt (approximate): 21,000 ft (6,400 m)

1.4 ORIENTATION AND MAXIMUM LATERAL DIMENSIONS OF SALT STOCK:

Major Axis: Length: 2.2 mi (3.6 km)  
Orientation: 045°

Minor Axis: Length: 2.1 mi (3.4 km)

Area: 3.7 mi<sup>2</sup> (9.6 km<sup>2</sup>)

Area of Planar Crest: 0.5 mi<sup>2</sup> (1.3 km<sup>2</sup>)

Percentage Planar Crest: 14%

1.5 SHAPE OF SALT STOCK:

General: Piercement stock

Plan: Circular (axial ratio = 1.05)

Cross Section:

Axis: Vertical, axial plunge 90°

Approximate Overall Symmetry: Axial

Crest: Conical-planar

Sides: Upward diverging from -6,000 ft to -8,000 ft (-1,829 m to -2,438 m);  
upward converging above -6,000 ft (-1,829 m); deepest data -8,000 ft  
(-2,438 m)

STEEN

**Overhang:** Moderate, circum-domal, symmetrical, elevation -6,000 ft (-1,829 m); maximum lateral overhang 1,000 ft (305 m) on S flank; percentage overhang 14%.

1.6 CAP ROCK:

**Maximum Stratigraphic Thickness:** 200 ft (61 m)

**Minimum Stratigraphic Thickness:** 9 ft (3 m)

**Composition:** Calcite, anhydrite

1.7 GEOMETRY OF ADJOINING STRATA:

**Lateral Extent of Rim Syncline:** 27,750 ft (8,450 m)

**Lateral Extent of Rim Anticline:** 12,000 ft (3,650 m)

**Vertical Variation in Maximum Limb Dip:**  $\Delta = -15^\circ$  at -8,200 ft (-2,500 m) Glen Rose  
 $\Delta = 0^\circ$  at -3,000 ft (914 m) Pecan Gap  
 $\Delta = +50^\circ$  at -4,000 ft (-1,200 m) Eagle Ford

**Angle Between Salt and Surrounding Strata:**  $\delta = 90^\circ$  -10,000 ft (-3,000 m) (l. Glen Rose) to -4,600 ft (-1,400 m) (Eagle Ford)

**Oldest Planar Overburden:** Claiborne Group

1.8 FAULTING OF ADJACENT STRATA:

**Faults at Flanks:** E side: normal, up-to-dome, antithetic, multiple-offset graben system on crest of broad anticline; growth faulting from Paluxy to Woodbine. W. side: normal, down-to-dome, homothetic fault (?Woodbine in age)

**Crestal Faults:** None

**Youngest Faulted Strata:** Woodbine Group

**Oldest Strata Brought to Surface:** Wilcox Group

2.0 GROWTH HISTORY:

2.1 PRIMARY PERIPHERAL SINK:

**Age of Initiation:** Pre-112 Ma

**Age of Cessation:** Pre-112 Ma

STEEN

Duration of Growth: Unknown

Distance of Axial Trace from Center of Dome: 3-4 mi (5-7 km)

2.2 SECONDARY PERIPHERAL SINK:

Age of Initiation: Pre-112 Ma

Age of Cessation: 73 Ma

2.3 TERTIARY PERIPHERAL SINK:

Age of Initiation: 73 Ma

Age of Cessation: Post-48 Ma

2.4 AGE OF MIGRATION OF SINK TO SALT-STOCK CONTACT: 104 Ma

2.5 DOME-RELATED UNCONFORMITIES: None recognized

Evidence for Extrusion and Erosion of Salt: None recognized

2.6 YOUNGEST DEFORMATION: Claiborne strata arch over dome

2.7 EVIDENCE FOR COLLAPSE:

Configuration of Overburden Strata: Claiborne strata arch over dome

Drainage System: Type 3, central supradomal depression, subcentripetal drainage

Sinkholes: None

Surface Salines: Present

3.0 RESOURCES AND USES:

3.1 HYDROCARBONS: Fender field

Number of Producing Wells: Current: 0

Total: 3

Production: Current: 11,790 bbls; 0 mcf

Total: 187,022 bbls; 0 mcf

Stratigraphic Reservoir: Rodessa Member

Traps: Beneath overhang

STEEN

3.2 BRINE:

3.3 SULFUR: None

3.4 GAS STORAGE: None

1.0 DOME NAME: WHITEHOUSE

1.1 LOCATION: S-Central Smith Co.;  
32° 13' 27" N; 95° 17' 03" W;

1.2 RESIDUAL GRAVITY EXPRESSION: -76 GU

1.3 DEPTH: Depth to Cap Rock: 485 ft (148 m)

Depth to Salt Stock: 535 ft (163 m)

Depth to Top of Louann Salt (approximate): 22,000 ft (6,700 m)

1.4 ORIENTATION AND MAXIMUM LATERAL DIMENSIONS OF SALT STOCK:

Major Axis: Length: 2.6 mi (4.2 km)      Major Axis: Length: >3.0 mi (>5.0 km)  
at -6,000 ft      at -10,000 ft

Orientation: 015°      Orientation: 007°

Minor Axis: Length: 1.3 mi (2.1 km)      Minor Axis: Length: >2.1 mi (>3.8 km)

Area: 2.6 mi<sup>2</sup> (6.7 km<sup>2</sup>)      Area: >5.3 mi<sup>2</sup> (>13.6 km<sup>2</sup>)

Area of Planar Crest: 0.2 mi<sup>2</sup> (0.5 km<sup>2</sup>)

Percentage Planar Crest: 8%

1.5 SHAPE OF SALT STOCK:

General: Piercement stock

Plan: Irregular lobate-elliptical (axial ratio = 1.3) at -15,000 ft (-4,572 m);  
elliptical (axial ratio = 2.0) at -6,000 ft (-1,829 m)

Cross Section:

Axis: Axial plunge 84°; tilt direction 095°; tilt distance 1,584 ft (483 m)

Approximate Overall Symmetry: Triclinic

Crest: Conical-planar

Sides: Upward converging from -8,000 ft to -15,000 ft (-2,438 m to -4,572 m);  
upward diverging from -6,000 ft to -8,000 ft (-1,829 m to -2,438 m);  
upward converging above -6,000 ft (-1,829 m); deepest data  
-15,000 ft (-4,572 m)

Overhang: Irregular, maximum development on NNE flank, elevation  
-6,000 ft (-1,829 m); maximum lateral overhang  
4,910 ft (1,447 m) on NNE flank; percentage overhang 53%

## WHITEHOUSE

### 1.6 CAP ROCK:

Maximum Stratigraphic Thickness: 70 ft (21 m)

Minimum Stratigraphic Thickness: 50 ft (15 m)

Composition: Anhydrite, calcite

### 1.7 GEOMETRY OF ADJOINING STRATA:

Lateral Extent of Rim Syncline: 21,750 ft (6,650 m)

Lateral Extent of Rim Anticline: 17,250 ft (5,250 m)

Vertical Variation in Maximum Limb Dip:  $\Delta = -1^\circ$  at -4,900 ft (1,500 m) Washita  
 $\Delta = 0^\circ$  at -4,000 ft (1,200 m) Eagle Ford  
 $\Delta = 10^\circ$  at -2,600 ft (-800 m) Pecan Gap  
 $\Delta = 30^\circ$  at -800 ft (-250 m) Claiborne

Angle Between Salt and Surrounding Strata:  $\delta = 20^\circ$  at -1,800 m (-6,000 ft),  
 $\delta = 50^\circ$  at -500 m (-1,700 ft) to crest at  
0 m

Oldest Planar Overburden: Quaternary strata

Dome-Related Unconformity: N Side: Woodbine Group (overlapped by Eagle Ford and Austin) pinches out domeward over unconformity on top of Washita Group

### 1.8 FAULTING OF ADJACENT STRATA:

Faults at Flanks: N Side: Normal, up-to-dome, multiple offset, antithetic (Fredericksburg age)

Crestal Faults: None

Youngest Faulted Strata: Fredericksburg Group

Oldest Strata Brought to Surface: Claiborne Group

### 2.0 GROWTH HISTORY:

#### 2.1 PRIMARY PERIPHERAL SINK:

Age of Initiation: Pre-112 Ma

Age of Cessation: Pre-112 Ma

WHITEHOUSE

Duration of Growth: Unknown

Distance of Axial Trace from Center of Dome: 4-5 mi (7-8 km)

2.2 SECONDARY PERIPHERAL SINK:

Age of Initiation: Pre-112 Ma

Age of Cessation: Pre-112 Ma

2.3 TERTIARY PERIPHERAL SINK:

Age of Initiation: Pre-112 Ma

Age of Cessation: Post-48 Ma

2.4 AGE OF MIGRATION OF SINK TO SALT-STOCK CONTACT: Unknown

2.5 DOME-RELATED UNCONFORMITIES: None recognized

Evidence for Extrusion and Erosion of Salt: None recognized

2.6 YOUNGEST DEFORMATION: Wilcox strata arch over dome

2.7 EVIDENCE FOR COLLAPSE:

Configuration of Overburden Strata: Claiborne strata flat lying

Drainage System: Type 3, subcentripetal drainage

Sinkholes: None

Surface Salines: None

3.0 RESOURCES AND USES:

3.1 HYDROCARBONS:

Number of Producing Wells: Current: 0

Total: 0

Production: Current: 0

Total: 0

WHITEHOUSE

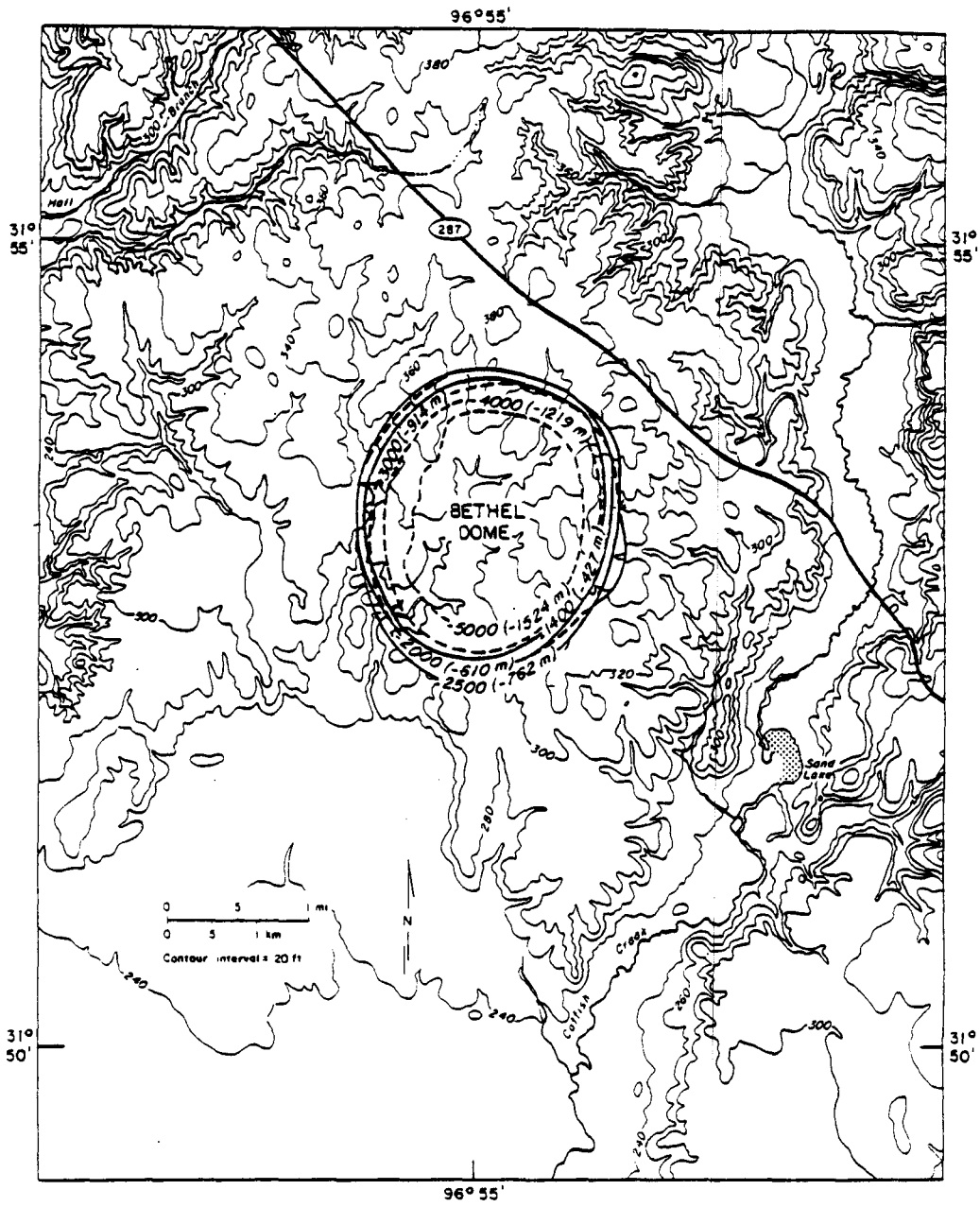
Stratigraphic Reservoir: None

Traps: None

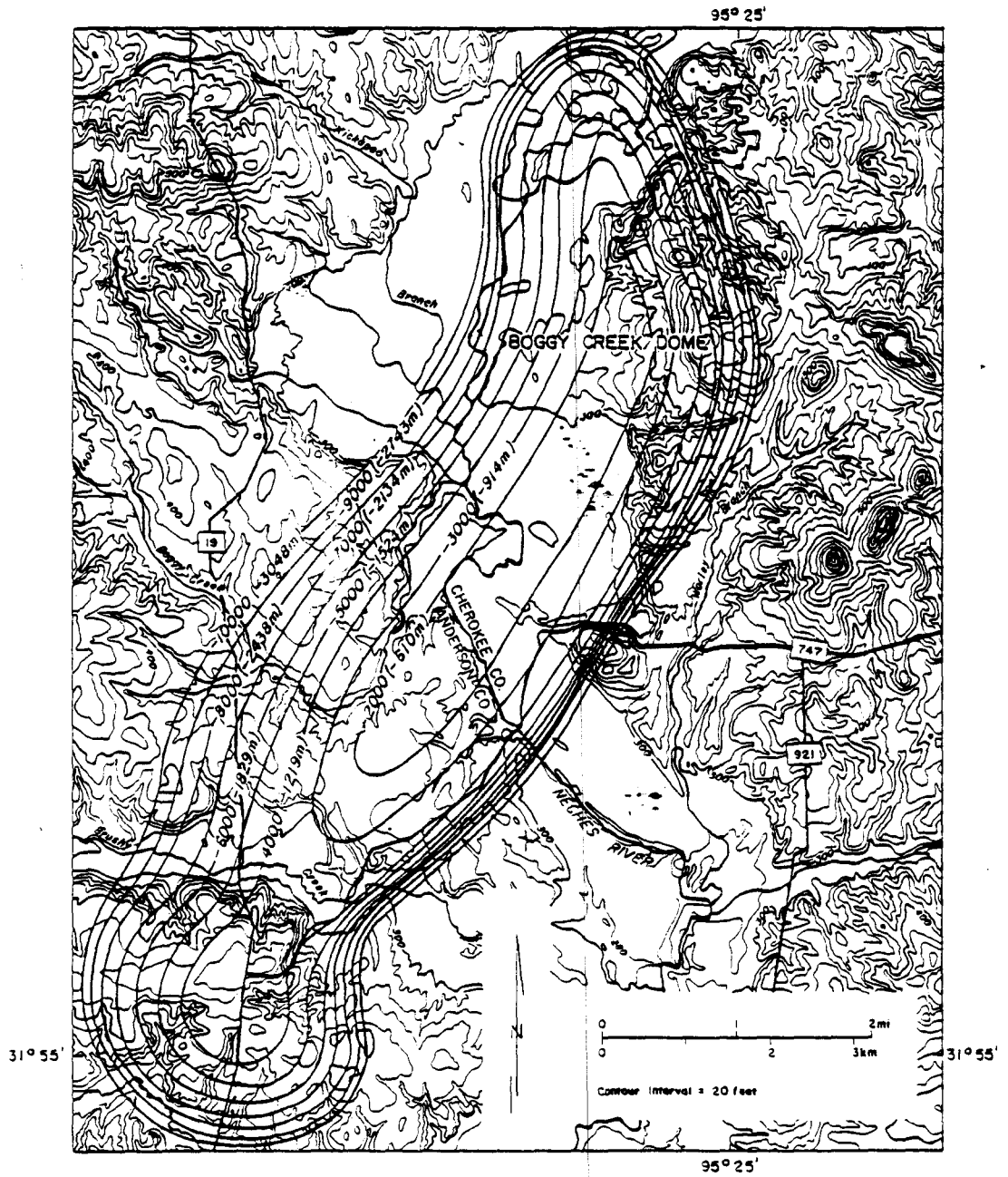
3.2 BRINE: None

3.3 SULFUR: None

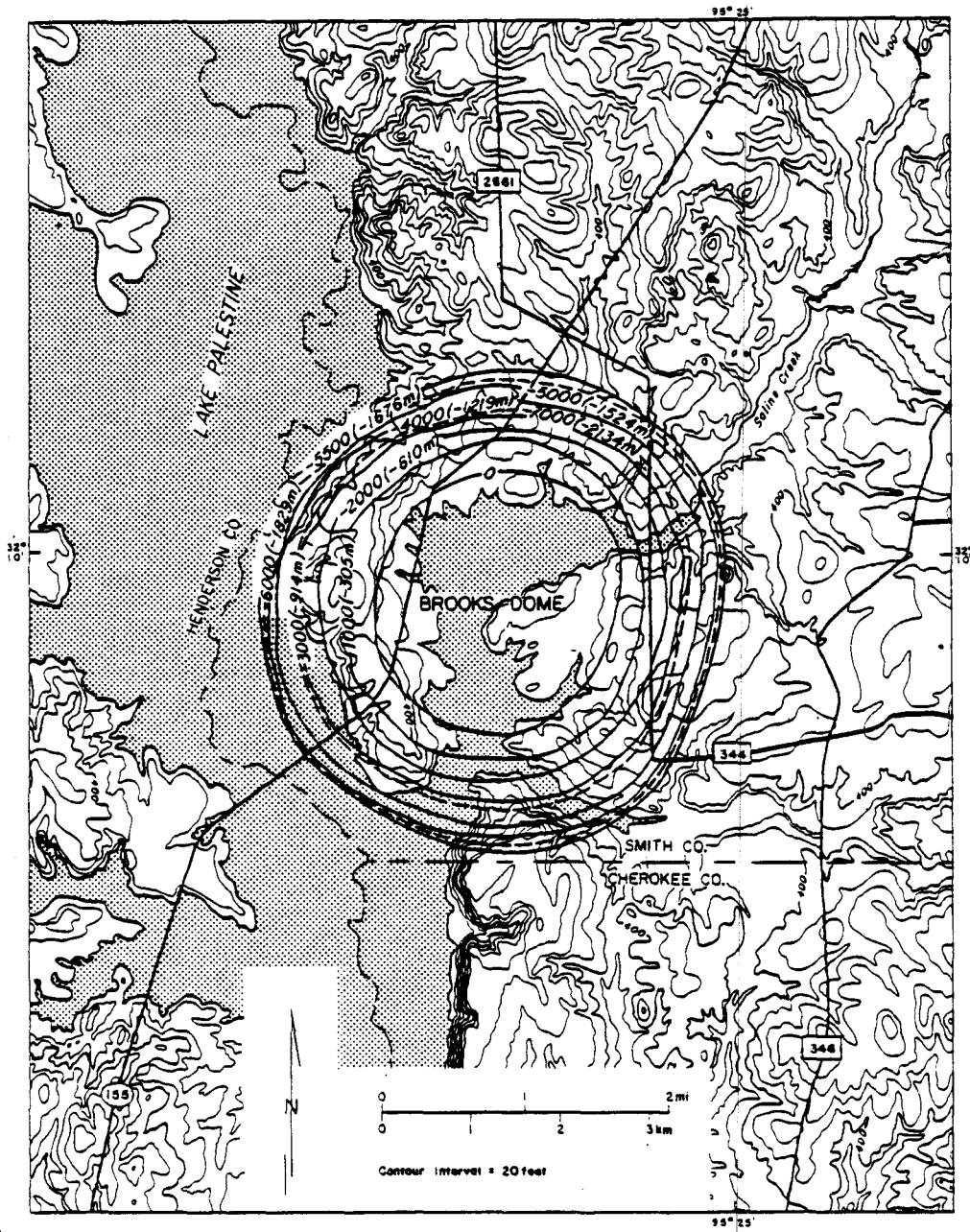
3.4 GAS STORAGE: None



DOMES SHAPE, LOCATION, TOPOGRAPHY, AND DRAINAGE (SECTIONS 1.1, 1.5, 2.7)  
 Salt structure contours in feet (meters) below sea level.



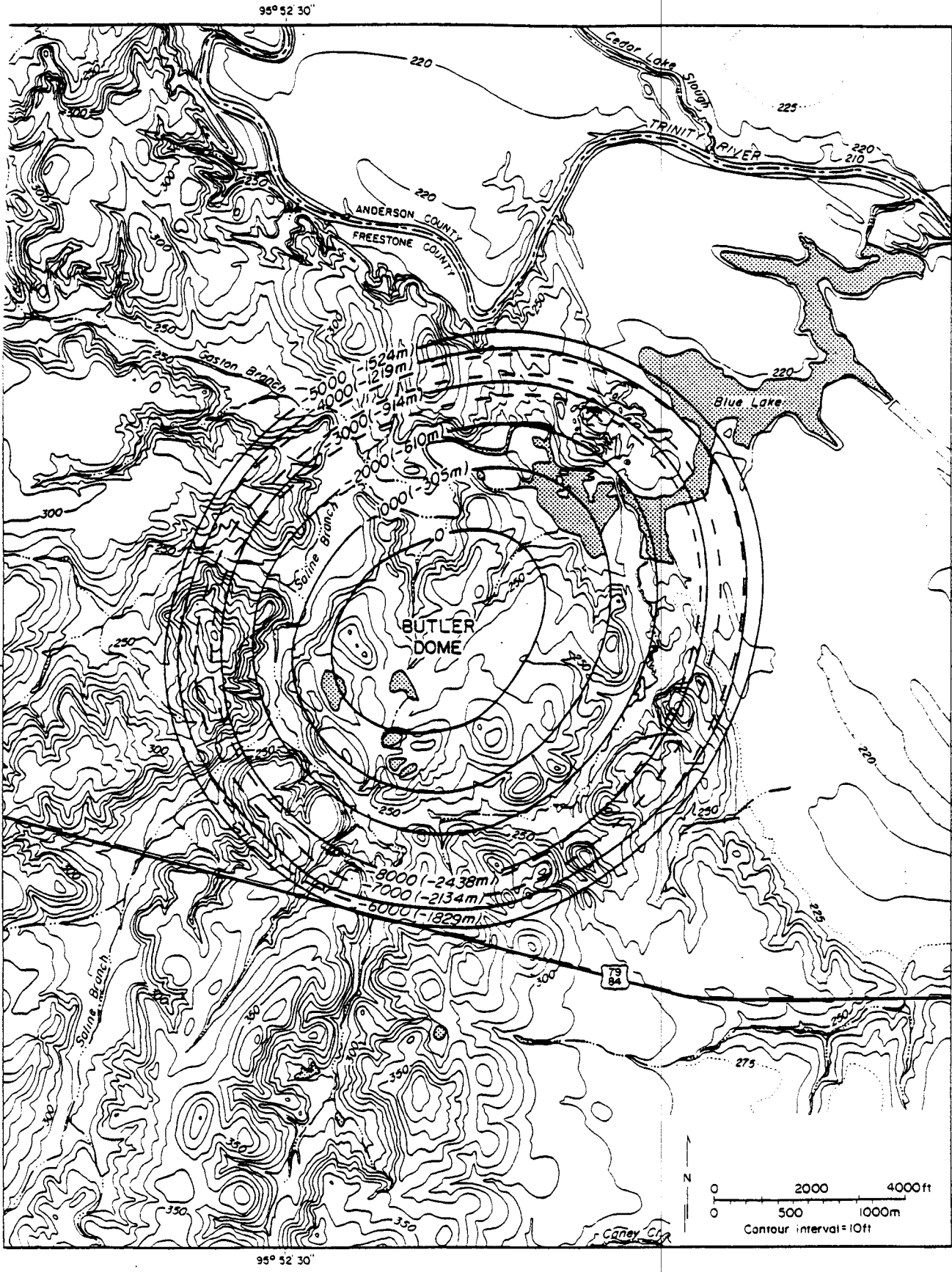
DOMESHAPE, LOCATION, TOPOGRAPHY, AND DRAINAGE (SECTIONS 1.1, 1.5, 2.7)  
 Salt structure contours in feet (meters) below sea level.



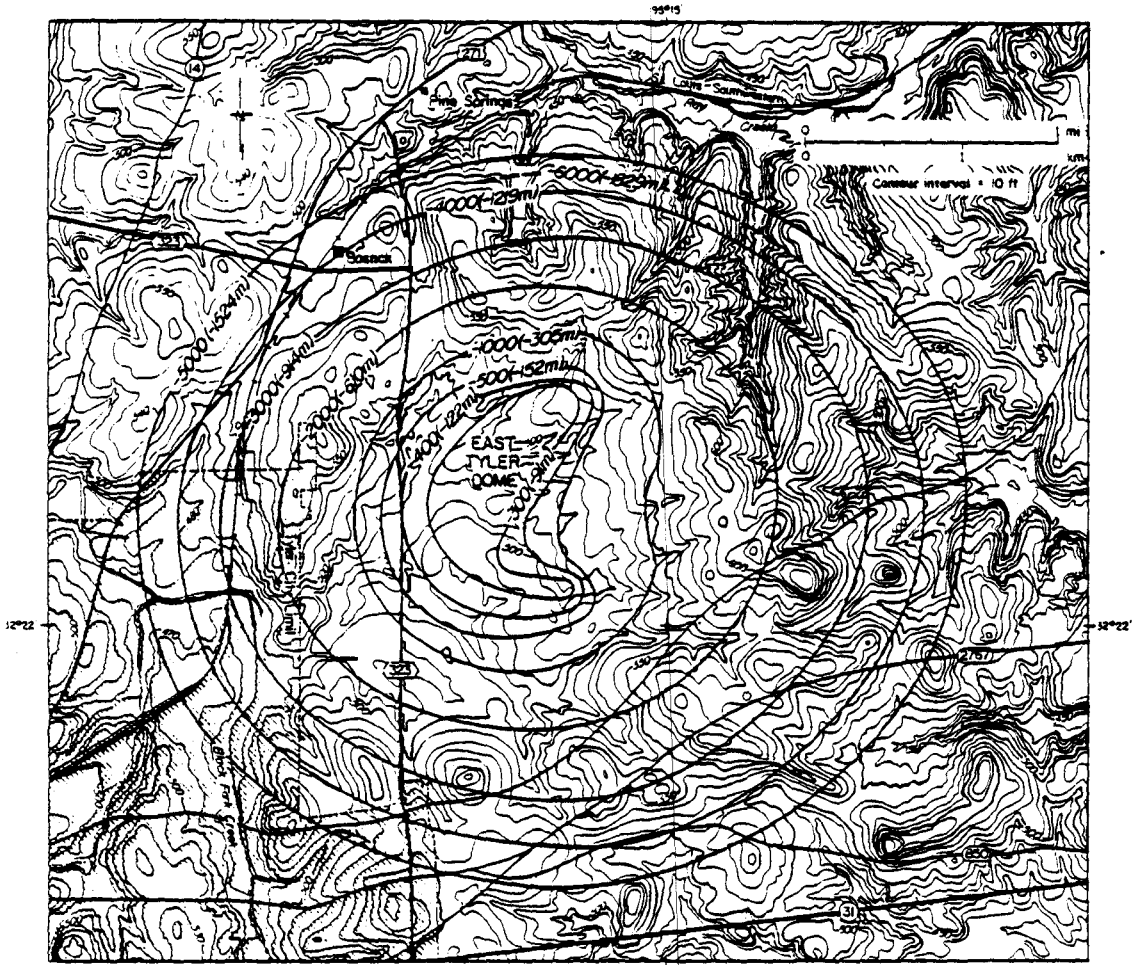
DOME SHAPE, LOCATION, TOPOGRAPHY, AND DRAINAGE (SECTIONS 1.1, 1.5, 2.7)  
 Salt structure contours in feet (meters) below sea level.



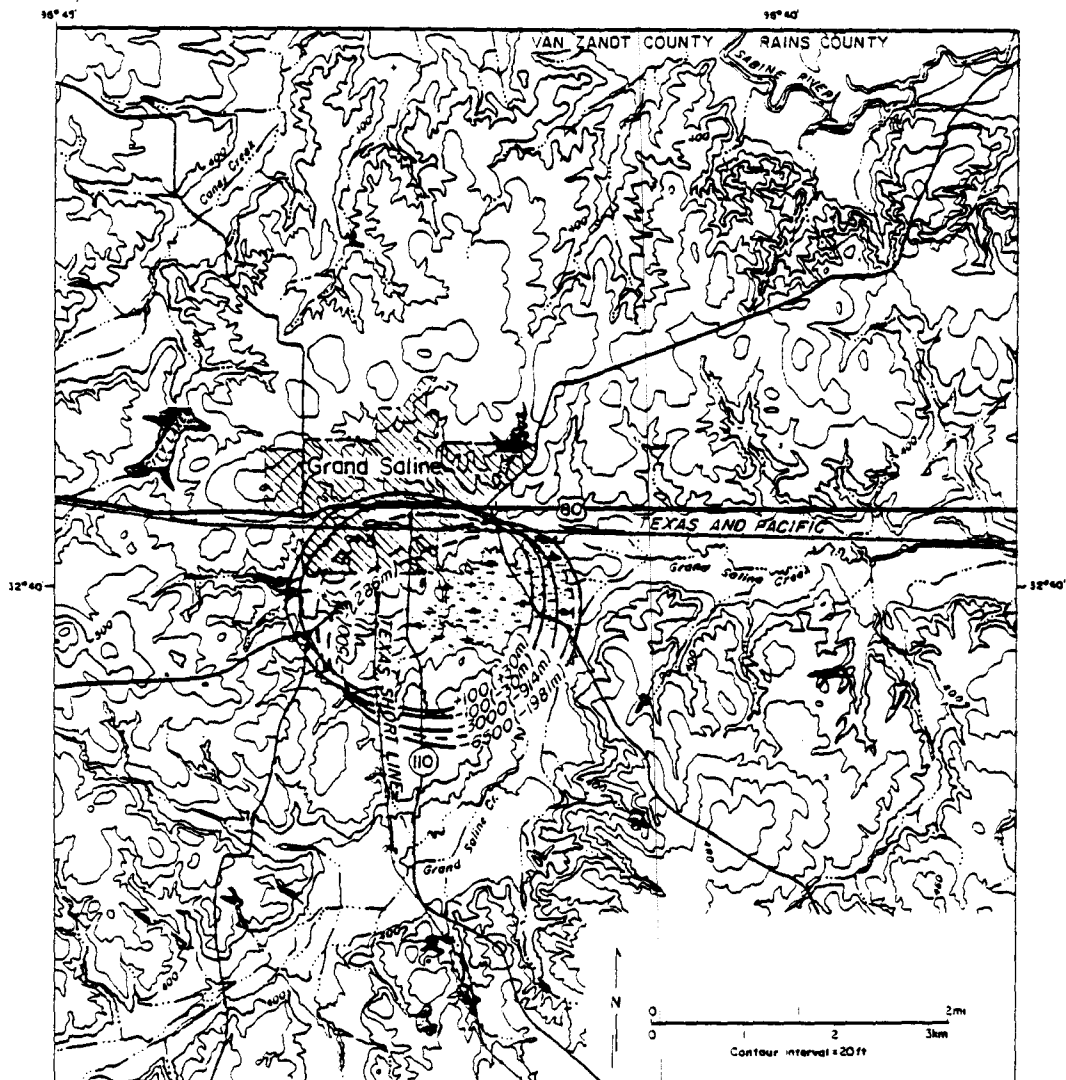
DOMESHAPE, LOCATION, TOPOGRAPHY, AND DRAINAGE (SECTIONS 1.1, 1.5, 2.7)  
Salt structure contours in feet (meters) below sea level.



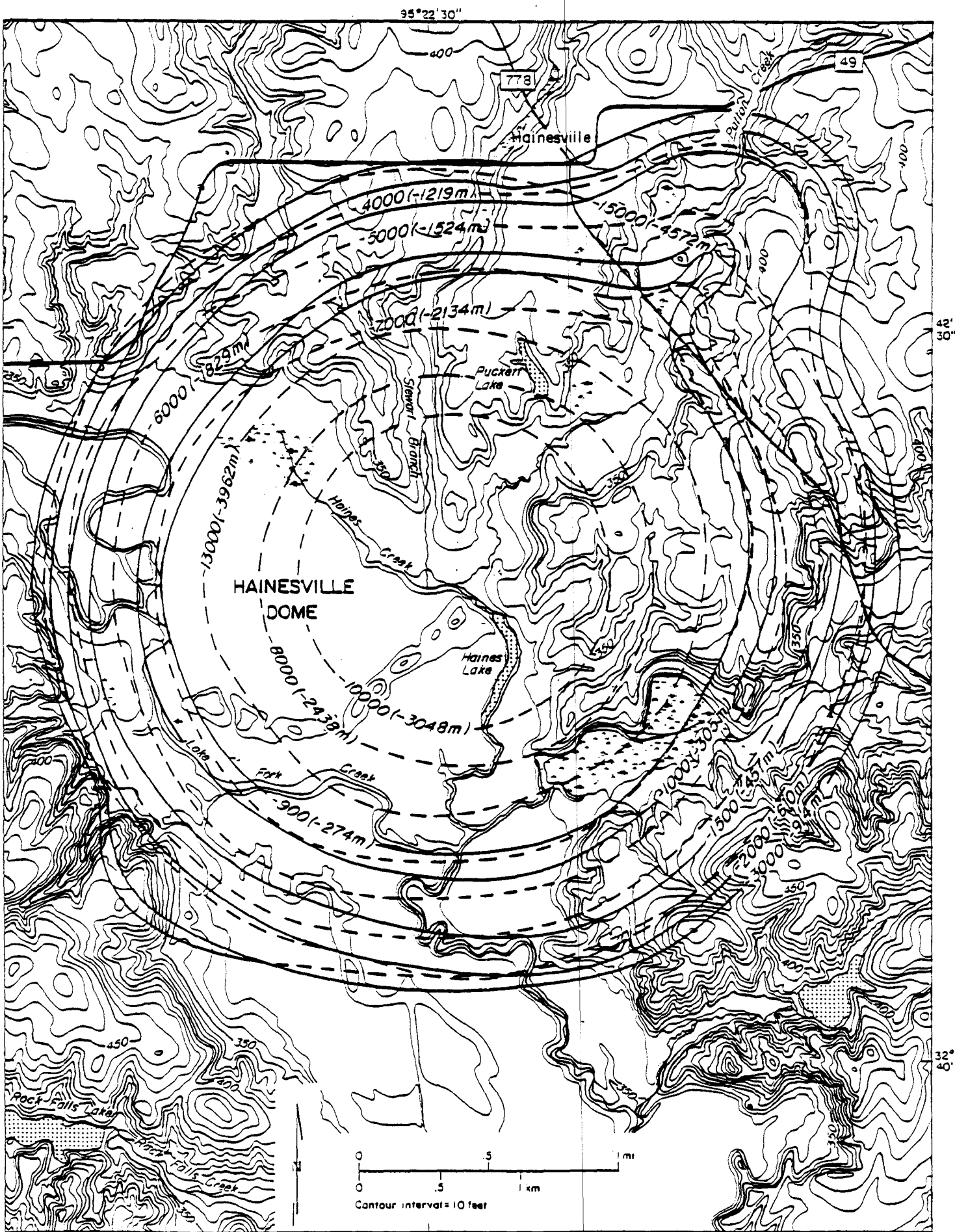
DOME SHAPE, LOCATION, TOPOGRAPHY, AND DRAINAGE (SECTIONS 1.1, 1.5, 2.7)  
 Salt structure contours in feet (meters) below sea level.



DOME SHAPE, LOCATION, TOPOGRAPHY, AND DRAINAGE (SECTIONS 1.1, 1.5, 2.7)  
 Salt structure contours in feet (meters) below sea level.



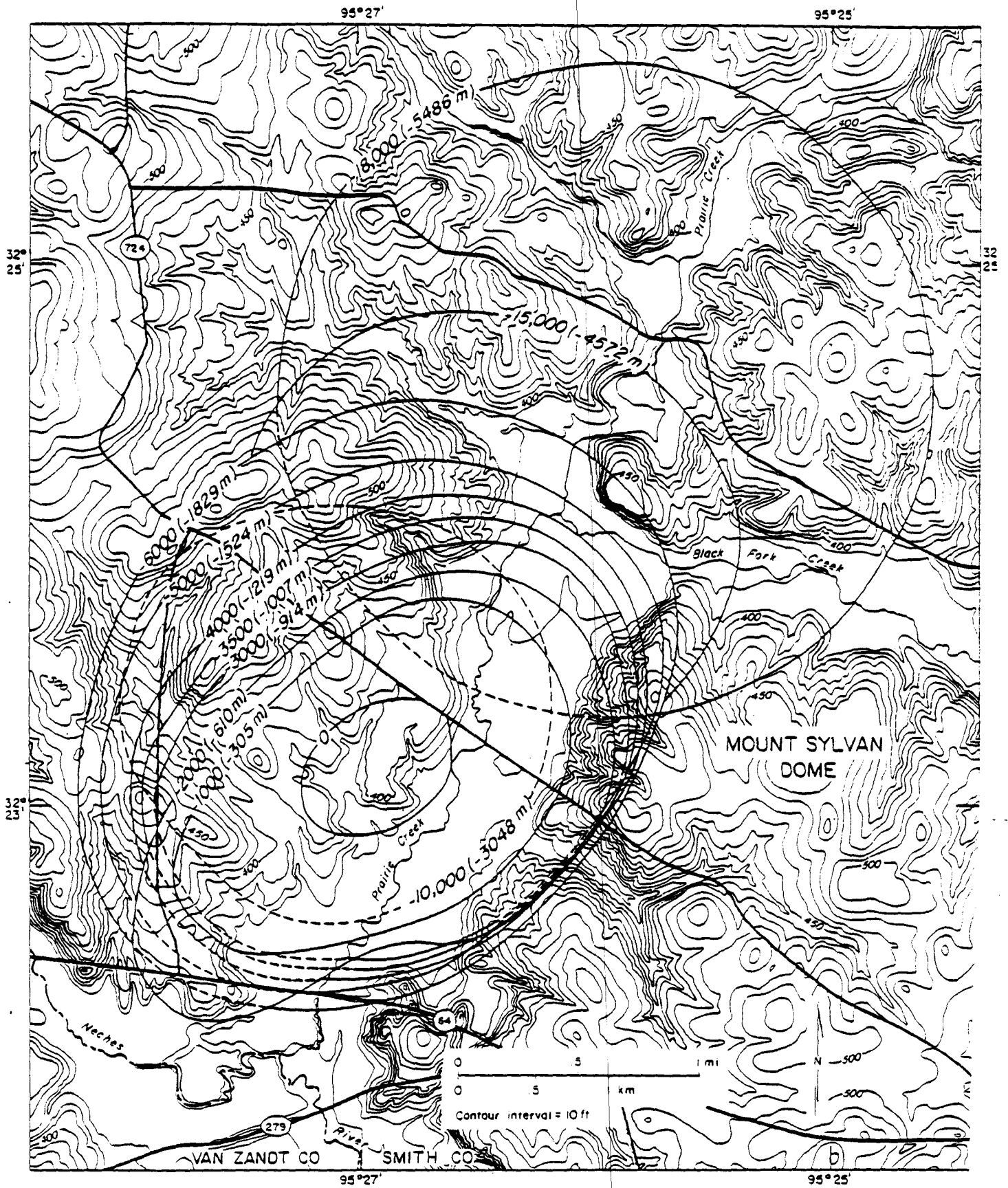
DOME SHAPE, LOCATION, TOPOGRAPHY, AND DRAINAGE (SECTIONS 1.1, 1.5, 2.7)  
 Salt structure contours in feet (meters) below sea level.



DOMES SHAPE, LOCATION, TOPOGRAPHY, AND DRAINAGE (SECTIONS 1.1, 1.5, 2.7)  
Salt structure contours in feet (meters) below sea level.

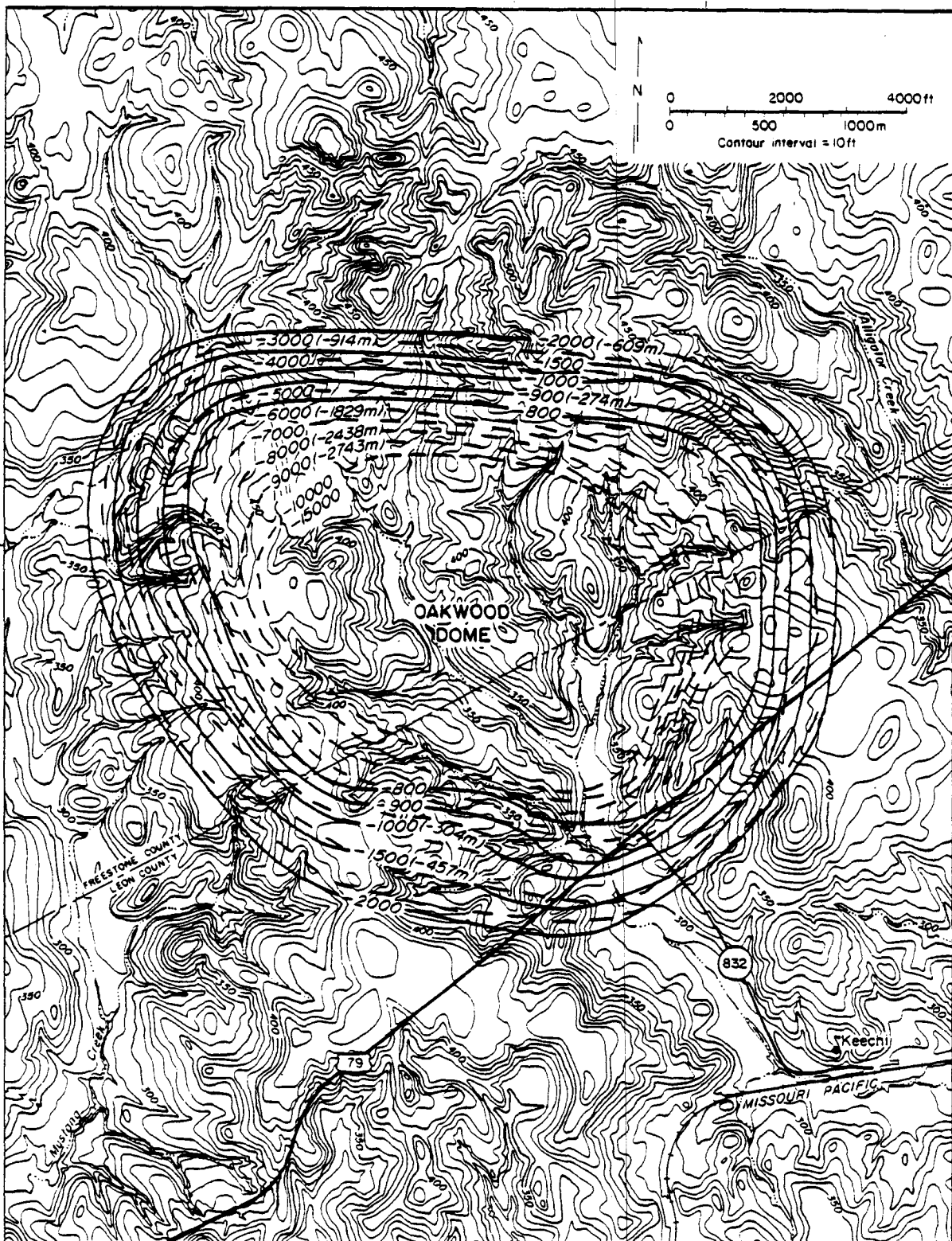


DOME SHAPE, LOCATION, TOPOGRAPHY, AND DRAINAGE (SECTIONS 1.1, 1.5, 2.7)  
 Salt structure contours in feet (meters) below sea level.



DOME SHAPE, LOCATION, TOPOGRAPHY, AND DRAINAGE (SECTIONS 1.1, 1.5, 2.7)  
 Salt structure contours in feet (meters) below sea level.

95° 57' 30"

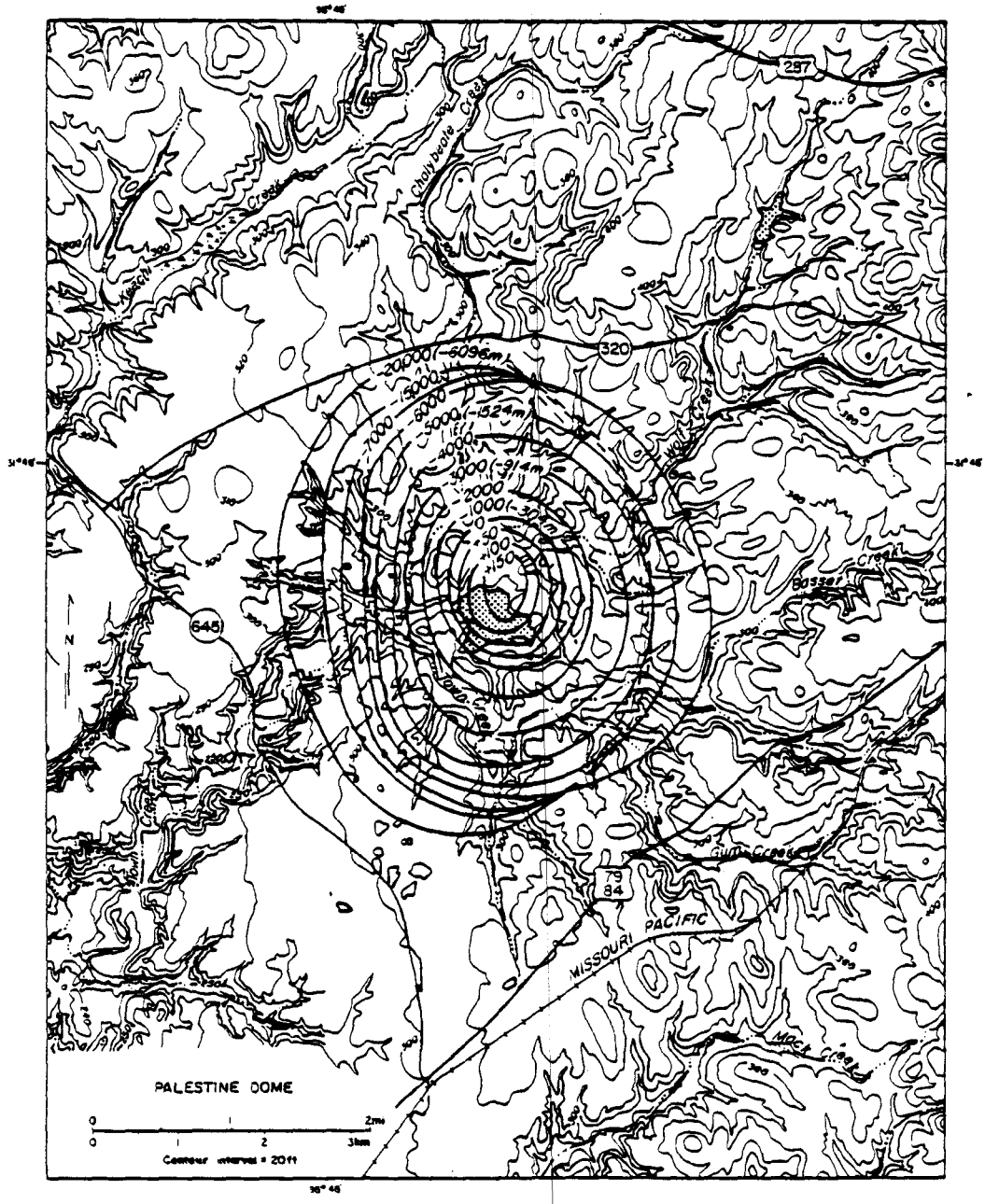


95° 57' 30"

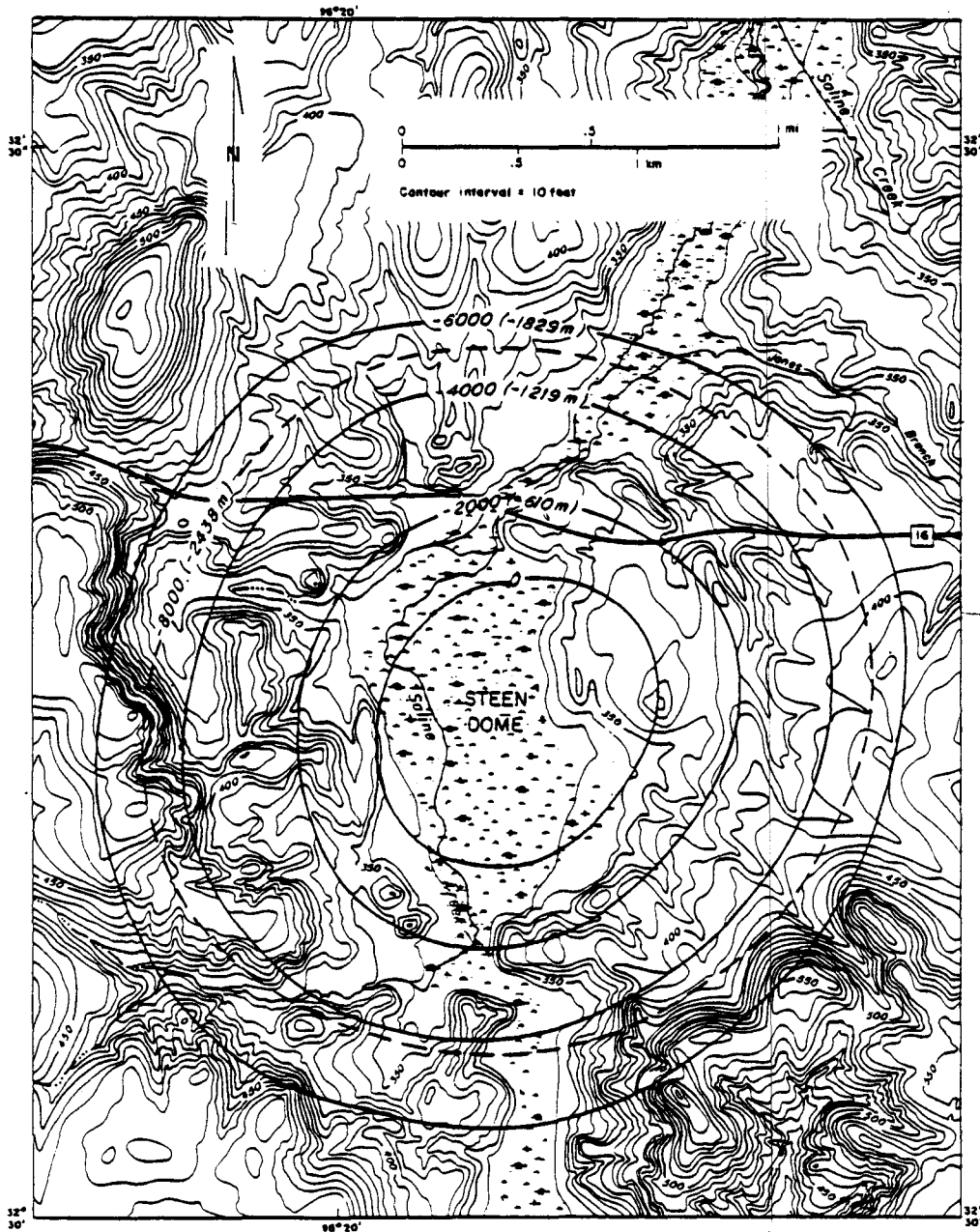
31° 32' 30"

31° 32' 30"

DOME SHAPE, LOCATION, TOPOGRAPHY, AND DRAINAGE (SECTIONS 1.1, 1.5, 2.7)  
Salt structure contours in feet (meters) below sea level.

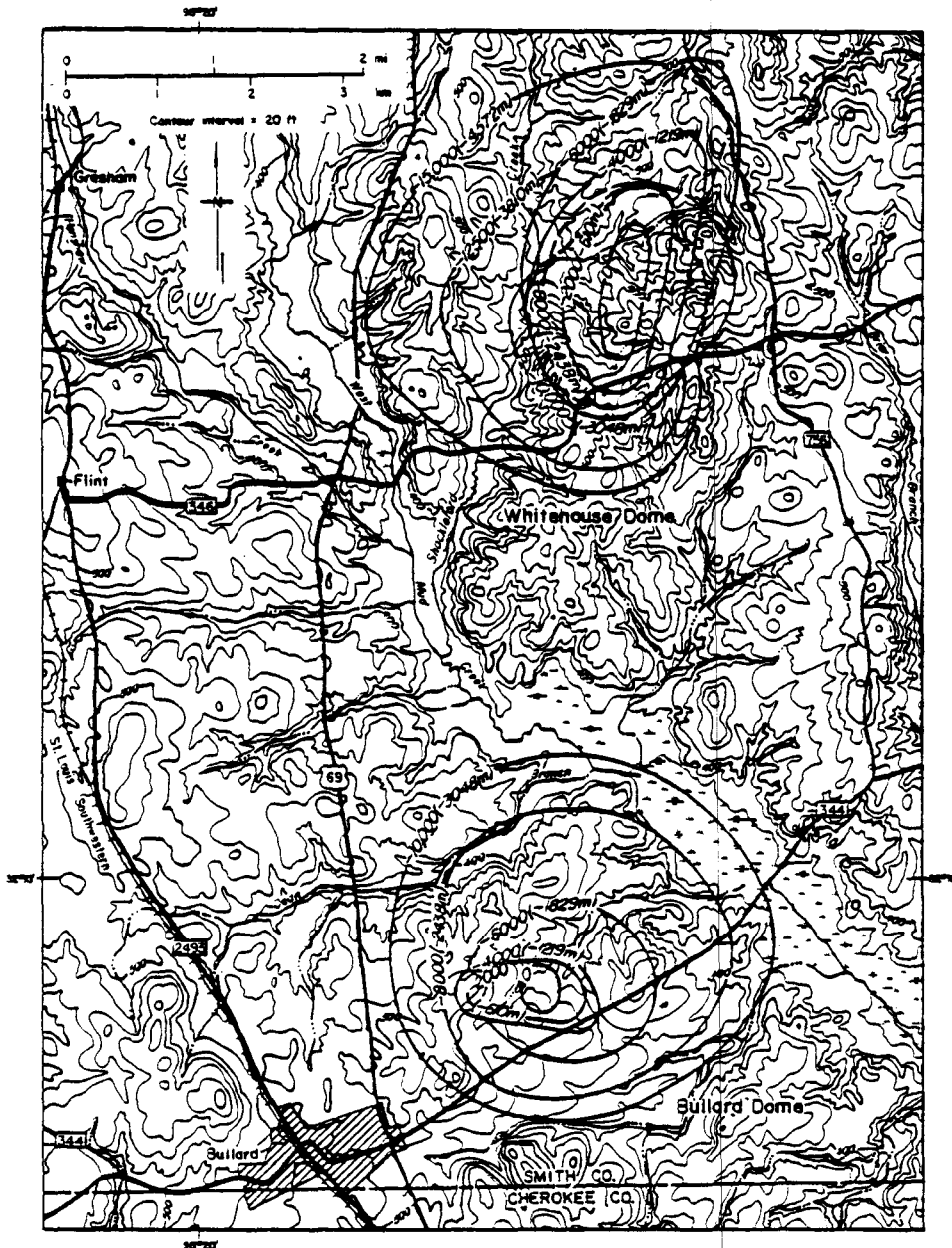


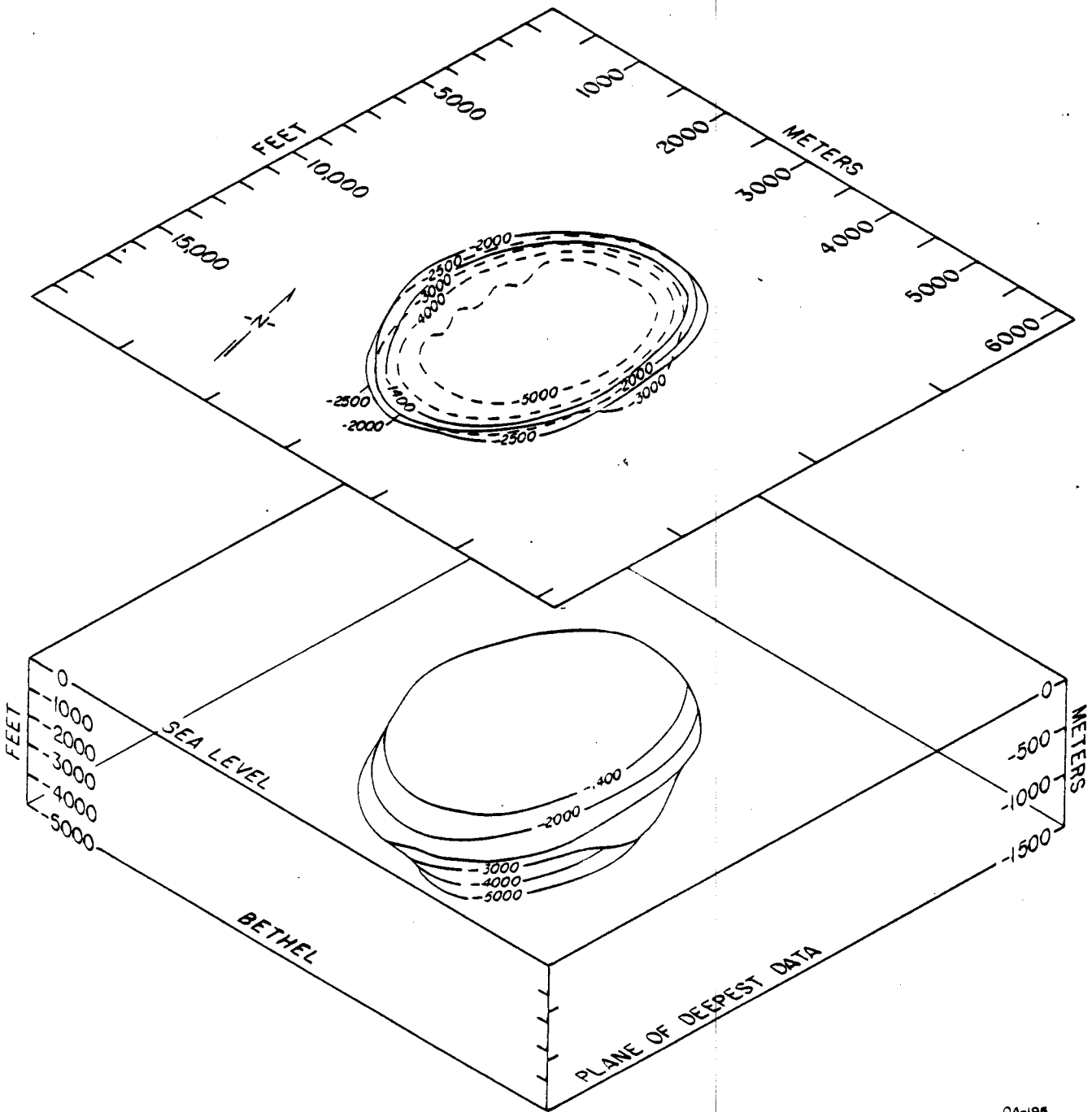
DOMESHAPE, LOCATION, TOPOGRAPHY, AND DRAINAGE (SECTIONS 1.1, 1.5, 2.7)  
 Salt structure contours in feet (meters) below sea level.



DOME SHAPE, LOCATION, TOPOGRAPHY, AND DRAINAGE (SECTIONS 1.1, 1.5, 2.7)  
 Salt structure contours in feet (meters) below sea level.

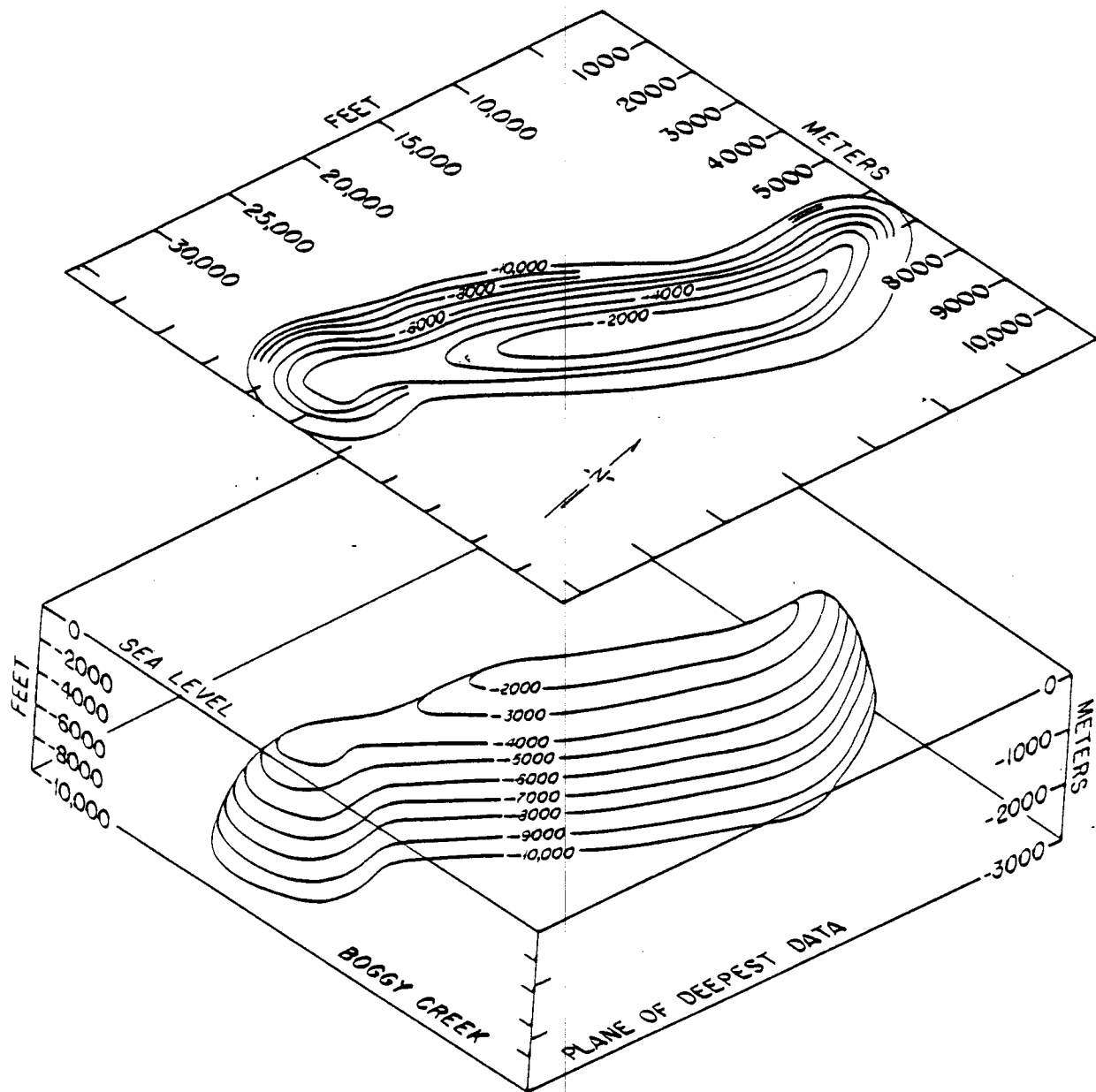
DOMES SHAPE, LOCATION, TOPOGRAPHY, AND DRAINAGE (SECTIONS 1.1, 1.5, 2.7)  
Salt structure contours in feet (meters) below sea level.





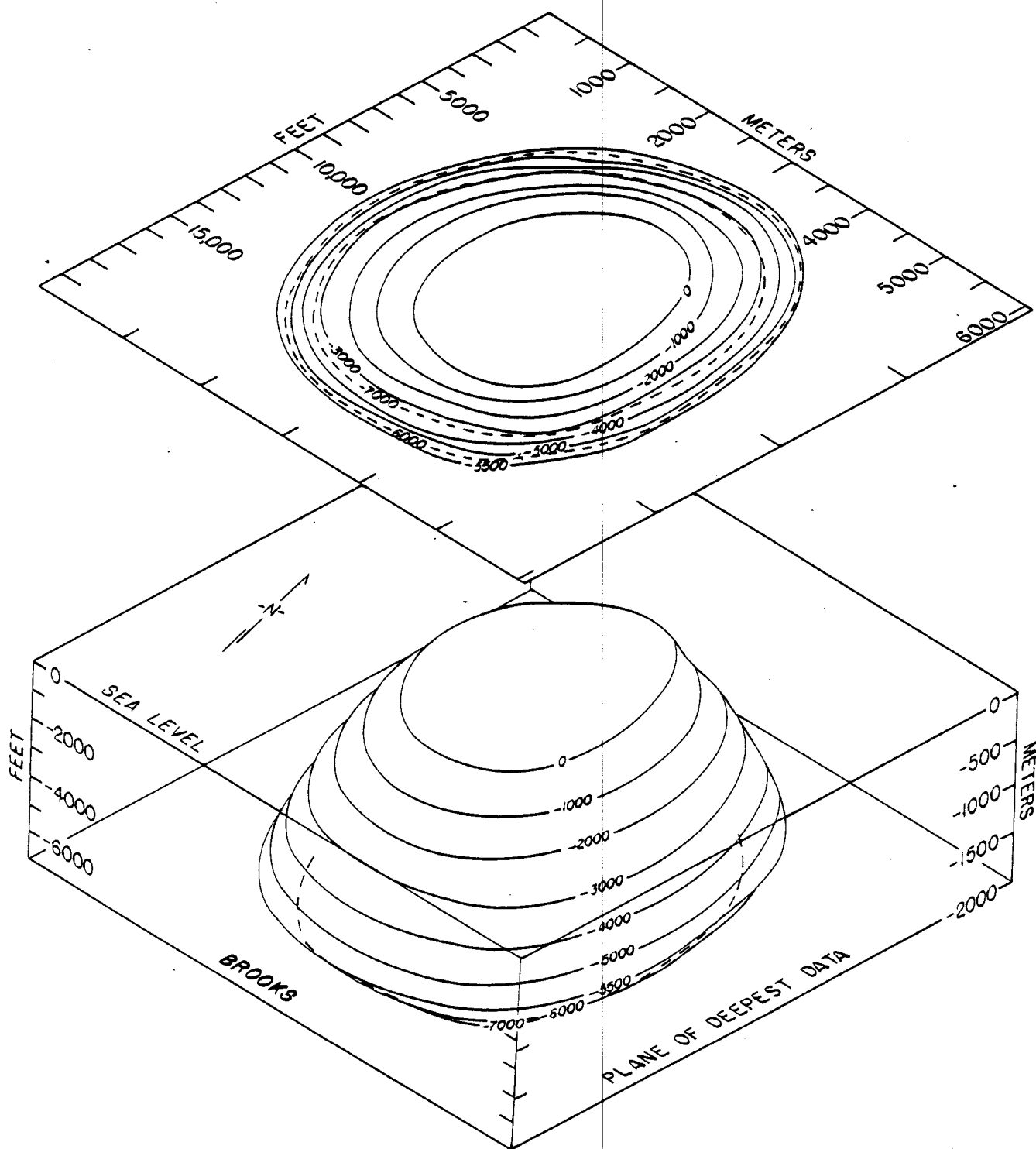
QA-195

ISOMETRIC BLOCK DIAGRAM OF SALT-STOCK SHAPE (SECTIONS 1.4, 1.5)  
Salt structure contours in feet below sea level.



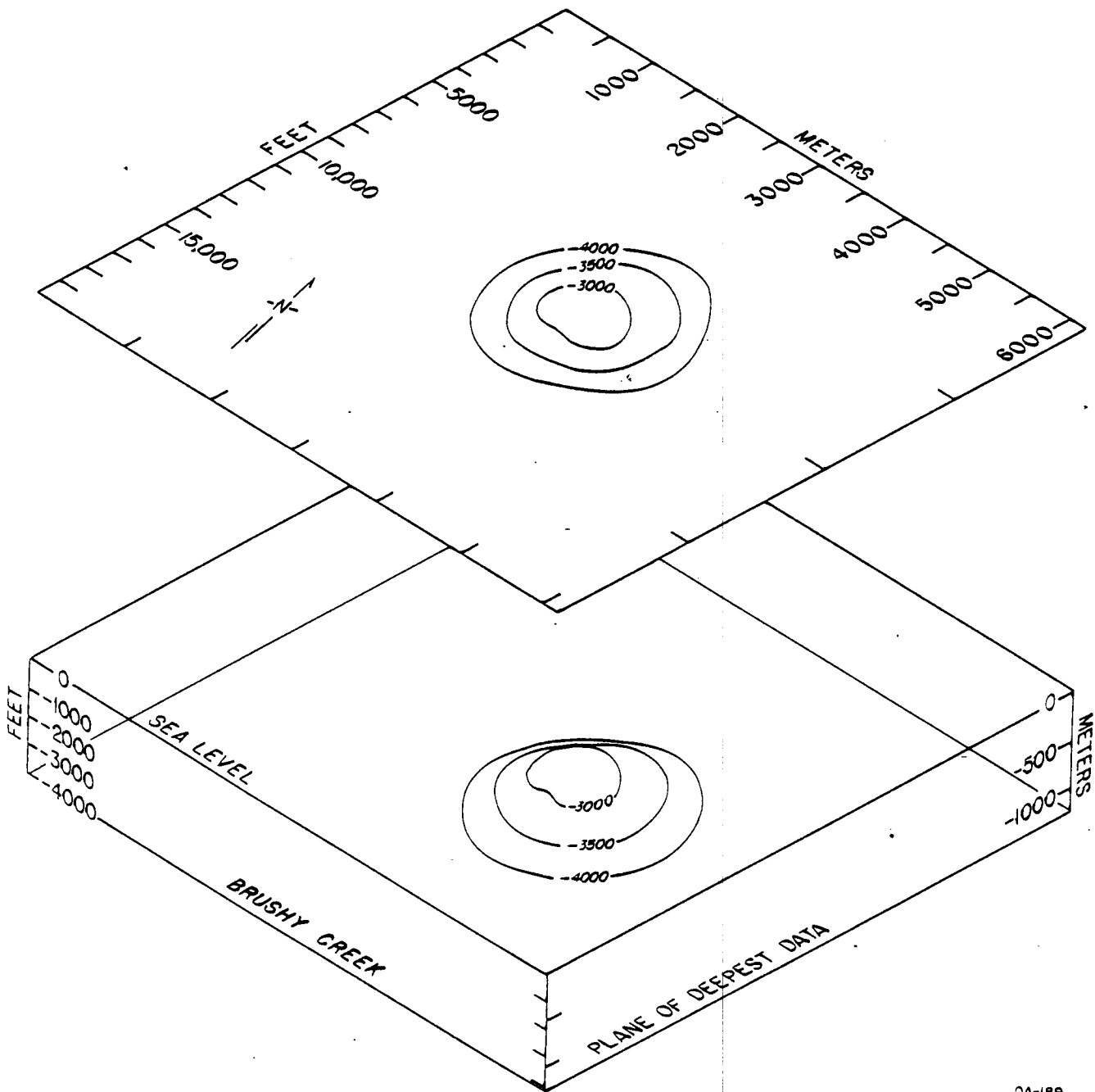
QA-200

ISOMETRIC BLOCK DIAGRAM OF SALT-STOCK SHAPE (SECTIONS 1.4, 1.5)  
Salt structure contours in feet below sea level.



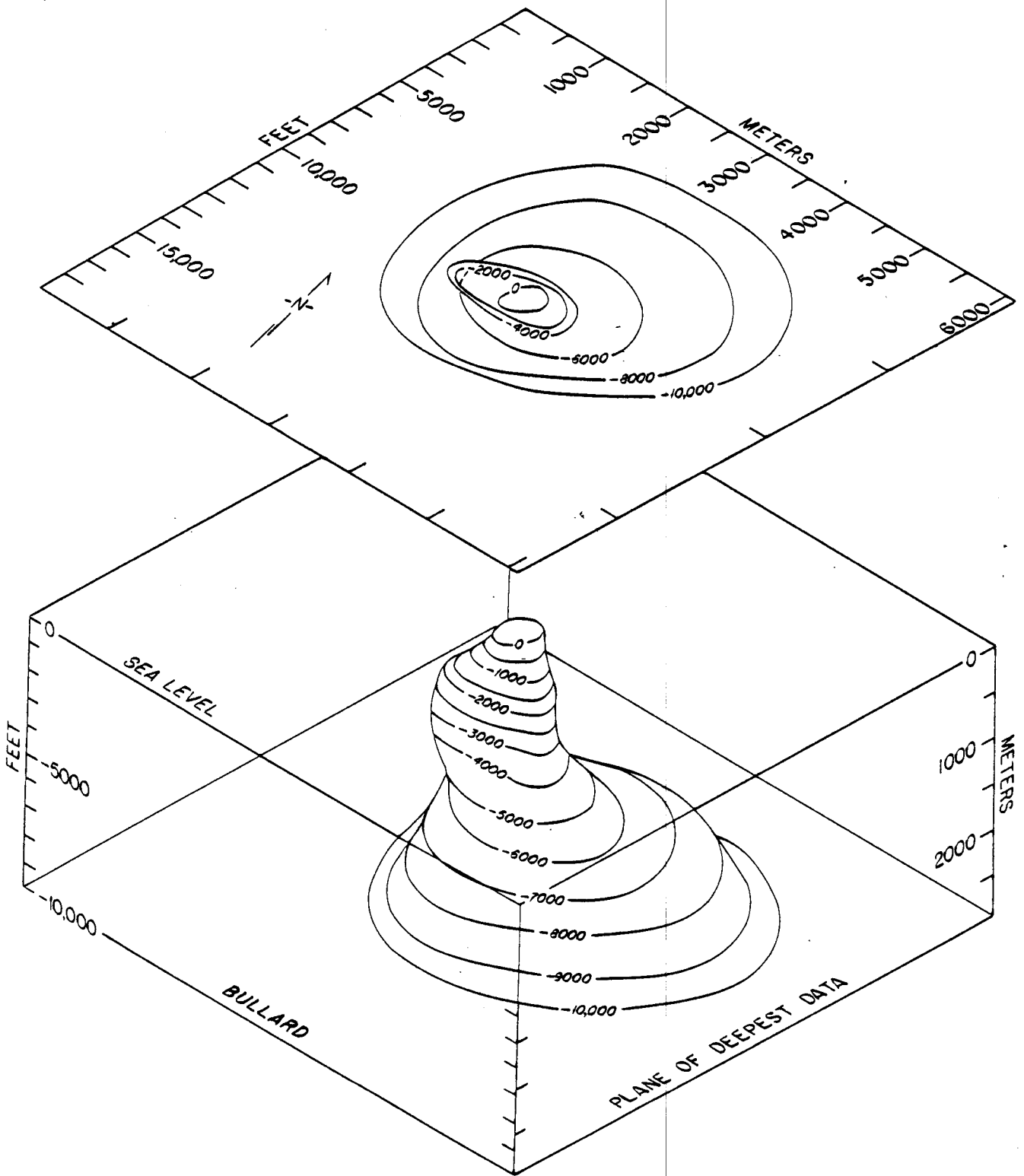
QA-198

ISOMETRIC BLOCK DIAGRAM OF SALT-STOCK SHAPE (SECTIONS 1.4, 1.5)  
Salt structure contours in feet below sea level.



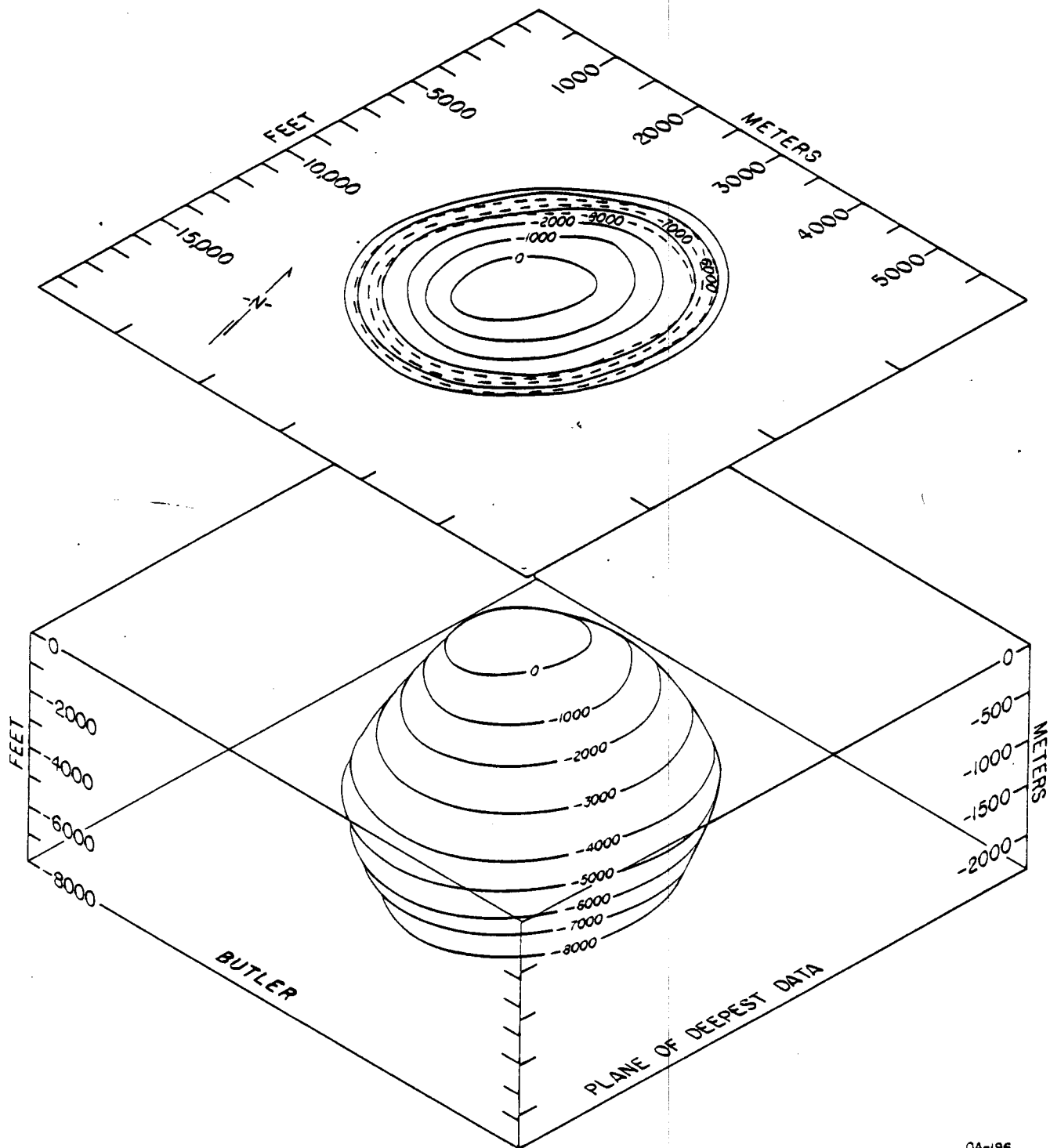
QA-189

ISOMETRIC BLOCK DIAGRAM OF SALT-STOCK SHAPE (SECTIONS 1.4, 1.5)  
Salt structure contours in feet below sea level.



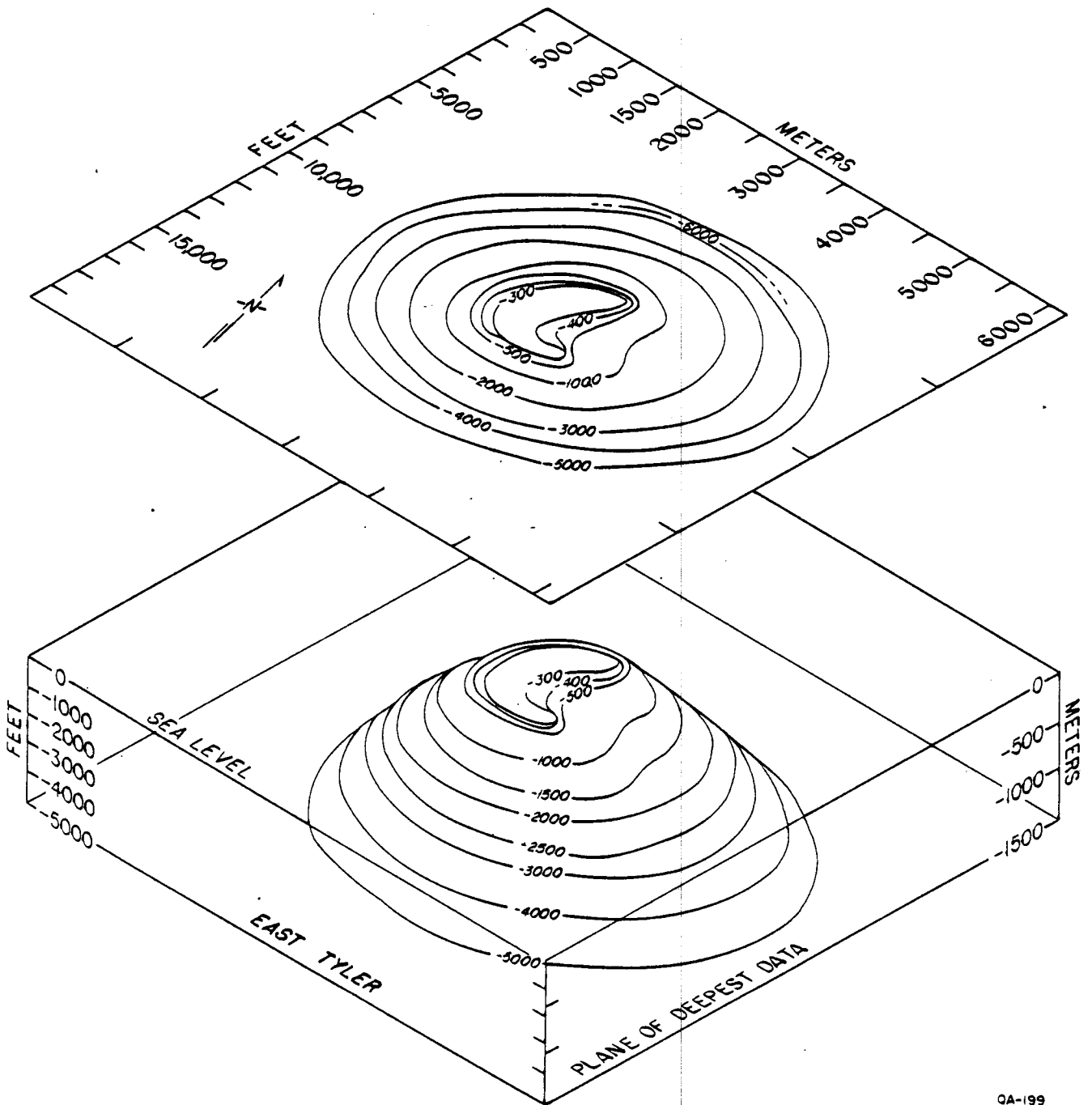
QA-191

ISOMETRIC BLOCK DIAGRAM OF SALT-STOCK SHAPE (SECTIONS 1.4, 1.5)  
Salt structure contours in feet below sea level.



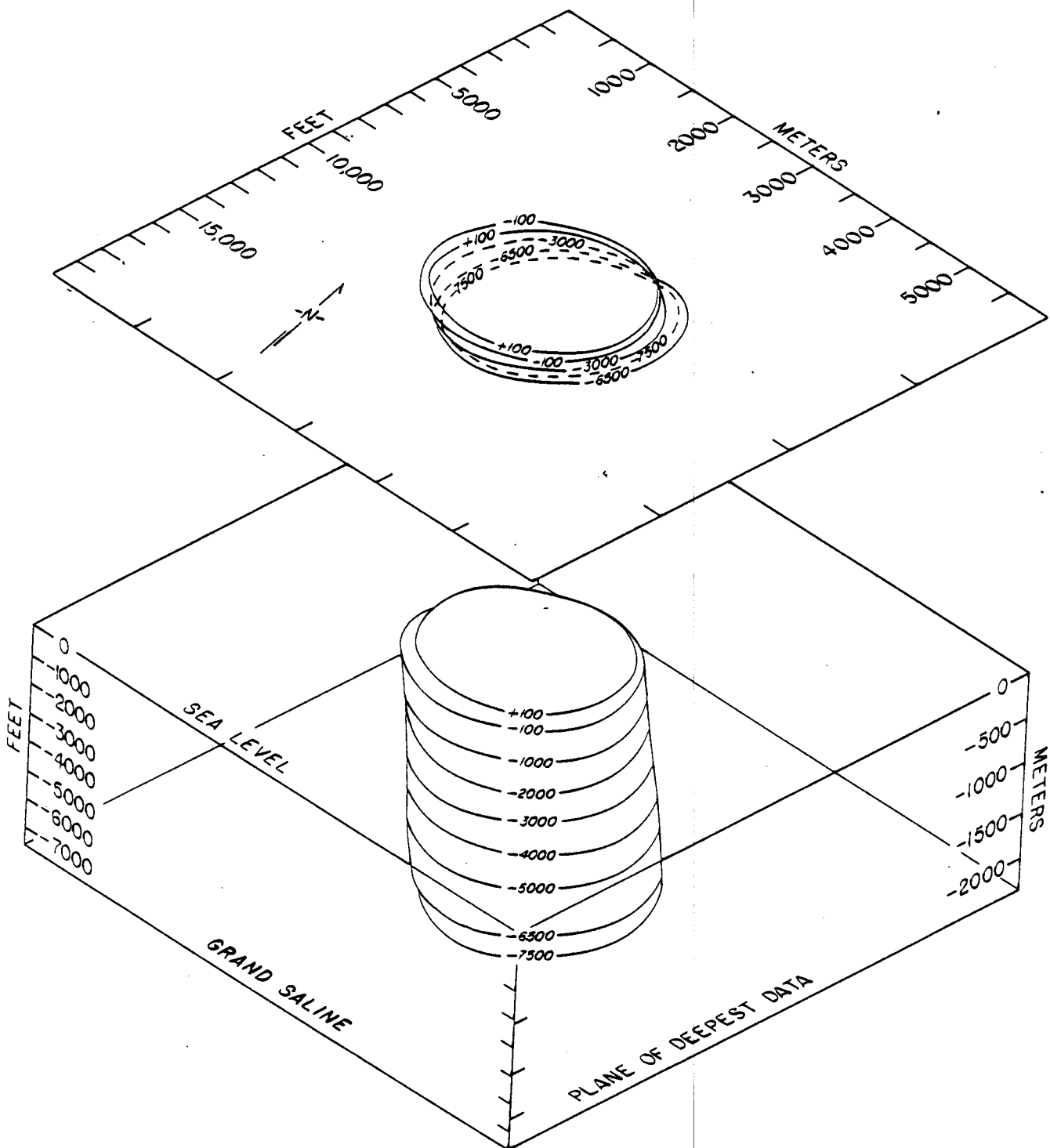
QA-196

ISOMETRIC BLOCK DIAGRAM OF SALT-STOCK SHAPE (SECTIONS 1.4, 1.5)  
Salt structure contours in feet below sea level.



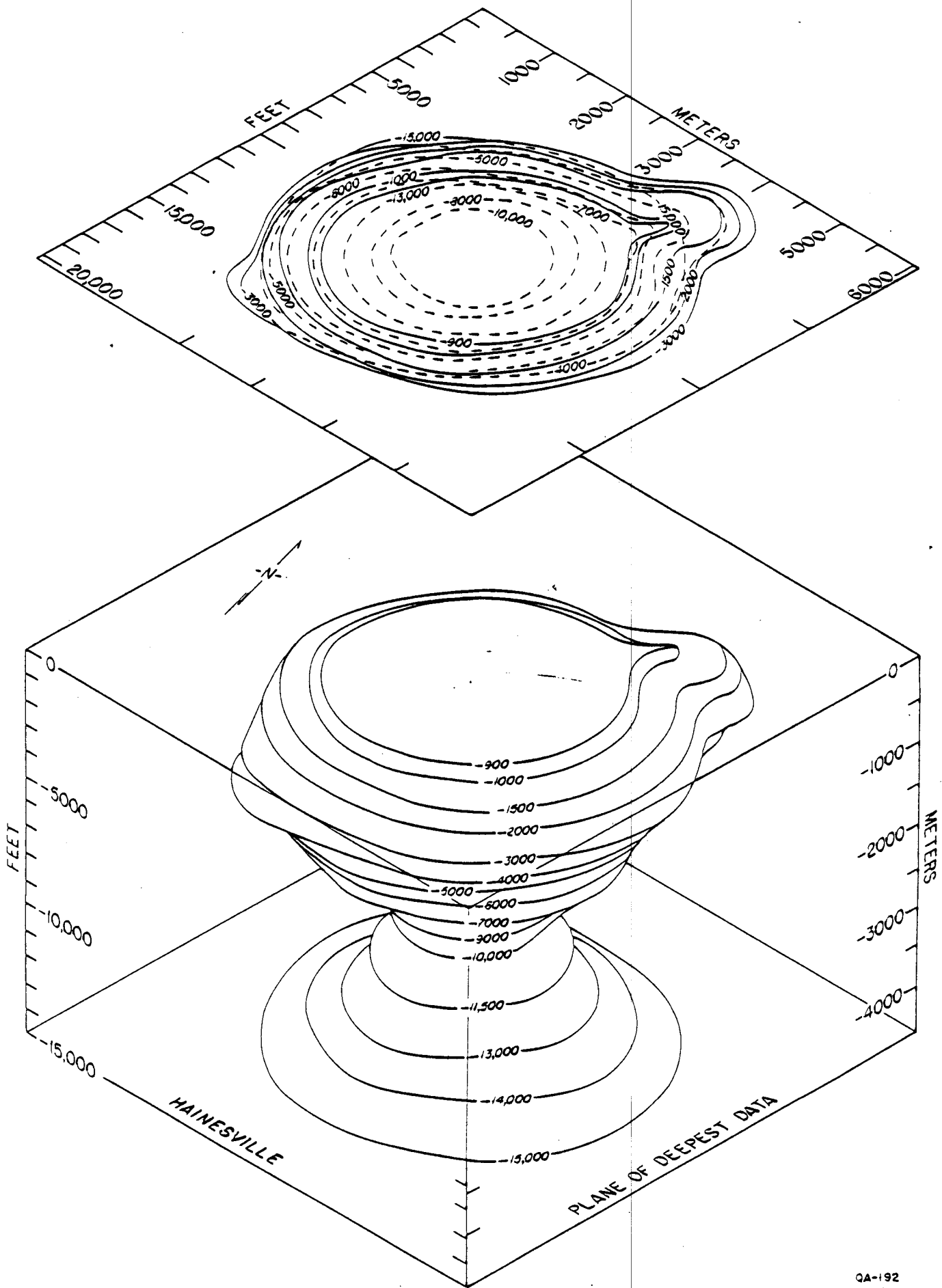
QA-199

ISOMETRIC BLOCK DIAGRAM OF SALT-STOCK SHAPE (SECTIONS 1.4, 1.5)  
Salt structure contours in feet below sea level.



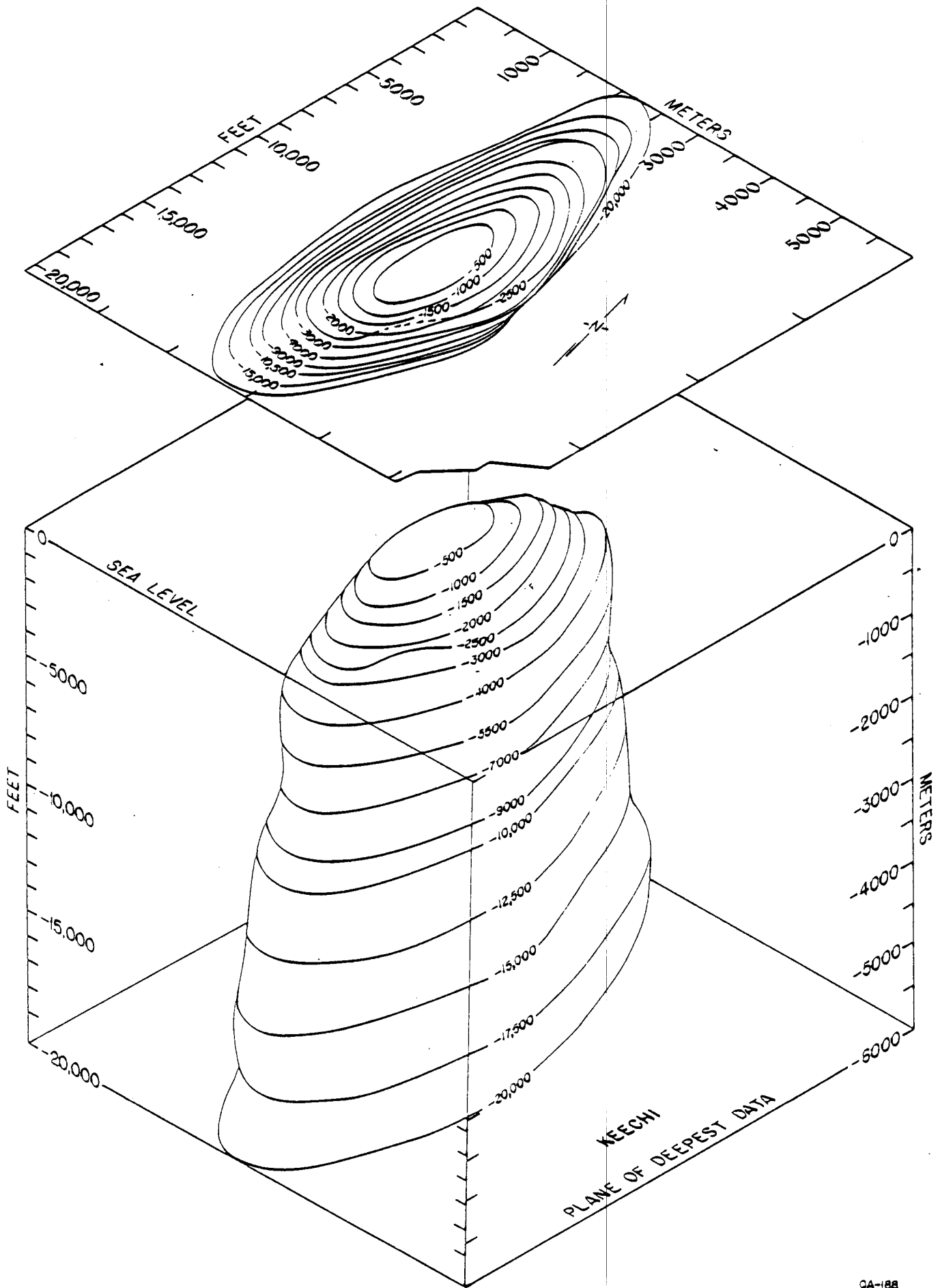
QA-193

ISOMETRIC BLOCK DIAGRAM OF SALT-STOCK SHAPE (SECTIONS 1.4, 1.5)  
Salt structure contours in feet below sea level.



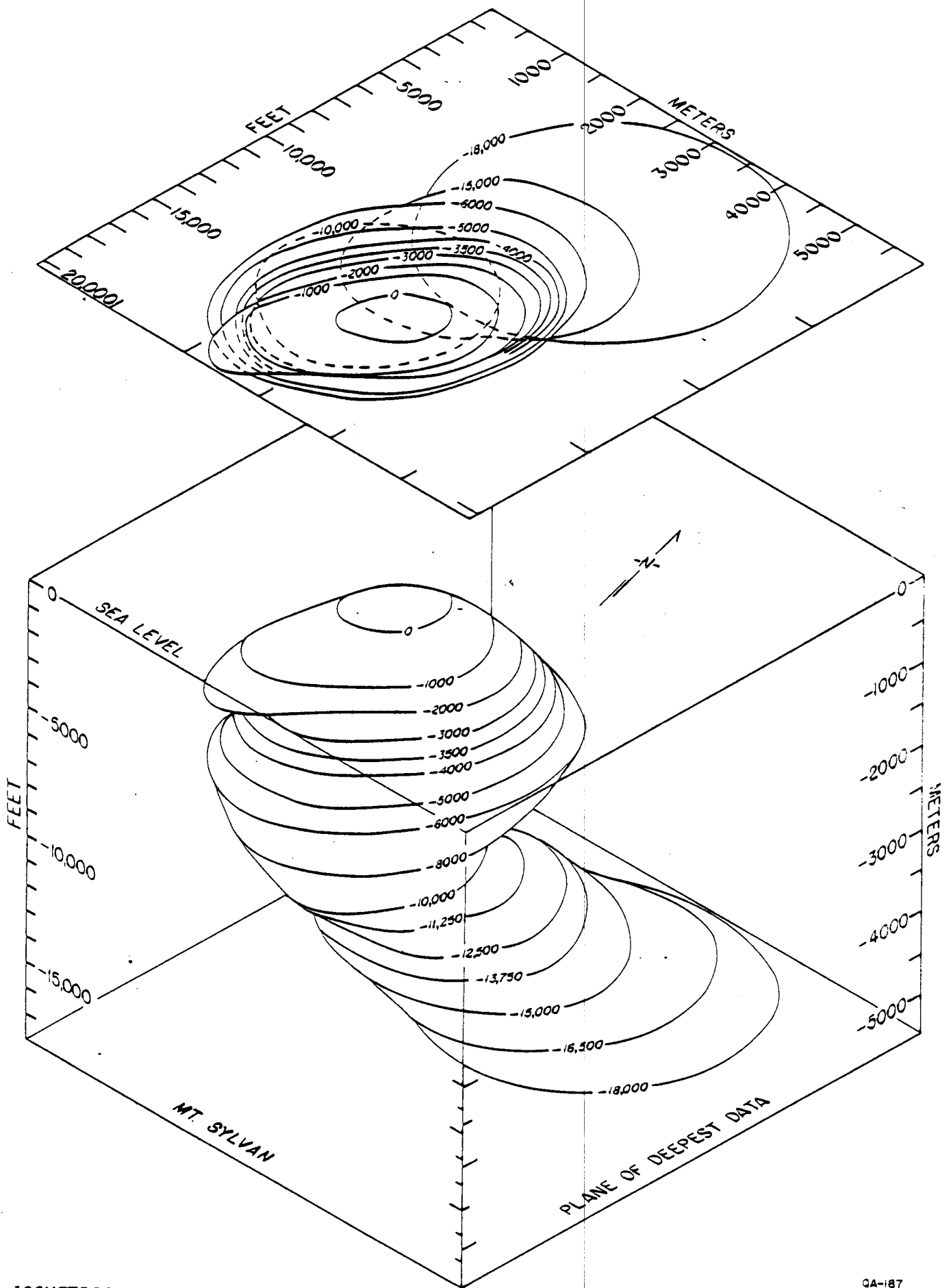
ISOMETRIC BLOCK DIAGRAM OF SALT-STOCK SHAPE (SECTIONS 1.4, 1.5)  
Salt structure contours in feet below sea level.

QA-192



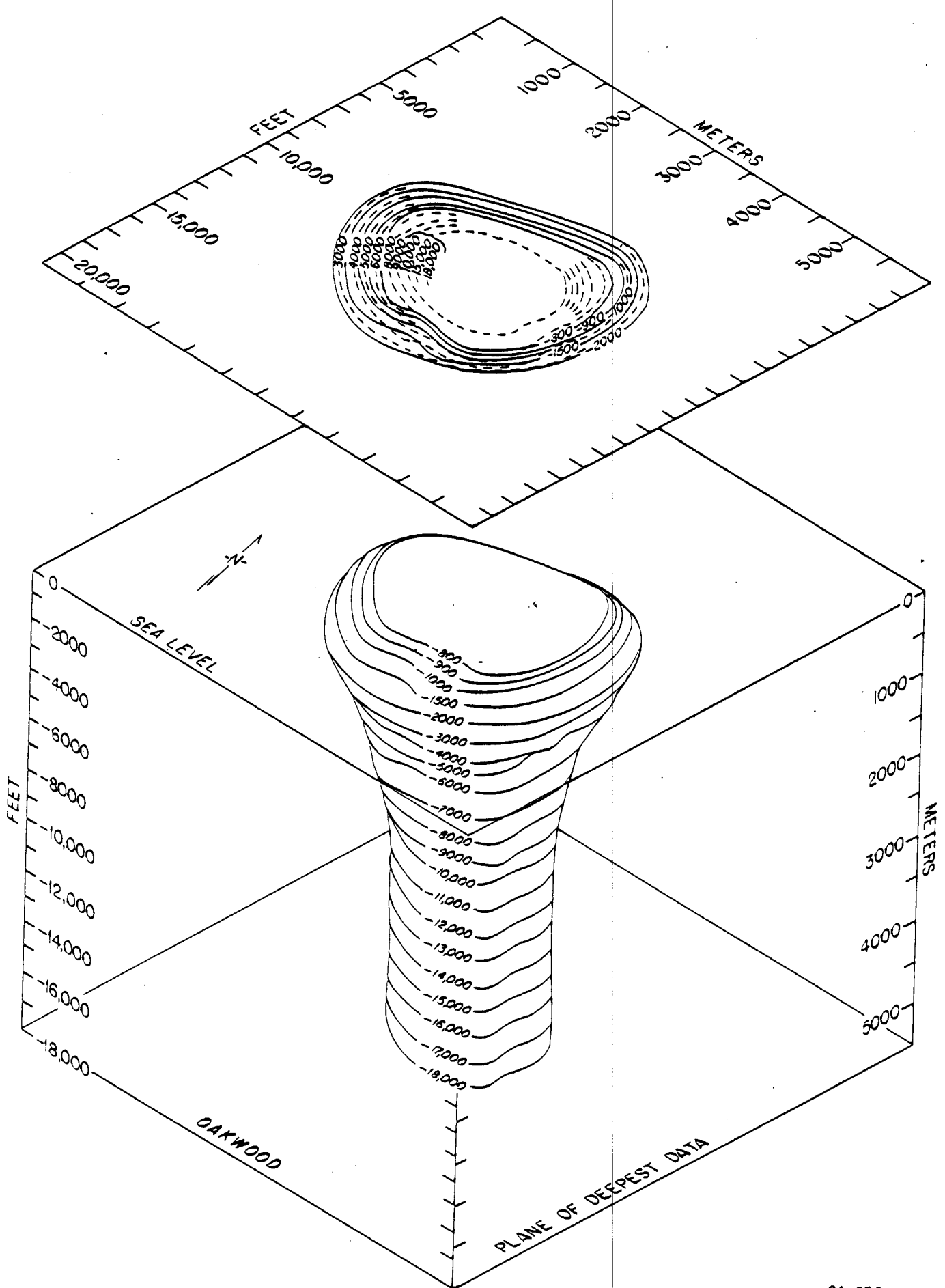
ISOMETRIC BLOCK DIAGRAM OF SALT-STOCK SHAPE (SECTIONS 1.4, 1.5)  
Salt structure contours in feet below sea level.

QA-188



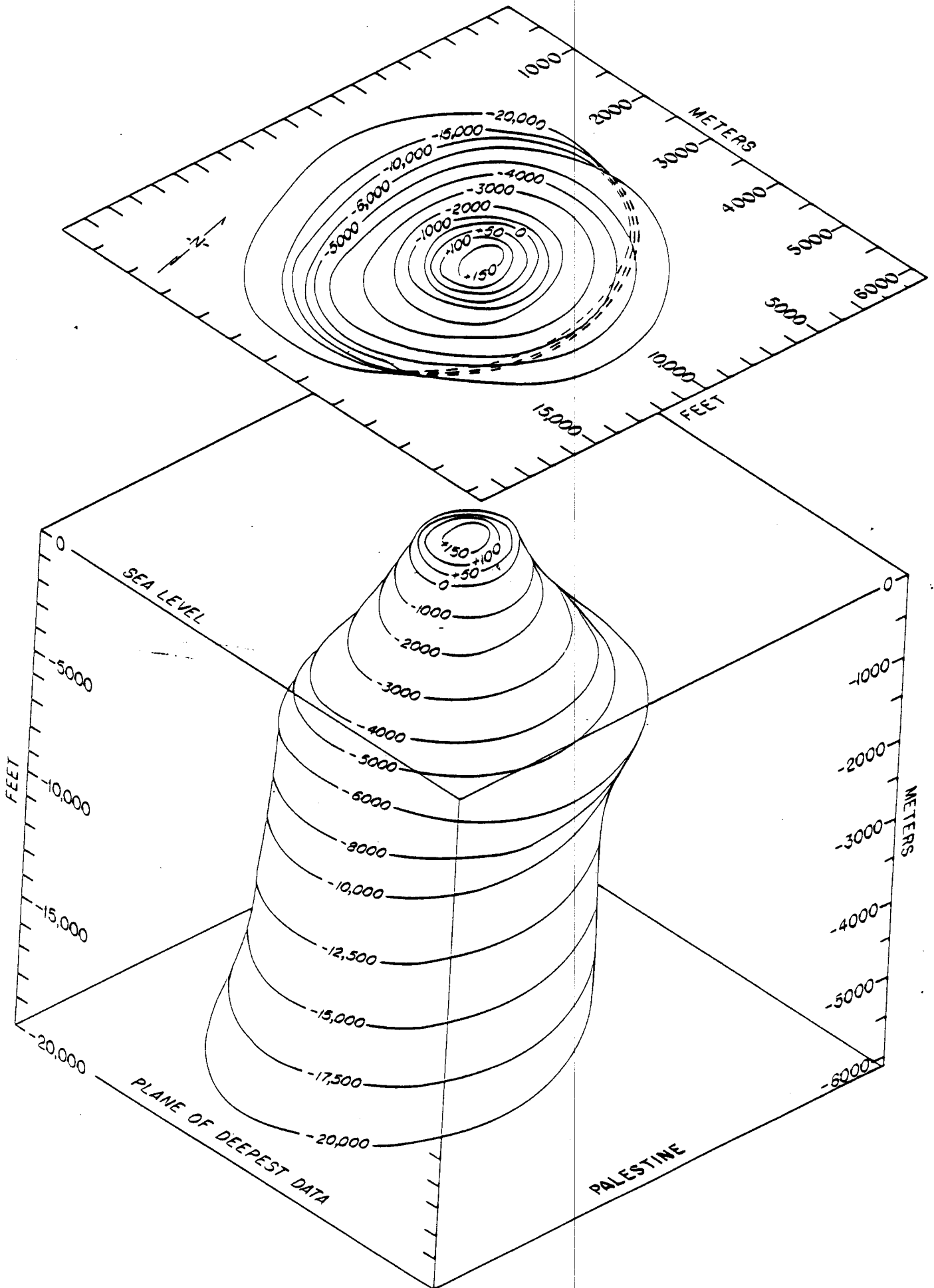
ISOMETRIC BLOCK DIAGRAM OF SALT-STOCK SHAPE (SECTIONS 1.4, 1.5)  
Salt structure contours in feet below sea level.

QA-187



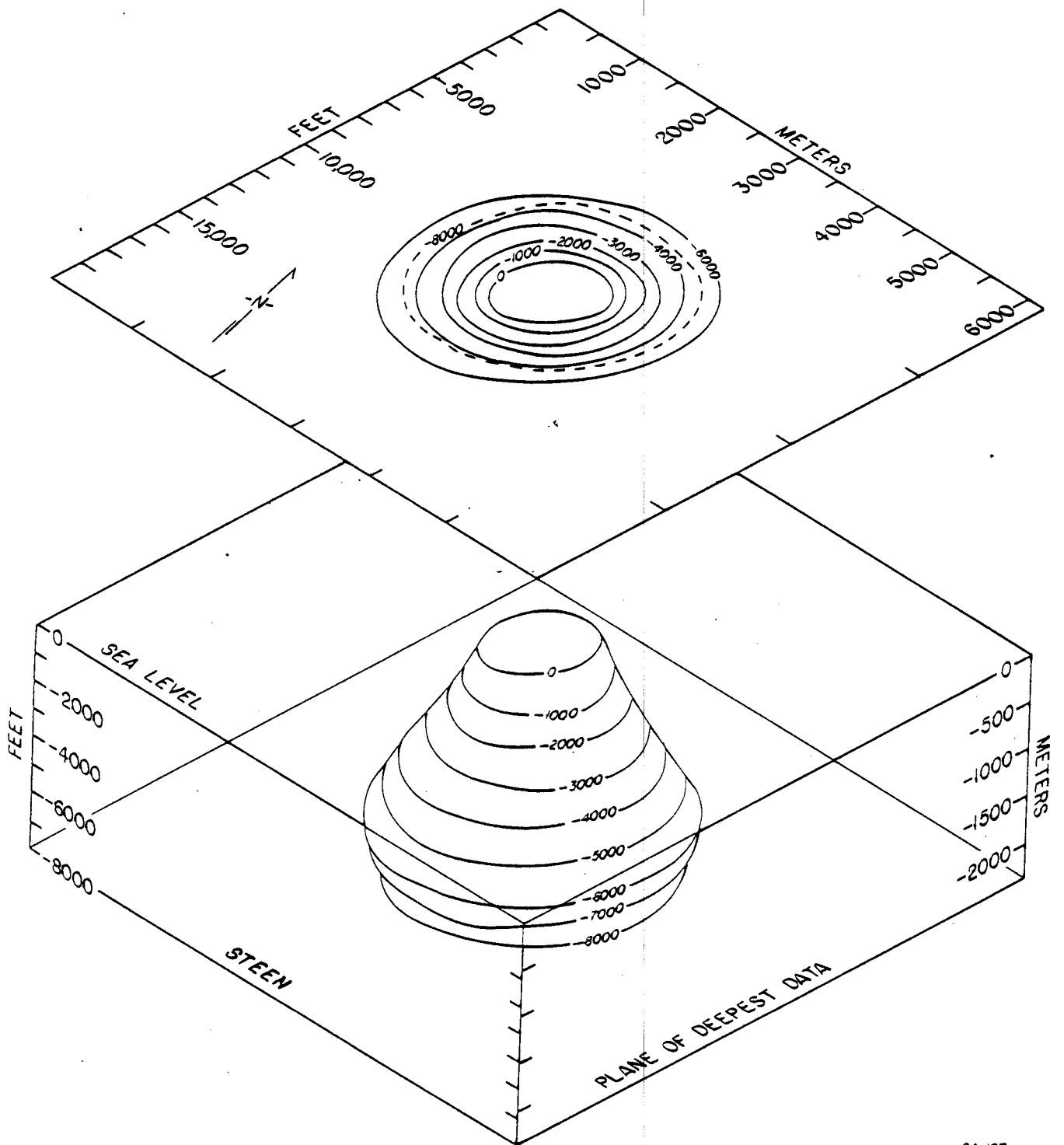
ISOMETRIC BLOCK DIAGRAM OF SALT-STOCK SHAPE (SECTIONS 1.4, 1.5)  
Salt structure contours in feet below sea level.

QA-256



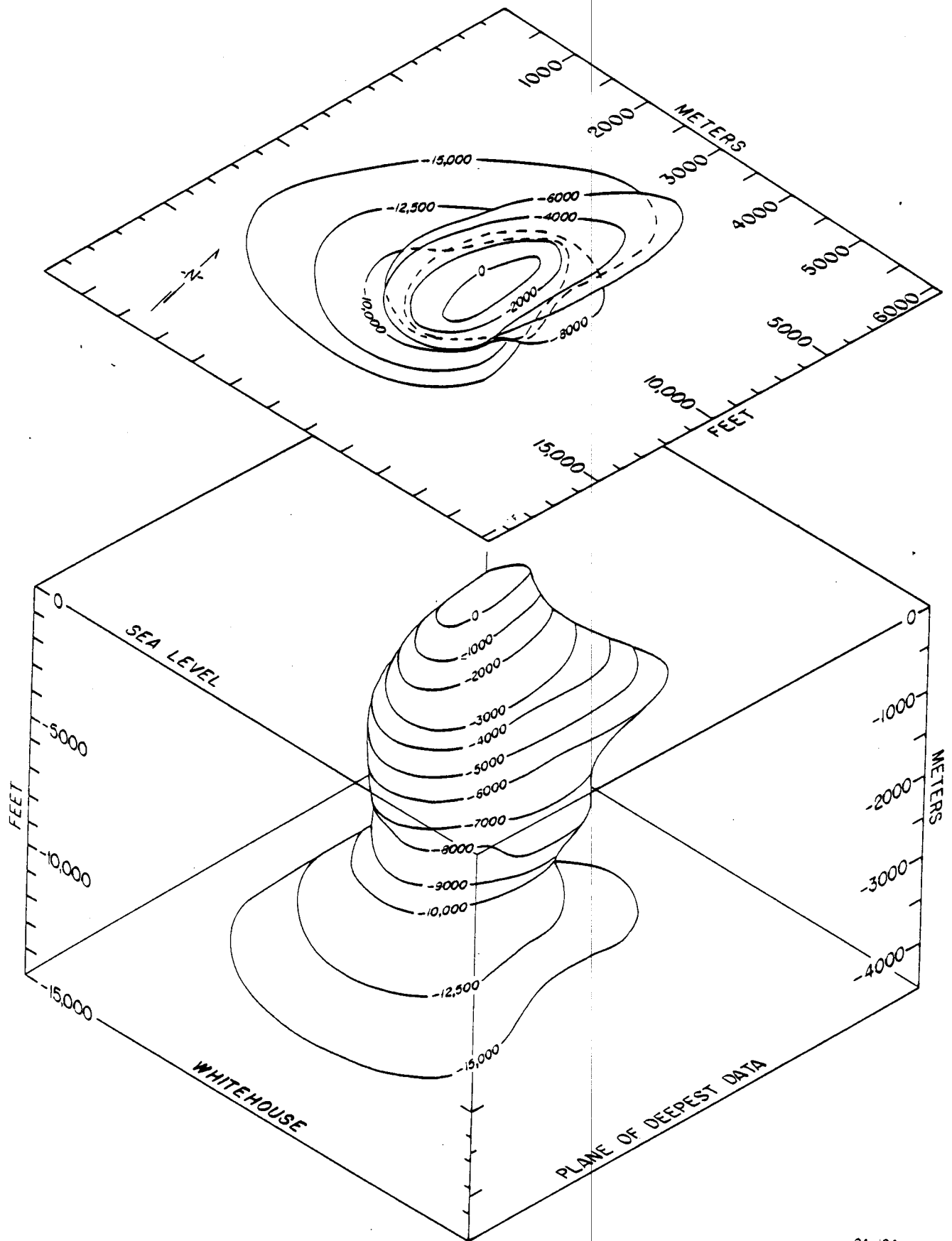
ISOMETRIC BLOCK DIAGRAM OF SALT-STOCK SHAPE (SECTIONS 1.4, 1.5)  
 Salt structure contours in feet below sea level.

QA-190



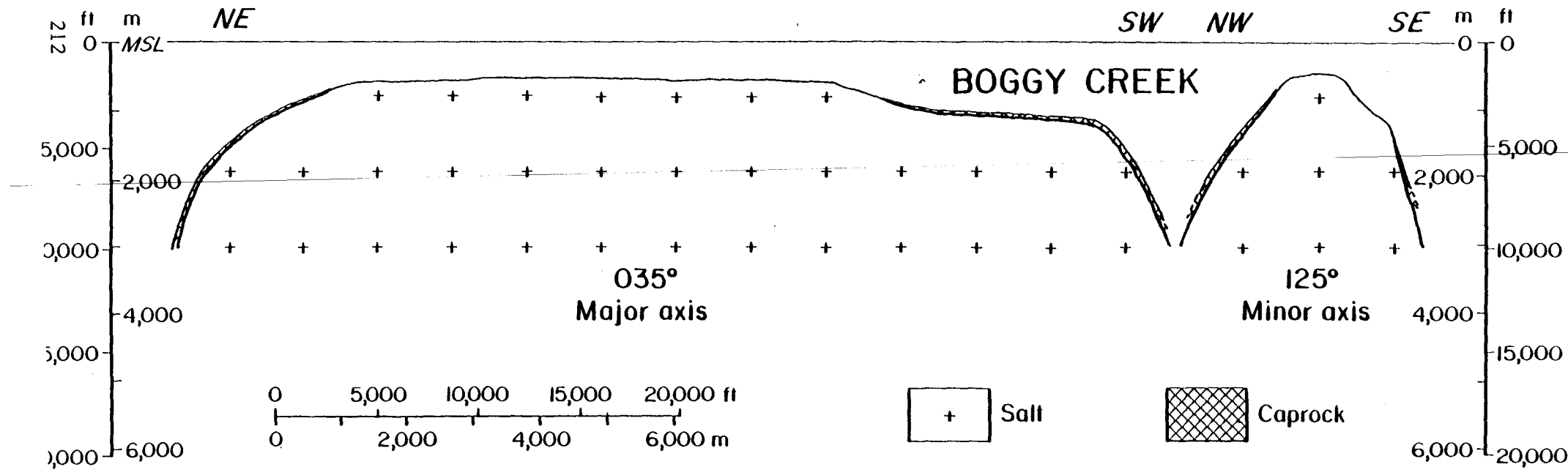
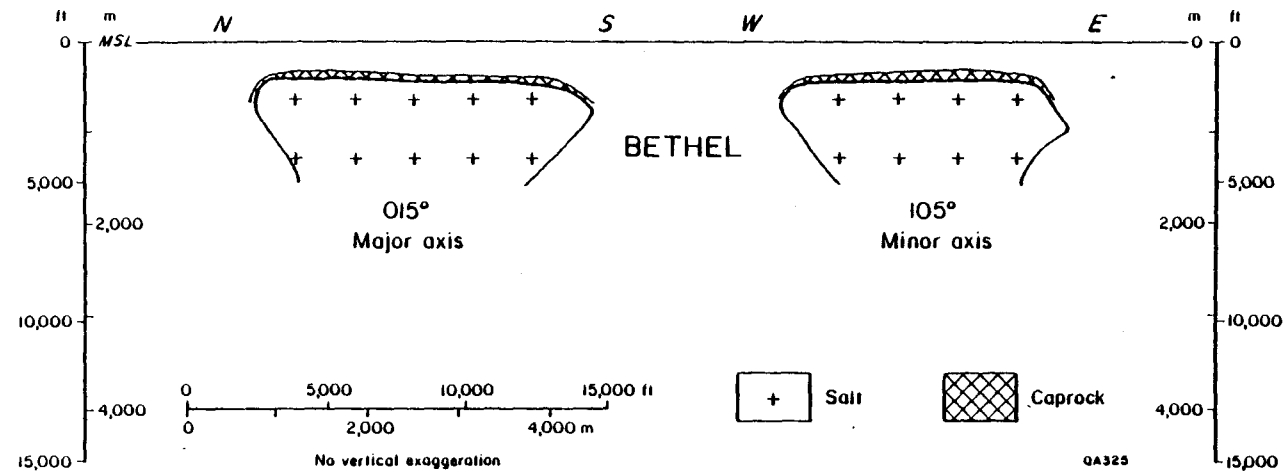
ISOMETRIC BLOCK DIAGRAM OF SALT-STOCK SHAPE (SECTIONS 1.4, 1.5)  
Salt structure contours in feet below sea level.

QA-197

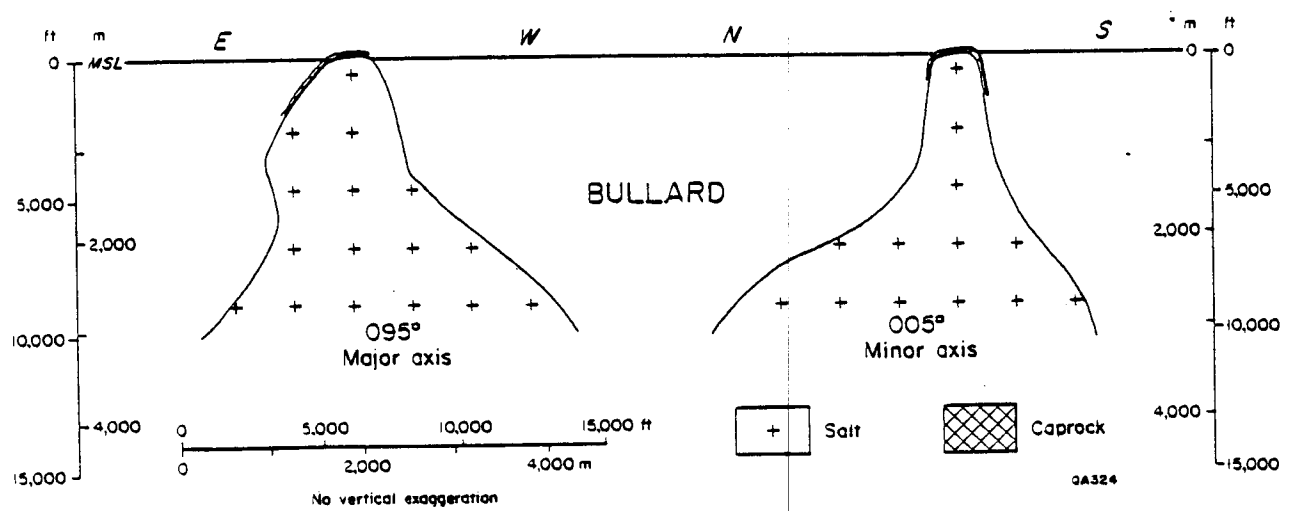
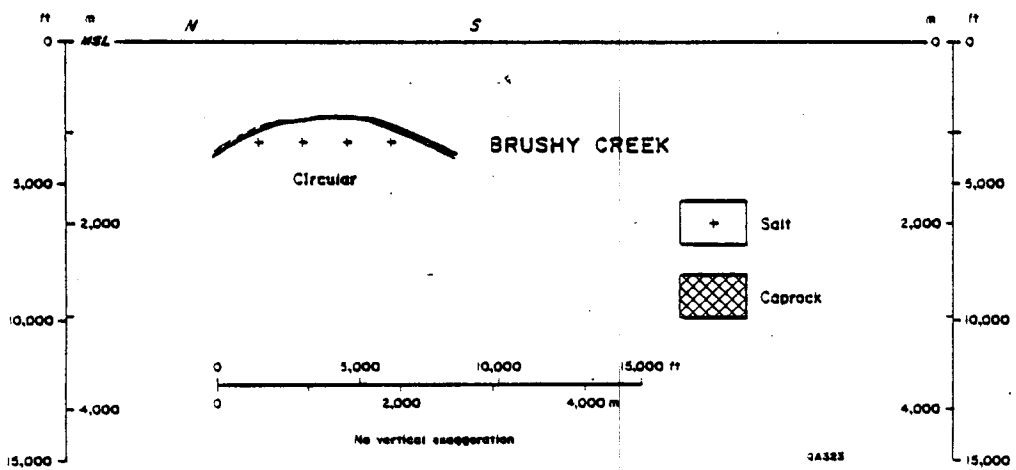
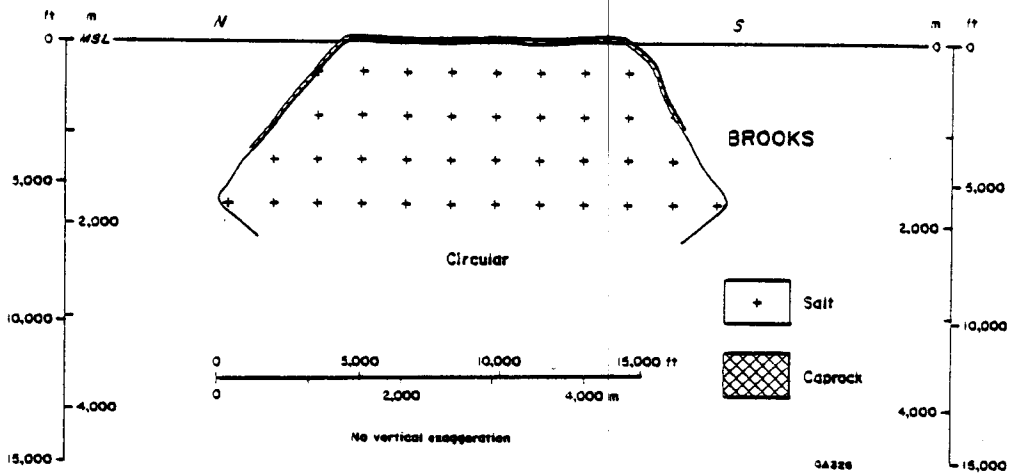


ISOMETRIC BLOCK DIAGRAM OF SALT-STOCK SHAPE (SECTIONS 1.4, 1.5)  
Salt structure contours in feet below sea level.

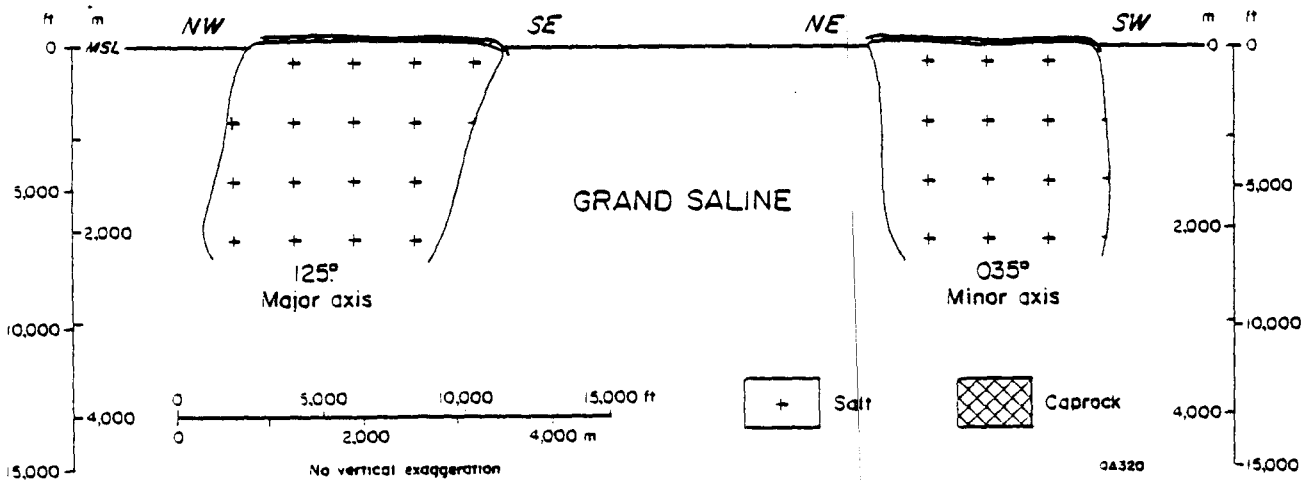
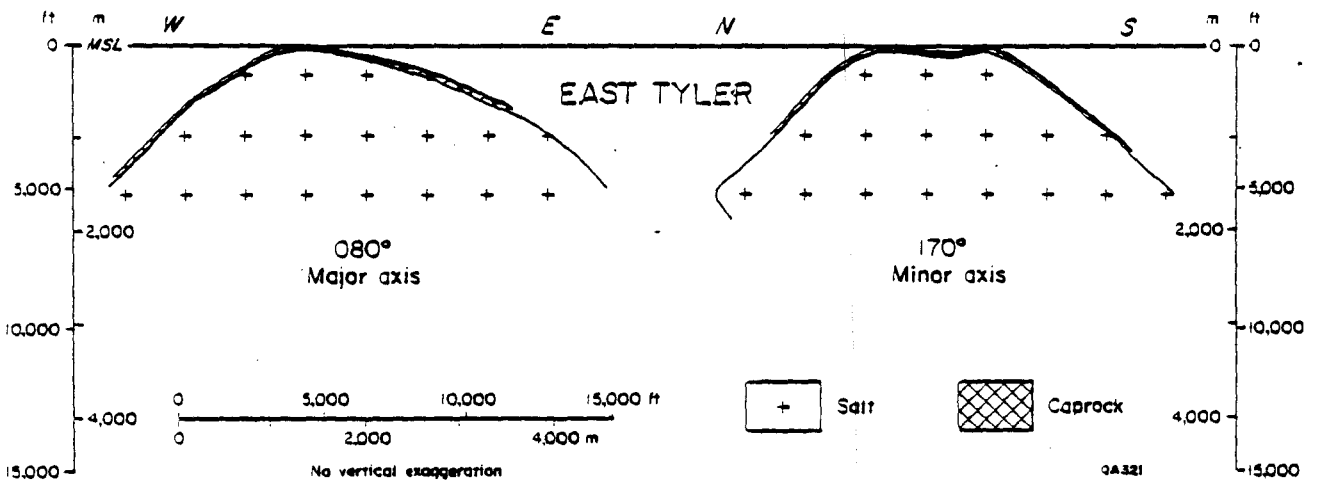
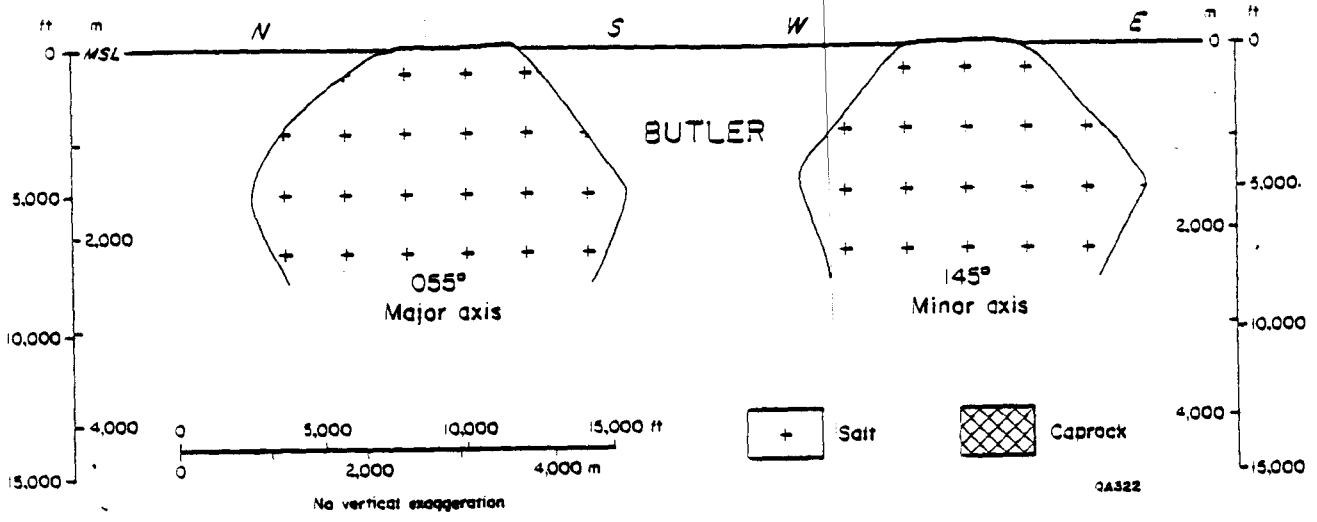
QA-194



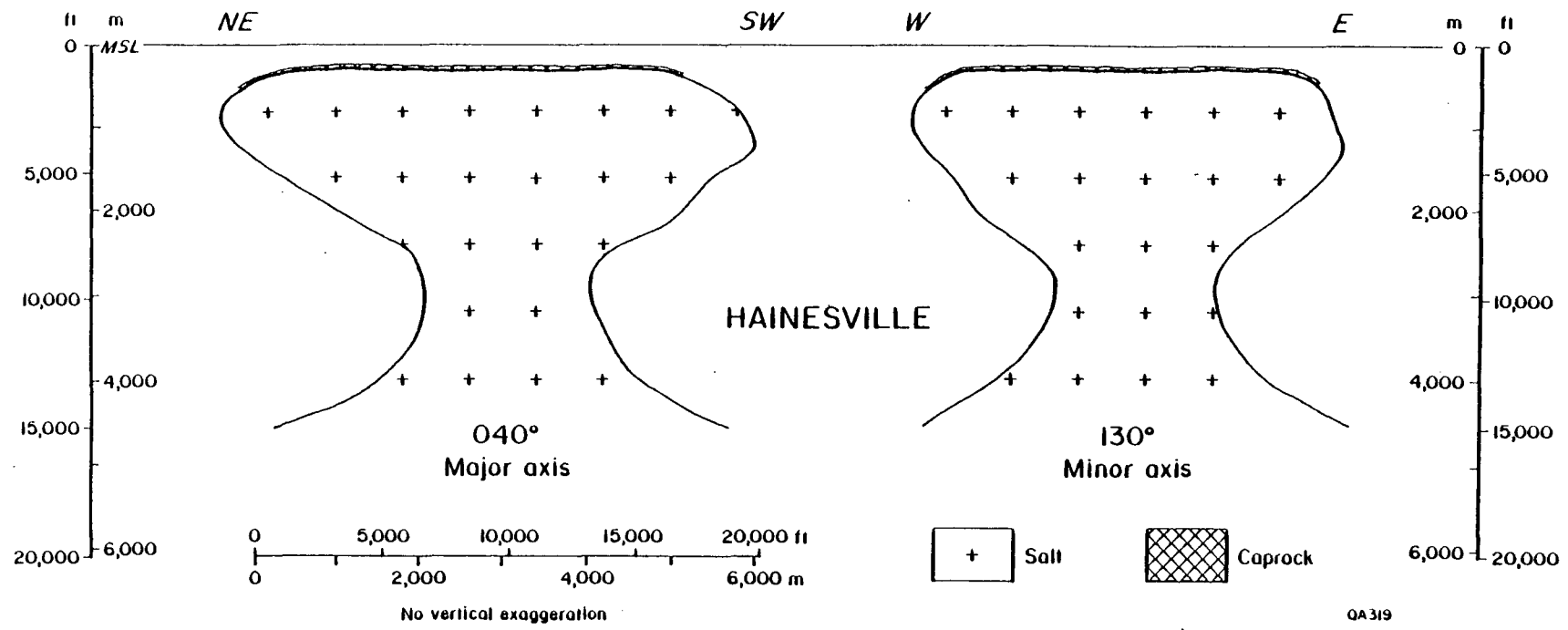
ORTHOGONAL CROSS SECTIONS THROUGH SALT STOCKS (SECTIONS 1.4, 1.5, 1.6)



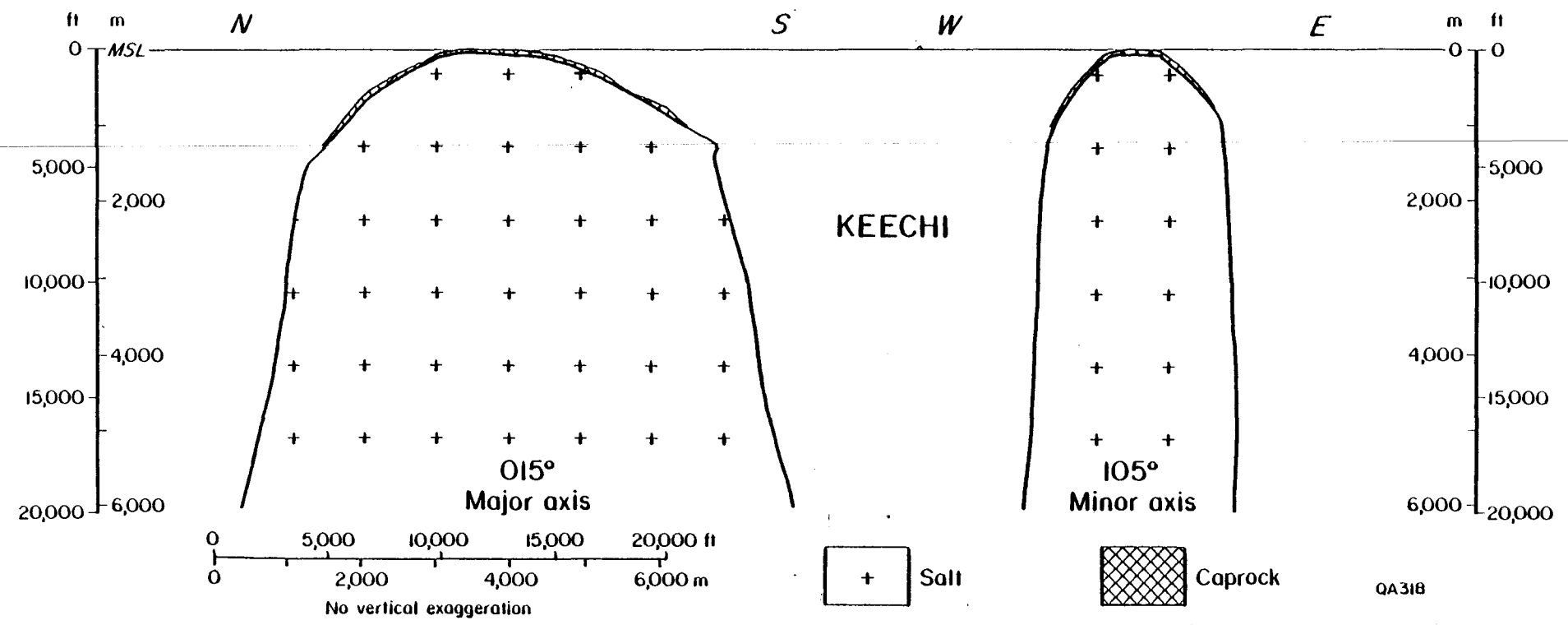
ORTHOGONAL CROSS SECTIONS THROUGH SALT STOCKS (SECTIONS 1.4, 1.5, 1.6)



ORTHOGONAL CROSS SECTIONS THROUGH SALT STOCKS (SECTIONS 1.4, 1.5, 1.6)

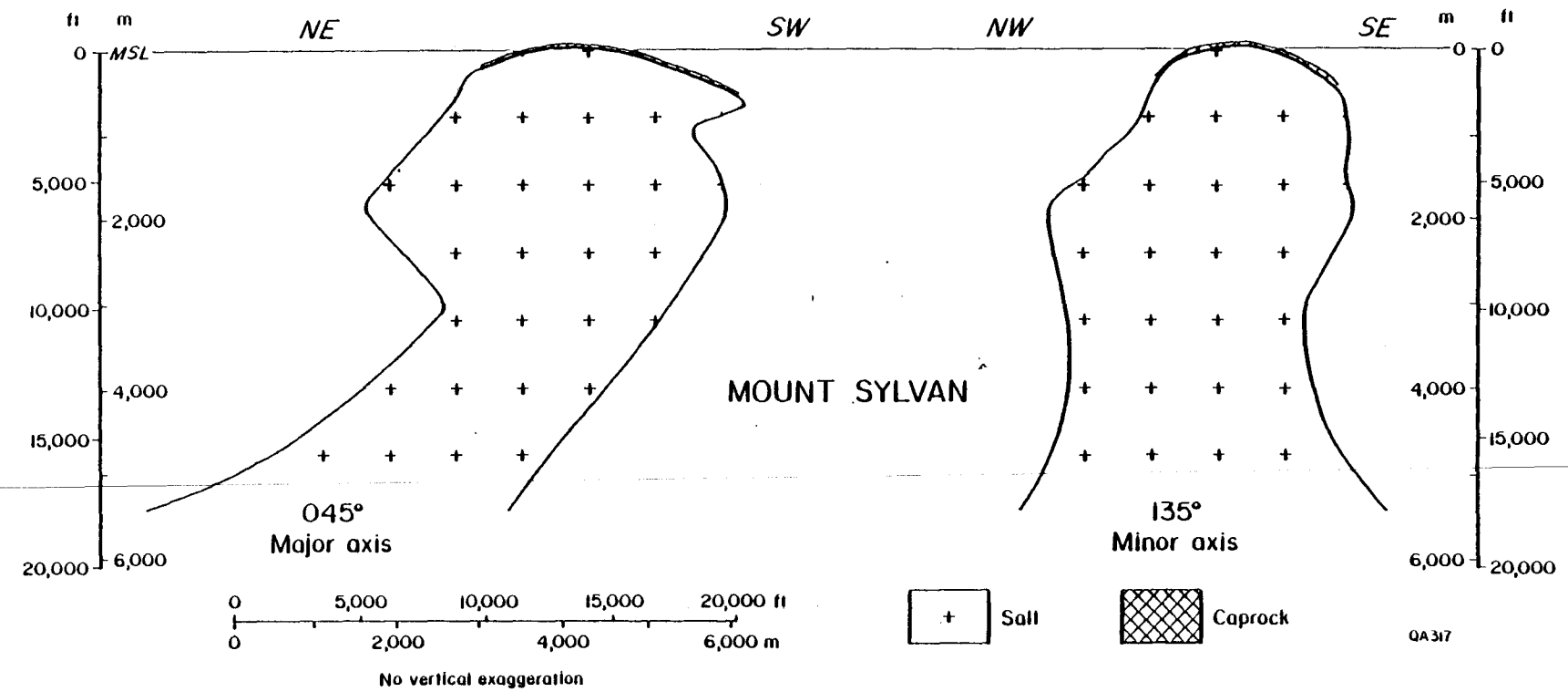


215

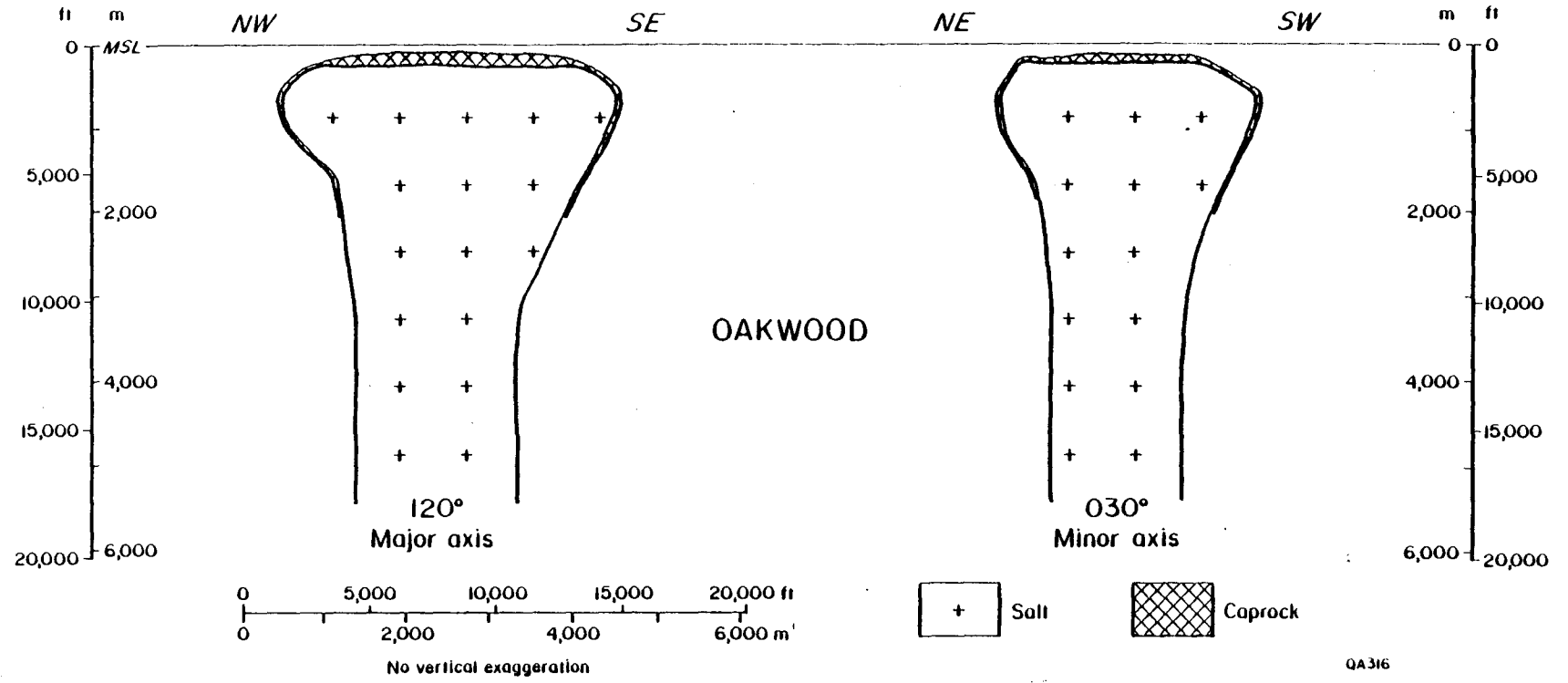


ORTHOGONAL CROSS SECTIONS THROUGH SALT STOCKS (SECTIONS 1.4, 1.5, 1.6)

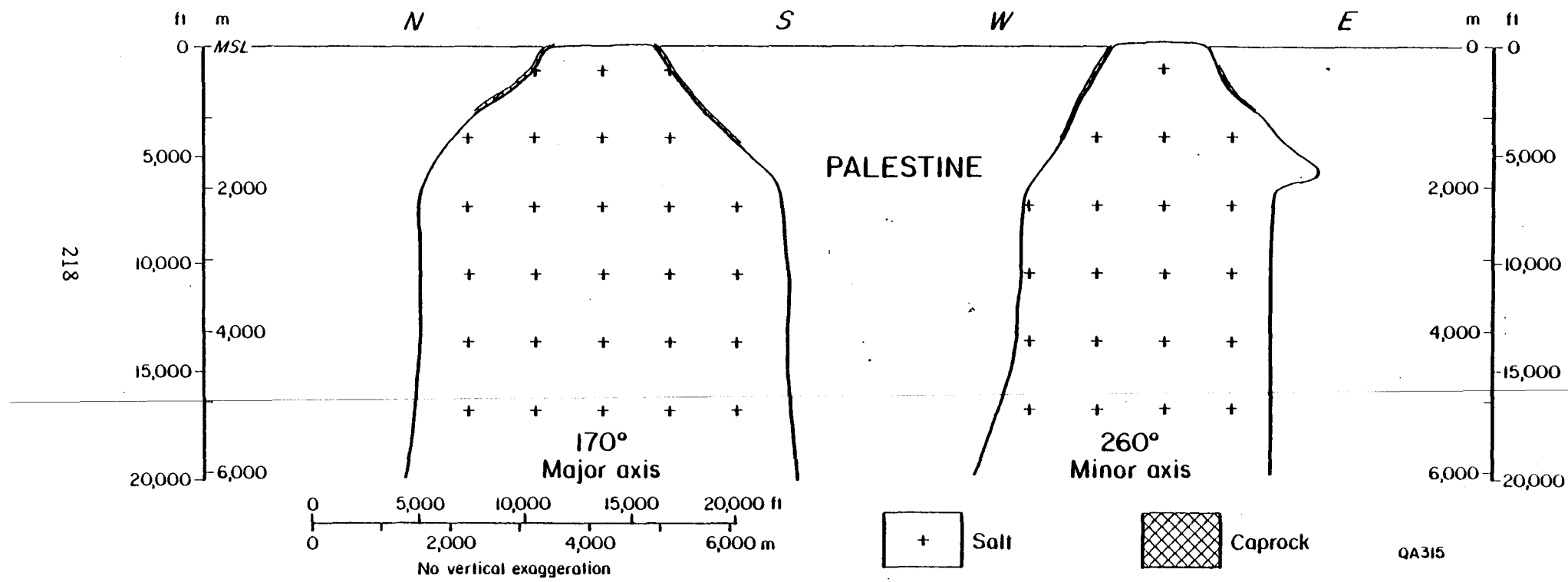
216



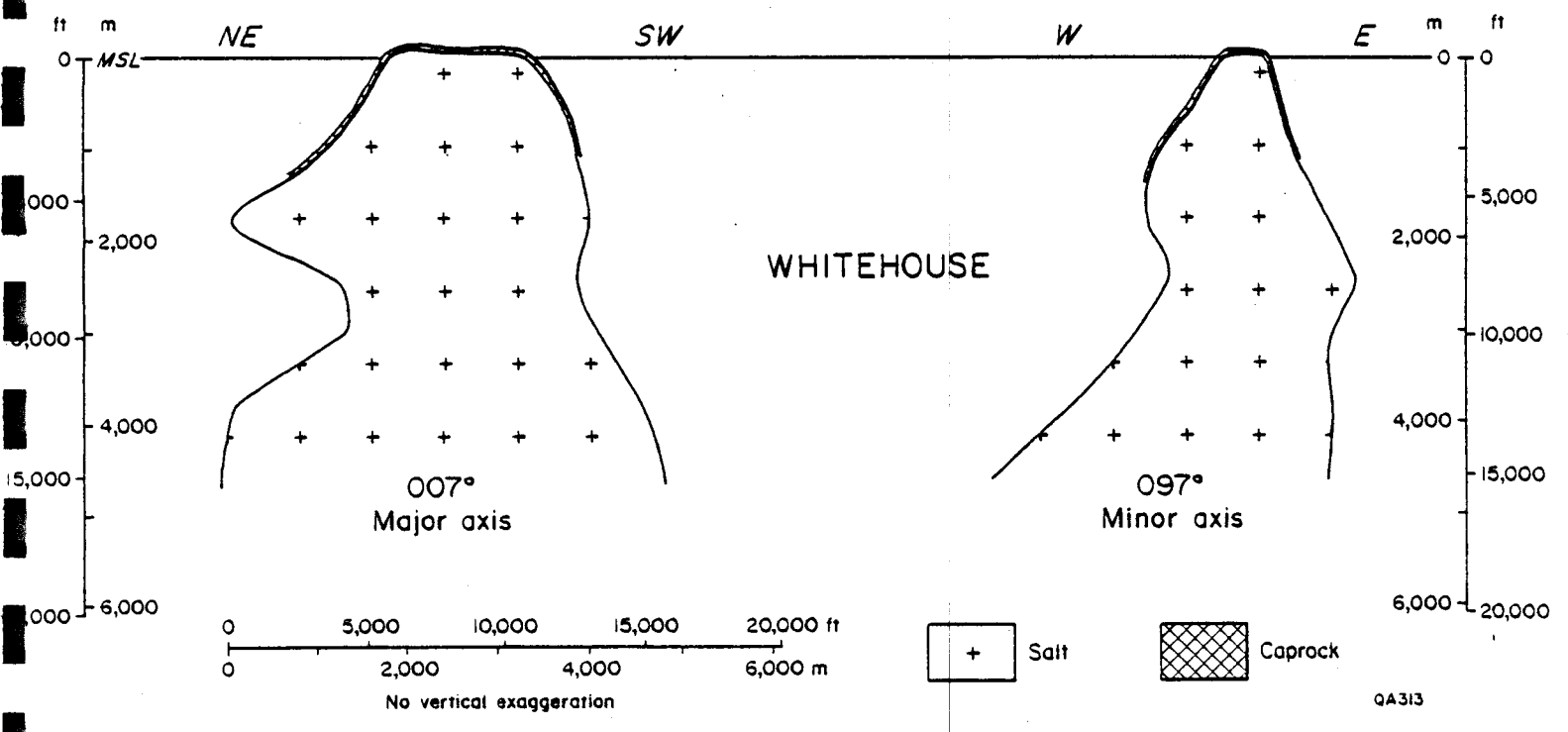
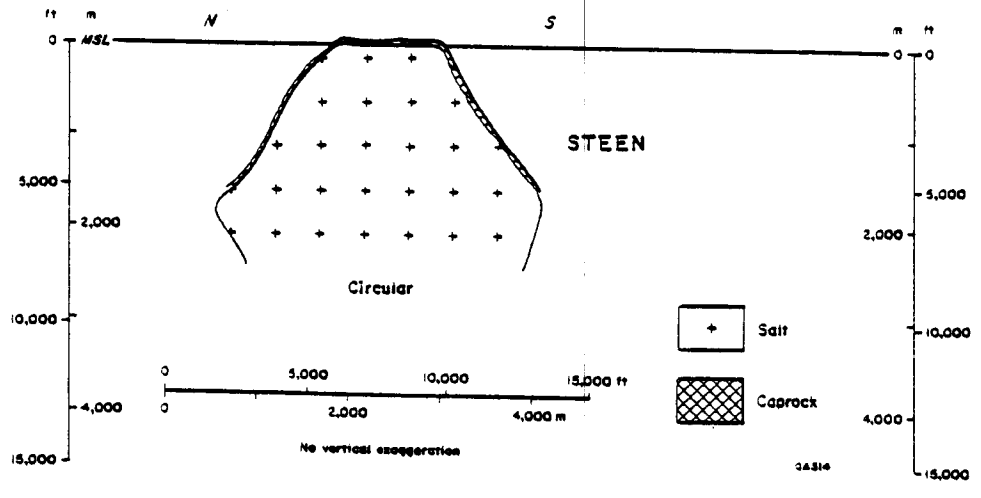
ORTHOGONAL CROSS SECTIONS THROUGH SALT STOCK (SECTIONS 1.4, 1.5, 1.6)



ORTHOGONAL CROSS SECTIONS THROUGH SALT STOCK (SECTIONS 1.4, 1.5, 1.6)

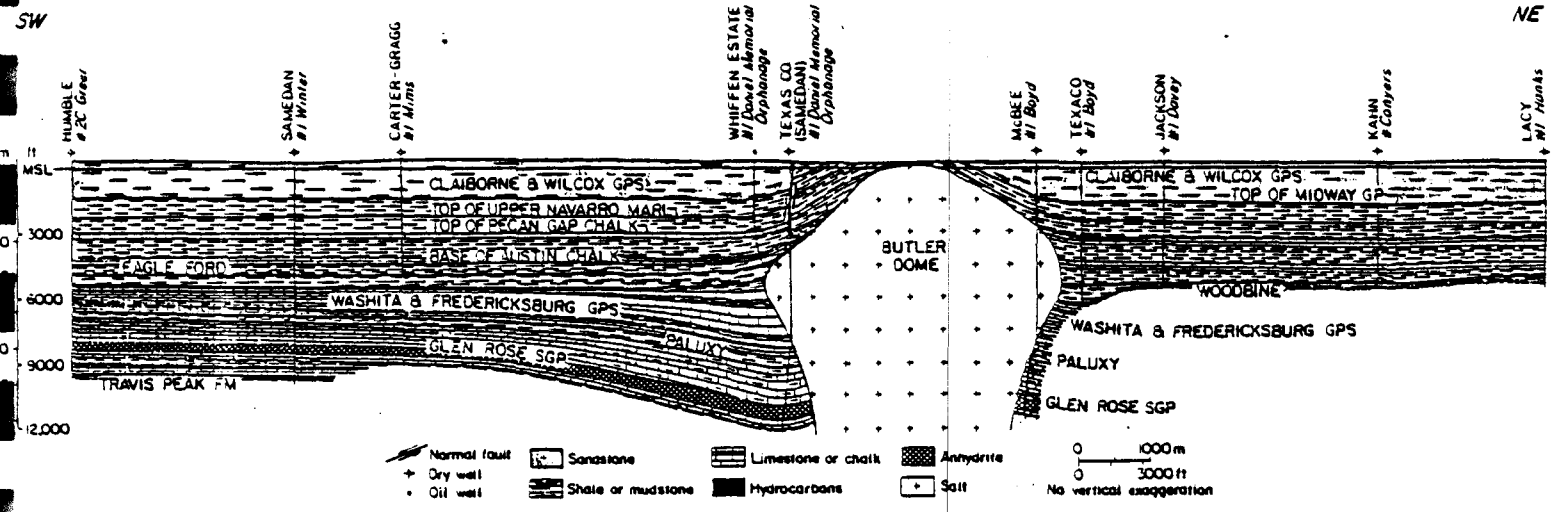
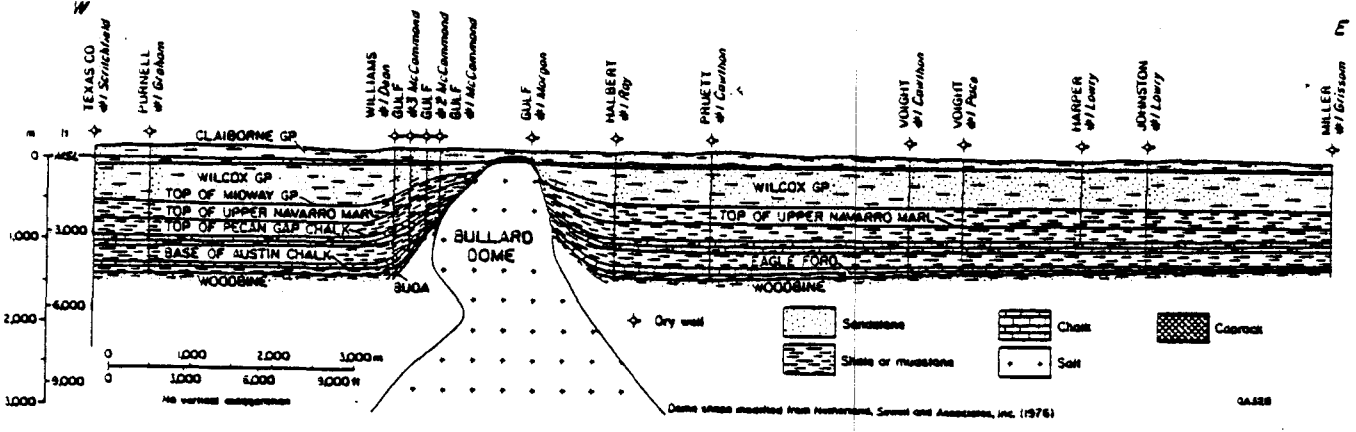
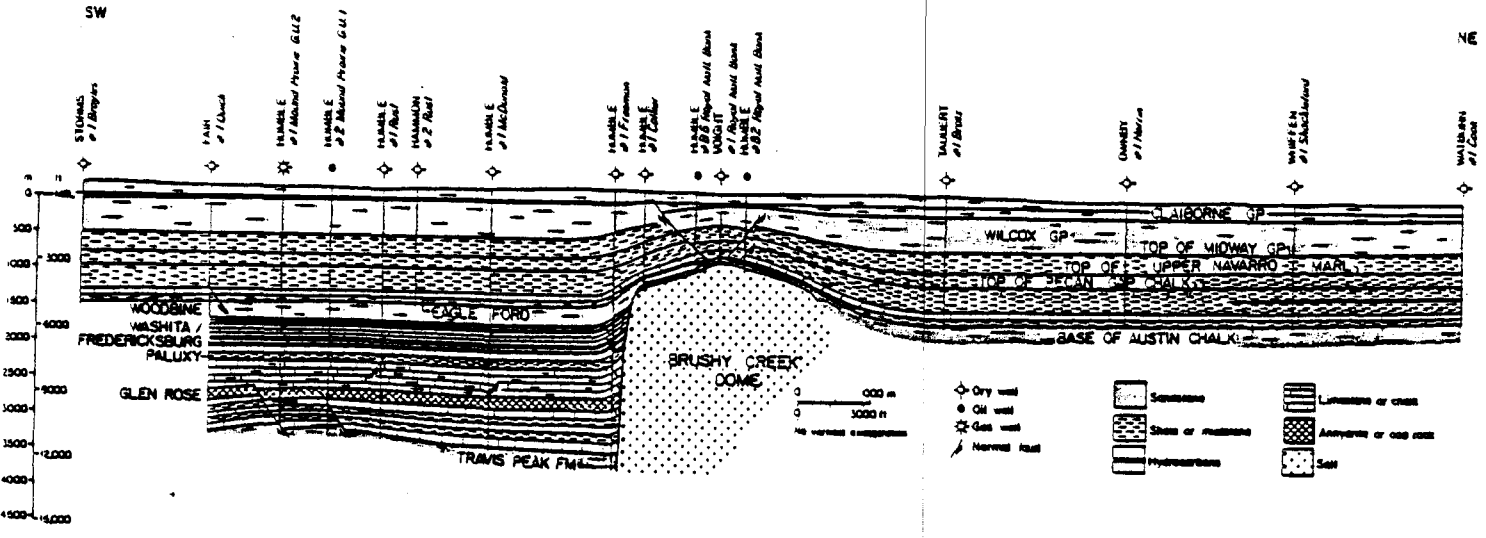


ORTHOGONAL CROSS SECTIONS THROUGH SALT STOCK (SECTIONS 1.4, 1.5, 1.6)

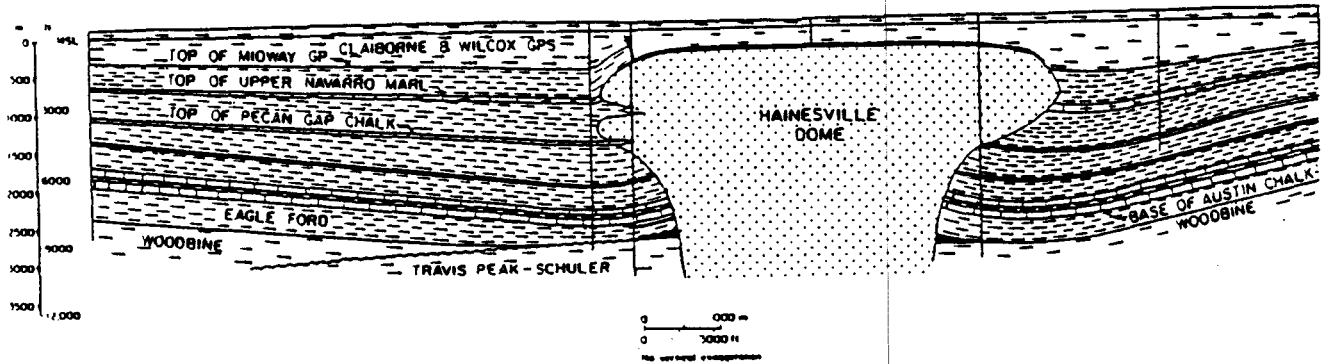
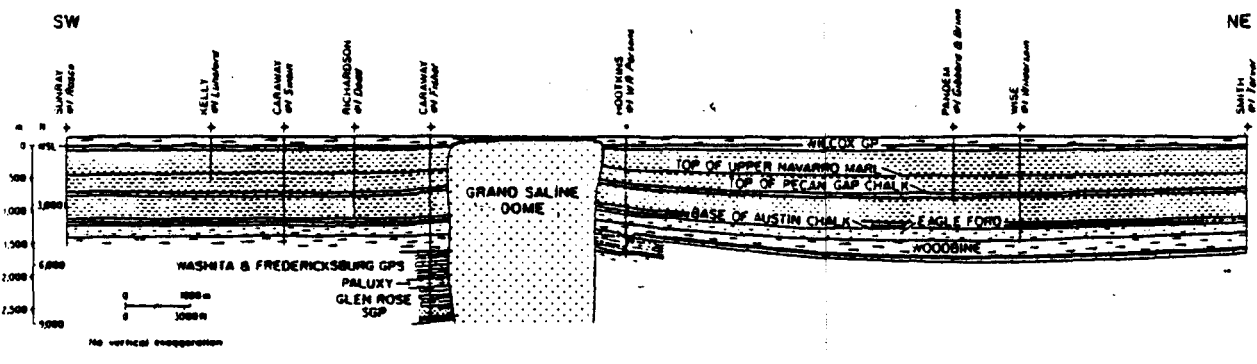
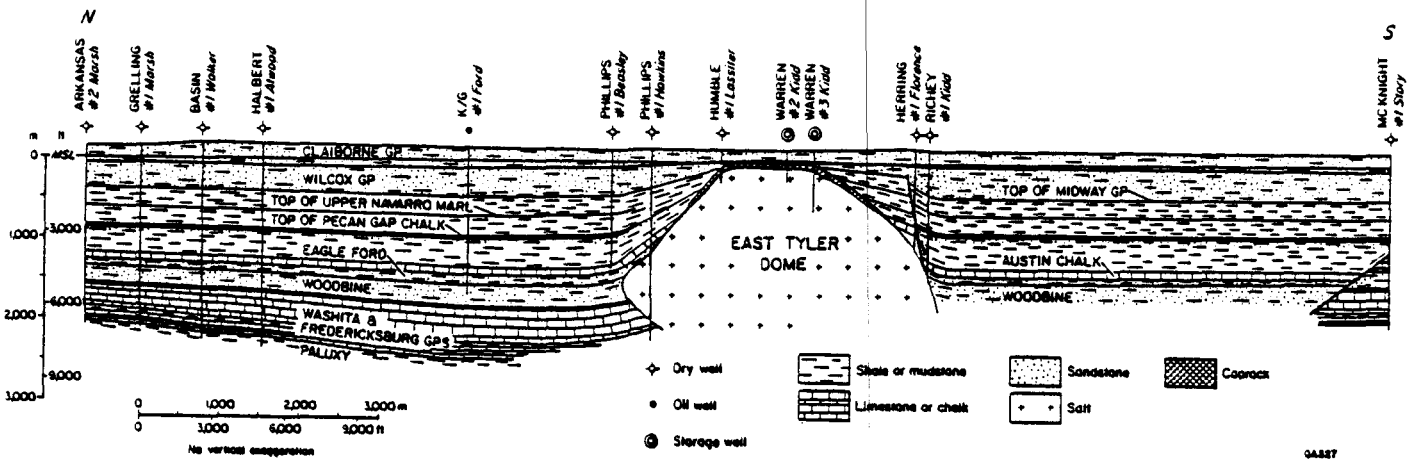


ORTHOGONAL CROSS SECTIONS THROUGH SALT STOCKS (SECTIONS 1.4, 1.5, 1.6)

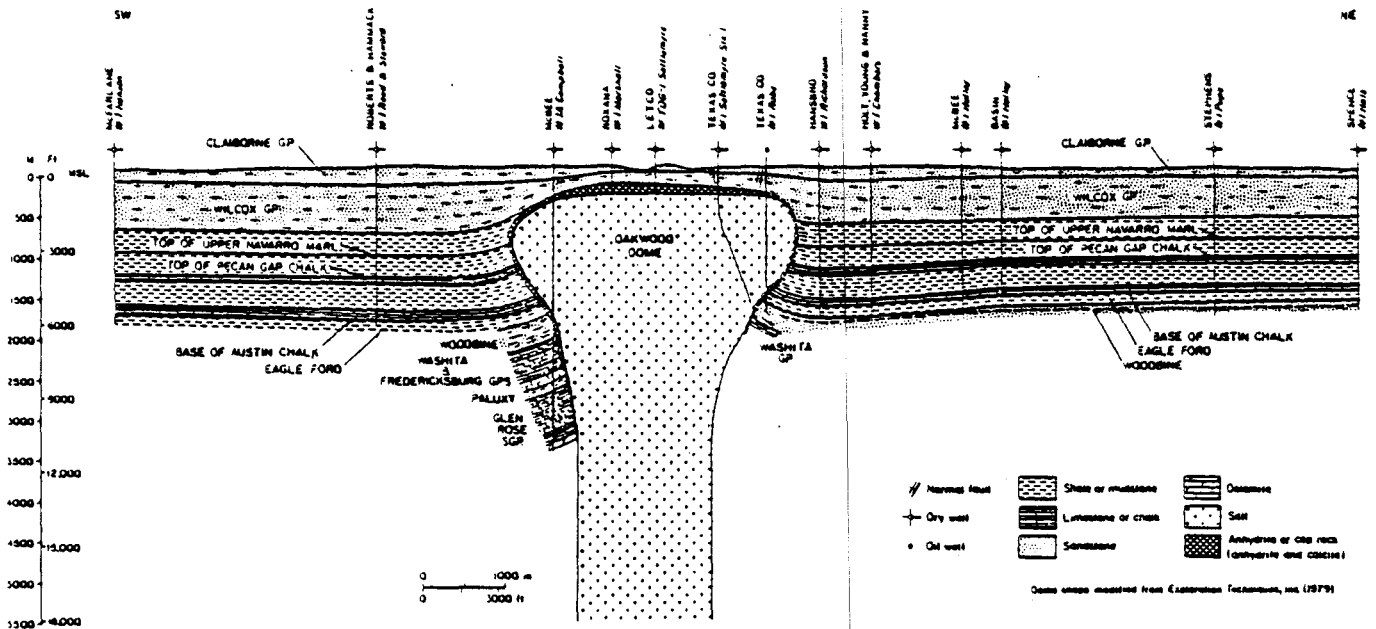
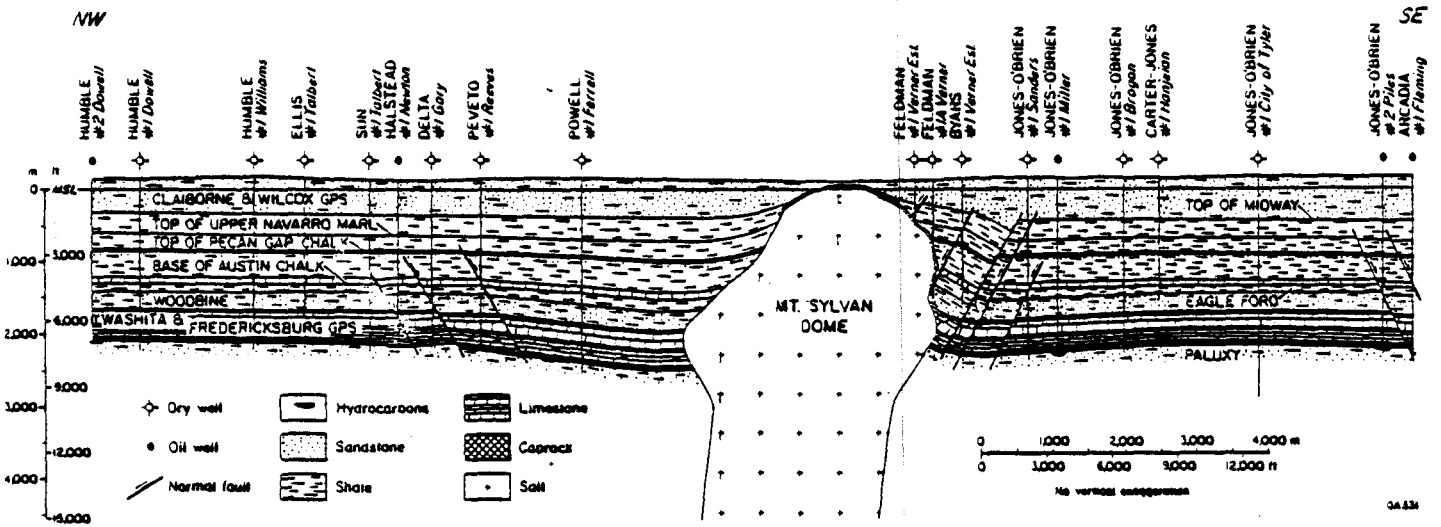
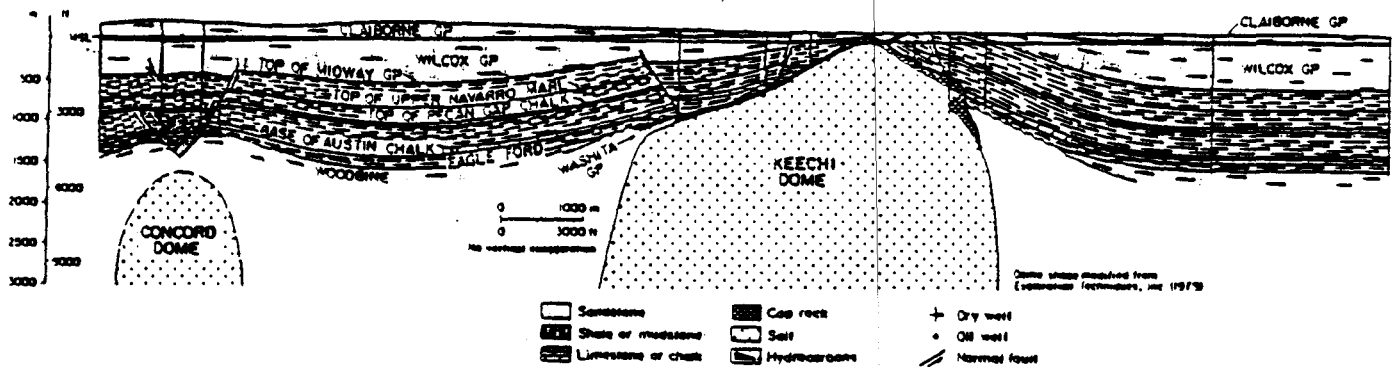




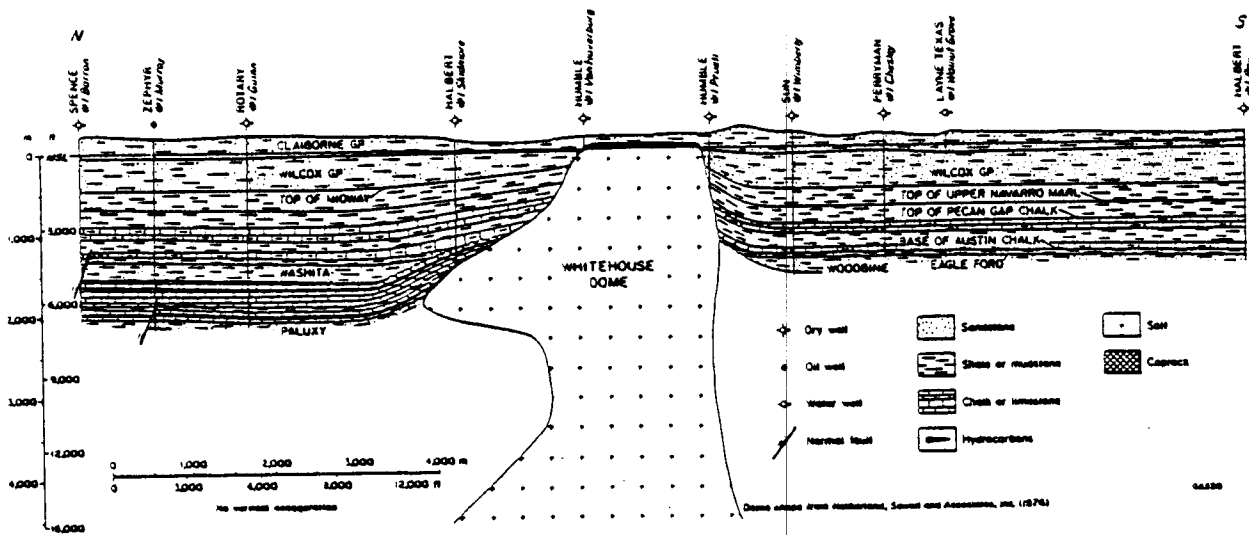
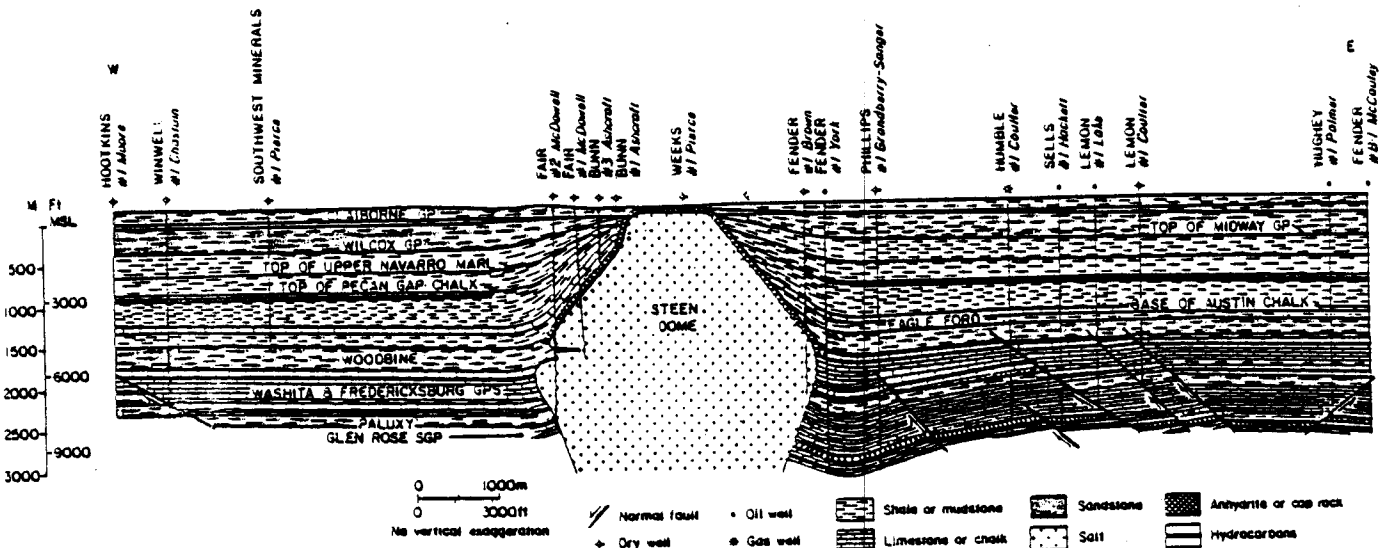
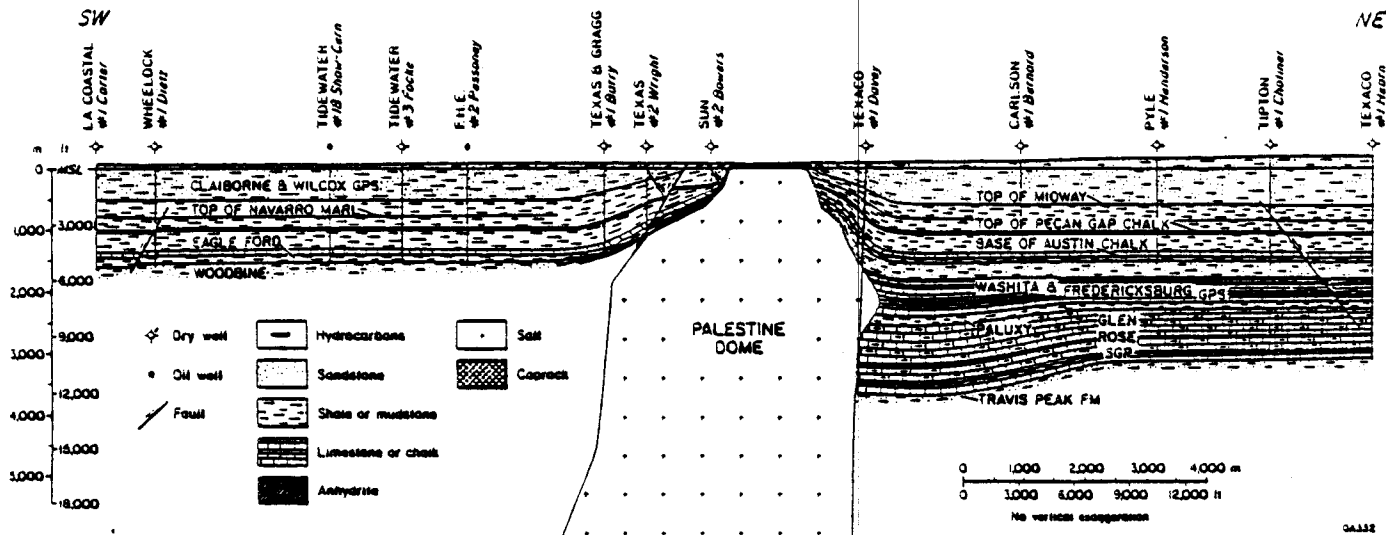
STRUCTURAL CROSS SECTIONS THROUGH STRATA AROUND SALT DOMES  
(SECTIONS 1.5, 1.6, 1.7, 1.8, 2.1, 2.2, 2.3, 2.4, 2.5, 2.6, 3.1)



STRUCTURAL CROSS SECTIONS THROUGH STRATA AROUND SALT DOMES  
(SECTIONS 1.5, 1.6, 1.7, 1.8, 2.1, 2.2, 2.3, 2.4, 2.5, 2.6, 3.1)



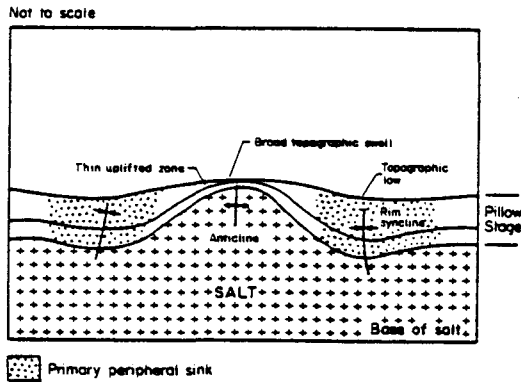
STRUCTURAL CROSS SECTIONS THROUGH STRATA AROUND SALT DOMES  
(SECTIONS 1.5, 1.6, 1.7, 1.8, 2.1, 2.2, 2.3, 2.4, 2.5, 2.6, 3.1)



STRUCTURAL CROSS SECTIONS THROUGH STRATA AROUND SALT DOMES  
(SECTIONS 1.5, 1.6, 1.7, 1.8, 2.1, 2.2, 2.3, 2.4, 2.5, 2.6, 3.1)

Appendix 3. Schematic stages of dome growth showing typical lithologic and thickness variations in strata around domes (from Seni and Jackson, 1983).

Pillow



Uplifted area

Sediments above pillow are thin over broad, equidimensional to elongate area. Maximum thinning over crest. Area extends 100-400 km<sup>2</sup> (40-150 mi<sup>2</sup>), depending on size of pillow. Percentage thinning, 10-100%.

Withdrawal basin

Sediments are overthickened in broad to elongate primary peripheral sink, generally located on up-dip side of salt pillow. Axial trace of sink parallels axial trace of elongate uplift, generally separated by 10-20 km (6-12 mi). Sink attains 300 km<sup>2</sup> (120 mi<sup>2</sup>) in extent, depending on size of pillow. Percentage thickening, 10-30%. Recognition of primary peripheral sink may be hindered by interference of nearby salt structures.

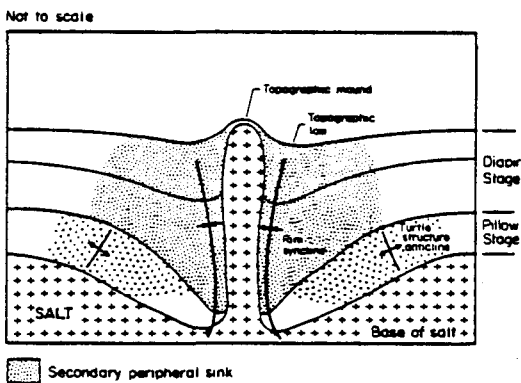
Facies

Thin, sand-poor, fluvial-deltaic deposits over crest of pillow include interchannel and interdeltic facies. Erosion common. Carbonate deposits on crest would include reef, reef-associated, and high-energy facies.

Facies

Thick, sand-rich fluvial-deltaic deposits in primary peripheral sink include channel axes and deltaic depocenters. Aggradation common in topographically low area of sink. Carbonate deposits in sink would include low-energy facies caused by increase in water depth.

Diapir



Uplifted area

Strata largely absent above dome. An 8-50 km<sup>2</sup> (3-20 mi<sup>2</sup>) area around diapir is thinned, depending on size and dip on flanks of dome.

Withdrawal basin

Sediments are thickened up to 215% in secondary peripheral sink. Sinks up to 1000 km<sup>2</sup> (390 mi<sup>2</sup>) in extent are equidimensional to elongate and preferentially surround single or multiple domes; several sinks flank domes; percentage thickening ranges from 50-215%.

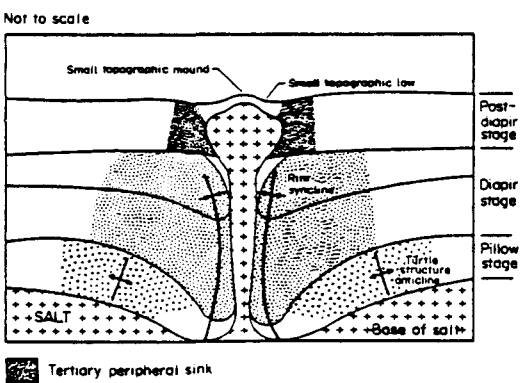
Facies

Facies immediately over dome crest not preserved because of piercing by diapir of all but the youngest strata. Sand bodies commonly pinch out against dome flanks.

Facies

Expanded section of marine facies dominate, including limestones, chalks, and mudstones; generally sink is filled with deeper-water low-energy facies caused by increased water depth. Elevated saddles between withdrawal basins are favored sites of reef growth and accumulated high-energy carbonate deposits.

Postdiapir



Uplifted area

Strata thin or absent in small 10-50 km<sup>2</sup> area over crest and adjacent to dome; area depends on size of dome and dip of flanks.

Withdrawal basin

Sediments within 20-200 km<sup>2</sup> (8-80 mi<sup>2</sup>) tertiary peripheral sink are thickened 0-40%, commonly by > 30 m (100 ft). Axial trace of elongate to equidimensional sink surrounds or flanks a single dome, or connects a series of domes.

Facies

Facies and strata over crest of dome not preserved in cases of complete piercement. Modern analogs have interchannel and interdeltic facies in uplifted area. Mounds above dome include thin sands. Carbonate strata would include reef or high-energy deposits; erosion common.

Facies

Modern analogs have channel axes in sink. Aggradation of thick sands common in subsiding sink. Carbonate strata would include low-energy facies.

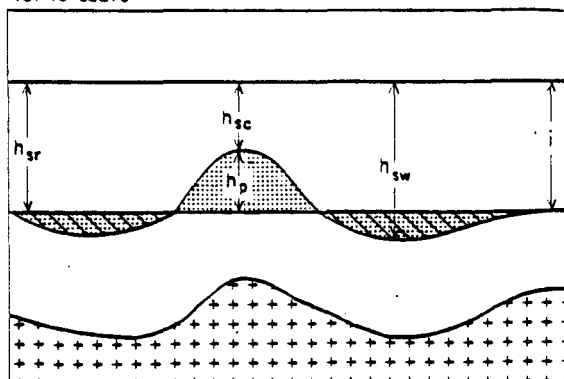
Appendix 4. Methods for calculating net and gross rates of diapir growth with applications, assumptions, restrictions and advantages (from Seni and Jackson, 1983).

Method

Application, Assumptions, Restriction, Advantages

A. Net growth by sediment thinning

Not to scale



Application: Pillow stage, post-diapir stage (only for non-pierced strata)

Assumptions: (1) Sediment thinning is syn-depositional  
(2) Sediment thinning is due to uplift of crest of structure

Restriction: Only records extension greater than shortening caused by extrusion or dissolution

Advantages: (1) Simple quantitative methodology  
(2) Can be measured from single cross section  
(3) Applicable to youngest strata not pierced by diapir, thus provides rates of most recent growth

$$h_p = h_{sr} - h_{sc}$$

$$G_n = h_p$$

$$\dot{G}_n = \frac{h_p}{t_i}$$

$h_p$  = Height of pillow

$h_{sr}$  = Regional mean sediment thickness

$h_{sc}$  = Minimum sediment thickness over crest of structure

$h_{sw}$  = Maximum sediment thickness in salt-withdrawal basin

$G_n$  = Net growth of pillow

$\dot{G}_n$  = Net growth rate of pillow

$t_i$  = Duration of stratigraphic interval (i)

Net growth calculated by sediment thinning will equal net growth calculated by sediment thickening only when

$$h_{sc} = 0$$

and  $h_{sw} = h_{sr}$

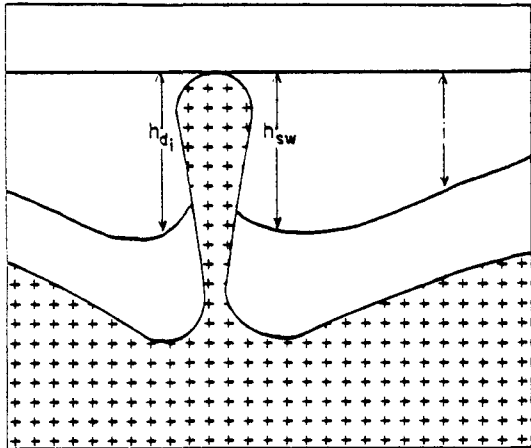
$$\therefore G_n = h_{sr} - h_{sc} = h_{sw}$$

Method

Application, Assumptions, Restriction, Advantages

B. Net growth by sediment thickening

Not to scale



$$G_n = h_{di} = h_{sw}$$

$$\dot{G}_n = \frac{h_{sw}}{t_i}$$

$h_{di}$  = height of diapir

$h_{sw}$  = Maximum thickness of stratigraphic interval measured in salt-withdrawal basin

$G_n$  = Net growth of diapir

$\dot{G}_n$  = Net growth rate of diapir

$t_i$  = Duration of stratigraphic interval (i)

Application:

Pillow stage, diapir stage, post-diapir stage

Assumptions:

- (1) Diapir remains near sediment surface during deposition
- (2) Rate of deposition controls or is controlled by diapir growth

Restriction:

Only records net extension greater than shortening caused by diapir extrusion or dissolution

Advantages:

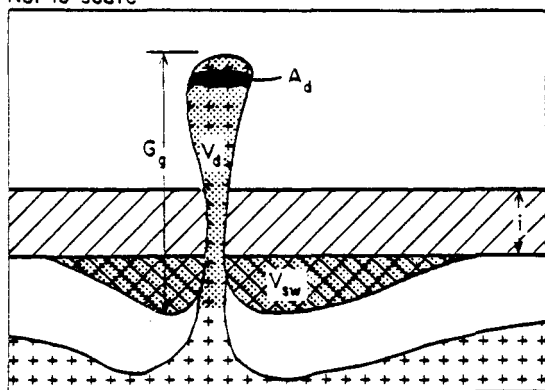
- (1) Simple quantitative methodology
- (2) Can be measured from single cross section

Method

Application, Assumptions, Restrictions, Advantage

C. Gross diapir growth

Not to scale



$$V_{sw} = V_d$$

$$G_g = \frac{V_{sw}}{A_d}$$

$$\dot{G}_g = \frac{V_{sw}/A_d}{t_i}$$

$V_{sw}$  = Volume of sediments in salt-withdrawal basin

$V_d$  = Volume of diapir

$A_d$  = Maximum cross-sectional area of diapir

$G_g$  = Gross growth of diapir

$\dot{G}_g$  = Gross growth rate of diapir

$t_i$  = Duration of stratigraphic interval (i)

Application:

Diapir stage only

Assumptions:

- (1) Present cross-sectional area of diapir equals cross-sectional area of diapir during filling of withdrawal basin
- (2) Volume of withdrawal basin equals volume of salt mobilized during filling of withdrawal basin
- (3) All salt mobilized during filling of withdrawal basin migrated into diapir

Restrictions:

- (1) Requires measuring volume of withdrawal basin and area of diapir, which requires close well spacing for map construction
- (2) Growth by tear-drop detachment of diapir base is not measurable

Advantage:

Records total extension independent of possible dissolution or extrusion

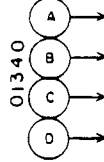
Appendix 5. Log of Oakwood Dome salt core (from Dix and Jackson, 1982).

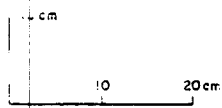
APPENDIX

Oakwood Salt-Core Log

Project name: GCSD-Texas  
 Project number: MV9620.20  
 Location: Oakwood Dome, Freestone-Leon County  
 Well number: TOG-1  
 Date commenced: 9-27-79  
 Date completed: 11-7-79  
 Total well depth: 411.8 m (1351 ft)  
 Net thickness of rock salt: 57.3 m (188 ft)

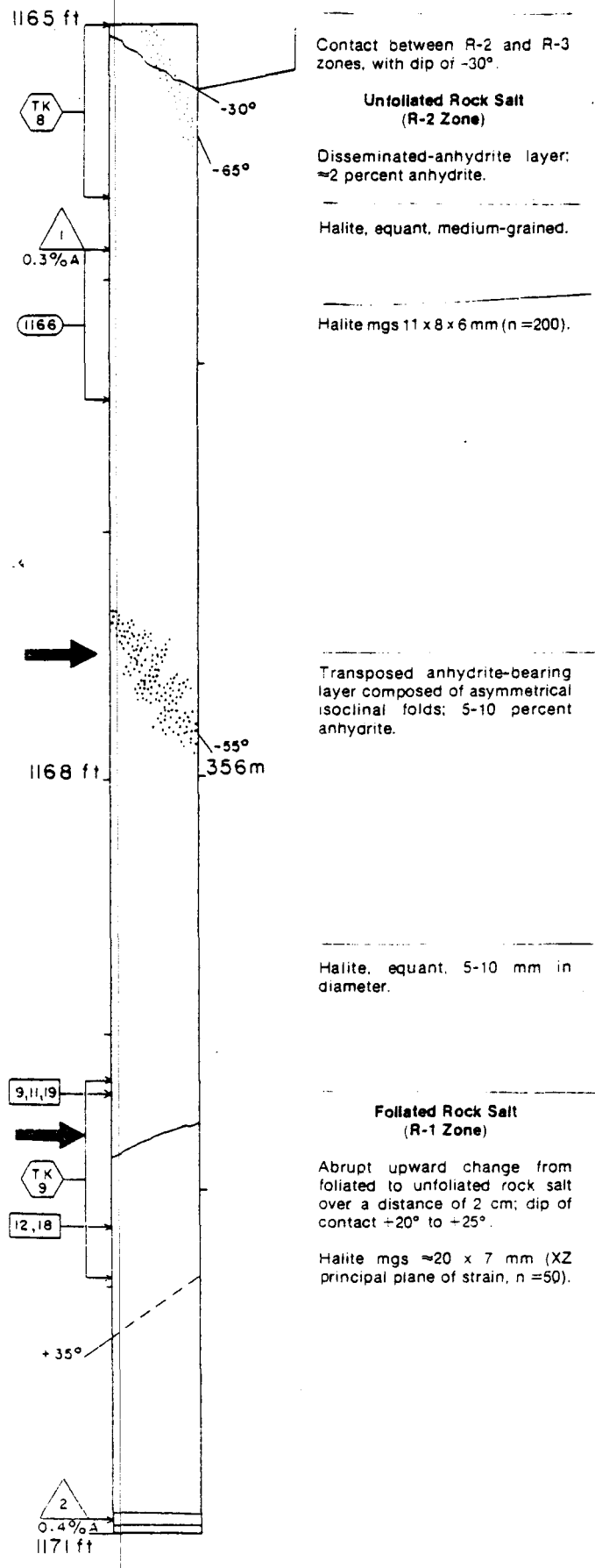
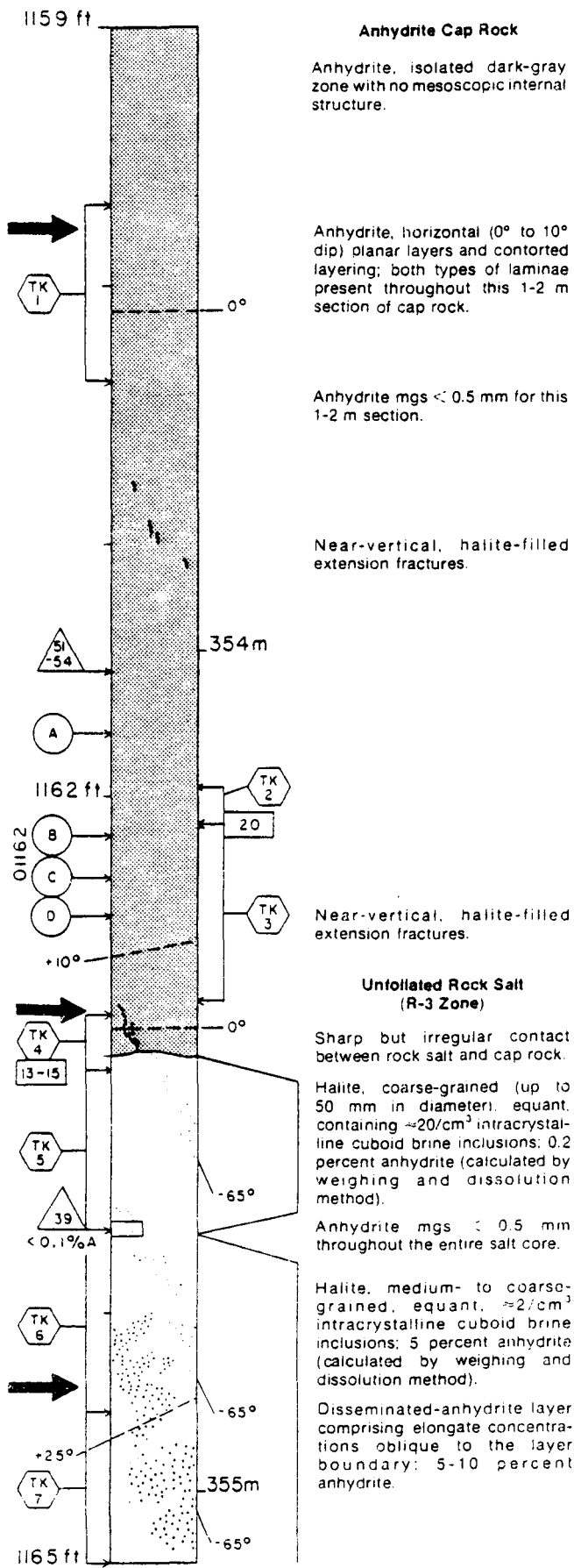
Explanation

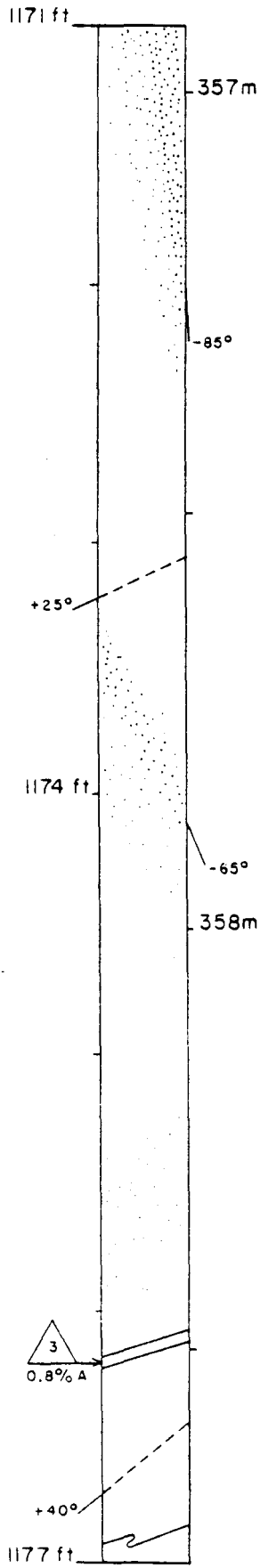
-  Detailed description in text
-  Location and number of thin section (< 1 mm thick)
-  Location and number of thick section (1-10 mm thick)
-  Location and number of sample used for geochemical analysis; exact location and orientation of sample shown on core profile; percentage anhydrite given below triangle
-  Location and number of sample for strain analysis
-  Location and number of plugs for magnetic anisotropy measurements
-  Missing core interval
-  Dip of foliation
-  Dip of contact, anhydrite layer or disseminated anhydrite
- $n=50$  Number of grains measured for grain-size determination (using only grains clearly visible to the naked eye)
- $n=200$  Number of grains measured for grain-size determination from strain analysis data (x 10 magnification)
- mgs Mean grain size



Halite grain sizes: fine grained < 5 mm  
 medium grained 6-20 mm  
 coarse grained 21-50 mm

Pure rock salt contains < 1 percent impurities



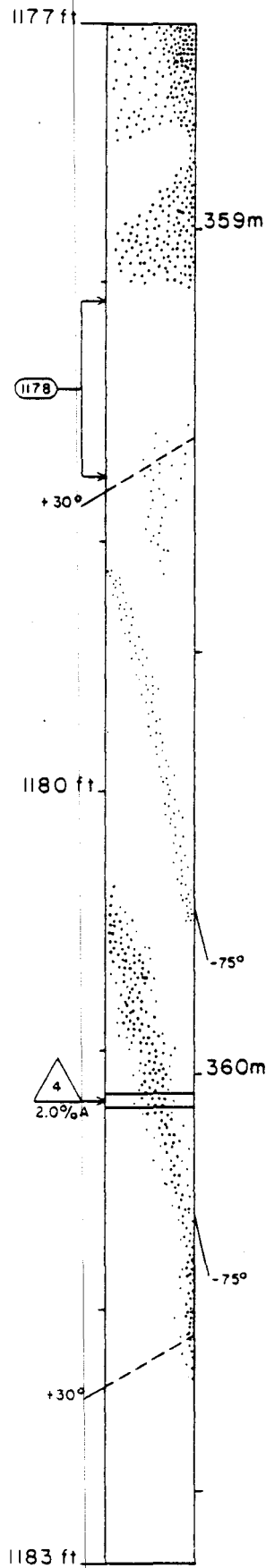


Disseminated-anhydrite layer:  
2-5 percent anhydrite; dark  
concentrations along halite grain  
boundaries due to some  
preferred location of anhydrite.

Halite mgs  $\approx 20 \times 7$  mm (XZ  
plane).

Disseminated-anhydrite layer  
(2-5 percent).

Disseminated anhydrite ( $\approx 2$   
percent); orientation not evident.



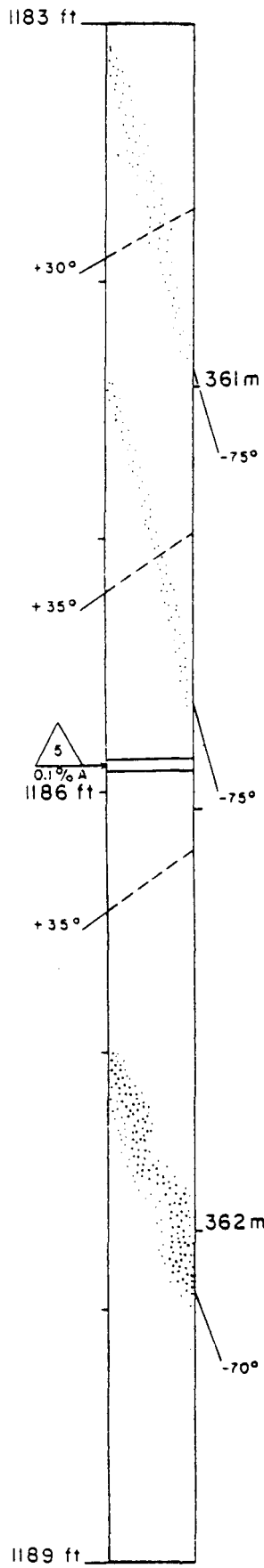
Disseminated anhydrite (5-10  
percent); orientation not evident.

Indistinct, disseminated  
anhydrite ( $\approx 2$  percent); halite  
mgs  $\approx 15 \times 6$  mm (XZ plane).

Indistinct, disseminated-  
anhydrite layer;  $\approx 2$  percent  
anhydrite.

Disseminated-anhydrite layer  
with mesoscopic folds; 5-10  
percent anhydrite.

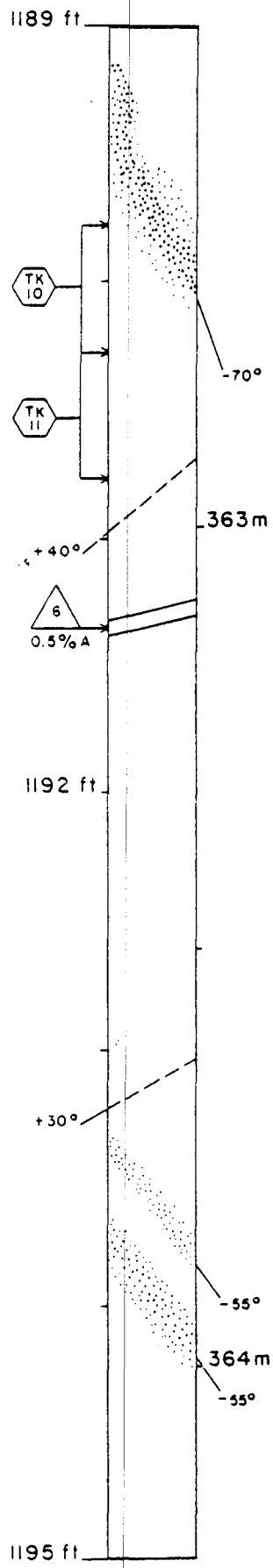
Dip of layer steepens to near  
vertical.



Indistinct, disseminated-anhydrite layer; ≈2 percent anhydrite.

Indistinct, disseminated-anhydrite layer; ≈2 percent anhydrite.

Disseminated-anhydrite layer with mesoscopic folds; 5-10 percent anhydrite.

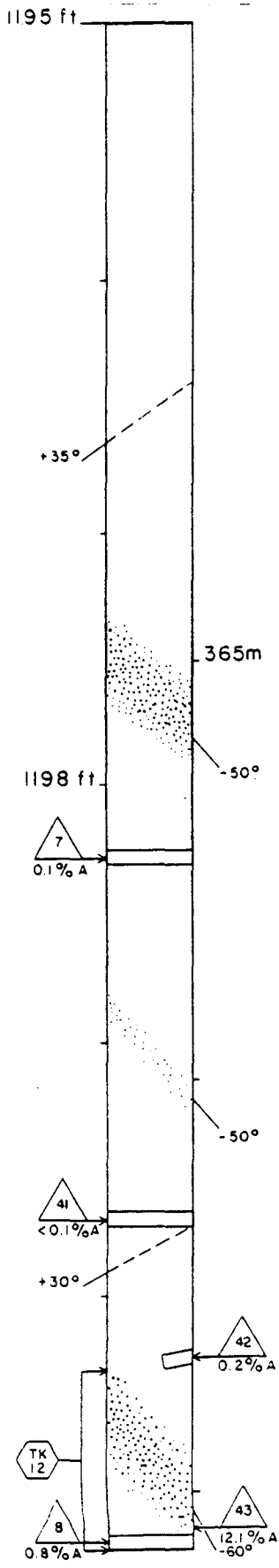


Disseminated-anhydrite layer with mesoscopic folds; 5-10 percent anhydrite; halite mgs ≈25 x 9 mm in pure rock salt (XZ plane), ≈18 x 7 mm adjacent to the layer, and ≈14 x 5 mm within the layering (n = 50 for each calculation).

Pure rock salt.

Indistinct, disseminated-anhydrite layer; ≈2 percent anhydrite.

Disseminated-anhydrite layer; 2-5 percent anhydrite.



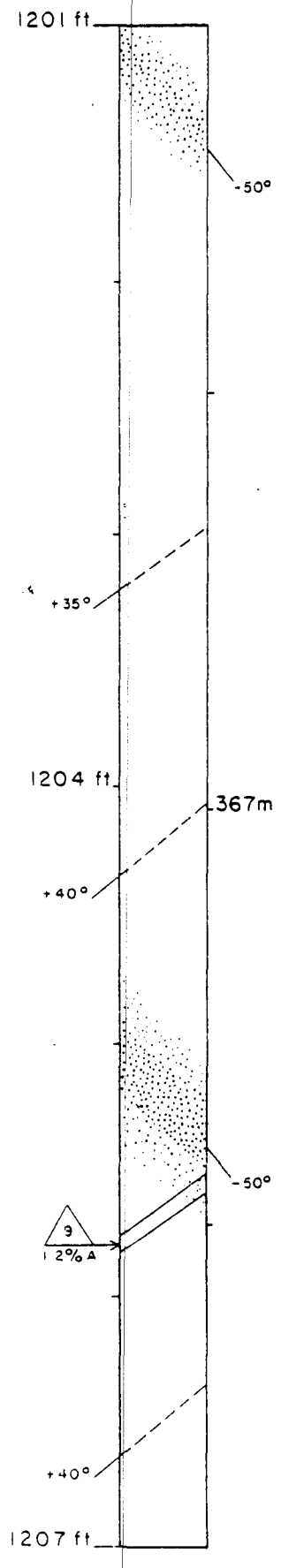
Pure rock salt.

Disseminated-anhydrite layer:  
5-10 percent anhydrite.

Indistinct, disseminated-  
anhydrite layer: ≈2 percent  
anhydrite.

Halite crystals up to 55 x 15 mm  
(XZ plane).

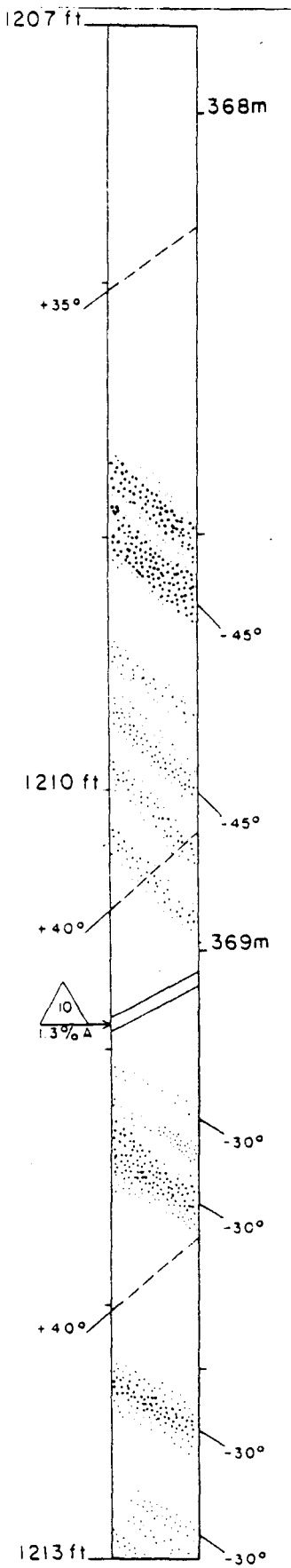
Disseminated-anhydrite layer:  
5-10 percent anhydrite; halite  
mgs in pure rock salt ≈20 x 9 mm  
(XZ plane, n = 50), and ≈13 x 6  
mm in the anhydrite layer; dip  
azimuth of layer is 180° to dip  
azimuth of foliation.



Disseminated-anhydrite layer:  
2-5 percent anhydrite.

Pure rock salt.

Disseminated-anhydrite layer:  
2-5 percent anhydrite.



Pure rock salt.

Two disseminated-anhydrite layers: 10-15 percent anhydrite.

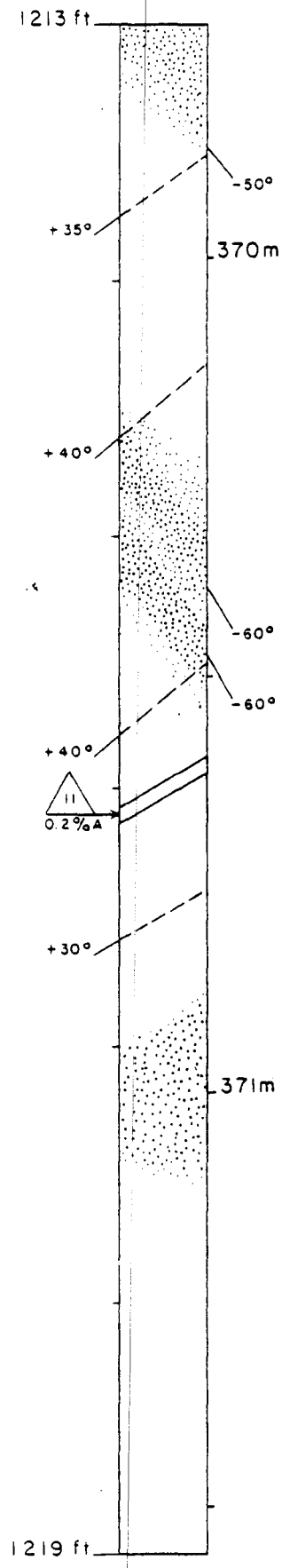
Four disseminated-anhydrite layers: 2-5 percent anhydrite; dip azimuth of anhydrite layers 140°-150° clockwise from dip azimuth of foliation.

Two indistinct disseminated-anhydrite layers: ≈2 percent anhydrite.

Disseminated-anhydrite layer: 5-10 percent anhydrite.

Disseminated-anhydrite layer: 5-10 percent anhydrite.

Three indistinct, disseminated-anhydrite layers: ≈2 percent anhydrite.

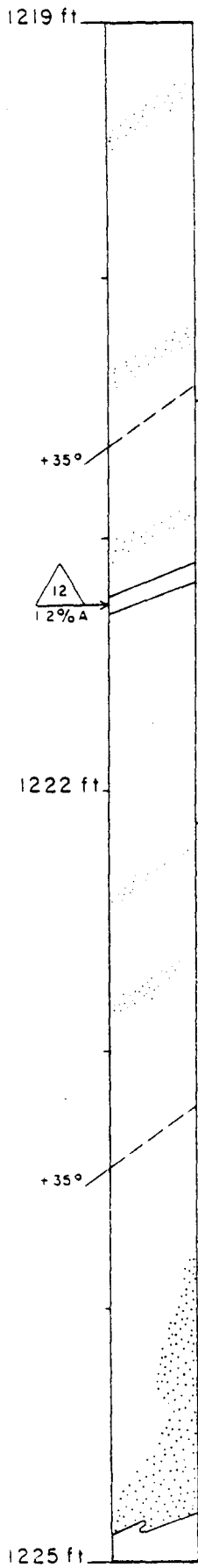


Disseminated anhydrite; 2-5 percent anhydrite; dark coloration along halite grain boundaries prominent.

Disseminated-anhydrite layer: 2-5 percent anhydrite.

Disseminated-anhydrite layer: 5-10 percent anhydrite.

Disseminated anhydrite (5-10 percent); orientation not evident; dark coloration along halite grain boundaries.



Indistinct, disseminated-anhydrite layer parallel to foliation; ≈2 percent anhydrite.

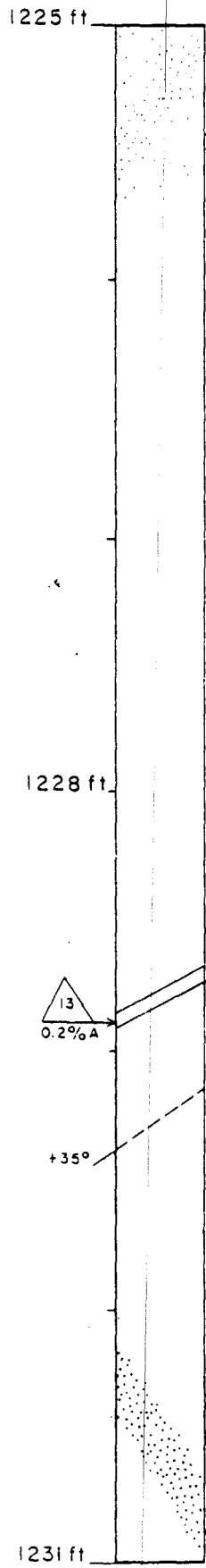
Indistinct, disseminated-anhydrite layer parallel to foliation; ≈2 percent anhydrite.

Indistinct, disseminated-anhydrite layer parallel to foliation; ≈2 percent anhydrite.

Two indistinct, disseminated-anhydrite layers parallel to foliation; ≈2 percent anhydrite.

Disseminated anhydrite (5-10 percent); dark coloration along halite grain boundaries.

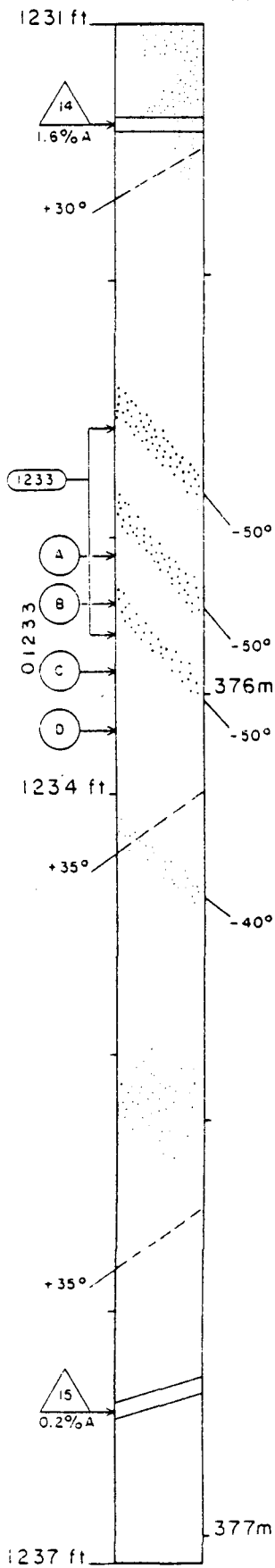
5 cm of core missing.



Disseminated anhydrite (≈2 percent); orientation not evident.

Pure rock salt.

Disseminated-anhydrite layer (5-10 percent).



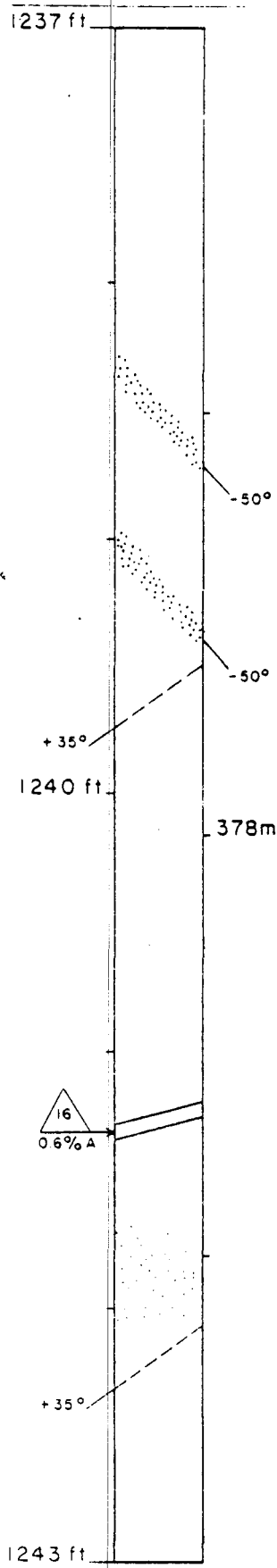
Disseminated anhydrite ( $\approx$ 2 percent); orientation not evident.

Disseminated-anhydrite layer; 5-10 percent anhydrite; dark blebs, and dark coloration along halite grain boundaries; halite mgs adjacent to layer  $\approx$ 15 x 6 mm (XZ plane).

Disseminated-anhydrite layers; 5-10 percent anhydrite.

Indistinct, disseminated-anhydrite layers;  $\approx$ 2 percent anhydrite.

Disseminated anhydrite ( $\approx$ 2 percent); orientation not evident; dark coloration along halite grain boundaries.

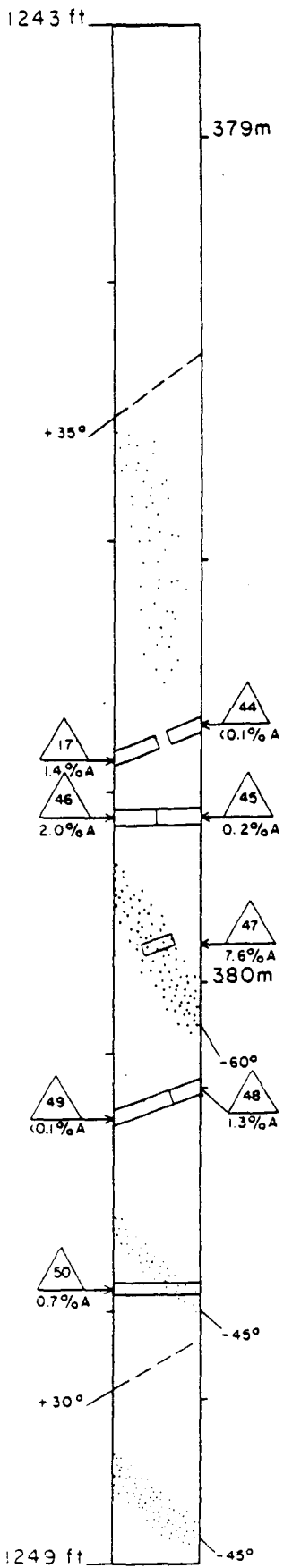


Pure rock salt.

Two disseminated-anhydrite layers; 5-10 percent anhydrite; dip azimuth of layering at 180° to dip azimuth of foliation; dark coloration along halite grain boundaries.

Pure rock salt.

Disseminated anhydrite ( $\approx$ 2 percent); orientation not evident.



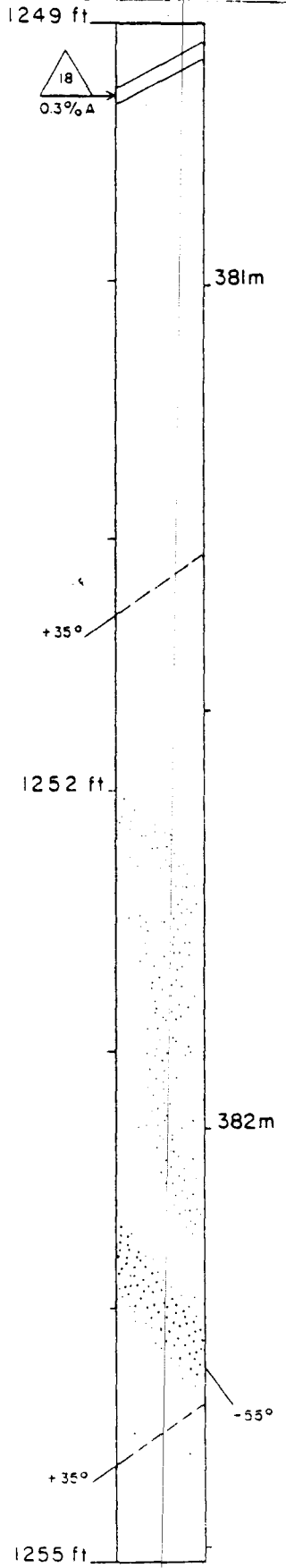
Pure rock salt.

Disseminated anhydrite (≈2 percent); orientation not evident.

Disseminated-anhydrite layer, 5-10 percent anhydrite, dark blebs, and dark coloration along halite grain boundaries; dip azimuth of layering 195° clockwise from dip azimuth of foliation.

Disseminated-anhydrite layer: ≈2 percent anhydrite.

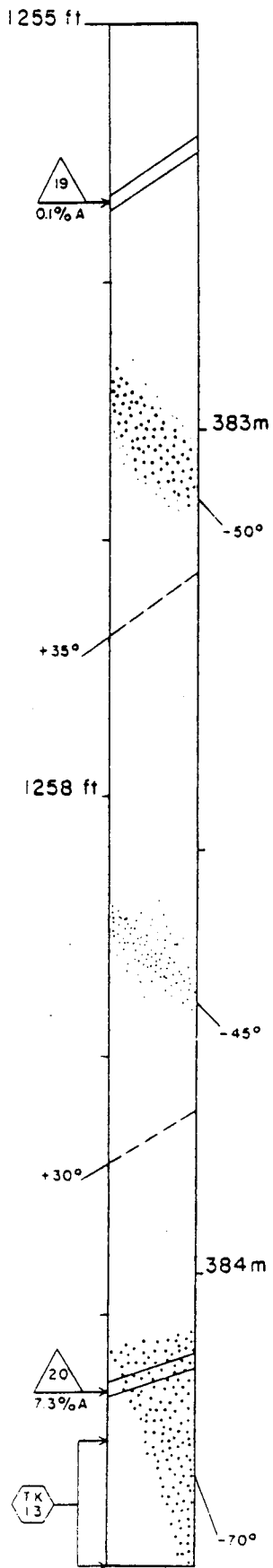
Disseminated anhydrite (≈2 percent); dark coloration along halite grain boundaries.



Pure rock salt.

Indistinct, disseminated anhydrite (≈2 percent); may represent a folded layer.

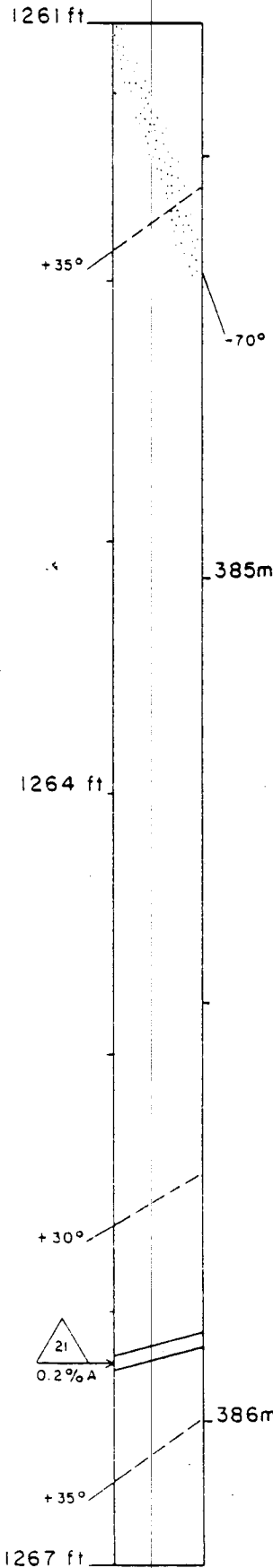
Disseminated-anhydrite layer, 5-10 percent anhydrite; dark coloration along halite grain boundaries; dip azimuth of layer 165° clockwise from dip azimuth of foliation.



Disseminated-anhydrite layer;  
5-10 percent anhydrite; dark  
coloration along halite grain  
boundaries; dip azimuth of layer  
180° to dip azimuth of foliation.

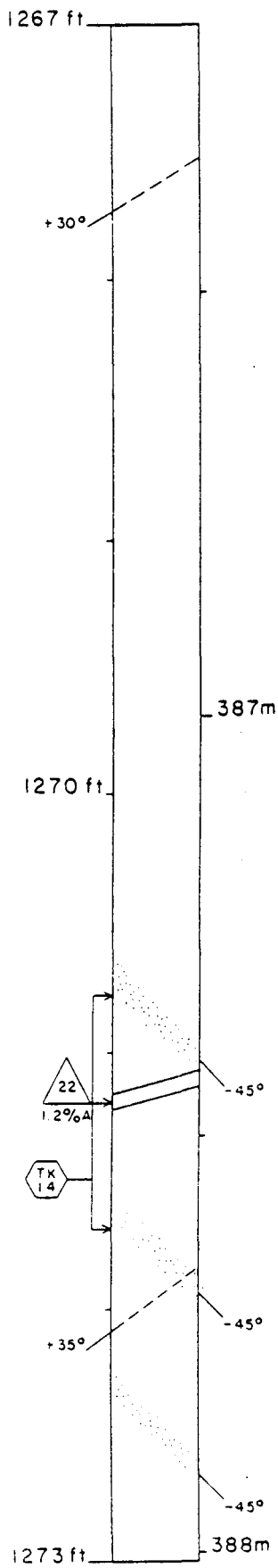
Indistinct, disseminated-  
anhydrite layer; ≈2 percent  
anhydrite; dark coloration along  
halite grain boundaries.

Disseminated anhydrite (5-10  
percent)

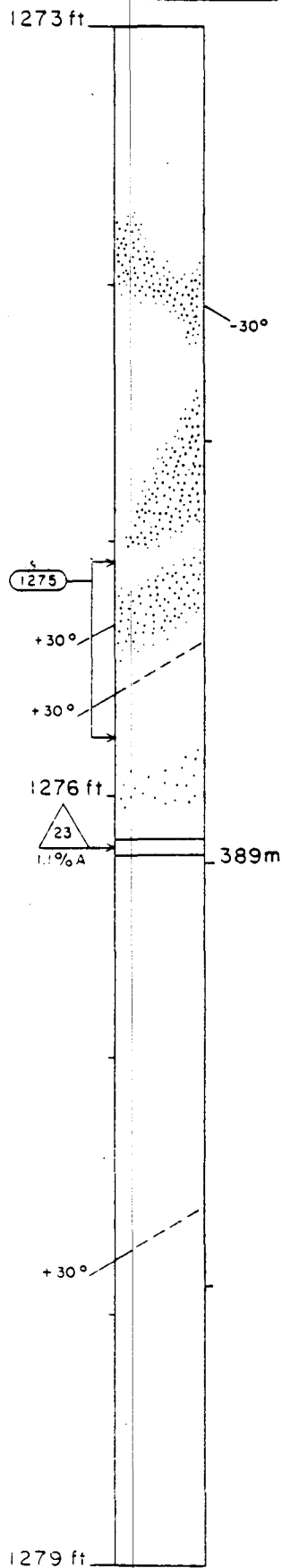


Disseminated-anhydrite layer;  
≈2 percent anhydrite.

Pure rock salt.



Three indistinct, disseminated-anhydrite layers: ≈2 percent anhydrite.



1279 ft

390m

Pure rock salt.

+35°

24  
<0.1% A

Halite mgs ≈25 x 10 mm (XZ plane), with a maximum in excess of 50 x 20 mm.

TX  
15

391m

Disseminated-anhydrite layers (≈2 percent) parallel to foliation.

+35°

Pure rock salt.

1285 ft

1285 ft

392m

Pure rock salt.

25  
<0.1% A

Disseminated anhydrite (≈2 percent) from 392.20 m to 392.75 m; orientation not evident.

1288 ft

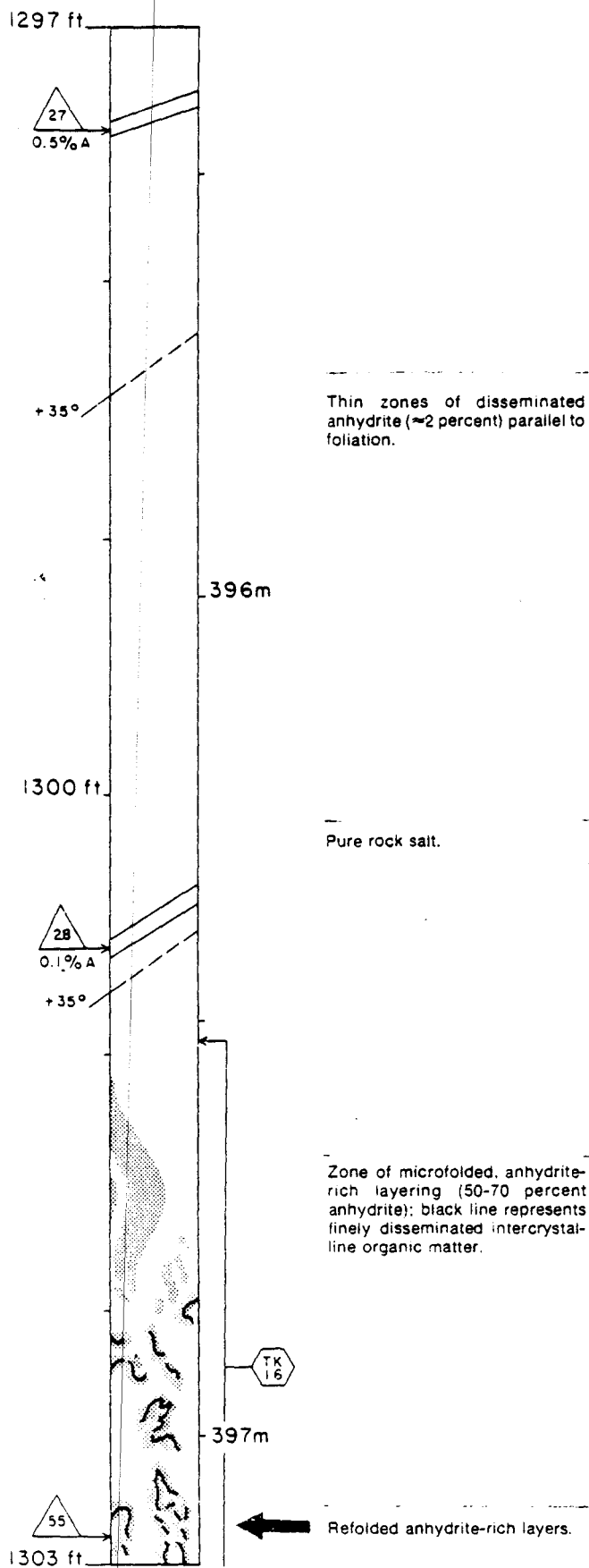
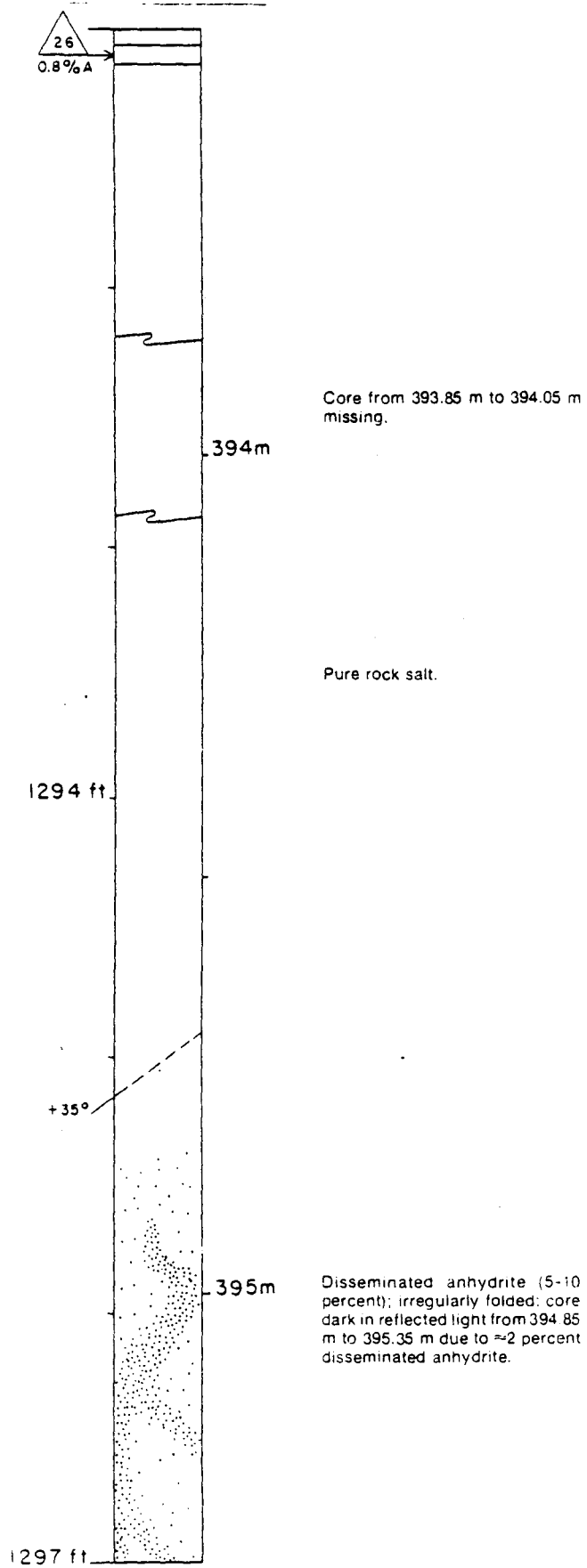
Pure rock salt.

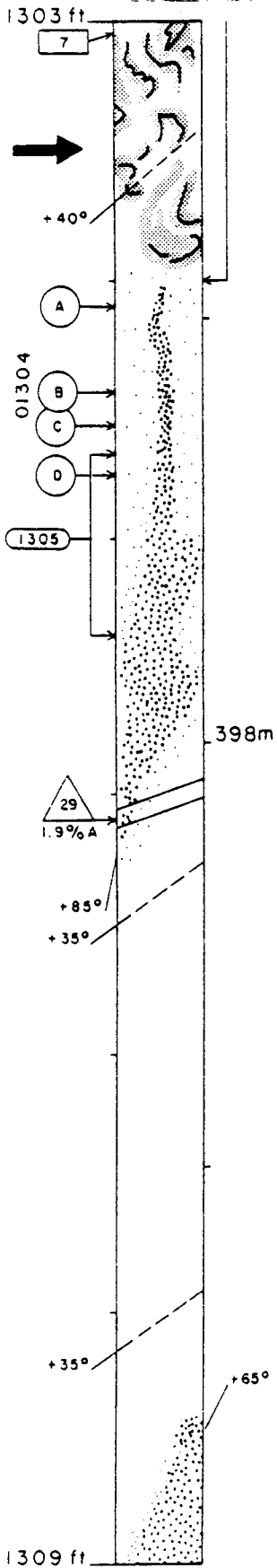
393m

+30°

Disseminated anhydrite (≈2 percent) from 393.25 m to 393.50 m; orientation not evident.

1291 ft





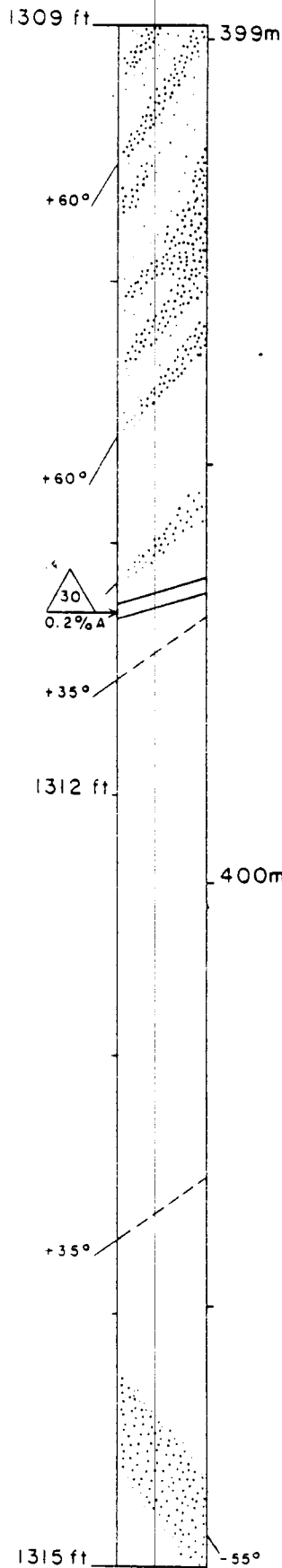
Refolded anhydrite-rich layers.

Lower limit of zone containing anhydrite-rich layers.

Disseminated-anhydrite layer; 10-15 percent anhydrite; halite mgs  $\approx 11 \times 4$  mm (XZ plane,  $n = 200$ ).

Pure rock salt

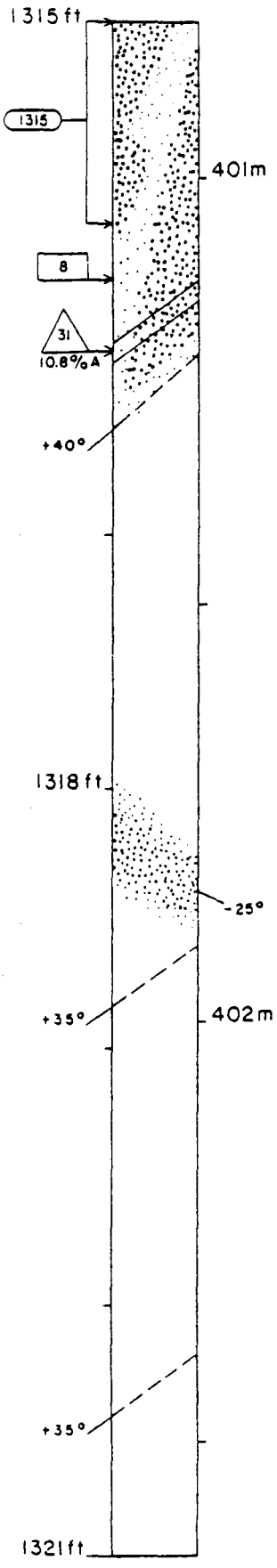
Disseminated-anhydrite layer; 10-15 percent anhydrite; dip azimuth of layer 35° clockwise from dip azimuth of foliation.



More than six disseminated-anhydrite layers; 5-10 percent anhydrite; some layers are discontinuous, others coalesce.

Pure rock salt.

Disseminated-anhydrite layer; 5-10 percent anhydrite; dip azimuth of layer 190° clockwise from dip azimuth of foliation.

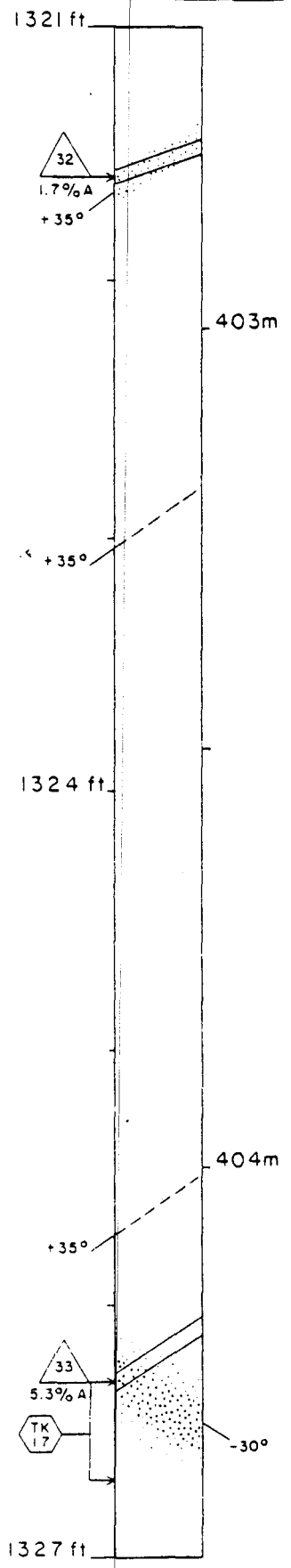


Two irregular disseminated-anhydrite layers: 10-15 percent anhydrite; halite mgs  $\approx 12 \times 4$  mm (XZ plane,  $n = 200$ ).

Pure rock salt.

Disseminated-anhydrite layer: 5-10 percent anhydrite.

Pure rock salt.

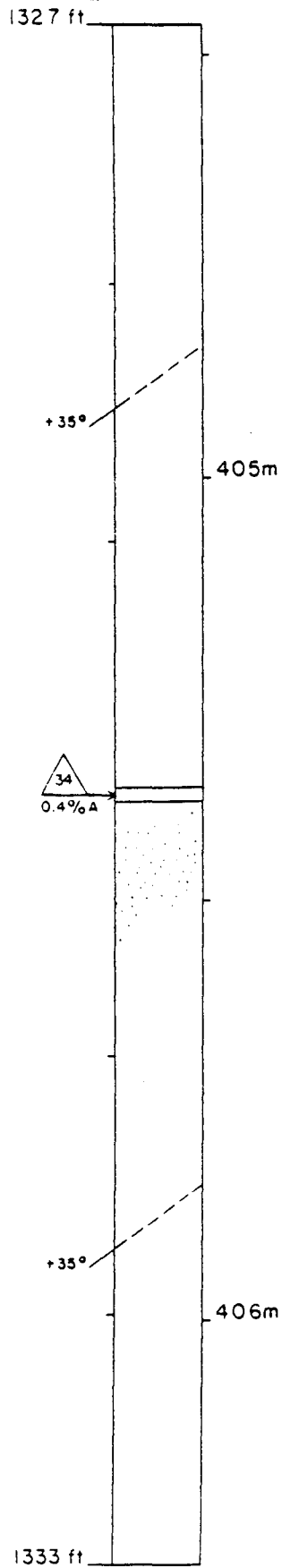


Indistinct, disseminated-anhydrite layer parallel to the foliation:  $\approx 2$  percent anhydrite.

Pure rock salt.

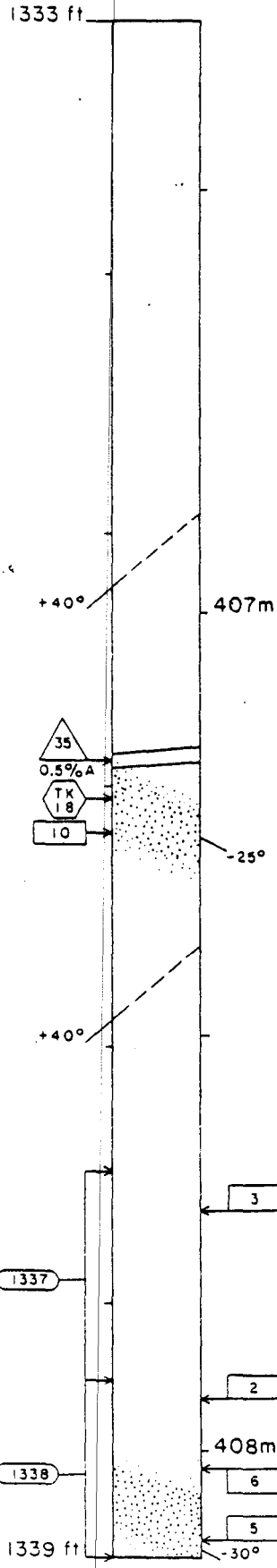
Pure rock salt.

Disseminated-anhydrite layer: 5-10 percent anhydrite.



Pure rock salt.

Disseminated anhydrite (≈2 percent).



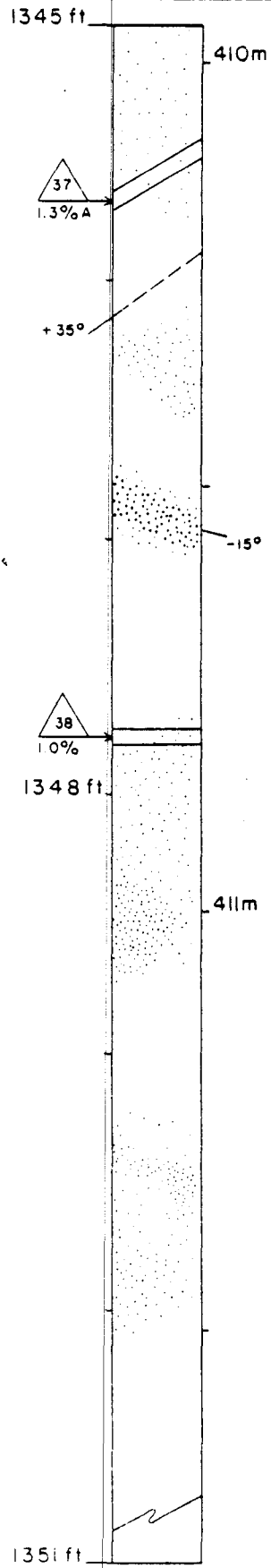
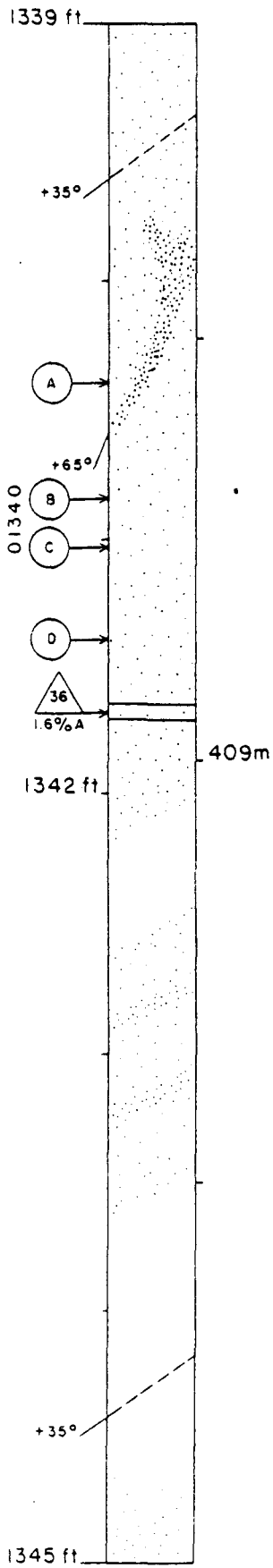
Pure rock salt.

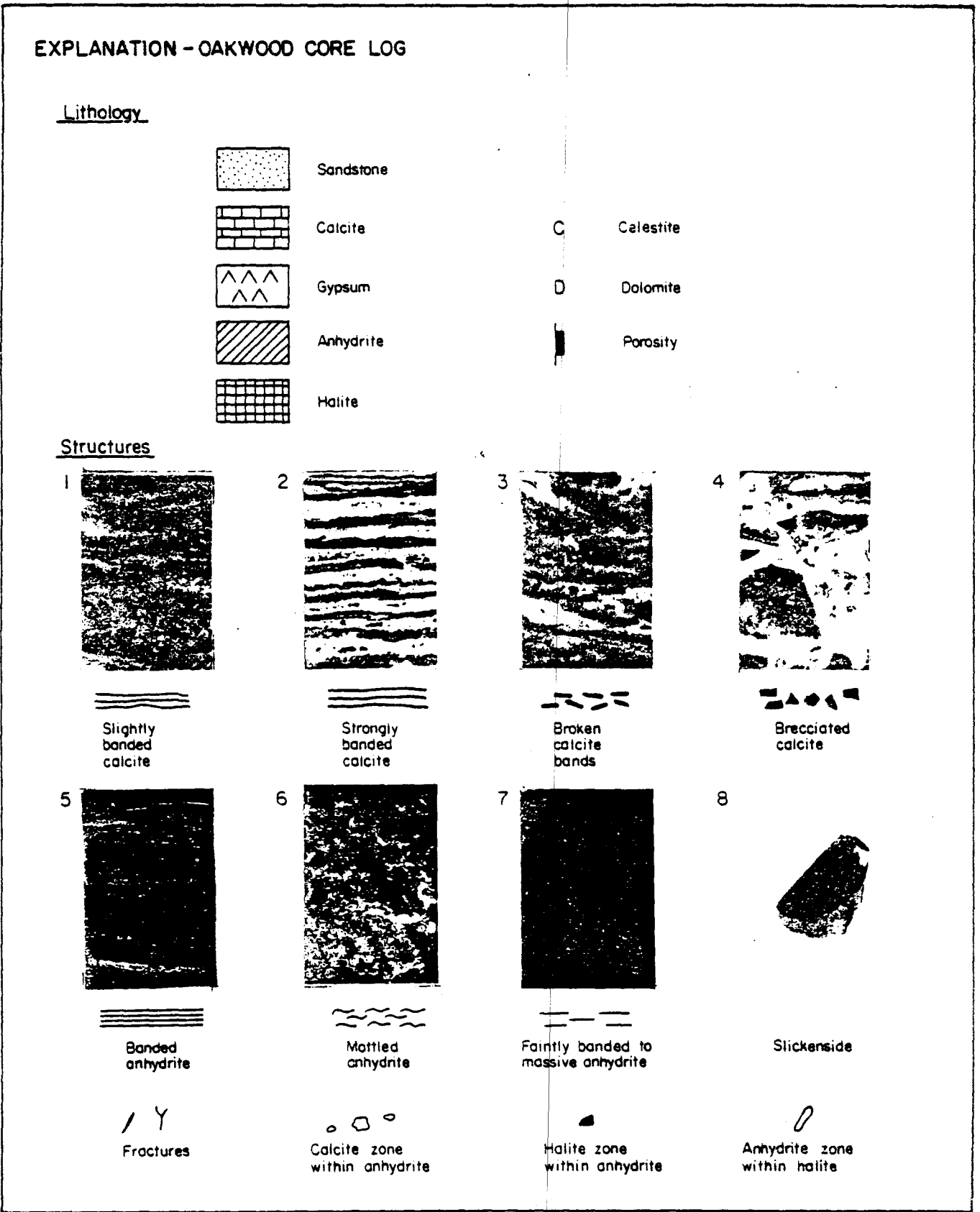
Disseminated-anhydrite layer; 5-10 percent anhydrite; dark coloration along halite grain boundaries.

Pure rock salt.

Halite mgs in pure rock salt ≈19 x 6 mm (XZ plane, n = 100).

Disseminated-anhydrite layer; 5-10 percent anhydrite; layer thins to the left, the thinnest point representing the hinge of a fold; dark coloration along halite grain boundaries; halite mgs ≈11 x 14 mm (XZ plane, n = 100).





Appendix 6 (cont.)

